EJA

European Journal of Anatomy

Volume 26 - Number 4 July 2022

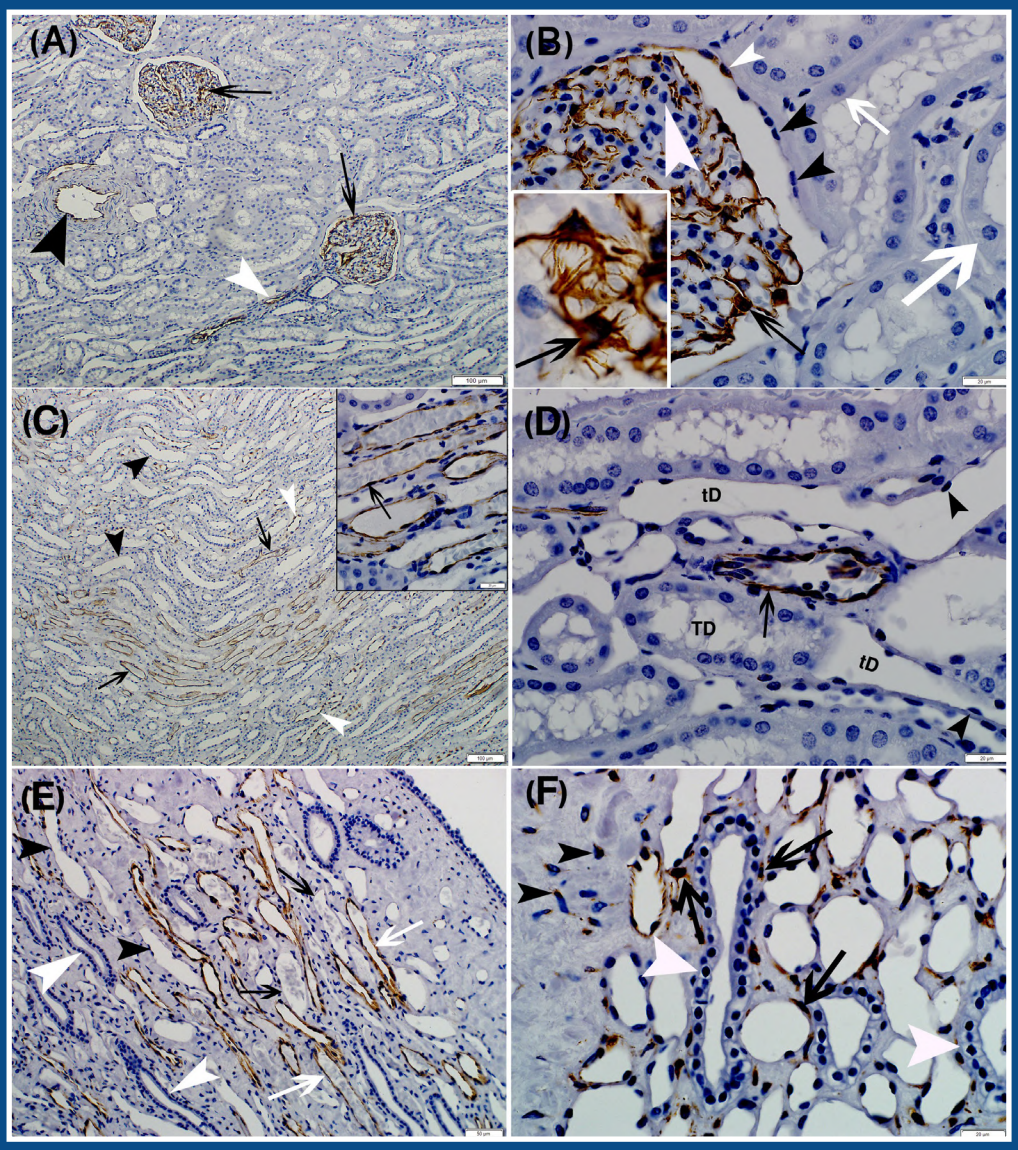

Indexed in:

CLARIVATE
- JCR:2020
- Q4 (21/23)
- I.F. J.C.I.: 0.19

DIALNET

EMBASE / Excerpta Medica

SCOPUS
- SJCR: 2020
- Q4 (31/39)
- I.F.: 0.162

Emerging Sources Citation Index

LATINDEX. Catálogo v1.0 (2002-2017)

Official Journal of the Spanish Society of Anatomy

www.eurjanat.com

EJA
European Journal of Anatomy
Volume 26 - Number 4 July 2022

OBITUARY

Prof. Dr. med. Dr. h.c. J. W. Rohen

On May 26, 2022, the Anatomist Prof. Dr. med. Dr. h.c. Johannes Wilhelm Rohen passed away.

Johannes W. Rohen was born on 18.9.1921 in Münster, attended the grammar schools in Oldenburg and Cologne. From 1940 to 1946 he studied human medicine in Cologne, Freiburg, Breslau and Danzig. After obtaining his doctorate in Tübingen and various clinical activities, he decided to pursue a scientific career at the Institute of Anatomy in Mainz, where he habilitated in 1953. Here he was able to deepen his interest in the functional view of the structures of the human organism. In 1963 he was appointed to an associate professorship in Giessen, and in 1964 to a chair of anatomy at the University of Marburg.

In 1974 he moved to the Friedrich Alexander University of Erlangen-Nürnberg, where he held the chair of anatomy until his retirement in 1991. His work as a teacher was characterized by his functional perspective and was reflected in the textbooks "Functional Human Anatomy", "Functional Histology", "Functional Neuroanatomy" and "Functional Embryology". With the "Photo Atlas of Anatomy" he edited together with Chihiro Yokochi an anatomical standard work was created that was translated into over 20 languages. He continued to work scientifically until he was 90 years old and up to this time he was still asked by students to give the traditional introductory lecture for students of human medicine.

Scientifically, he concentrated mainly on the elaboration of the functional morphology of the visual organ and larynx. Research visits took him to the Department of Ophthalmology at Washington University in St. Louis, USA, to Ahwaz, Iran and to Kampala, Uganda.

He described the three-dimensional structure of the iris-ciliary muscle system and its influence on the resistance of aqueous humor outflow and found that the outflow resistance for aqueous humor is mainly localized under the inner wall of Schlemm's canal (in the subendothelial region of the trabecular meshwork). These findings were the basis for the development of the glaucoma surgeries trabeculectomy and trabeculotomy. Electron microscopic and histochemical workup of the surgical material from trabeculectomies sent to him internationally then enabled him to differentiate the various forms of glaucoma. He was one of the first to culture trabecular cells to further investigate the causes of glaucoma.

With the advent of scanning electron microscopy, he was able to extend Helmholtz's theory of accommodation by describing new zonular systems and made significant contributions to the non-lenticular region of presbyopia, which played an important role in the development of intraocular lenses. His work on the functional morphology of the ciliary epithelium and conjunctiva was also of clinical importance.

His research has been recognized by highly prestigious awards, including the Albrecht von Graefe Award of the German Ophthalmological Society, twice the highly endowed Alcon Research Award, USA and the prestigious Helen Keller Award, USA as well as the Anton Waldeyer prize of the Anatomische Gesellschaft (German Anatomical Society).

In addition, he obtained a honorary doctor of the University of Uppsala, Sweden, and he was member of the Leopoldina (German Academy of Sciences) in Halle (Saale) and the Academy of Sciences and Literature in Mainz (Germany).

We coworkers, students and friends remember our revered teacher with heartfelt gratitude.

Prof. Dr. med. Elke Lütjen-Drecoll
(Emerita of the Institute of Anatomy, Chair II),
FAU Erlangen-Nürnberg, Germany

Dimension variability of the M2 human molar teeth: comparisons between prehistoric and medieval samples

Ozana-Maria Petraru[1,2], Vasilica-Monica Groza[1], Luminita Bejenaru[1,2], Mariana Popovici[1]

[1] Romanian Academy – Iaşi Branch, "Olga Necrasov" Center of Anthropological Research, Iasi, Romania; Th. Codrescu Street, no. 2, 700479, Iasi, Romania

[2] "Alexandru Ioan Cuza" University of Iaşi, Faculty of Biology, Iasi, Romania; Carol I Boulevard, no. 20A, 700505, Iași, Romania

SUMMARY

Teeth are a valuable source of information for studies regarding past human populations in archaeological and forensic contexts. In dental anthropology, the linear measurements of tooth crowns are used for assessing morphological variability and sexual dimorphism in both modern and past human populations. The aim of this research is to evaluate the M2 molar crown variability in archaeological human populations from Prehistory (Chalcolithic and Bronze Age, ~ 5000-1150 BCE) and Middle Ages (13th-17th centuries) discovered in sites from North-Eastern Romania. The objectives of this study emphasize on the diachronic comparison of the M2 molar crown variables between prehistoric and medieval samples (1), and the assessment of sexual dimorphism expression (2). The two crown measurements, mesio-distal (MD) and bucco-lingual (BL) diameters, were performed using ImageJ software on occlusal digital images acquired stereo-microscopically. The crown index (CI), crown area (CA) and the sexual dimorphism index (SDI), along with the two linear measurements, were subjected to univariate and multivariate statistical analysis.

Our results show that the variation coefficient (CV) differs for the MD variable in the female upper M2 molars, being higher in the medieval sample than the prehistoric one; also, a higher variability is remarked for the mandibular molar in the medieval sample than in prehistoric one. In females, the MD and CA variables for mandibular M2 molars and the BL and CA for maxillary molars showed significant statistical differences between the medieval and prehistoric mandibular teeth, with higher values for the exemplar from Middle Ages. Similar result was obtained in males, for the CA variable in the upper M2 molars. In our study, the sexual dimorphism manifested at the M2 crown molar was highlighted in the prehistoric sample, though less in the medieval one.

Key words: M2 molar teeth – Crown measurements – Sexual dimorphism – Archaeological human populations – Nord-Eastern Romania

INTRODUCTION

Dental anthropology is an interdisciplinary research area that involves several directions of study such as physical anthropology, dentistry,

Corresponding author:
Luminita Bejenaru. Romanian Academy – Iaşi Branch, "Olga Necrasov" Center of Anthropological Research, Iasi, Romania; Th. Codrescu Street, no. 2, 700479, Iasi, Romania. E-mail: lumib@uaic.ro

Submitted: December 6, 2021. **Accepted:** March 14, 2022

https://doi.org/10.52083/SAYF5787

biology, paleontology, and paleopathology (Moreno-Gómez, 2013). The unique preservation of teeth is based on their hard tissues (i.e., enamel, dentine, and cementum), teeth being a valuable source of information for studies regarding the past human populations in archaeological and forensic contexts (Eboh, 2017; Jeon et al., 2020; Higgins and Austin, 2013; Hillson, 2005; Watson and Haas, 2017). In physical anthropology, teeth have been studied by various methodologies concerning age at death estimation (Bertrand et al., 2019; Brothwell, 1981), dental wear and dental calculus as bioindicators of diet (Green and Croft, 2018; Cummings et al., 2018; Fiorenza et al., 2018), cultural modifications (Wasterlain et al., 2016; Smith-Guzmán et al., 2020), dental diseases (Hillson, 2001; Wasterlain et al., 2020; Garot et al., 2019; Marchewka et al., 2014), inter- and intra-populational variations of shape and size (Gómez-Robles et al., 2015; Black, 2014; Takahashi et al., 2007; Kondo et al., 2005).

A number of studies showed that genetic, environmental, and epigenetic factors have a great influence on dental morphology (Kondo and Manabe, 2016; Townsend et al., 2012; Farzin et al., 2020).

Several studies of dental anthropology approached the linear measurements of tooth crowns for assessing the sexual dimorphism in both modern human populations (Zorba et al., 2011; Zúñiga et al., 2021) and past ones (Petraru et al., 2020; Yoo et al., 2016; Górka et al., 2015), as well the dental variability between ethnic groups (Brook et al., 2009; Hasegawa et al., 2007). Most studies of the tooth crown size variability are based on the measurement of the mesio-distal and bucco-lingual diameters (Petraru et al., 2020; Zorba et al., 2011; Kondo et al., 2005; Yoo et al., 2016), although other alternative measurements have been reported (Hillson et al., 2005; Zorba et al., 2013). Due to their sexual dimorphism and resistance to postmortem alteration process, teeth, by crown dimensions, are essential in assessing sex when other skeletal parameters are not reliable (Zorba et al., 2013; Petraru et al., 2020). Several studies showed that the canine (particularly the mandibular canine) is the most sexually dimorphic tooth (Scherer, 2018; Magalhães et al., 2021). The adjacent teeth around the canines (i.e., lateral incisors and first premolars), along with the molar teeth (especially the mandibular teeth) also show dimensional variations due to sexual dimorphism (Zorba et al., 2011; Kondo et al., 2005).

Although odontometric research is well-known in both archaeological human populations and forensic contexts, there are few studies regarding dental variability and sexual dimorphism on molar crown in samples from North-Eastern Romania (Petraru et al., 2020; Petraru et al., 2017). Considering the consequences of genetic influence, environmental factors, like variation of food resources exploitation, and the interference of cultural factors, we suppose that dental variability is increasing in time being correlated with a decreasing sexual dimorphism in teeth.

The aim of this study is to assess M2 molar crown variability in samples of archaeological human populations discovered in North-Eastern Romania. Knowing the importance of teeth as indicators of the intra- and inter-population variability, the objectives of this study emphasize the diachronic comparison of the M2 crown variables (mesio-distal and bucco-lingual diameters, crown area, and crown index) between medieval and prehistoric samples (1), and the expression of sexual dimorphism at the M2 molar crown (2).

MATERIALS AND METHODS

Material

The dental material is represented by the M2 molars (maxillary and mandibular molars) (Fig. 1) (n = 284) belonging to human skeletons discovered in archaeological sites from North-Eastern Romania (Fig. 2; Table 1). The M2 molar was chosen, while for the first molar - M1, was avoided due to its variable morphology and usually high degree of wear. Furthermore, only the molars without pathologies, an integrated tooth crown and an occlusal wear that does not exceed a 'moderately advanced wear' (Smith, 1984, Tomczyk et al., 2020) were considered. All molars, related to different age categories (Table 1), were considered for the size analysis, as, once

formed, teeth do not change their size (Górka et al., 2015). The material under study dates, according to the archaeological inventory, from Prehistory (Chalcolithic and Bronze Age ~ 5000-1150 BCE), and the Middle Ages (13th-17th centuries) (Table 2). Some published data regarding the dimensional variability of M2 molar dating from the Bronze Age (n = 54) (i.e., Trușești and Cândești samples published previously by Petraru et al. (2020)) were included in this research due to the comparative approach. The molars from the "Curtea Domnească" necropolis of the 17th century, which have been subjected to a previously odontometric study based on caliper measurements (Petraru et al., 2017), were reanalyzed with Image J (n = 133) and no statistically significant differences were obtained between the two dimensioning (BL: t = 0.321, p = 0.749; MD: z = 0.289 p = 0.772); thus, all dental material was studied by the same method in order to avoid error interpretation. The human skeletons discovered in the mentioned archaeological sites were previously studied in terms of age at death and sex estimations, demography, pathologies and odontometrics (Petraru et al., 2017; Petraru et al., 2020) (Table 2). The dental material used in this study is currently preserved in the osteological collection of the "Olga Necrasov" Center of Anthropological Research, Romanian Academy - Iași Branch.

Methods

The molars selected to be studied were prepared for measurements by removing the exogenous grit/ impurities using ethanol, hydrogen peroxide, and cotton wool (Petraru et al., 2020). The teeth were placed under the stereomicroscope being situated in the dental alveoli, or positioned in the specific anatomical orientation if the teeth

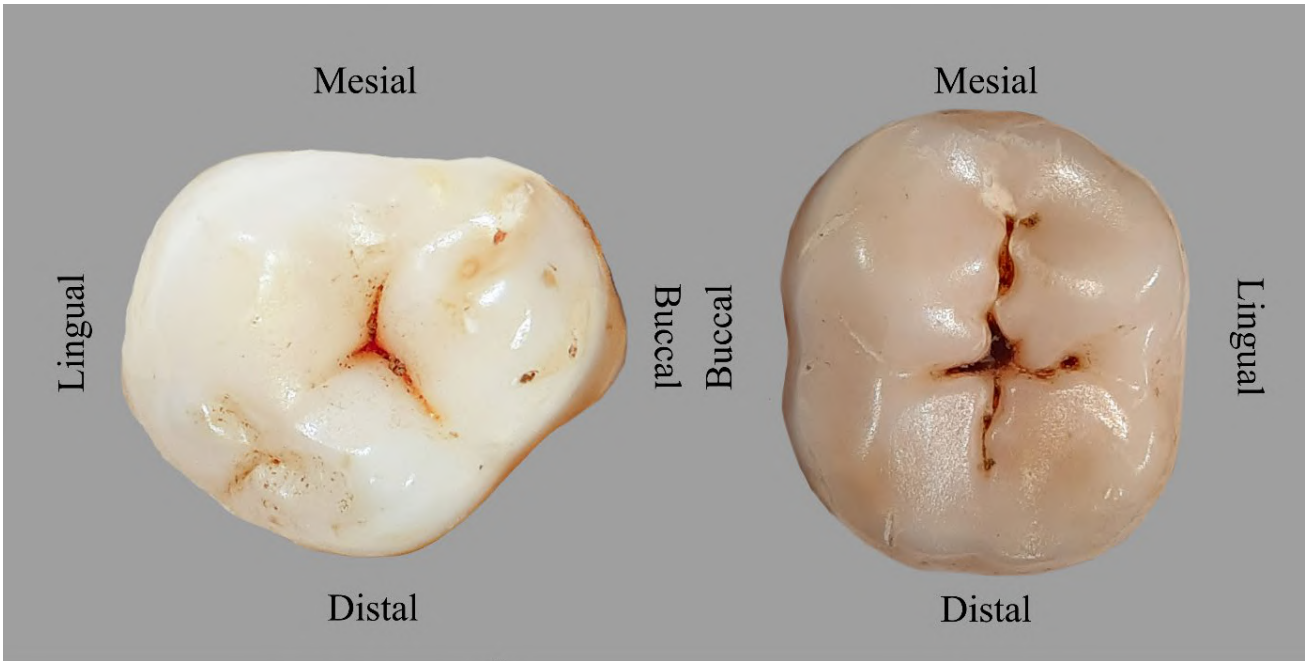

Fig. 1.- Occlusal surface of left maxillary M^2 molar (left) and left mandibular M_2 molar (right).

Table 1. M2 molar teeth selected for the study.

Distribution of M2 molars according to the position in the skull			
Upper right M2 molar (M^2_r)	Upper left M2 molar (M^2_l)	Lower right M2 molar (M_{2r})	Lower left M2 molar (M_{2l})
n = 71	n = 70	n = 79	n = 64
Distribution of M2 molars according to age at death category proposed by Buikstra and Ubelaker (1994)			
Adolescents (12-20 years)	Young adults (20-35 years)	Middle adults (35-50)	Old adults (> 50 years)
n = 28	n = 118	n = 115	n = 23

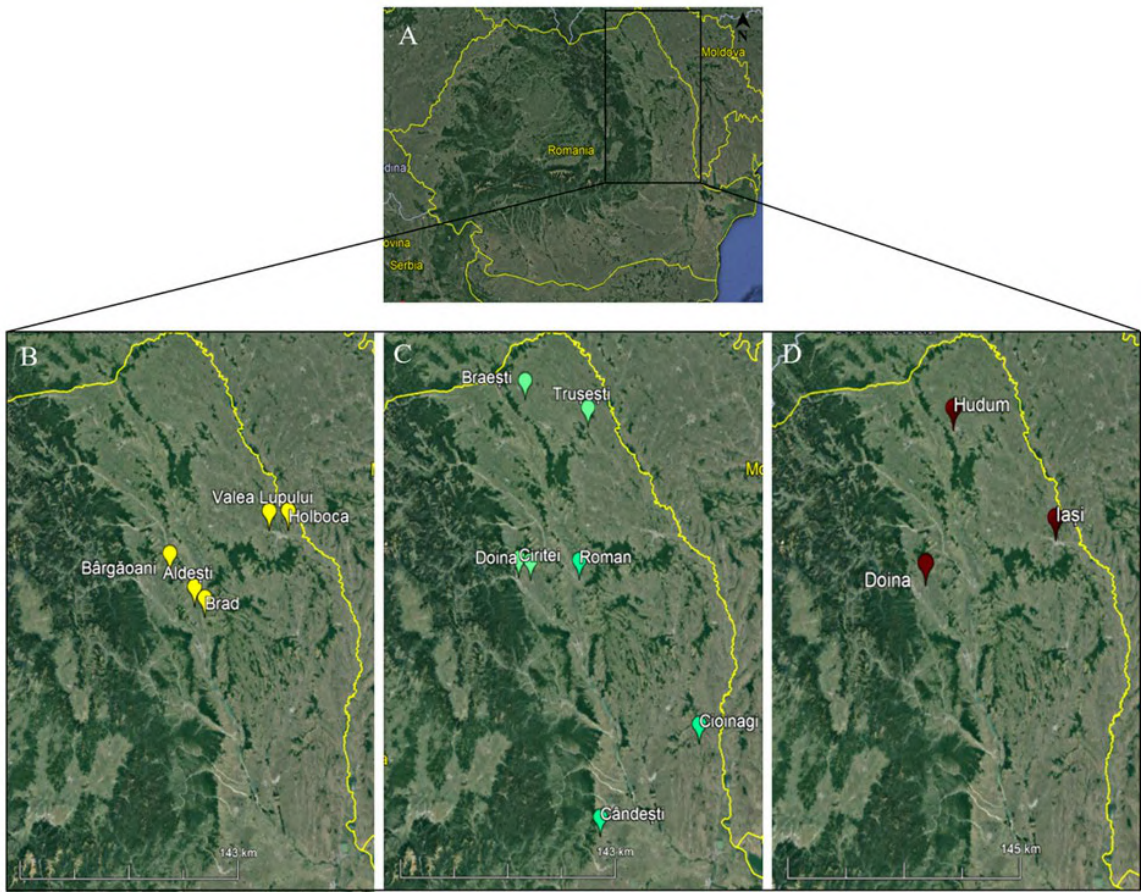

Fig. 2.- Location of archaeological sites: **A** – Nord-Eastern Romania area; **B** – archaeological sites from Chalcolithic (5000-3800/3700 BCE), **C** – archaeological sites from Bronze Age (3500-1200/1150 BCE); **D** – archaeological sites from Middle Ages (13th – 17th centuries).

Table 2. List of archaeological sites considered in the study.

Period		**Archaeological site / County**	**Dental samples**	**Skeleton sample Reference**	**Odontometric *ImageJ* data Reference**
Prehistory	Chalcolithic	Brad / Neamț	n = 3	Necrasov and Onofrei (1972)	Inedit
		Aldești / Neamț	n = 3		Inedit
		Valea Lupului / Iași	n = 3	Antoniu and Roșca-Gramatopol (1966)	Inedit
		Holboca / Iași	n = 19	Necrasov and Cristescu (1957)	Inedit
		Bârgăoani / Neamț	n = 3	Necrasov et al. (1972)	Inedit
	Bronze Age	Cioinagi / Galați	n = 7	Cristescu et al. (1965)	Inedit
		Cândești / Vrancea	n = 20	Miu (1999)	(Petraru et al., 2020)
		Roman / Neamț	n = 3	Diaconu et al. (2016)	Inedit
		Trușești / Botoșani	n =34	Cristescu and Miu (1999)	(Petraru et al., 2020)
		Ciritei / Neamț	n = 3	Cristescu (1961)	Inedit
		Brașești / Botoșani	n = 4	Miu (1992)	Inedit
		Doina / Neamț	n = 2	Archive data*	Inedit
Middle Ages	13th-14th centuries	Hudum / Botoșani	n = 34	Miu et al. (2003); Archive data*	Inedit
		Doina / Neamț	n = 13	Necrasov and Botezatu (1964); Archive data*	Inedit
	17th century	"Curtea Domnească"/ Iași	n = 133	Groza (2015)	Inedit

* Data from the Archive of "O. Necrasov" Centre of Anthropological Research

were detached from the skull (Petraru and Bejenaru, 2019). The teeth were placed under stereomicroscope so that the cement-enamel junction plane was perpendicularly situated to the optical axis of the camera lens (Galbany et al., 2016; Górka, 2016; De Castro and Nicolas, 1995; Al-Khatib et al., 2011; de Castro et al., 2001; Martín-Albaladejo et al., 2017).

Dental micrometry

Digital images of occlusal surfaces of the M2 molars were recorded using a Carl Zeiss Stemi 2000-C stereomicroscope with a Canon Power Shot G9 attached. The images were processed and calibrated (in mm) using ImageJ software (Abràmoff et al., 2004). Two maximum crown diameters were taken by ImageJ software: bucco-lingual (BL) diameter and mesio-distal (MD) diameter. The MD diameter was taken as the maximum width of the tooth crown in the mesio-distal plane (Kazzazi and Kranioti, 2018), while BL diameter was taken as the widest point of the tooth crown in the bucco-lingual plane, perpendicular to the MD (Nava et al., 2021; Takahashi et al., 2007; Pilloud and Scott, 2020). In the dental samples in which inter-proximal facets were observed, the MD length was estimated according to the method proposed by Wood and Abbott (1983). The crown index (CI = BL diameter x 100/MD diameter), and the crown area (CA = BL diameter x MD diameter) were used to characterize the overall crown size, but no the shape (Kondo et al., 2005; Kondo and Manabe, 2016). The sexual dimorphism index (SDI = M-F/ F x 100; M - male mean value; F - females mean value) was also used (Harris and Foster, 2014; Zorba et al., 2011).

Statistical analysis

Intra-observer error of dental measurements was achieved by blind tests in which 20 molars were randomly examined. The BL, and MD variables were measured twice with one month between measurements, by the same researcher. The Shapiro-Wilk test was computed for the data distribution in order to perform the asymmetry analysis, bivariate analysis of the M2 molar variables (BL, MD, CA, CI). Student's T-test and Mann-Whitney tests were used to compare the BL and MD values as independent groups of the left and right mandibular/maxillary molars.

Descriptive statistics and relationships between measurements were investigated through univariate and multivariate statistical analysis using XLSTAT and PAST softwares (Hammer et al., 2001). Pearson's and Spearman's tests were used to analyze the correlations between the BL and MD measurements (Ratner, 2009; Razali and Wah, 2011).

To evaluate the accuracy of the BL, MD, CA and IC variables in assessing sexual dimorphism, the Discriminant Analysis (DA) was used. The analysis was achieved for every category of data: upper and lower M2 molars in every period (Prehistory and Middle Ages). Hoteling's test indicates how convenient is a given molar variable in the discriminant analysis; the F Statistic determines how much variation exists between the sexes and the significance level of the variance.

RESULTS

The result of the *t* test was not statistically significant (BL: N = 20; t = 0.27; p > 0.78; MD: N = 20, t = 0.37, p = 0.71).

The diameters' asymmetry between the left and right mandibular/maxillary molars was analysed and no statistically significant result was revealed (Table 3); therefore the left and right mandibular/maxillary molars were analyzed simultaneously.

Table 3. Test results for asymmetry between the left and right mandibular/maxillary BL and MD.

Test type	$M_{2\ right}$ *vs.* $M_{2\ left}$		$M^{2\ right}$ *vs.* $M^{2\ left}$	
	BL diameter	**MD diameter**	**BL diameter**	**MD diameter**
Shapiro-Wilk	W = 0.98, p = 0.66 W = 0.96, p = 0.1	W = 0.95, p = 0.005 W = 0.95, p = 0.019	W = 0.97, p = 0.28 W = 27, p = 0.26	W = 0.98, p = 0.50 W = 0.98, p = 0.60
T test/ Mann-Whitney	t = 1.02, **p = 0.307**	Z = 0.62**, p = 0.53**	t = 1.47, **p = 0.16**	t = 0.19, **p = 0.84**

The summary statistics of the bidimensional diameters are comparative shown by sex, position of the molars (mandibular and maxillary), and period, in Table 4. The bidimensional diameters for the mandibular M_2 molars are characterized by a higher mean in males comparative to females, probably due to sexual dimorphisms (BL = 9.42 mm in females and 9.72 mm in males; MD = 10.10 mm in females and 10.43 mm in males). The differences between the BL and MD variables in males *vs.* females are statistically significant (BL: z = 3.05, p = 0.002; MD: z = 2.60, p = 0.009). A difference was also observed for the superior molars M^2 but not supported by statistical significance (BL t test: t = 0.518, p = 0.605; MD t test: t = 0.906, p = 0.3665). When the dimensions were divided by period (*i.e.,* Prehistory, Middle Ages), the BL and MD values were similar for the inferior M_2 molars. In this study, the variability degree of the M2 dimensions is indicated by the coefficient of variation (CV%). Thus, constant CV% values were observed for the mandibular molars dating from Prehistory (CV% = 6.71 for BL diameter, and 6.87 for MD diameter), while a greater variability was observed for the medieval teeth from both 13th-14th centuries (CV% = 7.99 for BL diameter, and 8.22 for MD diameter) and 17th century (CV% = 5.93 for BL diameter, and 6.83 for MD diameter). In contrast with the dimension variability of the mandibular molars, for the superior M^2 molars a higher variability coefficient is observed for both diameters in the 13th-14th centuries (CV% = 10.73 for BL diameter, and 10.79 for MD diameter). Similar high CV% was noted for the MD diameter of the M^2 from prehistoric sample (CV% = 10.53), while BL diameter was characterized by lower variability (CV% = 7.23).

To compare the molar dimensions in terms of diachronic and sex criteria, the medieval teeth of 13th-14th centuries and those of the 17th century were considered together. In order to merge the samples, parametric and non-parametric tests, depending on the data distribution, were performed to test whether there are differences between the odontometric data of the 13th -14th centuries and those of the 17th century. The results showed no statistical differences between the variables of the mandibular M2 molars (BL: t = 0.73, p =0.46; MD: z = 0.03, p = 0.96) and the maxillary ones (BL: t = 0.08, p = 0.93; MD: t = 1.44, p = 0.15). The upper M^2 molars from the female dataset are characterized by a similar variability of the mesio-distal diameter for both prehistoric and medieval samples (CV%= 8.76, and 8.20 respectively), in contrast with the variability of the bucco-lingual diameter which varies less in the prehistoric molars (CV% = 4.43) than in medieval ones (CV% = 7.05). In contrast with the dimensions of the superior molar in females, the dimensions of the mandibular molar are characterized by lower variability in the sample from Prehistory (CV% = 3.45 in BL diameter, and 4.75 in MD diameter), while in the medieval sample the variability is higher (CV% = 7.22 in BL diameter, and 6.41 in MD diameter). In the male samples, comparable CV% values were observed for the inferior molars, and for the BL diameter in the maxillary M^2 molars (CV% = 8.14 in prehistoric molars, and 7.69 in medieval ones), while different CV% values were obtained for the MD diameter in the prehistoric molars (CV% = 11.24), and medieval ones (CV% = 8.82).

The bidimensional measurements analyzed on the criterium of tooth position in the skull (mandibular and maxillary) have shown a non-normal distribution in the mandibular M_2 molars for the MD diameter (W = 0.95, p = 0.0002), and a normal distribution for the BL diameter (W = 0.98, p = 0.08). In the maxillary M^2 molars, the diameter values showed a normal distribution (BL diameter: W = 0.98, p = 0.08; MD diameter: W = 0.99, p = 0.48). When sex criteria were applied, the data for the mandibular male molars showed a non-normal distribution for the MD diameter (W = 0.96, p = 0.01), and a normal distribution data for the BL diameter (W = 0.98, p = 0.45). In the male maxillary molars, both diameter values showed a normal distribution (BL diameter: W = 0.98, p = 0.40; MD diameter: W = 0.97, p = 0.11). Similar distribution of data diameters was observed in the female molars: non-normal distribution data in the mandibular molars (BL diameter: W = 0.86, p = 0.0003; MD diameter: W = 0.91, p = 0.009), and normal data distribution in the maxillary ones (BL and MD diameters: W = 0.95, p = 0.15).

Table 4. Summary statistics of bucco-lingual (BL) and mesio-distal (ML) diameters in the M2 molars by position in skull, sex, and periods (N – number, Min – minimum, Max – maximum, Std. error – standard error, Var. – variance, Std. dev. – standard deviation, Coeff. Var. – coefficient of variance).

Tooth	N	Sex	Variable	Min	Max	Mean	Std. error	Var.	Std. dev.	Median	Coeff. Var.
M_2	143	-	BL	8.41	11.37	9.65	0.05	0.41	0.64	9.64	6.64
		-	MD	9.02	12.61	10.37	0.06	0.55	0.74	10.27	7.14
M^2	141	-	BL	7.82	12.82	10.9	0.07	0.70	0.83	10.84	7.67
		-	MD	6.53	11.61	9.00	0.07	0.71	0.84	9.05	9.36
Dimension variability of M2 molars by sex											
M_2	101	Male	BL	8.41	11.37	9.72	0.06	0.41	0.64	9.7	6.59
			MD	9.02	12.61	10.43	0.07	0.54	0.73	10.33	7.08
M_2	38	Female	BL	8.71	11.03	9.42	0.09	0.33	0.58	9.31	6.17
			MD	9.14	12.24	10.10	0.09	0.37	0.61	9.99	6.05
M^2	102	Male	BL	7.82	12.82	10.92	0.08	0.74	0.86	10.88	7.92
			MD	6.53	11.61	9.03	0.08	0.77	0.88	9.07	9.74
M^2	34	Female	BL	9.62	12.8	10.83	0.13	0.64	0.80	10.66	7.42
			MD	7.7	10.45	8.88	0.13	0.57	0.76	9.05	8.55
Dimension variability of M2 molars by period											
Prehistory (~ 5000-1150 BCE)											
M_2	53	-	BL	8.42	11.3	9.59	0.08	0.41	0.64	9.51	6.71
			MD	9.14	12.46	10.24	0.09	0.49	0.70	10.08	6.87
M^2	51	-	BL	8.9	12.68	10.6	0.10	0.58	0.76	10.61	7.23
			MD	6.53	11.62	8.79	0.12	0.82	0.91	8.86	10.53
Middle Ages (13th-14th centuries)											
M_2	27	-	BL	8.56	11.38	9.77	0.15	0.61	0.78	9.88	7.99
			MD	9.03	11.94	10.45	0.16	0.73	0.85	10.33	8.22
M^2	20	-	BL	7.83	12.82	11.05	0.26	1.40	1.18	11.34	10.73
			MD	7.08	10.37	8.90	0.21	0.92	0.96	9.01	10.79
Middle Ages (17th century)											
M_2	63	-	BL	8.46	11.03	9.66	0.07	0.32	0.57	9.6	5.93
			MD	9.22	12.61	10.44	0.08	0.50	0.71	10.42	6.83
M^2	70	-	BL	9.56	12.8	11.07	0.08	0.50	0.71	10.97	6.43
			MD	7.02	10.74	9.18	0.08	0.51	0.72	9.22	7.83
*Dimension variability of M2 molars by period and sex**											
Prehistory (~ 5000-1150 BCE)											
M_2	34	Male	BL	8.42	11.3	9.76	0.11	0.48	0.69	9.72	7.15
			MD	9.36	12.46	10.37	0.12	0.50	0.70	10.21	6.84
M^2	33	Male	BL	8.9	12.68	10.70	0.15	0.76	0.87	10.64	8.14
			MD	6.53	11.62	8.80	0.17	0.97	0.98	8.89	11.24
M_2	17	Female	BL	8.72	9.98	9.22	0.07	0.10	0.31	9.19	3.45
			MD	9.14	10.79	9.87	0.11	0.22	0.46	9.8	4.75
M^2	15	Female	BL	9.63	11.1	10.32	0.11	0.20	0.45	10.37	4.43
			MD	7.72	10.46	8.68	0.19	0.58	0.76	8.59	8.76
Middle Ages (13th – 17th centuries)											
M_2	67	Male	BL	8.46	11.38	9.70	0.07	0.37	0.61	9.69	6.33
			MD	9.03	12.61	10.46	0.09	0.57	0.75	10.43	7.22
M^2	69	Male	BL	7.83	12.82	11.02	0.10	0.72	0.84	10.96	7.69
			MD	7.02	10.74	9.15	0.09	0.65	0.80	9.19	8.82
M_2	21	Female	BL	8.76	11.03	9.59	0.15	0.48	0.69	9.42	7.22
			MD	9.36	12.24	10.28	0.14	0.43	0.65	10.27	6.41
M^2	19	Female	BL	9.86	12.8	11.24	0.18	0.62	0.79	11.22	7.05
			MD	7.7	10.27	9.04	0.17	0.55	0.74	9.22	8.20

* 9 molars were removed from the descriptive statistics due to the indeterminate sex of the individuals

Our results show a strong and positive correlation between the BL and MD diameters for the mandibular M_2 molars (Spearman coefficient = 0.75, $p < 0.001$), and moderate one in the maxillary M^2 molars (Pearson coefficient = 0.32, $p < 0.001$) (Fig. 3A, B). When a sex criterium was applied, the dental measurements in the mandibular M_2 molars (i.e., BL, and MD) were strong correlated in males (Spearman coefficient = 0.76, $p < 0.001$), and moderate positive correlated in females (Spearman coefficient = 0.64, $p < 0.001$) (Fig. 3C, E). In contrast with these results, for the maxillary M^2 molars, dental measurements showed a moderate positive correlation in males (Pearson coefficient = 0.39, $p < 0.001$), and no correlation in females (Pearson coefficient = 0.083, $p < 0.64$) (Fig. 3D, F). The MD and BL diameters were less correlated in the maxillary M^2 molar than in the mandibular M_2 (10%, and 57% respectively). This aspect is highlighted especially in the female molars (47% in the mandibular M_2, and 0.69% in the maxillary M^2) in contrast with the male molars (56% in mandibular M_2 and 15% in the maxillary M^2).

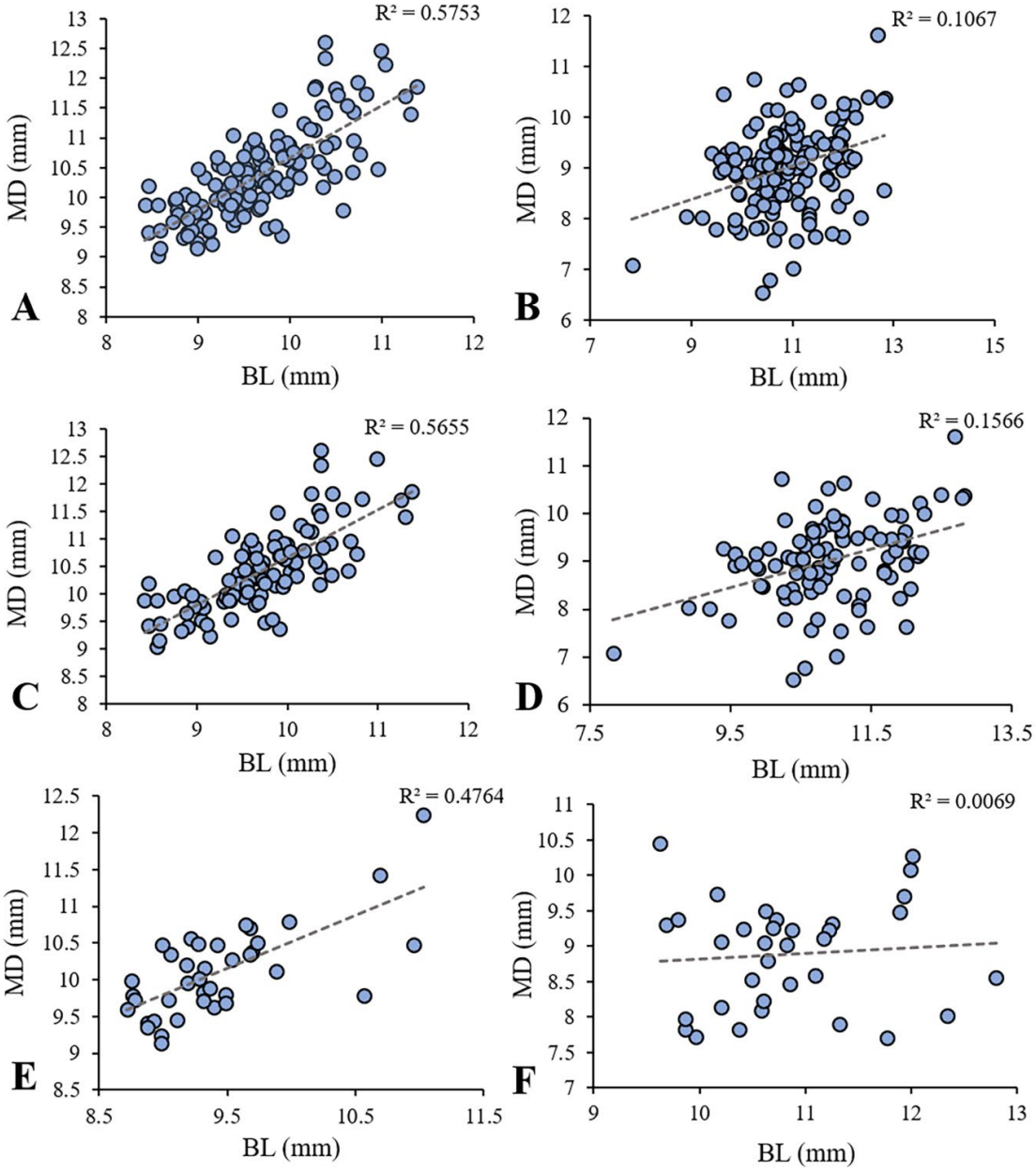

Fig. 3.- Dimension variability of the M2 human molars belonging to the archaeological populations from North-Eastern Romania: **A** – dimensions of the M_2 molars; **B** – dimensions of the M^2 molars; **C** – dimensions of the M_2 molars in males; **D** – dimensions of the M^2 molars in males; **E** – dimensions of the M_2 molars in females; **F** – dimensions of the M^2 molars in females.

The crown index (CI) can be used to obtain data regarding the crown proportions, especially in a comparative approach (Kondo et al., 2005). The CI frequency values are shown by sex and tooth position in the skull in Fig. 4. The distribution of the CI values was assessed using the Shapiro-Wilk test. The results showed that the CI values have non-normal distribution in the maxillary M^2 molars in males (W = 0.94, p = 0.002); therefore, the Mann-Whitney pairwise test was used. According to the Mann-Whitney test, a significant statistical difference was revealed between the mandibular M_2 molars in female vs. male (p < 0.001), probably due to the sexual dimorphism that influenced the crown proportion.

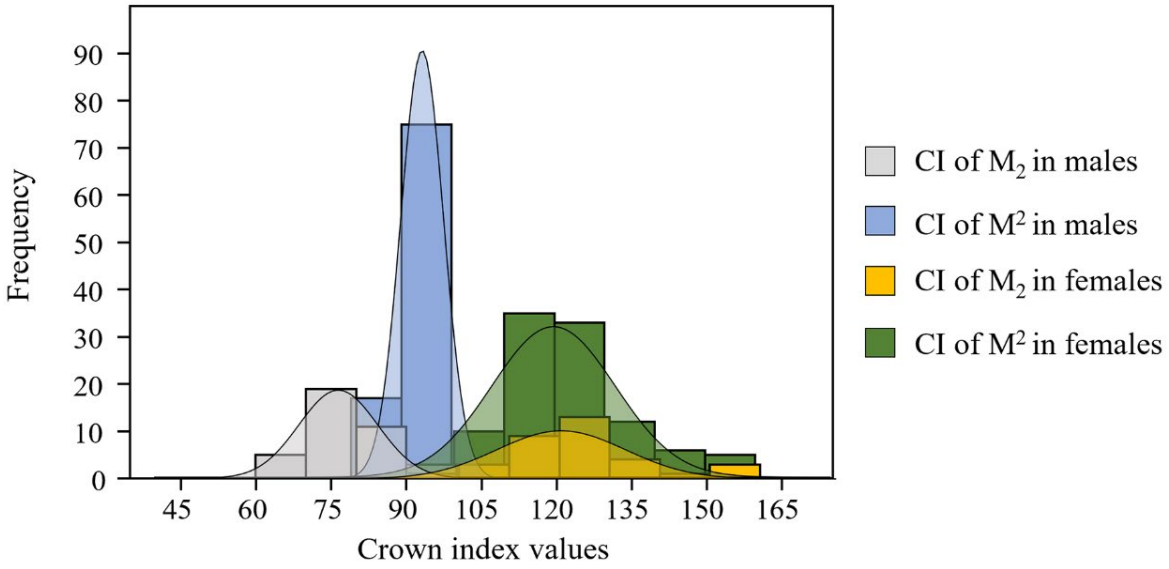

Fig. 4.- Crown index of the M2 molars by sex.

To analyze the dynamic of the tooth crown proportion in the upper and lower M2 molars, the medio-distal (MD) and bucco-lingual (BL) measurements, along with the crown area (CA), and crown index (CI) were diachronically compared. The results of data normality test are shown in Table 5.

Three variables register statistically significant differences between the prehistoric and the medieval periods in the female teeth (Fig. 5A). For the lower M2 molar, the mesio-distal (MD) diameter recorded a mean value greater in the medieval sample (MD = 10.28 mm) comparative with that of prehistoric one (MD = 9.87 mm) (U test = 109; p = 0.042). Also, the crown area (CA) of the mandibular molar M_2 recorded higher values in the medieval sample (98.97 mm^2) compared to the prehistoric one (91.08 mm^2) (U test = 102; p = 0.02).

In the upper M^2 molars, the bucco-lingual diameter (BL) and the crown area (CA) registered significant higher values for the medieval sample (U test = 46; p = 0.00 and U test = 51; p = 0.001), namely 11.24 mm in BL and 101.66 mm^2 in CA, comparative with 10.32 mm and 89.56 mm^2 for prehistoric sample.

In the male dataset, the Mann-Whitney test results highlight significant differences between the mean values only for the crown area (CA) of upper M^2 molars (U test =743; p = 0.008) (Fig. 5B). The CA registered higher values for this molar in the medieval sample (101 mm^2) than in the prehistoric one (96.22 mm^2).

Sexual dimorphism

In our study, the sexual dimorphism was calculated for each period separately: Prehistory and Middle Ages. In the prehistoric mandibular M_2, of the four variables investigated (MD, BL, CI, CA), the sexual dimorphism was manifested in three of them: BL (U test = 112; p = 0.001), MD (U test = 138; p = 0.01), and CA (U test = 114; p = 0.001).

Table 5. Normality test result for BL, MD, CA, CI variables.

Prehistory									
Lower M_2 molar – male					**Lower M_2 molar – female**				
Normality test	**Variables**				**Normality test**	**Variables**			
	BL	**MD**	**CI**	**CA**		**BL**	**MD**	**CI**	**CA**
W	0.979	0.868	0.984	0.916	W	0.958	0.963	0.946	0.925
p - value	0.790	0.001	0.921	0.021	p - value	0.592	0.694	0.394	0.176
Upper M^2 molar – male					**Upper M^2 molar – female**				
Normality test	**Variables**				**Normality test**	**Variables**			
	BL	**MD**	**CI**	**CA**		**BL**	**MD**	**CI**	**CA**
W	0.986	0.942	0.976	0.874	W	0.946	0.935	0.877	0.950
p - value	0.950	0.088	0.673	0.001	p - value	0.459	0.319	0.043	0.525
Middle Ages									
Lower M_2 molar – male					**Lower M_2 molar – female**				
Normality test	**Variables**				**Normality test**	**Variables**			
	BL	**MD**	**CI**	**CA**		**BL**	**MD**	**CI**	**CA**
W	0.985	0.978	0.980	0.975	W	0.893	0.900	0.848	0.886
p - value	0.622	0.303	0.389	0.200	p - value	0.029	0.035	0.004	0.019
Upper M^2 molar – male					**Upper M^2 molar – female**				
Normality test	**Variables**				**Normality test**	**Variables**			
	BL	**MD**	**CI**	**CA**		**BL**	**MD**	**CI**	**CA**
W	0.958	0.973	0.941	0.978	W	0.976	0.938	0.836	0.966
p - value	0.020	0.141	0.003	0.274	p - value	0.883	0.246	0.004	0.692

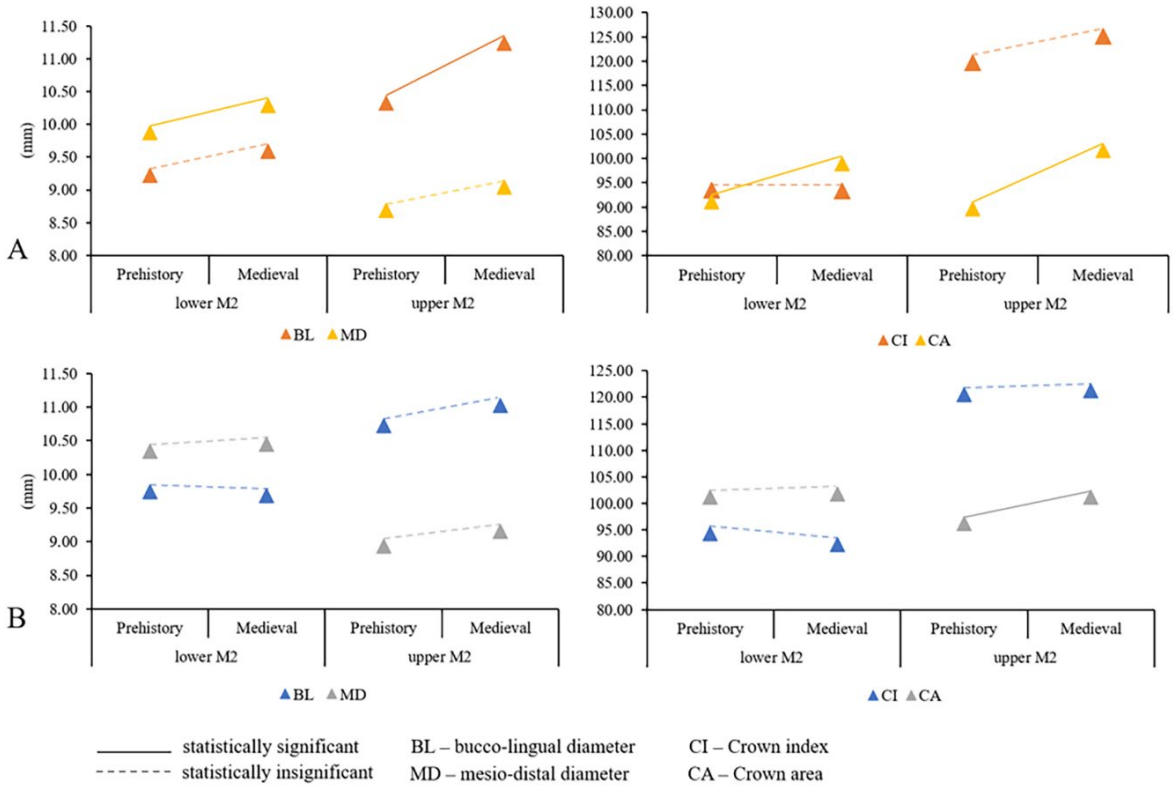

Fig. 5.- Comparative representation of the M2 molar variables (BL, MD, CA, CI) between medieval and prehistoric samples: **A**. Females, **B**. Males.

Table 6. Discriminant analysis statistics.

Stepwise discriminant analysis of dental variables					
Period	**Molar**	**Hotelling's value**	**F test**		**P value**
Prehistory	Lower M_2 molar	12.17	2.84		0.03*
	Upper M^2 molar	3.4	0.8		0.52
Middle Ages	Lower M_2 molar	1.04	0.25		0.9
	Upper M^2 molar	2.4	0.58		0.67
The correlations between the factors (F1) and original variables					
Variables	**Lower M_2 molar Prehistory**	**Upper M^2 molar/ Prehistory**	**Lower M_2 molar Middle Ages**		**Upper M^2 molar Middle Ages**
BL	0.926	-0.701	0.62		0.646
MD	0.771	-0.583	0.893		-0.347
CI	0.213	0.021	-0.421		0.783
CA	0.896	-0.796	0.821		0.105
Canonical discriminant function coefficients and Functions at Group Centroid					
Molar	**Variable**	**F1**	**Function of Group centroid**		
Lower M_2 molar Prehistory	Constant	-39.596	Female: -0.675 Male: 0.383		
	BL	14.077			
	MD	2.583			
	CI	-0.549			
	CA	-0.714			
Upper M^2 molar/ Prehistory	Constant	-74.156	Female: 0.395 Male: -0.185		
	BL	-6.111			
	MD	9.012			
	CI	0.602			
	CA	-0.142			
Lower M_2 molar Middle Ages	Constant	-102.491	Female: -0.194 Male: 0.063		
	BL	-13.542			
	MD	9.865			
	CI	1.198			
	CA	0.191			
Upper M^2 molar Middle Ages	Constant	-38.829	Female: 0.315 Male: -0.087		
	BL	10.339			
	MD	3.255			
	CI	-0.275			
	CA	-0.709			
Confusion matrix for the cross-validation results:					
M2	**from \ to**	**F**	**M**	**Total**	**% Correct**
Lower M_2 molar Prehistory	F	14	3	17	82.35%
	M	16	14	30	46.67%
	Total	30	17	47	59.57%
Upper M^2 molar/ Prehistory	F	9	6	15	60.00%
	M	12	20	32	62.50%
	Total	21	26	47	61.70%
Lower M_2 molar Middle Ages	F	1	20	21	4.76%
	M	7	58	65	89.23%
	Total	8	78	86	68.60%
Upper M^2 molar Middle Ages	F	0	19	19	0.00%
	M	5	64	69	92.75%
	Total	5	83	88	72.73%
Discriminant function for M2 mandibular molar – Prehistory: F1= (-39.596) + 14.077*BL + 2.583*MD + (-0.549*CI) + (-0.714*CA).					

*Statistically significant p-value

The SDI values are close for the two variables: 6.09% for BL, and 5.06% for MD. So, for that we consider that indeed both variables play a more important role in the sexual differentiation. This idea is strengthened by the area of the dental crown (CA), calculated precisely on these two variables (BL x MD). The SDI value of CA shows a much more dimorphic role than for the two variables analyzed separately (SDI = 11.74%).

The role of variables in the sexual discrimination was also tested with Discriminant Analysis. Discriminant Analysis was achieved for every category of data: upper and lower M2 molars, and every period (Prehistory and Middle Ages). The analysis only reinforces the findings of the previous test.

The Table 6 shows the results of Discriminant Analysis. It includes the Hotelling's test, which highlights the role of the dental variables in the stepwise analysis, while F test determines how much variation exists between sexes and the significance level of variance. The DA results show that BL variable is the one that makes the biggest contribution to the functions obtained, and a stronger correlation between the variables is noticed in the test of the mandibular molar from the Prehistoric period. Also, in Table 6 the canonical discriminant coefficient and function at group centroid are presented. A group centroid is the mean discriminant score for each of the sexes. The formula to identify the sex by M2 is derived from the discrimination function coefficients (unstandardized coefficients), clearly categorizing the subjects as male or female. After calculating F value from the formula, it will be compared with the section point which is calculated as 0.

In the present study, classification accuracy in the stepwise discriminant analysis ranged between 59.57-72.73% (Table 6). Maximum accuracy of sex diagnosis was observed in the maxillary second molar (72.73% in Middle Ages, and 61.70% in Prehistory), followed by the mandibular second molar (59.57% in Prehistory, and 68.60% in Middle Ages). If we referred at the function statistically significant (p value<0.05), namely the one of the prehistoric samples, we can notice a higher accuracy for females (82.35%) than for males (46.67%).

DISCUSSION

This study explores the dental variability of permanent molar crowns in past human populations from Prehistory (~ 5000-1150 BCE) and the Middle Ages (13th-17th centuries), Northeastern Romania. In this research, the M2 molar teeth have been subjected to linear measurements of tooth crown (i.e., medio-distal diameter MD, and bucco-lingual diameter BL), along with two indexes (i.e., crown area CA, and crown index CI). Several studies on tooth characterization used these variables in both past human populations (Brook et al., 2009; Nava et al., 2021; Lukacs, 2019; Viciano et al., 2012) and actual ones (Zúñiga et al., 2021; Abaid et al., 2021). The results of the present study show that mandibular M2 molars in females are characterized by a mean BL value of 9.42 mm, and a mean MD value of 10.10 mm (Table 4). A higher mean value of the BL variable was obtained by Pajević and Glišić (2017) in samples from Mesolithic-Neolithic to Middle Ages from Serbia. In our study, comparable mean values to those attained by Pajević and Glišić (2017) were also obtained for the male mandibular molars. The same study conducted by Pajević and Glišić (2017) showed higher values in the male maxillary M2 molars in comparison with the data obtained for the samples belonging to archaeological sites from North East Romania.

When the period criterium was considered, differences regarding the tooth diameters were observed between the molars from Prehistory and Middle Age.

Several comparative studies on tooth dimension reveal that tooth size decreases from the prehistoric populations to the medieval ones (Christensen, 1998; Brace et al., 1987; Pinhasi et al., 2008). Pajević and Glišić (2017) reported that the BL diameter of the maxillary M2 molar decreases from the Mesolithic-Neolithic samples to the medieval ones. In contrast, our results show that the BL diameter of the maxillary molar increases from Prehistory to the Middle Ages, while the MD diameter values for mandibular molars are higher in the medieval period in comparison with Prehistory. Same increasing tendency of dental diameters was noted for the male molars, but not statistically supported. A study of Mockers et al.

(2004) shows that the MD diameter of mandibular teeth belonging to the prehistoric population from Roaix, Southern France, is smaller when compared to its size in modern Caucasian populations. Moreover, the mean value for the MD diameter of prehistoric mandibular M2 molars from Nord Eastern Romania (10.24 mm) is higher than the value obtained by Mockers et al. (2004) for the prehistoric molars from a population in Roix, France (9.75 mm). Regarding the BL and MD diameters of the medieval mandibular molars, comparable mean values were obtain by Vodanović et al. (2007) in a study approaching dental metrics in medieval samples from Eastern Croatia; the female maxillary molars from North East Romania showed slightly lower values than ones from Croatia. The crown area (CA), also known as the robustness index, is often used to characterize the overall crown size (Hillson et al., 2005; Petraru et al., 2020; Nowaczewska et al., 2013; Schmidt et al., 2011). The M2 molars from Norh East Romania show an increasing CA from the prehistoric period to the medieval one in both mandibular and maxillary molars in females. The same tendency is maintained for the upper M^2 molar in males. Similar CA values of medieval maxillary M2 molars in females from Croatia were obtained by Vodanović et al. (2007), while higher values were found in both mandibular and maxillary male molars in comparison with the data obtained for the dental samples from Romania.

Sexual dimorphism refers to systematic morphological differences between males and females of the same species (Abaid et al., 2021; Magalhães et al., 2021). Sexual dimorphism can be reflected in the human dentition especially in permanent teeth (Shankar et al., 2013; Zúñiga et al., 2021). The molars are considered among the most dimorphic teeth (El Sheikhi and Bugaighis, 2016) and even if the overall trend is known in any population, the degree of sexual dimorphism of each variable involved remains a population-specific characteristic (Garn et al., 1964; Acharya and Mainali, 2007; Zorba et al., 2011; Shankar et al., 2013). Previous studies have found that there is a statistically significant difference in tooth size between males and females, and this is due to the differences in the body size of the two sexes that occur in any human population (Schwartz and Dean, 2005; Ateş et al., 2006; Saunders et al., 2007).

While the prehistoric dental sample has been found highly dimorphic by sex, not a similar result was found in the medieval material, according to the Mann-Whitney test. As in another study conducted by İşcan and Kedici (2003), the lower M_2 is more dimorphic than the upper M^2.

The tooth dimensions typically are larger in males than in females, but the difference is not constant across populations (Barrett et al., 1964; Barrett et al., 1963; Harris and Foster, 2014). There are studies conducted on more recent material suggesting that mandibular BL is more dimorphic than mandibular MD (Yamada and Sakai, 1992; Garn et al., 1966; Zorba et al., 2011; Prabhu and Acharya, 2009), in contrast to others which mention that MD dimension is better suited than BL for sex discrimination; however, they found that better results are obtained when both MD and BL dimensions are used together (Acharya and Mainali, 2007; Barrett et al., 1964; Barrett et al., 1963). Our view is closer to the latter one if we consider the obtained results.

The stepwise discriminant analysis was done to find a reliable result on sex discrimination.

Lakhanpal et al. (2013) considered that, although BL dimension is more easily measured, its ability to correct classifications of individuals is moderate when used independently. Furthermore, if one has the opinion of choosing between the two types of linear measurements, MD should be preferred, even if it is more difficult to measure. We consider that better accuracy can be obtained when several variables are correlated. In our material, CI has a small contribution to sex discrimination, compared to the other three variables (BL, MD and CA). CI is the relationship between BL and MD and while the linear dimensions in males are usually larger than in females, this may not be true when they are taken as a relative measure (Kondo and Townsend, 2004). There are opinions according to which the crown index does not quantify the tooth size, as the crown area and linear measurements do. Harris and Rathburn (1991), and Garn et al. (1967) consider the crown

index to be a description of the tooth shape rather than tooth size, being a more relevant indicator of population variations and not of sex differences.

A comparison between the maxillary and mandibular molars showed that the upper ones were more dimorphic than the mandibular molars, but statistically insignificant (p value > 0.05). Between the two sexes, the classification accuracy was higher in females than in males for cross-validated data. This could mean that males have the greatest variability of dental size and they can more often be misclassified than females. This result is in concordance with those of İşcan and Kedici (2003), Ateş et al. (2006), Peckmann et al. (2015) on crown mesiodistal and buccolingual measurements, which reported higher classification accuracy in females. A study conducted by Zorba et al. (2013) also provided similar results but for the diagonal measurements of molar teeth in a modern Greek population.

CONCLUSIONS

This paper approached dental measurements in archaeological human populations in order to assess M2 molar crown variability. The results of our study show a greater variability in the medieval female M2 teeth compared to prehistoric sample, in both maxillary (MD variable) and mandibular molars (MD and BL variables). Also, the two diameters were less corelated in the maxillary M^2 molar than in the mandibular M_2 molar, especially in females. In males, a higher variability of the mesio-distal (MD) variable was observed in the prehistory maxillary molars compared with the medieval ones. In the mandibular female teeth, significative statistical differences were obtained between the prehistoric and medieval samples (MD variable and CA variable). Also, in the maxillary molars the bucco-lingual (BL) and crown area (CA) variables showed higher values in the medieval samples.

In the male maxillary molars, the crown area (CA) variable showed significative higher values in the medieval sample than in the prehistoric one.

The discriminant analysis confirmed the sexual dimorphism on the mandibular M_2 crown in the prehistoric sample.

Further multidisciplinary studies are required to provide information concerning the influence of genetic, epigenetic and environmental factors on the dental variations.

REFERENCES

ABAID S, ZAFAR S, KRUGER E, TENNANT M (2021) Mesiodistal dimensions and sexual dimorphism of teeth of contemporary Western Australian adolescents. *J Oral Sci,* 20: 0596.

ABRÀMOFF MD, MAGALHÃES PJ, RAM SJ (2004) Image processing with ImageJ. *Biophotonics Int,* 11: 36-42.

ACHARYA AB, MAINALI S (2007) Univariate sex dimorphism in the Nepalese dentition and the use of discriminant functions in gender assessment. *Forensic Sci Int,* 173: 47-56.

AL-KHATIB A, RAJION Z, MASUDI S, HASSAN R, ANDERSON P, TOWNSEND G (2011) Tooth size and dental arch dimensions: a stereophotogrammetric study in Southeast Asian Malays. *Orthod Craniofac Res,* 14: 243-253.

ANTONIU S, ROȘCA-GRAMATOPOL ME (1966) Studiul antropologic al scheletelor din complexul mormintelor cu ocru de la Valea Lupului. *An Șt Univ „Al I Cuza" Iași, s Șt nat,* XII: 49-66.

ATEŞ M, KARAMAN F, IŞCAN MY, ERDEM TL (2006) Sexual differences in Turkish dentition. *Leg Med,* 8: 288-292.

BARRETT M, BROWN T, ARATO G, OZOLS I (1964) Dental observations on Australian aborigines: buccolingual crown diameters of deciduous and permanent teeth. *Aust Dent,* 9: 280-285.

BARRETT MJ, BROWN T, MACDONALD M (1963) Dental observations on Australian aborigines: mesiodistal crown diameters of permanent teeth. *Aust Dent,* 8: 150-156.

BERTRAND B, CUNHA E, BÉCART A, GOSSET D, HÉDOUIN V (2019) Age at death estimation by cementochronology: Too precise to be true or too precise to be accurate? *Am J Phys Anthropol,* 169: 464-481.

BLACK W (2014) Dental morphology and variation across Holocene Khoesan people of southern Africa (Doctoral thesis). University of Cape Town, South Africa.

BRACE CL, ROSENBERG KR, HUNT KD (1987) Gradual change in human tooth size in the late Pleistocene and post-Pleistocene. *Evolution,* 41: 705-720.

BROOK A, GRIFFIN R, TOWNSEND G, LEVISIANOS Y, RUSSELL J, SMITH R (2009) Variability and patterning in permanent tooth size of four human ethnic groups. *Arch Oral Biol,* 54: S79-S85.

BROTHWELL DR (1981) *Digging up bones.* New York, Cornell University Press.

BUIKSTRA J, UBELAKER D (1994) *Standards for Data Collection from Human Skeletal Remains: Research Seminar* Fayetteville, Arkansas Archaeological Survey Research Series, No 44.

CHRISTENSEN AF (1998) Odontometric microevolution in the Valley of Oaxaca, Mexico. *J Hum Evol,* 34: 333-360.

CRISTESCU M (1961) Contribuție la studiul antropologic al unor schelete de la sfârșitul Epocii Bronzului (Cultura Noua) și începutul Epocii Fierului din Moldova. *Arh Mold,* I. p. 129-148.

CRISTESCU M, ANTONIU S, KLUGER R (1965) Studiul antropologic al scheletelor de la Cioinagi - Bălințești. *SCA,* 2: 29-42.

CRISTESCU M, MIU G (1999) Studiul Paleoantropologic al Scheletelor din Necropola Civilizației Noua de la Trușești - Țuguieta. In: Dîmbovița MP, Florescu M, Florescu AC (eds.) *Trușești: Monografie Arheologică.* București: Ed. Academiei Române.

CUMMINGS LS, YOST C, SOŁTYSIAK A (2018) Plant microfossils in human dental calculus from Nemrik 9, a Pre-Pottery Neolithic site in Northern Iraq. *Archaeol Anthropol Sci,* 10: 883-891.

DE CASTRO JMB, NICOLAS ME (1995) Posterior dental size reduction in hominids: the Atapuerca evidence. *Am J Phys Anthropol,* 96: 335-356.

DE CASTRO JMB, SARMIENTO S, CUNHA E, ROSAS A, BASTIR M (2001) Dental size variation in the Atapuerca-SH Middle Pleistocene hominids. *J Hum Evol,* 41: 195-209.

DIACONU V, HÂNCEANU GD, SIMALCSIK A, DANU M (2016) Un grup de morminte din Epoca Bronzului descoperit la Roman - Arhiepiscopie. *Arh Mold,* XXXIX: 347-370.

EBOH D (2017) A dimorphic study of maxillary first molar crown dimensions of Urhobos in Abraka, South-Southern Nigeria. *J Morphol Sci,* 29: 96-100.

EL SHEIKHI F, BUGAIGHIS I (2016) Sex discrimination by odontometrics in Libyan subjects. *Egypt J Forensic Sci,* 6: 157-164.

FARZIN M, GITI R, HEIDARI E (2020) Age-related changes in tooth dimensions in adults in Shiraz, Iran. *J Int Oral Health,* 12: 24.

FIORENZA L, BENAZZI S, OXILIA G, KULLMER O (2018) Functional relationship between dental macrowear and diet in Late Pleistocene and recent modern human populations. *Int J Osteoarchaeol,* 28: 153-161.

GALBANY J, IMANIZABAYO O, ROMERO A, VECELLIO V, GLOWACKA H, CRANFIELD MR, BROMAGE TG, MUDAKIKWA A, STOINSKI TS, MCFARLIN SC (2016) Tooth wear and feeding ecology in mountain gorillas from Volcanoes National Park, Rwanda. *Am J Phys Anthropol,* 159: 457-465.

GARN SM, LEWIS AB, KEREWSKY RS (1964) Sex difference in tooth size. *J Dent Res,* 43: 306-306.

GARN SM, LEWIS AB, KEREWSKY RS (1966) Sexual dimorphism in the buccolingual tooth diameter. *J Dent Res,* 45: 1819-1819.

GARN S, LEWIS A, KEREWSKY R (1967) Sex difference in tooth shape. *J Dent Res,* 46: 1470-1470.

GAROT E, COUTURE□VESCHAMBRE C, MANTON DJ, BEKVALAC J, ROUAS P (2019) Differential diagnoses of enamel hypomineralisation in an archaeological context: A postmedieval skeletal collection reassessment. *Int J Osteoarchaeol,* 29: 747-759.

GÓMEZ-ROBLES A, DE CASTRO JMB, MARTINÓN-TORRES M, PRADO-SIMÓN L, ARSUAGA JL (2015) A geometric morphometric analysis of hominin lower molars: Evolutionary implications and overview of postcanine dental variation. *J Hum Evol,* 82: 34-50.

GÓRKA K (2016) Dental morphology and dental wear as dietary and ecological indicators: sexual and inter-group differences in traditional human populations (doctoral thesis). University of Barcelona, Barcelona.

GÓRKA K, ROMERO A, PÉREZ-PÉREZ A (2015) First molar size and wear within and among modern hunter-gatherers and agricultural populations. *Homo,* 66: 299-315.

GREEN JL, CROFT DA (2018) Using dental mesowear and microwear for dietary inference: a review of current techniques and applications. In: Croft DA, Su DF, Simpson SW (eds.) *Methods in Paleoecology.* Switzerland: Springer.

GROZA V-M (2015) *Cercetări paleoantropologice privind populația Iașului Medieval.* Iași, Editura Universității „Alexandru Ioan Cuza" Iași.

HAMMER Ø, HARPER D, RYAN P (2001) PAST-Palaeontological statistics software package for education and data analysis. *Palaeontol Electron,* 4: 9.

HARRIS E, RATHBURN TA (1991) Ethnic differences in the apportionment of tooth size. In: Kelley MA, Larsen CS (eds.) *Advances in dental anthropology.* New York: Wiley-Liss.

HARRIS EF, FOSTER CL (2014) Discrimination between American blacks and whites, males and females, using tooth crown dimensions. In: Berg GE, Ta'ala SC (eds.) *Biological affinity in forensic identification of human skeletal remains: beyond black and white.* USA: CRC Press.

HASEGAWA Y, ROGERS JR, KAGEYAMA I, NAKAHARA S, TOWNSEND GC (2007) Comparison of permanent mandibular molar crown dimensions between Mongolians and Caucasians. *Dent anthropol,* 20: 1-6.

HIGGINS D, AUSTIN JJ (2013) Teeth as a source of DNA for forensic identification of human remains: a review. *Sci Justice,* 53: 433-441.

HILLSON S (2001) Recording dental caries in archaeological human remains. *Int J Osteoarchaeol,* 11: 249-289.

HILLSON S (2005) *Teeth.* USA, Cambridge University Press.

HILLSON S, FITZGERALD C, FLINN H (2005) Alternative dental measurements: proposals and relationships with other measurements. *Am J Phys Anthropol,* 126: 413-426.

İŞCAN MY, KEDICI PS (2003) Sexual variation in bucco-lingual dimensions in Turkish dentition. *Forensic Sci Int,* 137: 160-164.

JEON CL, PAK S, WOO EJ (2020) The correlation between the tooth wear of the first molar and the estimated age from the auricular surfaces in a Joseon Dynasty population, South Korea. *Int J Osteoarchaeol,* 30: 759-768.

KAZZAZI SM, KRANIOTI EF (2018) Sex estimation using cervical dental measurements in an archaeological population from Iran. *Archaeol Anthropol Sci,* 10: 439-448.

KONDO S, TOWNSEND G (2004) Sexual dimorphism in crown units of mandibular deciduous and permanent molars in Australian Aborigines. *Homo,* 55: 53-64.

KONDO S, TOWNSEND GC, YAMADA H (2005) Sexual dimorphism of cusp dimensions in human maxillary molars. *Am J Phys Anthropol,* 128: 870-877.

KONDO S, MANABE Y (2016) Analytical methods and interpretation of variation in tooth morphology. *J Oral Biosci,* 58: 85-94.

LAKHANPAL M, GUPTA N, RAO N, VASHISTH S (2013) Tooth dimension variations as a gender determinant in permanent maxillary teeth. *JSM Dent,* 1: 1014.

LUKACS JR (2019) Deciduous dental variation in Chalcolithic India: methods, metrics and meaning. *Homo*: 3-14.

MAGALHÃES LV, BORGES BS, PINTO PHV, ALVES CP, DA SILVA RHA (2021) Sexual dimorphism applying the mandibular canine index in a Brazilian sample: a pilot study. *Acta Sci Health Sci,* 43: e54202-e54202.

MARCHEWKA J, SKRZAT J, WRÓBEL A (2014) Analysis of the enamel hypoplasia using micro-CT scanner versus classical method. *Anthropol Anz,* 71.

MARTÍN-ALBALADEJO M, MARTINÓN-TORRES M, GARCÍA-GONZÁLEZ R, ARSUAGA JL, DE CASTRO JB (2017) Morphometric analysis of Atapuerca-Sima de los Huesos lower first molars. *Quat Int,* 433: 156-162.

MIU G (1992) Caracteristicile antropologice ale scheletelor descoperite la Brăești (județul Botoșani) aparținând culturii Noua. *SCA,* 29: 17-23.

MIU G (1999) Cercetări paleoantropologice complexe asupra populațiilor aparținând Culturii Monteoru (Doctoral thesis). Universitatea „Alexandru Ioan Cuza" din Iași, Iași.

MIU G, SIMALCSIK R, STUPU M (2003) La nécropole féodale de Hudum (Département de Botoșani) XIII^{e}-XIV^{e} siècles. Analyse démographique. *Ann Roum Anthropol,* 40: 3-9.

MOCKERS O, AUBRY M, MAFART B (2004) Dental crowding in a prehistoric population. *Eur J Orthod,* 26: 151-156.

MORENO-GÓMEZ F (2013) Sexual dimorphism in human teeth from dental morphology and dimensions: A dental anthropology viewpoint. In: Moriyama H (ed.) *Sexual Dimorphism.* IntechOpen.

NAVA A, FIORIN E, ZUPANCICH A, CARRA M, OTTONI C, DI CARLO G, VOZZA I, BRUGNOLETTI O, ALHAIQUE F, CREMONESI RG (2021) Multipronged dental analyses reveal dietary differences in last foragers and first farmers at Grotta Continenza, central Italy (15,500–7000 BP). *Sci Rep,* 11: 1-14.

NECRASOV O, CRISTESCU M (1957) Contribuție la studiul antropologic al scheletelor din complexul mormintelor cu ocru de la Holboca - Iași. *Probleme de Antropologie,* III: 73-147.

NECRASOV O, BOTEZATU D (1964) Studiu antropologic al scheletelor feudale timpurii de la Doina (sec. XIII-XIV). *SCA,* 2: 137-155.

NECRASOV O, ONOFREI M (1972) Contribution a l'anthropologie de la population neoeneolithique du complexe Horodistea-Foltesti. *Ann Roum Anthropol,* 9: 3-9.

NECRASOV O, ANTONIU S, FEDOROVICI C (1972) Sur la structure anthropologique des tribus neo-eneolithiques appartenant a la culture des amphores spheriques. *Ann Roum Anthropol,* 9: 9-25.

NOWACZEWSKA W, DĄBROWSKI P, STRINGER CB, COMPTON T, KRUSZYŃSKI R, NADACHOWSKI A, SOCHA P, BINKOWSKI M, URBANOWSKI M (2013) The tooth of a Neanderthal child from Stajnia Cave, Poland. *J Hum Evol,* 64: 225-231.

PAJEVIĆ T, GLIŠIĆ B (2017) Dental occlusion analysis in the Mesolithic–Neolithic Age, Bronze Age, and Roman to Medieval times in Serbia: Tooth size comparison in skeletal samples. *Arch Oral Biol,* 77: 44-50.

PECKMANN TR, MEEK S, DILKIE N, MUSSETT M (2015) Sex estimation using diagonal diameter measurements of molar teeth in African American populations. *J Forensic Leg Med,* 36: 70-80.

PETRARU O-M, BEJENARU L (2019) Overview on microscopic methods for dental wear evaluation in paleodiet studies. *Ann Roum Anthropol,* 56: 5-14.

PETRARU O-M, GROZA V-M, BEJENARU L (2017) Morphometric variability of the molar tooth M2 in the skeletal series discovered in the 17th century necropolis from Iasi (Iasi county, Romania). *An Şt Univ „Al I Cuza" Iaşi, s Biol anim,* 63: 55-61.

PETRARU O-M, BEJENARU L, GROZA V-M, POPOVICI M (2020) Dimensional variability of the human second molar (M2) in Bronze Age populations from North-East Romania. *RAASI*: 101-109.

PILLOUD MA, SCOTT GR (2020) Dentition in the estimation of sex. In: Klales AR (ed.) *Sex Estimation of the Human Skeleton.* San Diego: Elsevier.

PINHASI R, ESHED V, SHAW P (2008) Evolutionary changes in the masticatory complex following the transition to farming in the southern Levant. *Am J Phys Anthropol,* 135: 136-148.

PRABHU S, ACHARYA AB (2009) Odontometric sex assessment in Indians. *Forensic Sci Int,* 192: 129. e1-129. e5.

RATNER B (2009) The correlation coefficient: Its values range between+ 1/– 1, or do they? *J Target Meas Anal Market,* 17: 139-142.

RAZALI NM, WAH YB (2011) Power comparisons of shapiro-wilk, kolmogorov-smirnov, lilliefors and anderson-darling tests. *JSMTA,* 2: 21-33.

SAUNDERS SR, CHAN AH, KAHLON B, KLUGE HF, FITZGERALD CM (2007) Sexual dimorphism of the dental tissues in human permanent mandibular canines and third premolars. *Am J Phys Anthropol,* 133: 735-740.

SCHERER AK (2018) Dental Metrics. In: Varela SLL (ed.) *The Encyclopedia of Archaeological Sciences.* Chichester: Wiley Blackwell.

SCHMIDT C, OUSLEY S, SCHMIDT M (2011) Brief communication: Correcting overestimation when determining two-dimensional occlusal area in human molars. *Am J Phys Anthropol,* 145: 327-332.

SCHWARTZ GT, DEAN MC (2005) Sexual dimorphism in modern human permanent teeth. *Am J Phys Anthropol,* 128: 312-317.

SHANKAR S, ANUTHAMA K, KRUTHIKA M, KUMAR VS, RAMESH K, JAHEERDEEN A, YASIN MM (2013) Identifying sexual dimorphism in a paediatric South Indian population using stepwise discriminant function analysis. *J Forensic Leg Med,* 20: 752-756.

SMITH-GUZMÁN NE, RIVERA-SANDOVAL J, KNIPPER C, ARIAS GAS (2020) Intentional dental modification in Panamá: New support for a late introduction of African origin. *J Anthropol Archaeol,* 60: 101226.

SMITH BH (1984) Patterns of molar wear in hunter–gatherers and agriculturalists. *Am J Phys Anthropol,* 63: 39-56.

TAKAHASHI M, KONDO S, TOWNSEND GC, KANAZAWA E (2007) Variability in cusp size of human maxillary molars, with particular reference to the hypocone. *Arch Oral Biol,* 52: 1146-1154.

TOMCZYK J, MYSZKA A, REGULSKI P, OLCZAK□KOWALCZYK D (2020) Case of pulp stones and dental wear in a Mesolithic (5900±100 bc) individual from Woźna Wieś (Poland). *Int J Osteoarchaeol,* 30: 375-381.

TOWNSEND G, BOCKMANN M, HUGHES T, BROOK A (2012) Genetic, environmental and epigenetic influences on variation in human tooth number, size and shape. *Odontology,* 100: 1-9.

VICIANO J, ALEMĀN I, D'ANASTASIO R, CAPASSO L (2012) Alternative dental measurements: Correlation between cervical and crown dimensions. *Boll Soc Ital Biol Sper,* 85.

VODANOVIĆ M, DEMO Ž, NJEMIROVSKIJ V, KEROS J, BRKIĆ H (2007) Odontometrics: a useful method for sex determination in an archaeological skeletal population? *J Archaeol Sci,* 34: 905-913.

WASTERLAIN S, NEVES M, FERREIRA M (2016) Dental modifications in a skeletal sample of enslaved Africans found at Lagos (Portugal). *Int J Osteoarchaeol,* 26: 621-632.

WASTERLAIN SN, RUFINO AI, FERREIRA MT (2020) Dental caries and intentional dental modification in a skeletal sample of enslaved Africans from Lagos, Portugal (15th–17th centuries). *Int J Osteoarchaeol,* 30: 109-113.

WATSON JT, HAAS R (2017) Dental evidence for wild tuber processing among Titicaca Basin foragers 7000 ybp. *Am J Phys Anthropol,* 164: 117-130.

WOOD B, ABBOTT S (1983) Analysis of the dental morphology of Plio-pleistocene hominids. I. Mandibular molars: crown area measurements and morphological traits. *J Anat,* 136: 197.

YAMADA H, SAKAI T (1992) Sexual dimorphism in tooth crown diameter of the Cook Islanders. In: Smith P, Tchernov E (eds.) *Structure, function and evolution of teeth.* London: Freund Publishing House, Ltd.

YOO H-I, YANG D-W, LEE M-Y, KIM M-S, KIM S-H (2016) Morphological analysis of the occlusal surface of maxillary molars in Koreans. *Arch Oral Biol,* 67: 15-21.

ZORBA E, MORAITIS K, MANOLIS SK (2011) Sexual dimorphism in permanent teeth of modern Greeks. *Forensic Sci Int,* 210: 74-81.

ZORBA E, SPILIOPOULOU C, MORAITIS K (2013) Evaluation of the accuracy of different molar teeth measurements in assessing sex. *Forensic Sci Med Pathol,* 9: 13-23.

ZÚÑIGA MH, VICIANO J, FONSECA GM, SOTO-ÁLVAREZ C, ROJAS-TORRES J, LÓPEZ-LÁZARO S (2021) Correlation coefficients for predicting canine diameters from premolar and molar sizes. *JDS,* 16: 186-194.

Immunolocalization of intermediate filaments in the kidney of the dromedary camel (*Camelus dromedarius*)

Lemiaa Eissa[1], Mortada M.O. Elhassan[1], Rasha B. Yaseen[1], Hassan A. Ali[2], Haider I. Ismail[1], M.-C. Madekurozwa[3]

[1] Department of Anatomy, College of Veterinary Medicine, University of Bahri, Khartoum, Sudan
[2] Department of Biomedical Sciences, College of Veterinary Medicine, Sudan University of Science and Technology, Khartoum, Sudan
[3] Department of Anatomy and Physiology, Faculty of Veterinary Science, University of Pretoria, Pretoria, South Africa

SUMMARY

Intermediate filaments belong to a large family of proteins which contribute to the formation of the cytoskeleton. The immunolocalization of cytoskeletal proteins has been used extensively in the diagnosis of various renal pathologies. The present study described the immunolocalization of the cytoskeletal proteins vimentin, desmin, smooth muscle actin, and cytokeratin 19 in the normal kidney of the dromedary camel. Kidney samples from eight adult camels were processed for histology and immunohistochemistry. The kidney was enclosed in a renal capsule composed of vimentin immunoreactive fibroblasts and smooth muscle actin immunoreactive smooth muscle cells. The smooth muscle cells in the renal capsule did not exhibit desmin immunoreactivity. Podocytes forming the visceral layer of the glomerular capsule were immunoreactive for vimentin. Immunoreactivity for vimentin and smooth muscle actin in the parietal layer of the glomerular capsule varied, with both reactive and non-reactive cells observed. Intraglomerular mesangial cells were immunoreactive for smooth muscle actin and desmin, but non-reactive to vimentin. The endothelial lining of blood vessels was vimentin immunoreactive, while smooth muscle actin and desmin were demonstrated in the smooth muscle cells of the vessels. The thin limbs of the loops of Henle in cortical nephrons displayed vimentin immunoreactivity. The proximal and distal convoluted tubules, as well as the collecting ducts were negative to vimentin, smooth muscle actin, desmin and cytokeratin 19 immunostaining. In conclusion, the present study has revealed that similarities and differences exist in the immunolocalization of cytoskeletal proteins in the camel when compared to other mammals. The presence of smooth muscle actin in the parietal cells of the glomerular capsule suggests a contractile function of these cells. The results of the study indicate that vimentin and smooth muscle actin can be used as markers for the identification of podocytes and intraglomerular mesangial cells, respectively, in the camel kidney.

Key words: Immunohistochemistry – Vimentin – Desmin – Smooth muscle actin – Cytokeratin 19 – Camelid

Corresponding author:
Mortada M.O. Elhassan. College of Veterinary Medicine, University of Bahri, P.O. Box 1660, Khartoum, Sudan. Phone: 0024991449. E-mail: mortadamahgoub@bahri.edu.sd

Submitted: January 19, 2022. **Accepted:** March 17, 2022

https://doi.org/10.52083/ODPI9847

INTRODUCTION

Camels exist in arid and semi-arid environments, and are well-equipped with mechanisms which allow them to withstand sub-optimal environmental conditions, such as limited water resources (Drosa et al., 2011(. One of these mechanisms, which is the maintenance of electrolyte and water balance during dehydration and fast rehydration, is attributed to the kidney (Jararr and Faye, 2015). For a better understanding of this renal mechanism, several investigations have been carried out on the histology of the kidney in the dromedary camel (Abdalla and Abdalla, 1979; Safer et al., 1988; Eissa et al., 2018; Eissa et al., 2019, Abdalla, 2020). However, despite these studies, several histological features of the camel kidney remain unknown.

Intermediate filaments form a large family of proteins that contribute to the formation of most of the cytoskeleton (Block et al., 2015; Lowery et al., 2015). More than 50 different intermediate filament proteins have been identified (Cooper and Hausman, 2006). A knowledge of the various types of these proteins is useful in comparing and contrasting their structural and functional properties. In this respect, it is widely accepted that the main functions of intermediate filaments are related to the support of cellular physiological activities and structural integrity (Satelli and Li, 2011; Chernoivanenko et al., 2015; Lowery et al., 2015; Snider, 2016). Intermediate filaments can also improve the resistance of cells to various forms of stress and damage caused by pathological processes (Toivola et al., 2010; Battaglia et al., 2017).

Vimentin, desmin, smooth muscle actin and cytokeratin 19 are cytoskeletal proteins which are present in the kidneys of several mammalian species (Şen et al., 2010; Novakovic et al., 2012; Laszczyńska et al., 2012). However, their expression and distribution vary depending on the species and type of renal epithelial cell concerned (Şen et al., 2010). Vimentin is a specific marker for cells of mesenchymal origin (Yang et al., 2019). Smooth muscle actin and desmin have been used as markers for muscle differentiation (Rangdaeng and Truong, 1991). Desmin is found in all muscle types (Robson et al., 2004; Lowery et al., 2015), while smooth muscle actin is restricted to smooth muscle cells, pericytes, myoepithelial cells and myofibroblasts (Rangdaeng and Truong, 1991). Cytokeratins are considered the most abundant cytoskeletal components, with an extensive localization in epithelial cells of the kidney, liver, and lung (Bragulla and Homberger, 2009; Pastuszak et al., 2015; Djudjaj et al., 2016; Werner et al., 2020).

Several researchers have studied cytoskeletal proteins in normal and pathological kidneys of humans (Şen et al., 2010; Sharma et al., 2019), rats (Herrmann, et al., 2012; Funk, et al., 2016), dogs (Gil da Costa et al., 2011), and polar foxes (Laszczyńska, et al., 2012). These studies have shown that the expression and distribution of intermediate filaments varies depending on the type of renal cell, the pathological condition, as well as the animal species concerned (Şen et al., 2010; Laszczyńska et al., 2012). Due to the lack of information on the immunolocalization of cytoskeletal proteins in the normal camelid kidney, the current study investigated the distribution of vimentin, desmin, smooth muscle actin, and cytokeratin 19 in the kidney of the one-humped camel. It is envisaged that the information provided in this study on the normal camelid kidney could form a baseline for the diagnosis of pathological renal lesions in the camel.

MATERIAL AND METHODS

Animals and tissues sampling

Eight non-pregnant female adult camels, aged between 7 and 10 years and weighing 300 to 350 kg, were used in this study. Animals were slaughtered at Assalam abattoir, Khartoum, Sudan. The purpose of slaughtering animals was to provide meat intended for human consumption. A total of 120 tissue samples were selected from the right kidneys of the animals. The right kidney was taken because it was reached without much delay after the abdominal cavity being opened during slaughtering process. Fifteen samples were taken from each kidney (5 samples from the cortex, outer medulla, and inner medulla). All procedures in this study were approved by the College Research Board, College of Veterinary Medicine, University of Bahri, Khartoum, Sudan.

Histological and immunohistochemical staining

Tissue samples were fixed in 10% neutral buffered formalin for five days. Specimens were then processed for routine histological techniques and embedded in paraffin wax. For a general histological overview, sections of 5 µm thickness were stained with hematoxylin and eosin.

The immunostaining technique was performed on additional 5 µm thick sections using a Biogenex super sensitive one-step polymer-HRP detection system kit (Emergo Europe, The Hague, The Netherlands). Sections were deparaffinized and endogenous peroxidase activity was blocked, using 3% (v/v) hydrogen peroxide solution in water for 5 min. The slides were then rinsed in a 0.01 M phosphate buffered saline solution (PBS, pH 7.4) for 5 min. For antigen retrieval, the sections selected for desmin, smooth muscle actin and vimentin immunostaining were microwaved at 750 W for three cycles of 7 min each. After being allowed to cool for 20 min the sections were rinsed in PBS. The sections for cytokeratin 19 immunostaining were incubated with Proteinase K (Dakocytomation, Glostrup, Denmark) in 0.05 mol/L Tris-HCl (pH 7.6) solution for 3 min.

The sections were incubated at room temperature with anti-cytokeratin 19, desmin, smooth muscle actin or vimentin antisera. After incubation with primary antibodies the slides were rinsed in PBS and then incubated with the one-step polymer-HRP reagent (Emergo Europe, The Hague, Netherlands). Slides were then rinsed in PBS and antibodies were visualized by addition of a 3,3'-diaminobenzidine tetrachloride solution (Emergo Europe, The Hague, The Netherlands). The sections were counterstained with Mayer's haematoxylin. Table 1 shows the type, source, and dilution of the primary and secondary antibodies used in this study.

The immunostained, and haematoxylin and eosin-stained sections were viewed using a light microscope (Olympus BX63-Japan) connected to a digital camera (OlympusDP72). Images were then captured using the Cell Sens 510 software program.

Assessment of the immunostaining intensity

Three experienced examiners participated in the semiquantitative assessment of immunohistochemical reactivity independently. Previously, they agreed on the immunostaining intensities being qualified as strong (+++), moderate (++), weak (+) or negative (-).

For negative controls, the primary antibodies utilized in this study were replaced with mouse IgG1 (Dakocytomation, Glostrup, Denmark) which was diluted to the same concentration as the primary antibodies. Smooth muscle was used as a positive control for desmin and smooth muscle actin, while tonsillar tissue was used as a positive control for vimentin. Skin was used as a positive control for cytokeratin 19. No background staining was detected in the negative control sections. The variations in the immunostaining of sections used in this study were minor.

Table 1. Source and dilutions of primary antibodies used in the immunohistochemical technique.

Product name	Source and code	Type of antibody	Dilution	Incubation time
Monoclonal Mouse Anti-Vimentin	Dakocytomation, Glostrup, Denmark, code M7020	Monoclonal Primary Antibodies	1:200	1 hour
Monoclonal Mouse Anti-Human Smooth Muscle Actin	Dakocytomation, Glostrup, Denmark, code M0851	Monoclonal Primary Antibodies	1:50	1 hour
Monoclonal Mouse Anti-Human Desmin	Dakocytomation, Glostrup, Denmark, code M0760	Monoclonal Primary Antibodies	1:50	1 hour
Monoclonal Mouse Anti-Human Cytokeratin 19	Dakocytomation, Glostrup, Denmark, code GA615	Monoclonal Primary Antibodies	1:50	1 hour
One-step polymer-HRP reagent	Emergo Europe, The Hague, The Netherlands, code HK59506K	Anti-mouse and anti-rabbit secondary antibodies labeled with enzyme polymer	Ready to use	15 minutes

RESULTS

General histological overview of the camel kidney

The kidney was covered by a thick fibrous capsule which was composed of inner and outer layers (Fig. 1A). The inner layer contained numerous smooth muscle cells, while the outer layer was predominately composed of dense irregular connective tissue (Fig. 1A). The kidney parenchyma was divided into an outer cortex and an inner medulla (Fig. 1A, B). Cortical and juxtamedullary nephrons were observed in the kidney. The renal corpuscles of cortical nephrons were located in the outer region of the cortex, while the corpuscles of juxtamedullary nephrons were situated in the inner cortical region. The loops of Henle in cortical nephrons were short in contrast to the long loops of juxtamedullary nephrons, which extended into the medulla. The cortical region of the kidney contained renal corpuscles, proximal and distal convoluted tubules, as well as blood vessels (Fig. 1C, D). The renal corpuscles were composed of a glomerulus and glomerular capsule (Bowman's capsule). The glomerulus was formed by glomerular capillaries and mesangial cells (Fig. 1C). The glomerular capsule was formed by an inner visceral and an outer parietal layer. The visceral layer was composed of podocytes, which contained large, irregular-shaped nuclei, while a simple squamous epithelium formed the parietal layer (Fig. 1C).

The medulla of the kidney was subdivided into outer and inner regions, both of which contained collecting ducts. The outer region of the medulla

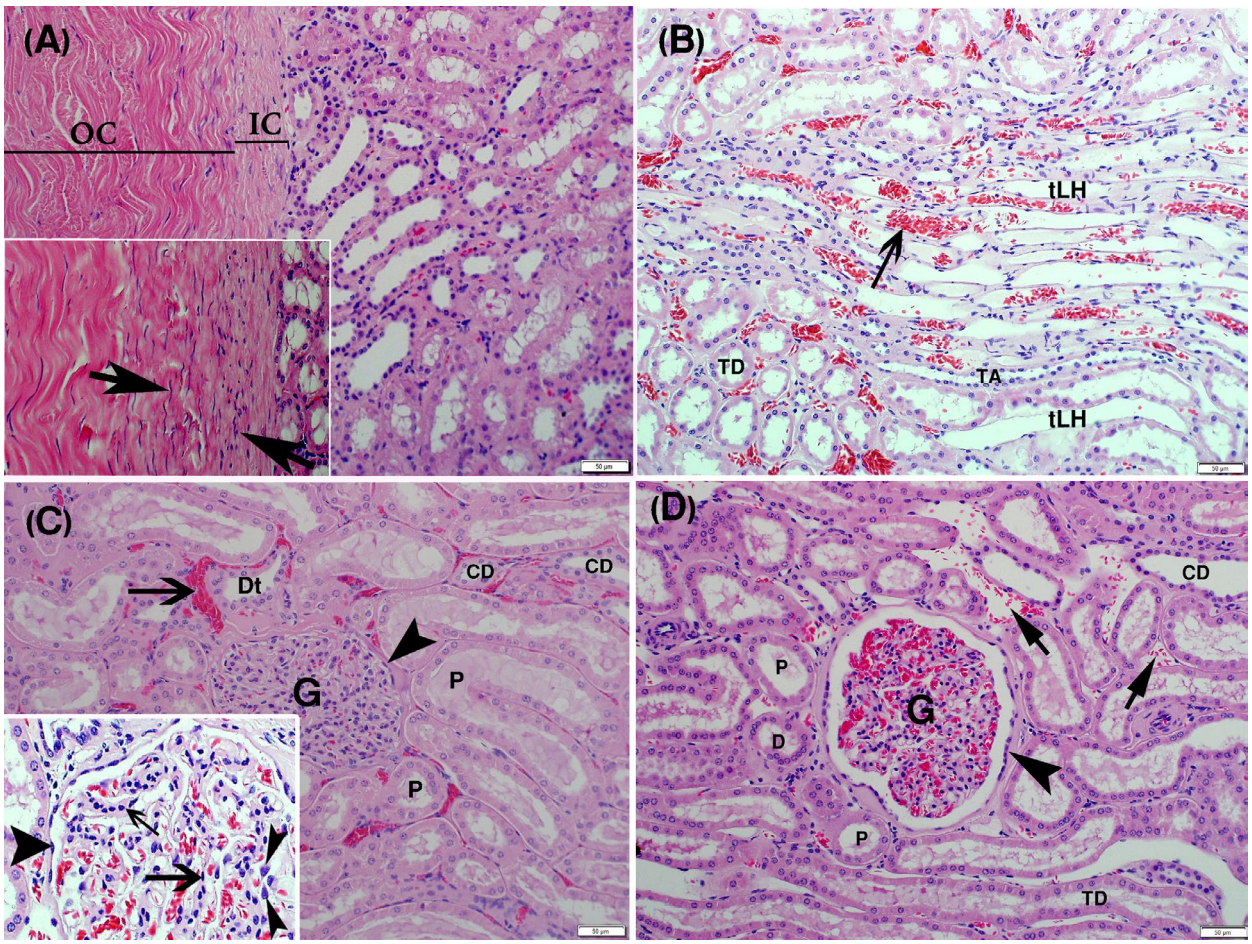

Fig. 1.- Photomicrographs of the cortex (A, C, D) and medulla (B) of the camel kidney. H&E staining. **(A)** Renal capsule and cortex. OC: Outer region of the renal capsule. IC: Inner region of the renal capsule. Inset: high magnification of inner region of the renal capsule containing smooth muscle cells (Arrows). **(B)** Outer region of the medulla. Limbs of the loop of Henle. TA: Thick ascending limb. TD: Thick descending limb. tLH: Thin limbs. Arrow: Vasa recta. **(C)** Renal cortex. G: Glomerulus. Arrowhead: Parietal layer of glomerular capsule. P: Proximal convoluted tubules. Dt: Distal convoluted tubule. CD: Collection ducts. Inset: Renal corpuscle. Small arrowheads: Podocytes. Small arrow: Intraglomerular mesangial cell. Large arrow: Endothelium of the glomerulus. Large arrowhead: Parietal layer of glomerular capsule. **(D)** Renal cortex. G: Glomerulus of a juxtamedullary nephron. Arrowhead: Parietal layer of a glomerular capsule. TD: Thick descending limb of the loop of Henle. CD: Collecting duct. P: Proximal convoluted tubules. Arrows: Blood vessels. Scale bars: 50 µm for A, B, C, D.

additionally contained the thick descending and ascending, as well as the thin limbs of the loop of Henle (Fig. 1B). In contrast, the thin limbs of the loops of Henle were the only tubular nephron components observed in the inner medulla.

Immunohistochemistry

The immunoreactivity of intermediate filaments in various regions of the camel kidney is shown in Table 2.

Vimentin

Strong vimentin immunostaining was demonstrated in podocytes which formed the visceral layer of the glomerular capsule (Fig. 2 A, B). Immunoreactivity was strong to moderate in cells forming the parietal layer of the glomerular capsule. However, interspersed between the vimentin immunoreactive cells were non-reactive cells (Fig. 2B). The thin limbs of the loops of Henle in cortical nephrons displayed strong vimentin immunoreactivity (Fig. 2C), whereas those of the juxtamedullary nephrons were non-reactive to vimentin (Fig. 2C, D and E).

Endothelial cells of renal blood vessels were predominantly immunoreactive to vimentin. In the cortex, these immunoreactive endothelial cells appeared to be mainly confined to cortical arteries and glomerular arterioles (Fig. 2A). In the medulla, strong immunoreactivity for vimentin was observed in the endothelial cells of the vasa rectae (Fig. 2C, D and E). However, in the medulla a few vasa rectae were lined by endothelia that non-reactive to vimentin (Fig. 2E).

Stromal cells in the interstitial tissue of the medulla and subepithelial connective tissue of the renal papilla exhibited strong immunoreactivity for vimentin (Fig. 2F). In addition, moderate to weak vimentin immunostaining was observed in fibroblasts located in the renal capsule, as well as in the trabeculae between nephrons.

No vimentin immunoreactivity was observed in the intraglomerular mesangial cells, epithelium of proximal and distal tubules (Fig. 2B), and collecting ducts (Fig. 2E, F).

Smooth muscle actin and desmin

Strong smooth muscle actin immunoreactivity was detected in intraglomerular mesangial cells (Fig. 3A, B). Strong smooth muscle actin immunoreactivity was also noted in the parietal cells of the glomerular capsules. However, some of the parietal cells were non-reactive to smooth muscle actin (Fig. 3B). Intense smooth muscle actin immunostaining was evident in smooth muscle cells forming the inner layer of the renal capsule (Fig. 3C). Additionally, strong smooth muscle actin immunostaining was demonstrated in the tunica media and tunica externa of muscular arteries (Fig. 3A, D), as well as in pericytes enclosing intertubular capillaries (Fig. 3C, D). In the medulla strong smooth muscle actin immunoreactivity was observed in the tunica media of vasa rectae (Fig. 3E, F).

Table 2. The intensity of the immunostaining of vimentin, smooth muscle actin, desmin, and cytokeratin 19 in the kidney of the camel.

Structures	Vimentin	SMA	Desmin	Cytokeratin 19
Podocytes	+++	-	-	-
Parietal cells of the glomerular capsule	-/++/+++	-/+++	-	-
Intraglomerular mesangial cells	-	+++	+	-
Cells of the thin limb of the loop of Henle*	+++	-	-	-
Endothelial cells	-/+++	-	-	-
Vascular smooth muscle cells	-	+++	+	-
Fibroblasts in the renal capsule	+	-	-	-
Smooth muscle fibres in the renal capsule	-	+++	-	-
Stromal cells below epithelium of renal papilla	+++	+++	-	-
Stromal cells in connective tissue trabeculae	+/++	+++	-	-
Fibroblasts in the interstitial tissue of medulla	+++	-	-	-

***** The loop of Henle of the outer cortical nephron

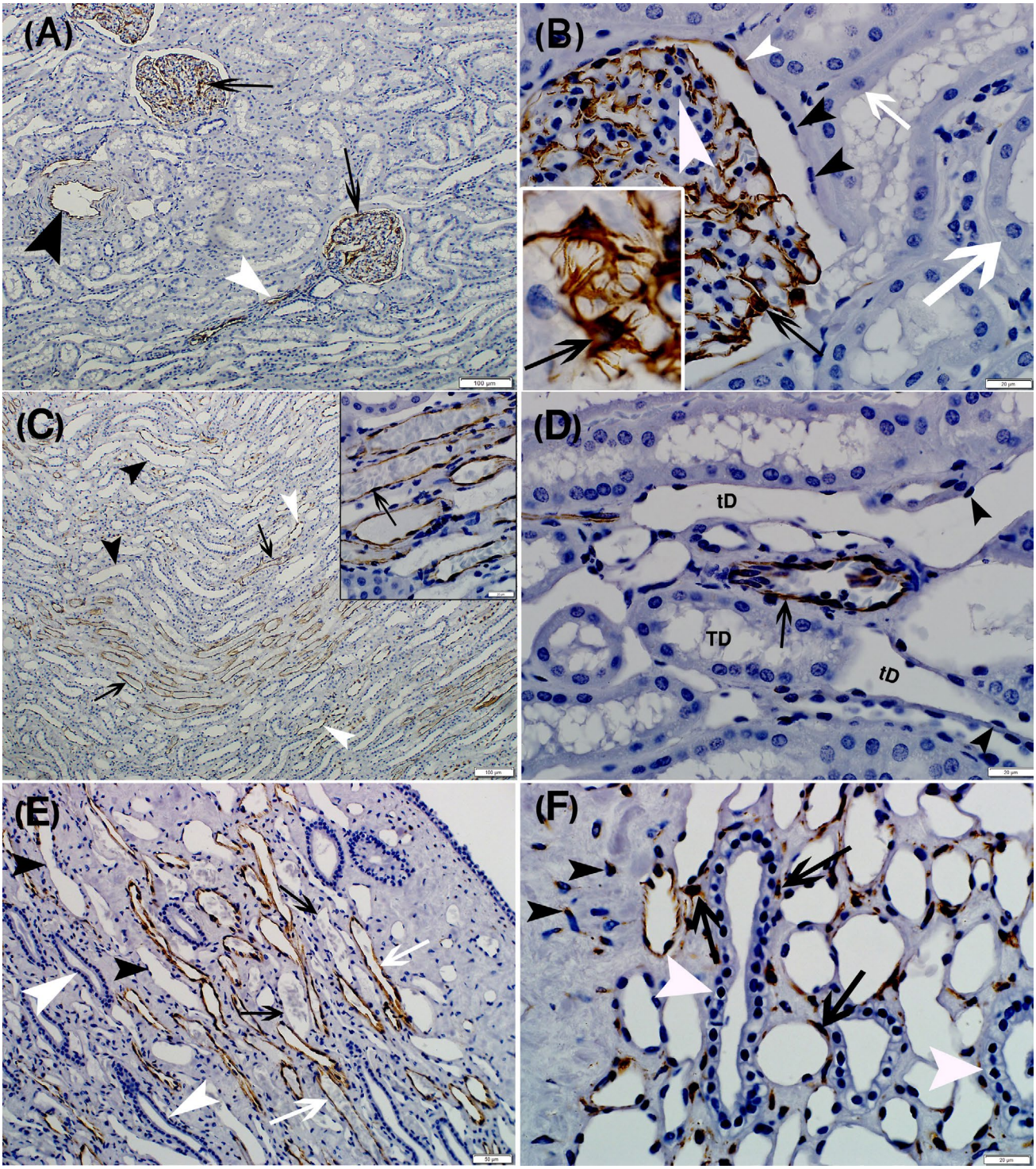

Fig. 2.- Photomicrographs of vimentin immunostaining in the cortex (A and B) and medulla (C, D, E and F) of the camel kidney. **(A)** Arrows: Strong vimentin immunopositive podocytes. Black arrowhead: Immunopositive endothelial cell of a small artery. White arrowhead: Immunopositive endothelial cell of a glomerular arteriole. **(B)** Black arrow: Strong vimentin immunostaining in a podocyte. Small white arrowhead: Strong vimentin immunostaining in a cell in the parietal layer of a glomerular capsule. Black arrowheads: Vimentin immunonegative cells in the parietal layer. Large white arrowhead: Vimentin immunonegative intraglomerular mesangial cell. Small white arrow: Vimentin immunonegative epithelium of a proximal convoluting tubule. Large white arrow: Vimentin immunonegative epithelium of a distal convoluting tubule. Inset: High magnification of a glomerulus and glomerular capsule. Arrow: Vimentin immunopositive podocyte. **(C)** White arrowheads: Vimentin immunopositive cells forming the thin limbs of the loop of Henle in superficial nephrons. Arrows: Immunopositive endothelial cells of vasa rectae in the outer medulla. Black arrowheads: Immunonegative cells of thin limbs of the loops of Henle in juxtamedullary nephrons. Inset: Arrow: Immunopositive endothelium of a vasa recta. **(D)** Arrowheads: Vimentin immunonegative cells lining the thin descending limbs (tD) of loops of Henle in juxtamedullary nephrons. Arrow: Immunopositive endothelium of a vasa recta at the junction between outer and inner regions of the medulla. TD: Thick descending limb of a loop of Henle. **(E)** White arrows: Immunopositive endothelial cells of vasa rectae in the inner medulla. Black arrows: Immunonegative endothelial cells. Black arrowheads: Immunonegative cells of thin limbs of the loops of Henle of juxtamedullary nephrons. White arrowheads: Immunonegative cells of collecting ducts. **(F)** Arrows: Immunopositive stromal cells in the interstitial tissue of the medulla. Black arrowheads: Immunopositive stromal cells in the subepithelial connective tissue of a renal papilla. White arrowheads: Immunonegative cells of collecting ducts. Scale bars: 100 µm for A, C; 20 µm for B, D, F; 50 µm for E.

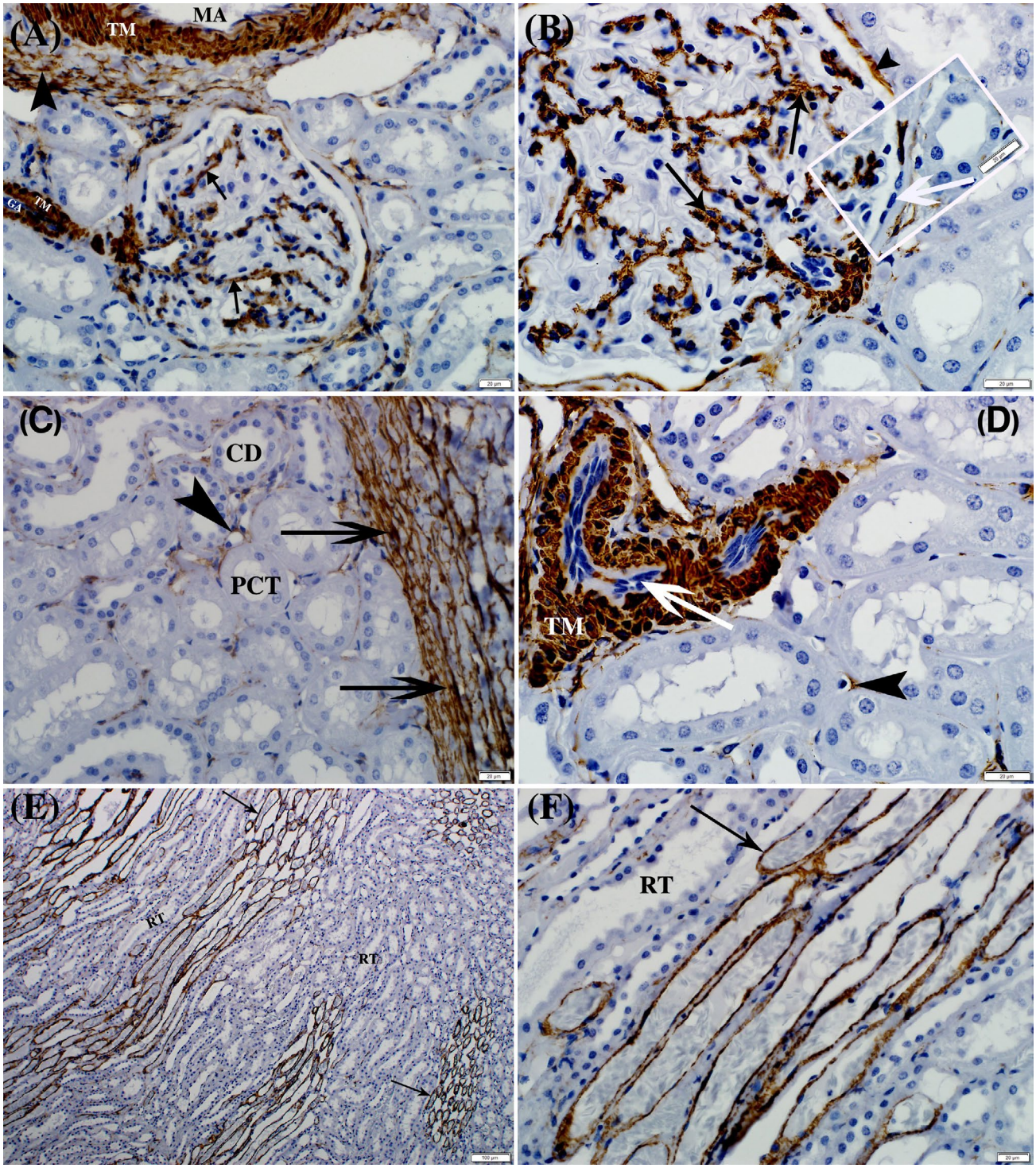

Fig. 3.- Photomicrographs of smooth muscle actin immunostaining in the cortex (A and B) and medulla (C, D, E and F) of the camel kidney. **(A)** Smooth muscle actin immunoexpression in intraglomerular mesangial cells (arrows), as well as in the tunica media (TM) of a muscular artery (MA) and glomerular arteriole (GA). Smooth muscle actin immunoexpression is also present in smooth muscle cells in the tunica externa (arrowhead) of the muscular artery. **(B)** Smooth muscle actin immunostaining in the cytoplasm of intraglomerular mesangial cells (arrows), as well as in the parietal cell layer (arrowhead) of the glomerular capsule. Inset: Arrow: Vimentin immunonegative cell in the parietal layer of a glomerular capsule. **(C)** Smooth muscle actin immunoreactivity in smooth muscle cells of the renal capsule (arrows), as well as in a pericyte of a capillary (arrowhead) interposed between a proximal convoluted tubule (PCT) and a cortical collecting duct (CD). **(D)** Strong smooth actin immunostaining in the tunica media (TM) of a muscular artery, as well as in a pericyte of an intertubular capillary (arrowhead). Arrow: Smooth muscle actin immunonegative endothelium. **(E) & (F)** Arrows: Strong smooth muscle actin immunoreactivity in smooth muscle cells of the tunica media of the vasa rectae. RT: Renal tubules. Scale bars: 20 µm for A, B, C, D, F; 100 µm for E.

Desmin immunostaining was restricted to intraglomerular mesangial and vascular smooth muscle cells (Fig. 4A, B). The proximal and distal convoluted tubules, as well as the collecting ducts were reactive to vimentin, smooth muscle actin, desmin, and cytokeratin 19.

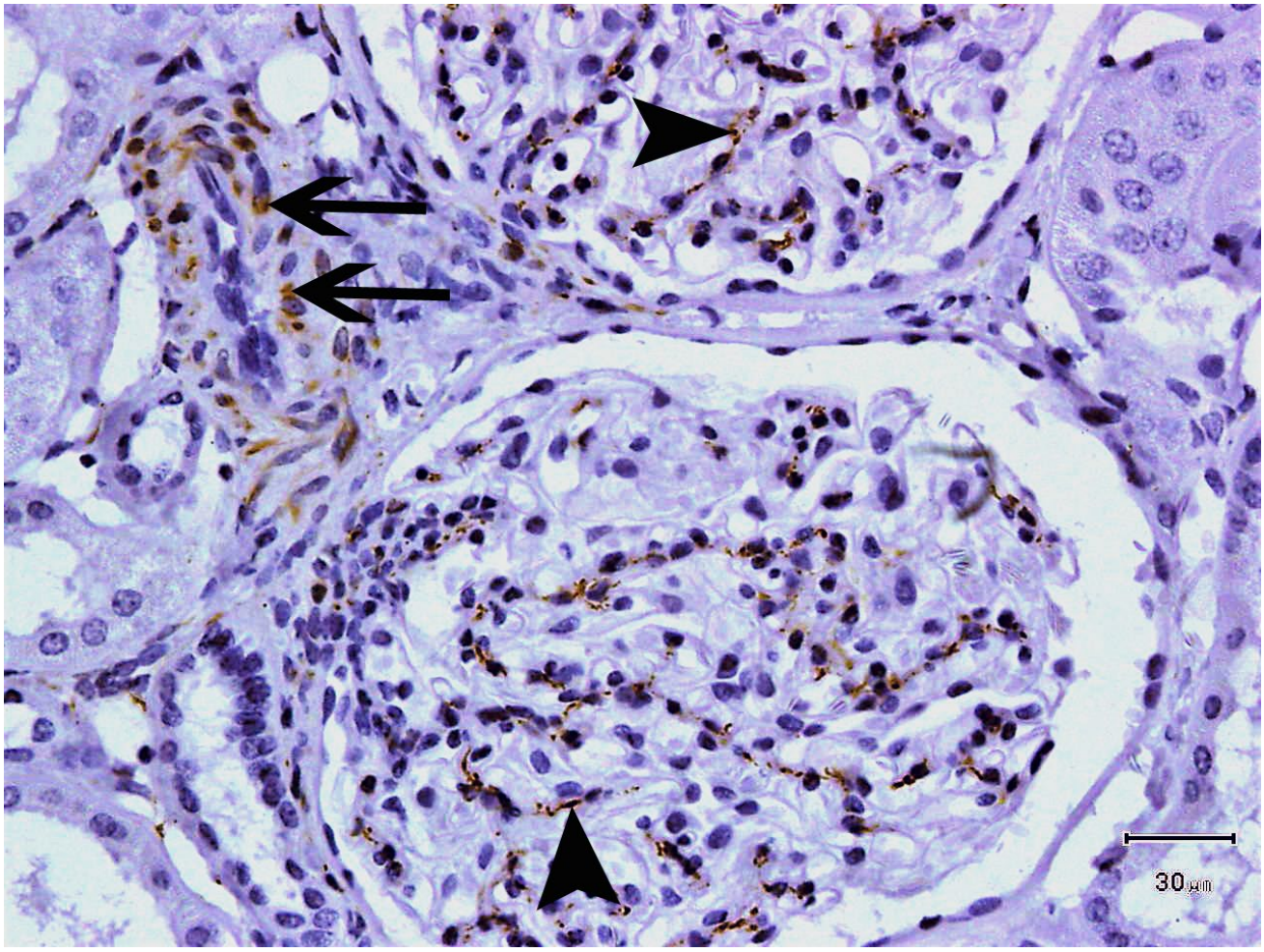

Fig. 4.- Photomicrograph of desmin immunostaining in the cortex of camel kidney. Immunopositive intraglomerular mesangial cells (arrowheads). Immunopositive smooth muscle cells of a glomerular arteriole (arrows). Scale bar: 30 µm.

Cytokeratin 19

No immunoreactivity for cytokeratin 19 was detected in the camel kidney.

DISCUSSION

Renal capsule

The renal capsule is known to play a role in the establishment of an effective renal interstitial pressure (Khraibi and Knox, 1989), and subsequently water excretion (Farrugia et al.,1992). The presence of smooth muscle cells in the inner capsular layer of camel kidney has previously been reported by Eissa et al. (2018), and confirmed in the current study. The present study has shown that the smooth muscle cells are immunoreactive for smooth muscle actin, but non-reactive to desmin. The occurrence of smooth muscle cells in the renal capsule has been reported in several mammalian species and is known to be involved in the contractile ability of the capsule (Kobayashi, 1978). In addition, the thick collagenous layer of the renal capsule functions to protect the kidney from traumatic injuries (Orchard et al., 2014). Thus, as shown in the current study, the main component of the outer region of the renal capsule dense irregular connective tissue with associated vimentin immunoreactive fibroblasts. Fibroblasts have been considered as one of the major components of renal capsule in several mammals, such as mouse, rat, guinea pig and rabbit (Kobayashi, 1978). In addition, fibroblast in the kidney were demonstrated by the immunolocalization of vimentin (Boor and Floege, 2012).

Renal parenchyma

The general histomorphological findings of the present study were similar to those reported in

previous investigations on the camel (Abdalla and Abdalla, 1979; Beniwal et al., 1998; Wenhui and Huaitao, 2000; Xu et al., 2009). Furthermore, the present study confirmed that the renal histology of the camel does not differ significantly from other mammalian species, such as the dog (Bulger et al., 1979), cattle (Mbassa, 1988), and sheep (Singh et al., 2018).

In this study, vimentin was immunolocalized in podocytes, vascular endothelial cells, and medullary interstitial fibroblasts. These findings are plausible as it is known that vimentin occurs in cells of mesenchymal origin (Leong et al., 2003; Satelli and Li, 2011). In addition, these results are in agreement with studies carried out on several mammals, including the human (Essawy et al., 1997), domestic ruminants (Maretta and Marettová, 1999; Yaoita et al., 1999), rodents (Zou et al., 2006; Yaoita et al., 1999; Sistani et al., 2013) dog (Yaoita et al., 1999), and polar fox (Laszczyńska et al., 2012). Intraglomerular mesangial cells, and the epithelia of proximal and distal tubules in the current study did not react with vimentin. These reports are contrary to observations made in the human and polar fox in which vimentin immunoreactivity was demonstrated in the epithelia of the proximal and distal tubules (Laszczyńska et al., 2012; Smeets et al., 2013). Furthermore, intraglomerular mesangial cells in humans, rats, ruminants, and polar foxes have been reported to be immunoreactive for vimentin (Stamenkovic et al., 1986; Oosterwijk et al., 1990; Scanziani et al., 1993; Essawy et al., 1997; Maretta and Marettová, 1999; Yaoita et al., 1999; Zou et al., 2006; Laszczyńska et al., 2012; Smeets et al., 2013). These results indicate that species variations exist in the immunolocalization of vimentin in the mammalian kidney. However, the functional significance of these interspecies variations is unknown.

In the current study smooth muscle actin immunoreactivity was detected in the tunica media of blood vessels throughout the renal tissue. This is similar to findings reported in the rat (Carey et al., 1992) and human (Essawy et al., 1997; Novakovic et al., 2012). Smooth muscle actin has also been demonstrated in myofibroblasts located in the interstitium of normal human kidney (Essawy et al., 1997; Gonlusen et al., 2001). In the present study no myofibroblasts appeared to be present.

The current findings revealed that smooth muscle actin immunostaining was demonstrated in the parietal layer of the glomerular capsule. This may suggest a contractile function of the parietal cells of camel kidney. Interestingly, the present study showed that some of the parietal cells of the glomerular capsule were non-reactive when stained either with vimentin or smooth muscle actin. It is plausible that the negative parietal cells for vimentin might display positive reactivity for smooth muscle actin, and the reverse is true. However, further double immunostaining studies will need to be conducted to confirm this assertion.

In this study, positive immunostaining for smooth muscle actin was observed in intraglomerular mesangial cells. This is in agreement with the findings of studies conducted on the human kidney (Schlöndorff and Banas, 2009; Young et al., 2014). It is known that intraglomerular mesangial cells contain the intermediate filaments actin and myosin (Davies, 1994; Stockand and Sansom, 1998). Consequently, intraglomerular mesangial cells are thought to have a contractile ability, which is utilized in the control of glomerular blood flow (Reece, 2015).

It is noteworthy that the immunostaining of desmin in this study was weaker than that of smooth muscle actin. One possible explanation for this difference could be that the fixation of renal tissue with formalin may significantly enhance the immunostaining sensitivity to smooth muscle actin rather than desmin (Rangdaeng and Truong, 1991). Desmin immunostaining in the present study was observed primarily in intraglomerular mesangial cells, as well as in vascular smooth muscle cells. Similar findings were reported in the human (Oosterwijk et al., 1990), rat (Zou et al., 2006) and polar fox (Laszczyńska et al., 2012). However, studies by Essawy et al. (1997), as well as Gonlusen et al. (2001) did not detect desmin immunoreactivity in the human kidney.

It is known that there are approximately twenty different types of cytokeratins, with at least two

occurring in most epithelial cells (Leong et al., 2003). In the human kidney, cytokeratin 19 has been demonstrated in the parietal layer of the glomerular capsule (Stamenkovic et al., 1986), as well as in the loop of Henle (Achtstätter et al., 1985), distal convoluted tubules (Oosterwijk et al., 1990) and collecting ducts (Şen et al., 2010). However, the current study did not detect cytokeratin 19 in the camel kidney. It has been reported that filaments generated from different types of cytokeratins have distinct physical properties, suggesting tailor-made networks of intermediate filaments suitable for tissue structural requirements of tensile strength, flexibility, and dynamics (Fuchs et al., 1994). Therefore, it is most likely that the epithelial cells of the camel kidney may have types of cytokeratins other than cytokeratin 19.

In conclusion, the results of the present study have shown that similarities and differences exist in the immunolocalization of cytoskeletal proteins in the camel when compared to other mammals. The presence of smooth muscle actin immunoreactivity in the parietal cell layer of the glomerular capsule suggests a contractile function of the parietal cells in the camel kidney. Significantly, the results of the study suggest that vimentin and smooth muscle actin can be used as markers for the identification of podocytes and intraglomerular mesangial cells, respectively, in the camel kidney.

REFERENCES

ABDALLA MA (2020) Anatomical features in the kidney involved in water conservation through urine concentration in dromedaries (*Camelus dromedarius*). *Heliyon*, 6: e03139.

ABDALLA MA, ABDALLA O (1979) Morphometric observation on the kidney of the *Camelus dromedarius*. *J Anat*, 129: 45-50.

ACHTSTÄTTER T, MOLL R, MOORE B, FRANKE WW (1985) Cytokeratin polypeptide patterns of different epithelia of the human male urogenital tract: Immunofluorescence and gel electrophoretic studies. *J Histochem Cytochem,* 33(5): 415-426.

BACHMANN S, KRIZ W, KUHN C, FRANKE WW (1983) Differentiation of cell types in the mammalian kidney by immunofluorescence microscopy using antibodies to intermediate filament proteins and desmoplakins. *Histochemistry,* 77: 365-394.

BATTAGLIA RA, KABIRAJ P, WILLCOCKSON HH, LIAN M, SNIDER NT (2017). Isolation of intermediate filament proteins from multiple mouse tissues to study aging-associated post-translational modifications. *J Vis Exp,* 123, e55655: 1-8.

BENIWAL G, SINGH K, JOSHI S (1998) Microscopic study of uriniferous tubules and collecting ducts of kidney in camel (*Camelus dromedarius*). *J Camel Pract Res,* 5(1): 107-109.

BLOCK J, SCHROEDER V, PAWELZYK P, WILLENBACHER N, KÖSTER S (2015) Physical properties of cytoplasmic intermediate filaments. *Biochim Biophys Acta,* 1853: 3053-3064.

BOOR P, FLOEGE J (2012). The renal (myo-)fibroblast: a heterogeneous group of cells. *Nephrol Dial Transplant,* 27: 3027-3036.

BRAGULLA HH, HOMBERGER DG (2009) Structure and functions of keratin proteins in simple, stratified, keratinized and cornified epithelia. *J Anat,* 214: 516-559.

BULGER RE, CRONIN RE, DOBYAN DC (1979) Survey of the morphology of the dog kidney. *Anat Rec,* 194: 41-66.

CAO Y, KARSTEN U, ZERBAN H, BANNASCH P (2000) Expression of MUC1, Thomsen-Friedenreich-related antigens, and cytokeratin 19 in human renal cell carcinomas and tubular clear cell lesions. *Virchows Arch,* 436(2): 119-126.

CAREY AV, CAREY RM, GOMEZ RA (1992) Expression of □-smooth muscle actin in the developing kidney vasculature. *Hypertension*, 19(2): 168-175.

CHERNOIVANENKO IS, MATVEEVA EA, GELFAND VI, GOLDMAN RD, MININ AA (2015) Mitochondrial membrane potential is regulated by vimentin intermediate filaments. *FASEB J,* 29: 820-827.

COOPER GM, HAUSMAN RE (2006) The Cell, a molecular approach, 2nd edition. Sinauer Associates, Inc. ISBN: 0878932194,9780878932191.

DAVIES M (1994) The mesangial cell: A tissue culture view. *Kidney Int,* 45: 320-327.

DJUDJAJ S, PAPASOTIRIOU M, BÜLOW RD, WAGNEROVA A, LINDENMEYER MT, COHEN, CD, STRNAD P, GOUMENOS DS, FLOEGE J, BOOR P (2016) Keratins are novel markers of renal epithelial cell injury. *Kidney Int,* 89(4): 792-808.

DROSA A, ELMALIK K, SALIH A, ABD-ELHDI O (2011) Some aspects of camel raising in the Butana area of the Sudan. Conference on International Research on Food Security, Natural Resource Management and Rural Development. University of Bonn. www.tropentag.de/2011/abstracts/full/274.pdf.

EISSA L, ISMAIL HI, ELHASSAN MMO, ALI HA (2019) Basement membranes in the kidney of the dromedary camel (*Camelus dromedarius*): An immunohistochemical and ultrastructural study. *Acta Histochem,* 121: 419-429.

EISSA L, ISMAIL HI, ELHASSAN MMO, YASEEN RB, ALI HA (2018) Comparative histology and histometry of the renal capsule in dromedary she camel (*Camelus dromedarius*), Cow (*Bos indicus*) and Ewe (*Ovis aires*). *J Camel Res Product*, 18(1): 9-16. http://repository.sustech.edu/handle/123456789/ 23596.

ESSAWY M, SOYLEMEZOGLU O, MUCHANETA-KUBARA EC, SHORTLAND J, BROWN CB, EL NAHAS AM (1997) Myofibroblasts and the progression of diabetic nephropathy. *Nephrol Dial Transplant,* 12: 43-50.

FARRUGIA E, LOCKHART JC, LARSON TS (1992) Relation between vasa recta blood flow and renal interstitial hydrostatic pressure during pressure natriuresis. *Circ Res,* 71(5): 1153-1158.

FUCHS E (1994) Intermediate filaments: structure, dynamics, function, and disease. *Annu Rev Biochem,* 63: 345-352.

FUNK J, OTT V, HERRMANN A, RAPP W, RAAB S, RIBOULET W, VANDJOUR A, HAINAUT E, BENARDEAU A, SINGER T, JACOBSEN B (2016) Semiautomated quantitative image analysis of glomerular immunohistochemistry markers desmin, vimentin, podocin, synaptopodin and WT-1 in acute and chronic rat kidney disease models. *Histochem Cell Biol,* 145: 315-326.

GHAYUR MN, KREPINSKY JC, JANSSEN LJ (2008) Contractility of the renal glomerulus and mesangial cells: Lingering doubts and strategies for the future. *Med Hypotheses Res,* 4(1): 1-9.

GIL DA COSTA RM, OLIVEIRA JP, SARAIVA AL, SEIXAS F, FARIA F, GÄRTNER F, PIRES MA, LOPES C (2011) Immunohistochemical characterization of 13 canine renal cell carcinomas. *Vet Pathol,* 48(2): 427-432.

GONLUSEN G, ERGIN M, PAYDAS S, TUNALI N (2001) The expression of cytoskeletal proteins (α-smooth muscle actin, vimentin, desmin) in kidney tissue: A comparison of fetal, normal kidneys, and glomerulonephritis. *Int Urol Nephrol,* 33(2): 299-305.

HERRMANN A, TOZZO E, FUNK J (2012) Semi-automated quantitative image analysis of podocyte desmin immunoreactivity as a sensitive marker for acute glomerular damage in the rat puromycin aminonucleoside nephrosis (PAN) model. *Exp Toxicol Pathol,* 64: 45-49.

JARARR B, FAYE B (2015) Normal pattern of the camel histology. Food and Agriculture Organization of the United Nations & Ministry of Agriculture Kingdom of Saudi Arabia. UTF/SAU/021/SAU.

JOHNSON RJ, GORDON K, GOWN AM (1991) Expression of smooth muscle cell phenotype by rat mesangial cells in immune complex nephritis. Alpha-smooth muscle actinis a marker of mesangial cell proliferation. *J Clin Invest,* 87(3): 847-858.

KHRAIBI AA, KNOX FG (1989) Effect of renal decapsulation on renal interstitial hydrostatic pressure and natriuresis. *Am J Physiol,* 257(1Pt2): R44-48.

KOBAYASHI K (1978) Fine structure of the mammalian renal capsule: The atypical smooth muscle cell and its functional meaning. *Cell Tissue Res,* 195: 381-394.

LASZCZYŃSKA M, OŻGO M, SZYMECZKO R, WYLOT M, SŁUCZANOWSKA-GŁĄBOWSKA S, PIOTROWSKA K, SKRZYPCZAK W (2012) Morphological, histochemical and immunohistochemical studies of polar fox kidney. *Folia Histochem Cytobiol,* 50(1): 87-92.

LEONG AS, COOPER K, LEONG FJW (2003) Manual of Diagnostic Antibodies for Immunohistology. 2nd Edition. Greenwich Medical Media Ltd. London, p 167.

LOWERY J, KUCZMARSKI ER, HERRMANN H, GOLDMAN RD (2015) Intermediate filaments play a pivotal role in regulating cell architecture and function. *J Biol Chem,* 290(28): 17145-17153.

MARETTA M, MARETTOVÁ E (1999) Immunohistochemical demonstration of vimentin and S-100 protein in the kidneys. *Gen Physiol Biophys,* 18(1): 100-102.

MBASSA GK (1988) Comparative histology of the kidney of Bos taurus and Bos indicus cattle. *Anat Histol Embryol,* 17: 157-163.

NOVAKOVIC ZS, DURDOV MG, PULJAK L, SARAGA M, LJTIC D, FILIPOVIC T, PASTAR Z, BENDIC A, VUKOJEVIC K (2012) The interstitial expression of alpha-smooth muscle actin in glomerulonephritis is associated with renal function. *Med Sci Monit,* 18(4): 235-240.

OOSTERWIJK E, VAN MUIJEN GNP, OOSTERWIJK-WAKKA JC, WARNAAR SO (1990) Expression of intermediate-sized filaments in developing and adult human kidney and in renal cell carcinoma. *J Histochem Cytochem,* 38(3): 385-392.

ORCHARD G, MUSKETT D, NATION B (2014) Kidney and urinary tract. In: Orchard G, Nation B (eds.). *Cell Structure and Function*. Oxford University Press, p 355.

PASTUSZAK M, GROSZEWSKI K, PASTUSZAK M, DYRLA P, WOJTUŃ S, GIL J (2015) Cytokeratins in gastroenterology. *Systematic review Prz Gastroenterol,* 10(2): 61-70.

RANGDAENG S, TRUONG LD (1991) Comparative immunohistochemical staining for desmin and muscle-specific actin. *Am J Clin Pathol,* 96(1): 32-45.

REECE WO (2015) Dukes' Physiology of Domestic Animals, 13th edition. Wiley-Blackwell, ISBN: 978-1-118-50139-9.

ROBSON RM, HUIATT TW, BELLIN RM (2004) Muscle intermediate filament proteins. *Methods Cell Biol,* 78: 519-553.

SAFER AM, EL-SAYED NK, ABO-SALEM K, AL-SHAER R (1988) Ultrastructure of the nephron of the One-humped Camel (*Camelus dromedarius*). *J Morphol,* 198(3): 287-301.

SATELLI A, LI S (2011) Vimentin as a potential molecular target in cancer therapy or vimentin, an overview and its potential as a molecular target for cancer therapy. *Cell Mol Life Sci,* 68(18): 3033-3046.

SCANZIANI E, GRIECO V, SALVI S (1993) Expression of vimentin in the tubular epithelium of bovine kidneys with interstitial nephritis. *Vet Pathol,* 30: 298-300.

SCHLÖNDORFF D, BANAS B (2009) The mesangial cell revisited: no cell is an island. *J Am Soc Nephrol,* 20: 1179-1187.

ŞEN S, SARSIK B, ŞİMŞİR A (2010) Immunohistochemical markers in renal tumors and findings in non-tumoral renal parenchyma. *Turk J Pathol,* 26(2): 120-129.

SHARMA P, ALSHARIF S, FALLATAH A, CHUNG BM (2019) Intermediate filaments as effectors of cancer development and metastasis: A Focus on keratins, vimentin, and nestin. *Cells,* 8: 497.

SINGH KN, JOSHI S, MATHUR R, KUMAR M, SENGAR SS (2018) Histological studies on the kidney of Marwari sheep (*Ovis aries*). *J Pharmacogn Phytochem,* 1: 994-996.

SISTANI L, RODRIGUEZ PQ, HULTENBY K, UHLEN M, BETSHOLTZ C, JALANKO H, TRYGGVASON K, WERNERSON A, PATRAKKA J (2013) Neuronal proteins are novel components of podocyte major processes and their expression in glomerular crescents supports their role in crescent formation. *Kidney Int,* 83(1): 63-67.

SMEETS B, BOOR P, DIJKMAN H, SHARMA SV, JIRAK P, MOOREN F, BERGER K, BORNEMANN J, GELMAN IH, FLOEGE J, VAN DER VLAG J, WETZELS JFM, MOELLER MJ (2013) Proximal tubular cells contain a phenotypically distinct, scattered cell population involved in tubular regeneration. *J Pathol,* 229(5): 645-659.

SNIDER NT (2016) Kidney keratins: cytoskeletal stress responders with biomarker potential. *Kidney Int,* 89(4): 738-740.

STAMENKOVIC I, SKALLI O, GABBIANI G (1986) Distribution of intermediate filament proteins in normal and diseased human glomeruli. *Am J Pathol,* 125(3): 465-475.

STOCKAND JD, SANSOM SC (1998) Glomerular mesangial cells: Electrophysiology and regulation of contraction. *Physiol Rev,* 78(3): 724-736.

TOIVOLA DM, STRNAD P, HABTEZION A, OMARY MB (2010) Intermediate filaments take the heat as stress proteins. *Trends Cell Biol,* 20(2): 79-91.

WENHUI W, HUAITAO C (2000) Studies on comparative histology of the kidneys in Bactrian camels (*Camelus bactrianus*). *J Lanzhou Univ,* (Naturl Science Edition) 36: 73-79.

WERNER S, KELLER L, PANTEL K (2020) Epithelial keratins: Biology and implications as diagnostic markers for liquid biopsies. *Mol Aspects Med,* 72: 100817.

XU C, BAO H, QI F, LIU Y, QIN J, GANDAHI JA, CHEN Q (2009) Morpho-histological investigation of the kidney of Bactrian camel (*Camelus bactrianus*). *J Camel Pract Res,* 16(2): 1-6.

YANG C, CHANG P, HSU W, CHANG H, CHEN C, LAI C, CHIU W, CHEN H (2019) Src and SHP2 coordinately regulate the dynamics and organization of vimentin filaments during cell migration. *Oncogene,* 38: 4075-4094.

YAOITA E, FRANKE WW, YAMAMOTO T, KAWASAKI K, KIHARA I (1999) Identification of renal podocytes in multiple species: higher vertebrates are vimentin positive/lower vertebrates are desmin positive. *Histochem Cell Biol,* 111: 107-115.

YOUNG B, O'DOWD G, WOODFORD P (2014) The urinary system. In: *Wheater's Functional Histology' A Text and Colour Atlas*. 6th edition. Elsevier, Churchill Livingstone.

ZOU J, YAOITA E, WATANABE Y, YOSHIDA Y, NAMETA M, LI H, QU Z, YAMAMOTO T (2006) Upregulation of nestin, vimentin, and desmin in rat podocytes in response to injury. *Virchows Arch,* 448: 485-492.

Radiographic assessment of maxillary sinus lateral wall and anatomy of posterior superior alveolar artery: A Cone-Beam Computed Tomographic

Renuka Devi KR, Mahima V. Guledgud, Karthikeya Patil, Sanjay CJ, Nagabhushana D, Harshitha N

Department of Oral Medicine and Radiology, JSS Dental College and Hospital, JSS Academy of Higher Education and Research, Mysore - 570 015, India

SUMMARY

The aims of the study were to determine the thickness of maxillary sinus (MS) lateral wall and to assess the prevalence, distance from maxillary sinus floor, diameter and course of posterior superior alveolar artery (PSAA) based on age, gender and dental status using cone-beam computed tomography (CBCT) that might be relevant to accomplish complication free surgeries in posterior maxilla. CBCT images of maxillary sinus (right and left) were obtained for 40 patients, which included 20 males and 20 females. Maxillary sinus lateral wall and PSAA parameters were measured and evaluated. The data obtained were then subjected to descriptive statistical analysis; independent t-test and one-way Anova test were performed and compared based on age, gender and dental status. The results showed that the average thickness of the lateral wall of the maxillary sinus was determined to be approximately around 2.50 mm. PSAA was observed in 25% of subjects with a maximum distance of 8.83 mm from the maxillary sinus floor and a minimum distance of 6.90 mm. PSAA had a diameter of 1-2 mm with the intraosseous course in most individuals. Comparison between CBCT images of the selected individuals among age groups, gender and dental status were not statistically significant on measuring the above mentioned parameters. This study concluded that CBCT provides valuable diagnostic information pertaining to sinus and related landmarks that assist during surgical procedures.

Key words: Maxillary sinus lateral wall – PSAA – CBCT – Dental implants

INTRODUCTION

Dental implants are frequently used to reconstruct edentulous areas of the posterior maxilla. Restoring of the posterior edentulous maxilla with dental implants is challenging due to insufficient height and width of the alveolar bone ridge (Talo Yildirim et al., 2019). To overcome these difficulties, two surgical methods utilised for maxillary sinus augmentation are the lateral

Corresponding author:
Dr. Mahima V, Guledgud, Professor. Department of Oral Medicine and Radiology, JSS Dental College and Hospital, JSS Academy of Higher Education and Research, Mysore - 570 015, India. Phone: +91 94480 86800. E-mail: dr.mahimavg@jssuni.edu.in

Submitted: March 10, 2022. **Accepted:** March 17, 2022

https://doi.org/10.52083/RLFI8348

window approach and the crestal method (Kiakojori et al., 2017). According to ancient medicine, sinuses as part of the skull's anatomy are intrinsically connected to vital organs. The maxillary sinuses undergo pneumatization as the age advances. The infraorbital artery (IOA) and the PSAA are branches of the maxillary artery that supply the superior membrane and lateral wall of the maxillary sinus (Van Cauwenberge et al., 2004) Maxillary sinus augmentation procedure is a safe and effective technique for the rehabilitation of the severely atrophic posterior maxilla with a significant predictability. Schneiderian membrane perforation and deterioration of the lateral wall's vascular supply are the most prevalent complications of this surgical approach. During intervention, it is necessary to predict probability of sinus membrane perforations; the thickness of the lateral sinus wall must be assessed. It is also critical to evaluate the anatomy of the maxillary sinus in order to avoid complications, since PSAA is closely related to the anatomy of the MS (Talo Yildirim et al., 2019; Van Cauwenberge et al., 2004). After the emergence of three-dimensional imaging mode, CBCT is deemed as the gold standard to evaluate the MS lateral wall thickness and its vascular anatomy owing to its accuracy, high resolution, and better tissue contrast by eliminating the overlap of surrounding structures (Van Cauwenberge et al., 2004).

In this backdrop, the present study was designed to measure the maxillary sinus lateral wall thickness, and also the prevalence, diameter and course of PSAA using CBCT. This study also correlates gender, age groups, and dental status with the MS and PSAA parameters which may provide significant information and assist the clinician in operative procedures.

MATERIALS AND METHODS

The study was approved by the Institutional Ethics Committee. Forty CBCT scans of 20 females and 20 males were reviewed summing up to 80 sinuses. The study samples were obtained from the outpatients attending the Department of Oral Medicine and Radiology, with age range of 21-86 years (mean age of 76 years). Prior to commencing the CBCT exposure, demographic data, complaint and past history of the patients were recorded. All of the subjects signed a formal consent form allowing their data to be used for research.

After precise placement of the study subject, ProMax 3D Mid CBCT machine was set to standard exposure parameters at 90 KvP, 8mA, 0.04 S, medium FOV on each side of the maxillary sinus for exposure. The resultant images, with slice thickness of 0.400 mm, were stored in DICOM format. Only high-quality images entirely encompassing the bilateral maxillary sinuses were included after an initial screening, while low-quality images and those with any artefacts were eliminated. Scans that detected unilateral and/or bilateral maxillary sinus developmental abnormalities, fractures, or any pathology such as a tumor or cyst were also excluded.

The axial, coronal and sagittal sections of selected CBCT images were reformatted and analyzed under optimum viewing conditions, and the following measurements were performed on coronal sections using Planmeca Romexis 5.3 (3D Software).

Measurement of Maxillary sinus lateral wall thickness

For the purpose of the study, the maximum distance perpendicularly from the inner point to the outermost point on the lateral wall of both right and left maxillary sinuses on coronal sections was considered to be the lateral wall thickness of the maxillary sinus. One vertical line was drawn on the coronal section 5mm from the maxillary sinus floor using a digital caliper. Taking this as a reference plane, a horizontal line drawn on the lateral wall of the maxillary sinus at the level of 5 mm measured the thickness of maxillary sinus lateral wall (Fig. 1).

Prevalence of PSAA

CBCT sections were checked for radiolucency interrupting the lateral wall of the maxillary sinus by scrolling it from anterior aspect to posterior aspect evaluated the prevalence of PSAA.

Measurement of distance of PSAA from the maxillary sinus floor

The maximum distance from the floor of the maxillary sinus to the area of visibility in the lateral wall of the maxillary sinus on coronal sections was considered to be the distance of PSAA from the maxillary sinus floor. One linear line drawn on the coronal section from the floor of the maxillary sinus to the level of visibility of posterior superior alveolar canal located in the lateral wall of the maxillary sinus using a digital caliper measured the distance of PSAA from maxillary sinus floor (Fig. 2).

Measurement of diameter and determining the course of PSAA

The longest anteroposterior distance from the point most anteriorly to the point most posteriorly on coronal sections was considered to be the diameter of PSAA. One horizontal line was drawn on the coronal section anteroposteriorly at the area of visibility of PSAA canal in the lateral wall of the maxillary sinus using a digital caliper measured the diameter of PSAA (Fig. 3). Based on the visibility, the path of the posterior superior alveolar artery was determined (Fig. 4).

The measurements were made at four different locations: the first premolar (P1), the second premolar (P2), the first molar (M1), and the second molar (M2) (M2). On the other side of the sinus, the same procedures were used.

Statistical Analysis

The data was generated on MS Office Excel Sheet (version 2019), and statistical analysis was performed using the Statistical Package for Social Sciences (SPSS). A comparison was made between gender, dental status, and age groups. The obtained data were then subjected to descriptive statistics, One-way Anova and Independent sample t-test to analyze the statistical significant difference between the means in groups.

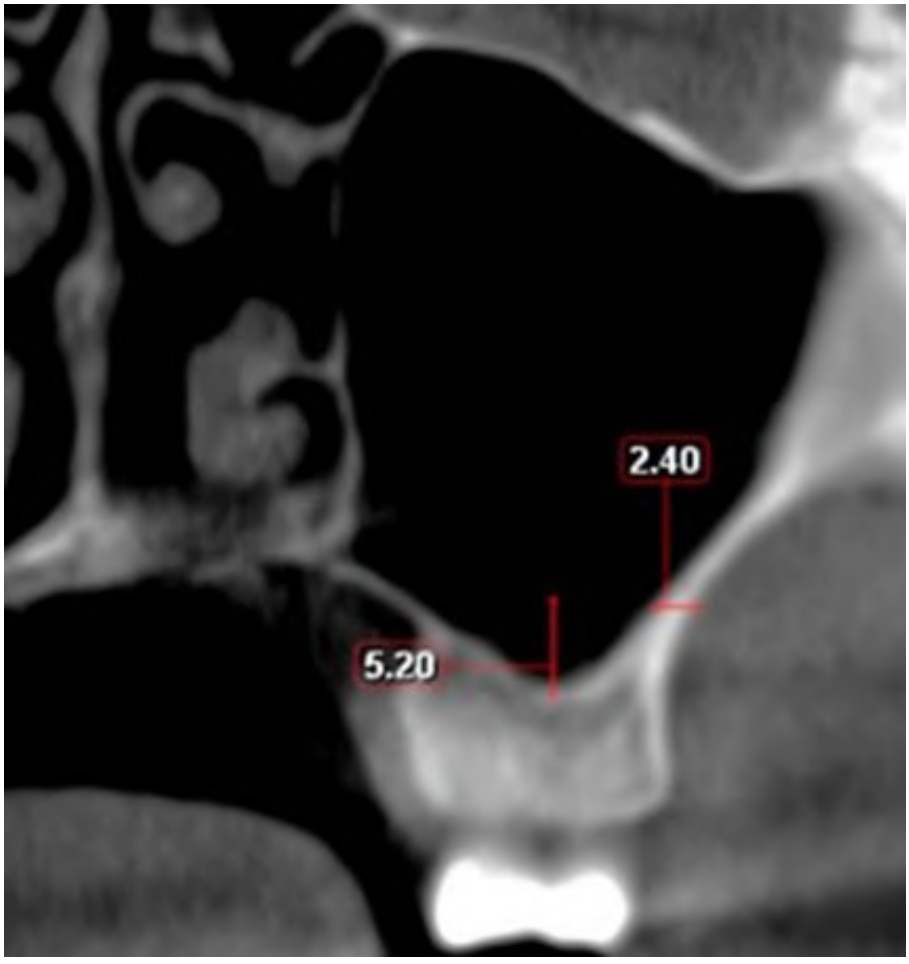

Fig. 1.- Measurement of maxillary sinus lateral wall thickness on coronal section.

Fig. 2.- Distance of PSAA from maxillary sinus floor on coronal section.

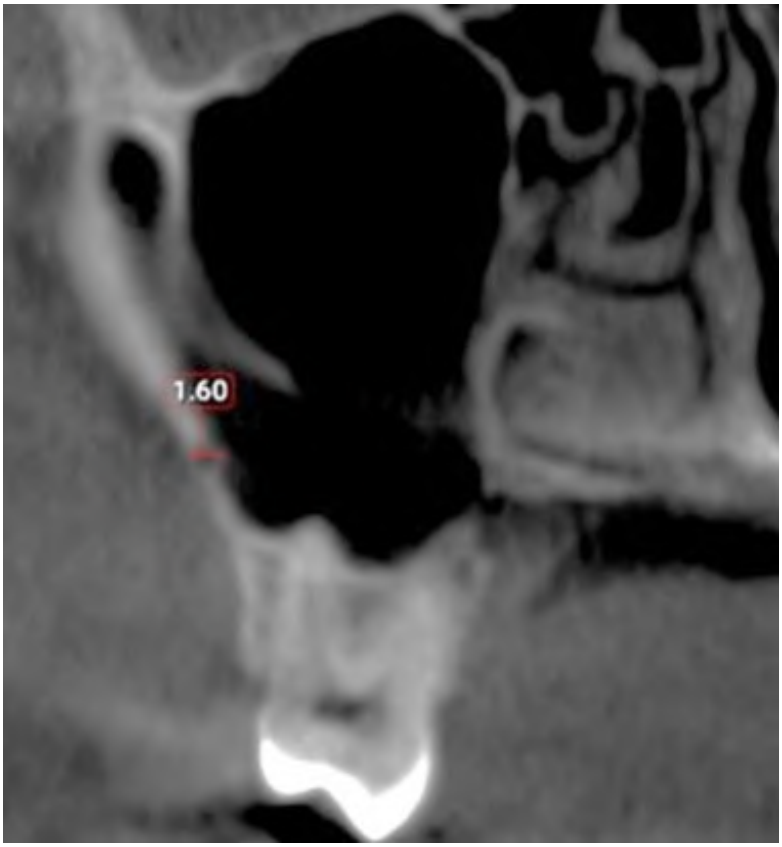

Fig. 3.- Diameter of PSAA on coronal section.

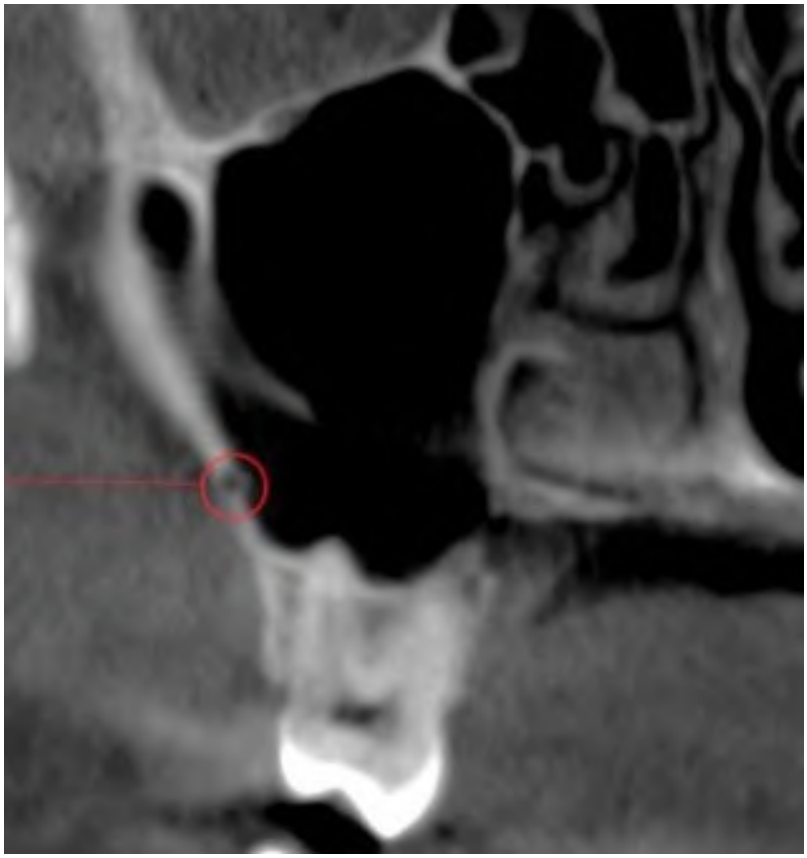

Fig. 4.- Course of PSAA on coronal section.

RESULTS

Among the 40 study subjects, 20 (50%) were males and 20 (50%) females, with a mean age of 44.000 and 37.3500 in males and females respectively. Thirty study subjects were dentulous (46.7%) and 10 were edentulous (10.0%).

The mean thickness of maxillary sinus lateral wall at P1 was 2.40 ± 0.57 mm**,** P2 was 2.57 ± 0.59 mm, M1 was 2.46 ± 0.71 mm and M2 was 1.98 ± 0.57 mm (Table 1).

Table 1. Maxillary sinus lateral wall thickness.

Maxillary sinus lateral wall thickness (mm) (n=40)		
TOOTH SITE	**MEAN**	**SD**
P1	2.40	± 0.57
P2	2.57	± 0.59
M1	2.46	± 0.71
M2	1.98	± 0.57

The maxillary sinus lateral wall thickness was compared between males and females: males appeared to have a thinner wall thickness than women with the exception at P2 location. Despite the fact that there was a mean value difference between genders, there were no statistically significant variations. The subjects' varying age groups and dental status (edentulous and non-edentulous) had no statistically significant influence on the lateral wall thickness (Table 2).

The presence of PSAA was detected on 25% of patients among the study subjects.

The mean distance of PSAA from the maxillary sinus floor was 6.90 ± 0.43 mm at P1, 7.44 ± 0.53 mm at P2, 8.58 ± 0.51 mm at M1 and 8.83 ± 1.54 mm at M2. The total mean distance of PSAA indicates that the distance from the maxillary sinus floor was found to be greater in molars than in premolars. PSAA distance from the maxillary sinus floor was substantially larger in dentulous people than in edentulous persons (Table 3).

PSAA vessel mean diameter was higher in molars than premolars. According to linear measurements, the mean diameter of the posterior superior alveolar artery at P1, P2, M1, M2 was reported to be less than 1 mm in 46.83% cases,1-2 mm in 51.89% of cases and more than 2mm in only one patient among the study subjects (Table 4).

Table 2. Differences in maxillary sinus lateral wall thickness by age, gender and dental status.

TOOTH SITE	GENDER	Mean ± SD	Sig (2-tailed)	DENTAL STATUS	Mean ± SD	P	AGE GROUPS	Mean ± SD	Sum of squares	sig
P1	Male Female	2.39 ±.549 2.40 ±.608	0.96	Dentate Edentulous	2.39 ± 0.56 2.40 ± 0 .63	0.95	21-30 31-40 41-50 51-60 71-80	2.45 ± 0.64 2.30 ± 0.38 2.33 ± 0.53 2.43 ± 0.65 2.60 ± 0.28	26.2	.903
P2	Male Female	2.64 ± .520 2.49 ± .667	0.26	Dentate Edentulous	2.56 ± 0 .59 2.59 ± 0.61	0.83	21-30 31-40 41-50 51-60 71-80	2.74 ± 0.59 2.38 ± 0.29 2.51 ± 0.72 2.49 ± 0.58 2.40 ± 0.00	28.3	.426
M1	Male Female	2.39 ± .753 2.53 ± .670	0.38	Dentate Edentulous	2.47 ± 0 .68 2.44 ± 0 .80	0.88	21-30 31-40 41-50 51-60 71-80	2.30 ± 0.52 2.60 ± 1.14 2.48 ± 0.49 2.57 ± 0.91 2.80 ± 0.56	40.0	.641
M2	Male Female	1.98 ± .547 1.99 ± .613	0.95	Dentate Edentulous	2.02 ± 0.59 1.87 ± 0 .52	0.28	21-30 31-40 41-50 51-60 71-80	1.97 ± 0.59 1.97 ±0 .83 2.04 ±0 .47 1.86 ± 0.46 2.80 ± 0.56	26.3	.294

Table 3. PSAA distance from maxillary sinus floor.

PSAA distance from maxillary sinus floor (mm) (n=40)		
TOOTH SITE	**MEAN**	**SD**
P1	6.90	± 0.43
P2	7.44	± 0.53
M1	8.58	± 0.51
M2	8.83	± 1.54

Table 4. Diameter of PSAA.

Diameter of PSAA (mm) (n=40)		
Category	**mm**	**%**
Category 1	<1	46.83%
Category 2	1-2	51.89%
Category 3	>2	1.26%

When age groups, gender, and dental status were compared, there was no variability in PSAA diameter and distance from the maxillary sinus floor (Tables 5 and 6).

On examining the course of PSAA at P1, 5% were intraosseous and 2.5 % were intrasinusal. At P2, 12.5% were intraosseous and 12.5% were intrasinusal. At M1, 1.3% were superficial, 11.3 % were intrasinusal and 15% were intraosseous. At M2, 1.3% were superficial, 15% were intrasinusal and 28.8 % were intraosseous (Table 4). As a result of the statistical comparison, the intraosseous form of PSAA was the most prevalent, followed by intrasinusal, and lastly superficial.

DISCUSSION

Osseointegration of dental implants needs appropriate bone quantity as well as bone quality. The MS is one of the most important anatomic features to consider when inserting implants in the posterior maxillary region. The length and location of implants are influenced by the reduced bone height produced by MS pneumatization. Thus, procedures such as maxillary sinus floor elevation (SFE), which facilitate the placement of longer implants in the posterior maxilla (Tarun Kumar and Anand, 2014). The most common intraoperative complication during sinus elevation is perforation of the Schneiderian membrane (Schwartz-Arad et al., 2015).

Infracture and wall-off are two methods for preparing the lateral window osteotomy. The lateral wall is tapped over the graft materials as a roof in the infracture method, while in the wall-off procedure, the lateral wall is removed to get access to the sinus. In addition to maxillary sinus floor elevation, surgical procedures must consider lateral wall thickness and PSAA (Wallace et al.,

2012; Raja, 2009). Data from earlier research that described the distance of the lower border of the window to the maxillary sinus floor were used to establish the measuring point of the lateral wall (Wallace et al., 2012; Woo and Le, 2004).

According to the literature, only a few studies have examined the impact of age, sex, and dental status on lateral wall thickness of maxillary sinus. Clinicians utilize the sinus floor as a reference point when designing the lateral window osteotomy's margins from a clinical standpoint (Wallace et al., 2012).

According to Zijderveld et al. (2008), 78% of patients had a thin lateral maxillary sinus wall. The thickness of the lateral wall should be measured before surgery, since it may compromise the sinus membrane's integrity (Kiakojori et al., 2017). In addition to maxillary sinus floor elevation, surgical procedures must consider lateral wall thickness and PSAA. Few researchers have

Table 5. Differences in distances of PSAA from maxillary sinus floor by age, gender and dental status.

TOOTH SITE	GENDER	Mean ± SD	Sig (2-tailed)	DENTAL STATUS	Mean ± SD	P	AGE GROUPS	Mean ± SD	Sum of squares	sig
P1	Male Female	6.86 ± 0.51 6.96 ± 0.40	0.78	Dentate Edentulous	6.92± 0.47 6.85± 0.49	0.85	21-30 31-40 41-50 51-60 71-80	6.98 ± 0.56 6.97 ± 0.00 6.96 ± 0.40 6.56 ± 0.00 6.50 ± 0.00	1.15	0.69
P2	Male Female	7.83 ± 0.53 7.92 ± 0.56	0.74	Dentate Edentulous	7.77 ± 0 .59 8.06 ± 0.38	0.29	21-30 31-40 41-50 51-60 71-80	7.83 ± 0.67 7.81 ± 0.00 7.70 ± 0.62 7.95 ± 0.35 8.50 ± 0.00	4.60	0.61
M1	Male Female	8.98 ±.0.30 8.96 ± 0.69	0.92	Dentate Edentulous	9.00 ± 0 .58 8.89 ± 0.35	0.66	21-30 31-40 41-50 51-60 71-80	8.83 ± 0.72 9.20 ± 0.50 8.96 ± 0.46 8.98 ± 0.40 8.95 ± 0.07	5.86	0.88
M2	Male Female	8.57± 2.25 9.03 ± 0.53	0.38	Dentate Edentulous	9.18 ± 0.60 7.99 ± 2.57	0.39	21-30 31-40 41-50 51-60 71-80	9.29 ± 0.59 9.29 ± 0.72 8.92 ± 0.71 7.91 ± 2.90 9.00 ± 0 .70	78.3	0.41

Table 6. Differences in diameter of PSAA by age, gender and dental status.

TOOTH SITE	GENDER	Mean ± SD	Sig (2-tailed)	DENTAL STATUS	Mean ± SD	P	AGE GROUPS	Mean ± SD	Sum of squares	sig
P1	Male Female	1.00 ± 0.23 1.03 ± 0.15	0.85	Dentate Edentulous	1.01 ± 0.18 1.00 ± 0.28	0.92	21-30 31-40 41-50 51-60 71-80	0.96 ± 0.20 0.85 ± 0.00 1.13 ± 0.54 0.11 ± 0.00 0.80 ± 0.00	0.40	0.29
P2	Male Female	0.95 ± 0.18 1.0 ± 0.36	0.68	Dentate Edentulous	1.06 ± 0.31 0 .83 ± 0.04	0 .10	21-30 31-40 41-50 51-60 71-80	0.97 ± 0.20 0.86 ± 0.00 1.04 ± 0.45 0.96 ± 0.18 0.80 ± 0.00	0.62	0.90
M1	Male Female	1.06 ±.0.25 1.12 ± 0.47	0.72	Dentate Edentulous	1.17 0.40 0 .91 ± 0.21	0.12	21-30 31-40 41-50 51-60 71-80	1.11 ± 0.38 1.26 ± 0.59 1.13 ± 0.32 0.95 ± 0.30 0.84 ± 0.06	0.28	0.70
M2	Male Female	1.05 ± 0.37 1.16 ± 0.34	0.37	Dentate Edentulous	1.09 ± 0.37 1.17 ± 0.31	0.60	21-30 31-40 41-50 51-60 71-80	0.99 ± 0.20 1.50 ± 0.42 1.03 ± 0.40 1.30 ± 0.36 1.20 ± 0 .00	1.02	0.14

Table 7. Course of PSAA.

Course of PSAA			
TOOTH SITE	**Intraosseous**	**Intrasinusal**	**Superficial**
P1	5%	2.5 %	-
P2	12.5%	12.5%	-
M1	15%	11.3%	1.3%
M2	28.8 %	15%	1.3%

explored into MS lateral wall thickness, PSAA, and possible relationships with patient's age, gender, and dental status (Kiakojori et al., 2017).

The present research demonstrated a thicker lateral wall in females in comparison to male subjects at the M1 location, and thicker lateral wall in male subjects at the P2 location. We noticed that the difference of lateral wall thickness between genders were not statistically significant.

Previous studies on lateral wall thickness found significant gender variations exclusively in the premolar area (Yang et al., 2012). Kang et al. (2013) discovered a substantial difference between males and females at a three-millimeter distance from the sinus floor. In terms of dental status, the findings of this study revealed that dentate people have thicker lateral walls than edentulous people, however the difference is statistically insignificant. In their investigation, Khajehahmadi et al. (2014) found no significant differences between dentulous and edentulous subjects. However, among dentate individuals, there was a trend toward a thicker lateral wall. Monje et al. (2014) analyzed the relationship between edentulous span and lateral wall thickness, and observed that the greater the edentulous span, the thinner the lateral wall. Also, that there was no statistically significant difference in age groups. Our findings are in agreement with statistics stated from earlier researches, which established that sinus lateral wall thickness does not increase with age (Kang et al., 2013; Monje et al., 2014). This is an interesting finding observed in our study. As the bone atrophy might progress further with time, it would have been noteworthy to study the association between duration of the edentulousness of the subjects with the lateral wall thickness. Further studies in this regard may shed more information on this aspect.

Various studies on PSAA prevalence rate observed the following: Ella et al. (2008), 10.5%; Rosano et al. (2009), 47%; Jung et al. (2011),52.8%; Apostolakis and Bissoon et al. (2014), 82%; Kang et al. (2013), 64.3%; Watanabe et al. (2014, 58.6%; Güncü et al. (2011), 64.5%, and Yang et al. (2012), 32.5% (see Kiakojori et al., 2017 for review). The prevalence of PSAA on CBCT in our current study data shows detection rate of around 26% (n=40) among the study subjects. Detection rate is higher in molar locations than premolars.

Discrepancy in many of the studies may be related to the lack of expertise of the clinicians, mode of imaging, and technical elements in assessing CBCT data (Kiakojori et al., 2017). Our CBCT images were obtained from a premium CBCT machine available in the market.

The distance of PSAA from maxillary sinus floor is significant in establishing the exact position of the PSAA, as well as the optimum length of an implant to be positioned in the edentulous area (Manjushri Waingade et al., 2021). The PSAA mean distance from the maxillary sinus floor was approximately about 6.00 mm to 8.00 mm for the P1, P2, M1, M2 areas. The distance of the posterior superior alveolar artery from sinus floor decreased towards the premolar region and increases as it approaches at the molar region. Other studies by Yang et al. (2012), Watanabe et al. (2014), Apostolakis and Bissoon (2014), Jung et al. (2011) and Yu et al. (2019), observed that the mean distance at P1, P2, M1, M2 were 7.75 mm, 9.57mm, 6.47 mm, 8.17 mm and 9.70 mm, respectively. In different orientations, the distance between the PSAA and the maxillary sinus floor varied substantially across individuals around the mean values (Apostolakis and Bissoon, 2014; Kiakojori et al., 2017).

Based on the hypothesis of Fayek et al. (2021), the mean diameter of PSAA was classified into three categories: Category 1: less than 1 mm; Category 2: between 1-2 mm; Category 3: more than 2 mm.

The mean diameter of PSAA obtained from our study was between 1-2 mm (Category 2) at P1, P2, M1, M2 locations. Very few individuals' PSAA diameter varied less than 1 mm (Category 1). Also, the diameters of PSAA in females are comparatively higher than males. Concerning the dental status, dentulous patients revealed larger PSAA vessels except in M2 region. A larger diameter might indicate serious bleeding, which could lead to intraoperative and postoperative problems such perforation of the Schneiderian membrane, graft material displacement, and hematoma of surrounding structures (Manjushri Waingade et al., 2021). There was no difference associated with age groups. Findings from our results exhibits no statistical difference between gender, dental status and age.

Studies by Kang et al. (2013), Güncü et al. (2011) and Apostolakis and Bissoon (2014), are in support of our study and show no statistical significance among gender and age groups. In contrast, comparison with younger age groups, Mardinger et al. (2007) found that elderly patients had larger diameter.

For the purpose of our study, the course of PSAA was divided into three types: Type I: Superficial; Type II: Intraosseous; and Type III: Intrasinusal.

When assessing the path of PSAA in relation to the lateral wall based on the visibility, we found Type II intraosseous course (30%) (n=40), followed by Type III intrasinusal (20%), (n=40) and then Type I superficial course (5%) (n=40) at all examined locations and remaining were not located.

Our findings show similar results to the previous studies revealing the most frequent course as intraosseous by Güncü et al. (2011) (68.2% of intraosseous course, 26% intrasinusal course). Ella et al. (2008) (71.4 % of intraosseous course, 14.3% intrasinusal course), Ilgüy et al. (2013) (71.1% of intraosseous course, 13% intrasinusal course), Kang et al. (2013) (64.3% of intraosseous course, 29.1% intrasinusal course).

The key anatomical points of the maxillary sinus and the position of PSAA were clearly demonstrated in this study. As a result, these parameters are recommended for offering complication-free implant planning operations.

The main observations made from the study are the following:

- Mean thickness of maxillary sinus lateral wall
- Prevalence and Course of PSAA
- Mean distance of PSAA from maxillary sinus floor
- PSAA mean diameter

The average thickness of the lateral wall of the maxillary sinus was determined to be approximately around 2.50 mm. PSAA was observed in 25% of subjects, with a maximum distance of 8.83mm from the maxillary sinus floor and a minimum distance of 6.90 mm. PSAA had a diameter of 1-2mm with the intraosseous course in most individuals.

The above parameters were found to be statistically insignificant between genders, dental status and age groups. It is concluded from the results of our study that the abovementioned observations are an important factor to address in order to reduce the probable consequences before and during surgery.

REFERENCES

APOSTOLAKIS D, BISSOON AK (2014) Radiographic evaluation of the superior alveolar canal: measurements of its diameter and of its position in relation to the maxillary sinus floor: a cone beam computerized tomography study. *Clin Oral Implants Res*, 25: 553-559.

ELLA B, SÉDARAT C, DA COSTA NOBLE R, NORMAND E, LAUVERJAT Y, SIBERCHICOT F, CAIX P, ZWETYENGA N (2008) Vascular connections of the lateral wall of the sinus: surgical effect in sinus augmentation. *Int J Oral Maxillofac Implants*, 23(6): 1047-1052.

FAYEK MM, AMER ME, BAKRY AM (2021) Evaluation of the posterior superior alveolar artery canal by cone-beam computed tomography in a sample of the Egyptian population. *Imaging Science in Dentistry*, 51: 35-40.

GÜNCÜ GN, YILDIRIM YD, WANG HL, TÖZÜM TF (2011) Location of posterior superior alveolar artery and evaluation of maxillary sinus anatomy with computerized tomography: a clinical study. *Clin Oral Implants Res*, 22(10): 1164-1167.

ILGÜY D, ILGÜY M, DOLEKOGLU S, FISEKCIOGLU E (2013) Evaluation of the posterior superior alveolar artery and the maxillary sinus with CBCT. *Braz Oral Res*, 27(5): 431-437.

JUNG J, YIM JH, KWON YD, AL-NAWAS B, KIM GT, CHOI BJ, LEE DW (2011) A radiographic study of the position and prevalence of the maxillary arterial endosseous anastomosis using cone beam computed tomography. *Int J Oral Maxillofac Implants*, 26(6): 1273-1278.

KANG SJ, SHIN SI, HERR Y, KWON YH, KIM GT, CHUNG JH (2013) Anatomical structures in the maxillary sinus related to lateral sinus elevation: a cone beam computed tomographic analysis. *Clin Oral Implants Res*, 24(Suppl A100): 75-81.

KHAJEHAHMADI S, RAHPEYMA A, HOSEINI ZARCH SH (2014) Association between the lateral wall thickness of the maxillary sinus and the dental status: cone beam computed tomography evaluation. *Iran J Radiol*, 11: e6675.

KIAKOJORI A, NASAB S, ABESI F, GHOLINIA H (2017) Radiographic assessment of maxillary sinus lateral wall thickness in edentulous posterior maxilla. *Electronic Physician*, 9: 5948-5953.

MANJUSHRI WAINGADE, SOMESHWARI SALUNKHE, RAGHAVENDRA S MEDIKERI (2021) Assessment of position of posterior superior alveolar artery in relation to maxillary sinus using cone-beam computed tomography. *J Orofacial Sci*, 13: 105-113.

MARDINGER O, ABBA M, HIRSHBERG A, SCHWARTZ-ARAD D (2007) Prevalence, diameter and course of the maxillary intraosseous vascular canal with relation to sinus augmentation procedure: a radiographic study. *Int J Oral Maxillofac Surg*, 36(8): 735-738.

MONJE A, CATENA A, MONJE F, GONZALEZ-GARCÍA R, GALINDO-MORENO P, SUAREZ F, WANG HL (2014) Maxillary sinus lateral wall thickness and morphologic patterns in the atrophic posterior maxilla. *J Periodontol*, 85:676– 682.

RAJA SV (2009) Management of the posterior maxilla with sinus lift: review of techniques. *J Oral Maxillofac Surg*, 67: 1730-1734.

ROSANO G, TASCHIERI S, GAUDY JF, DEL FABBRO M (2009) Maxillary sinus vascularization: a cadaveric study. *J Craniofac Surg*, 20(3): 940-943.

SCHWARTZ-ARAD D, HERZBERG R, DOLEV E (2015) The prevalence of surgical complications of the sinus graft procedure and their impact on implant survival. *J Periodontol*, 75: 511-516.

TALO YILDIRIM T, GÜNCÜ G, COLAK M, TÖZÜM T, F (2019) The relationship between maxillary sinus lateral wall thickness, alveolar bone loss, and demographic variables: a cross-sectional cone-beam computerized tomography study. *Med Princ Pract*, 28: 109-114.

TARUN KUMAR AB, ANAND U (2015) Maxillary sinus augmentation. *J Int Clin Dent Res Organ*, 7, Suppl S1: 81-93.

VAN CAUWENBERGE P, SYS L, DE BELDER T, WATELET JB (2004) Anatomy and physiology of the nose and the paranasal sinuses. *Immunol Allergy Clin North Am*, 24: 1-17.

WALLACE SS, TARNOW DP, FROUM SJ, CHO SC, ZADEH HH, STOUPEL J, DEL FABBRO M, TESTORI T (2012) Maxillary sinus elevation by lateral window approach: evolution of technology and technique. *J Evid Based Dent Pract*, 12(Suppl 3): 161-171.

WATANABE T, SHIOTA M, GAO S, IMAKITA C, TACHIKAWA N, KASUGAI S (2014) Verification of posterior superior alveolar artery distribution in lateral wall of maxillary sinus by location and defect pattern. *Quintessence Int*, 45: 673-678.

WOO I, LE BT (2004) Maxillary sinus floor elevation: review of anatomy and two techniques. *Implant Dent*, 13: 28-32.

YANG SM, PARK SI, KYE SB, SHIN SY (2012) Computed tomographic assessment of maxillary sinus wall thickness in edentulous patients. *J Oral Rehabil*, 39: 421-428.

YU SJ, LEE YH, LIN CP, WU AYJ (2019) Computed tomographic analysis of maxillary sinus anatomy relevant to sinus lift procedures in edentulous ridges in Taiwanese patients. *J Periodontal Implant Sci*, 49(4): 237-247.

ZIJDERVELD SA, VAN DEN BERGH JP, SCHULTEN EA, TEN BRUGGENKATE CM (2008) Anatomical and surgical findings and complications in 100 consecutive maxillary sinus floor elevation procedures. *J Oral Maxillofac Surg*, 66: 1426-1438.

Insulin improves ovarian function during the ovarian cycle in adult mice

Ali Younesi[1,2*], Mohammad Hossein K. Godaneh[1,2*], Mohammad Mahdi Gheibi[1,2], Mohammad A.T. Zavareh[1], Sanaz Ziaeipour[1], Abbas Aliaghaei[1], Amirhosein Hasani[1], Amirreza Khosravi[1], Vahid Ebrahimi[3], Amir Raoofi[4], Shabnam Abdi[5], Mohammad-Amin Abdollahifar[1,2]

[1] Cellular and Molecular Biology Research Center, Shahid Beheshti University of Medical Sciences, Tehran, Iran

[2] Department of Biology and Anatomical Sciences, School of Medicine, Shahid Beheshti University of Medical Sciences, Tehran, Iran

[3] Department of Anatomy and Cell Biology, School of Medicine, Mashhad University of Medical Sciences, Mashhad, Iran

[4] Leishmaniasis Research Center, Department of Anatomy, Sabzevar University of Medical Sciences, Sabzevar, Iran

[5] Department of Anatomical Sciences and Cognitive Neuroscience, Faculty of Medicine, Tehran Medical Sciences, Islamic Azad University, Tehran, Iran

SUMMARY

Folliculogenesis is controlled by numerous inside and outside ovarian factors such as endocrine, paracrine, and autocrine signals. Among these factors, insulin is an important molecule that regulates processes in the female reproductive system. So, the purpose of this study was to determine the impact of insulin treatment on ovary tissue during the ovarian cycle. For this probe, 18 adult female NMRI mice were randomly divided into two groups: control and insulin (100 µL with a 72-hour interval by intraperitoneal injection for 30 days). Blood samples for hormonal evaluation were obtained from the heart, and the serum levels of FSH, LH, progesterone, and estradiol were measured. Then, right and left ovaries were extracted for real-time PCR and stereology, respectively. According to our results, insulin administration increased mRNA levels of INS-R, Ki67, while reduced Caspase-3, IGF-1, and FOXO-1. Insulin administration augmented the concentrations of female reproductive hormones. Histological analyses showed that the total volume of ovary in mice receiving insulin was significantly reduced. Likewise, a significant decrease in the number of antral follicles, Graafian follicles, and the number of corpora lutea were seen following the use of insulin. In contrast, the results showed a significant growth in the number of primordial and primary follicles in the insulin group compared with the control group. Briefly, insulin administration is able to increase the expression of genes related to insulin receptor and cell proliferation, as well as the amount of female reproductive hormones, but simultaneously, has a dual effect on the histological parameters of the ovary.

Corresponding author:
Mohammad-Amin Abdollahifar, Cellular and Molecular Biology Research Center, Shahid Beheshti University of Medical Sciences, Tehran, Iran and Department of Biology and Anatomical Sciences, School of Medicine, Shahid Beheshti University Tehran, Iran. Arabi Ave, Daneshjoo Blvd, Velenjak, Tehran, Iran. Post Code: 19839-63113. Phone: +98 21 22 43 97 70. Orcid: 0000-0001-6947. E-mail: m_amin58@yahoo.com / abdollahima@sbmu.ac.ir

Submitted: March 7, 2022. **Accepted:** April 4, 2022

https://doi.org/10.52083/NJHH1910

**These two authors contributed equally to this work.*

Key words: Ovarian function – Ovarian cycle – Insulin – Adult mice

INTRODUCTION

An oocyte is a female germ cell which is required in female reproduction. The oocyte develops during the process of oogenesis (folliculogenesis) in the ovarian follicle, a specialized unit of the ovarian cortex (Virant-Klun et al., 2015). It is commonly accepted that human ovaries consist of a fixed number of primordial follicles which are formed before birth, decrease with age and are depleted in menopause (Bendsen et al., 2006; Forabosco and Sforza, 2007). In general, oogenesis, as well as folliculogenesis, are regulated by a large number of intra-ovarian factors and extra-ovarian factors. On the other hand, follicular development as well as oocyte maturation are regulated by the highly complex coaction of endocrine, paracrine, and autocrine signals. Different organs, such as the hypothalamus, the anterior pituitary gland, the gonads and also the hypothalamic-pituitary-gonadal axis have a pivotal role in the follicular development as well as oocyte maturation (Nagahama and Yamashita, 2008; Edson et al., 2009). Among the effective factors in female reproductive system, insulin is one of the most effective molecules that regulate ovarian development and oogenesis (Saltiel and Kahn, 2001).

It was reported that insulin-signaling is essential for ovulation, differentiation of granulosa cell, and female fertility (Sekulovski et al., 2020). And it is also accepted that in humans, hypoinsulinemia or hyperinsulinemia is in connection with ovarian function (Chang et al., 2005). Based on previous studies, the insulin receptor is a member of the ligand-activated receptor as well as tyrosine kinase family of transmembrane-signaling proteins which basically have a substantial role in the regulation of cell differentiation, cell growth and metabolism (Lee and Pilch, 1994).

Insulin receptor is expressed both in the thecal granulosa compartment as well as the oocyte surface, and it is right to point that, signaling pathways which are dependent on Insulin receptor promote oocyte maturation and follicular development (Das et al., 2016).

It has been reported that insulin is a key regulator of female reproduction, and insulin-sensitizing drugs are actually the only choice to reverse reproductive dysfunctions associated with metabolic disorders, such as insulin resistance, diabetes, and obesity (Das and Arur, 2017). On the other hand, polycystic ovary syndrome is one of the most prevalent systemic reproductive endocrine diseases as well. Recent studies have demonstrated that the main etiology and primary endocrine disorder of PCOS are hyperandrogenemia as well as insulin resistance (Wang et al., 2019). Based on other studies, insulin and insulin-like growth factors play a pivotal role in modification of the FSH-dependent cellular differentiation related to human granulosa cells (Garzo and Dorrington, 1984), and both insulin and somatotrophin can also lead to increase the level of IGF-I production by ovarian follicles. So that even insulin is significantly effective in reducing atresia and increasing progesterone during follicular culture (Cox et al., 1997). It has been reported that insulin, IGF-I and IGF-II are survival factors for early stage of human follicular development (Louhio et al., 2000).

The connection between the female reproductive system and the beneficial effects of insulin has been reported in previous studies, but more detailed understanding of insulin's action in regulation of oogenesis and folliculogenesis may be utilizable in opening the door to important medical applications. Thus, the aim of this study is evaluation of the effects of exogenous insulin on follicular development and some genes' expression related to this issue in adult female mice.

MATERIALS AND METHODS

Animals

For this study, 18 adult female NMRI mice weighing 25-30 g were attained from the Pasteur Institute, Tehran, Iran. All animals were cared under animal house standard conditions, including limitless access to water and food, 12-12-hour light/dark cycle, and normal room temperature (22±2°C). Then, the mice were randomly divided into two main control and insulin groups.

Treatments and sampling

Insulin (Sigma, St. Louis, MO, USA) was prepared by diluting in water. Each animal in experimental group received 100 µL of insulin with a 72-hour interval by intraperitoneal (IP) injection for 30 days. Control mice also were treated with similar amounts of water.

Hormonal measurement

Following deep anesthesia, blood samples for hormonal evaluation were gained from the heart of animals. Then, the blood samples were centrifuged at 6000 g at 4°C for 5 min before keeping them at -80°C until ready to be used. Subsequently, specific ELISA kit (EIA: Enzyme Immunoassay) for mice was applied to measure the blood serum levels of FSH, LH, progesterone, and estradiol using, according to the manufacturer's instructions. Results of FSH and LH were reported as Iu/mL, while progesterone as ng/mL and estradiol as pg/mL.

Total RNA extraction and real-time PCR

At the end of the treatment period, right ovaries were extracted for real-time PCR. For this purpose, whole RNA samples were extracted from ovary tissue, by means of the High Pure RNA Isolation kit, based on the manufacturer's instructions (Roche, Basel, Switzerland) and treated with DNase I (Roche, Basel, Switzerland) to eliminate genomic DNA contamination. Next, cDNA was synthesized in a total volume of 20 µl using a kit (Fermentas, Lithuania) at 42 °C for 60 min. Then, applied real-time PCR (TaqMan) was used based on QuantiTect SYBR Green kit (Takara Bio Inc, Japan) aimed at quantification of mRNA expression levels of INS-R, Ki67, Caspase-3, IGF-1, and FOXO-1 among two groups. All reverse and forward primer pairs were designed according to Primer 3 Plus software in exon-exon junction way to discriminate cDNA and genomic DNA. Beforehand, PCR primers were checked by Primer-Blast tool (Ebrahimi et al., 2019).

Stereological evaluation

Mice were profoundly anesthetized and sacrificed by IP injection of sodium pentobarbital. Subsequently, transcardial perfusion was made using chilled normal saline and fresh fixative solution, containing 4% paraformaldehyde (PFA) in 0.1 M phosphate-buffered saline (PBS). Finally, the left ovary samples of animals were extracted, placed in 10% formalin solution, sectioned into 5µm slices, and prepared for histological hematoxylin and eosin (HandE) staining and stereological analysis. The following factors were estimated in ovarian tissue: volume of ovary and the total number of primordial, primary, antral, Graafian follicles, and finally, the total number of corpora lutea. The total volume of the ovary was estimated using the Cavalieri method and following formula:

$$V\_total = \sum P \times \frac{a}{p} \times t$$

In this formula, Σp is the total number of points superimposed on the microscopic photos, and (a/p) is the area associated with each point, and t is the thickness of the microscopic sections.

Besides, the total number of ovarian cells and corpora lutea was measured via the optical dissector technique and also succeeding principles: The numerical density (N_v) was considered as:

$$N_v = \frac{\sum Q}{\sum P \times h \times \frac{a}{f}} \times \frac{t}{BA}$$

In this formula, ΣQ is the number of the cell nuclei, ΣP is the total number of the unprejudiced calculating frame in all fields of ovarian tissue, h is the height of the dissector, ratio a to f (a/f) is the frame area, t is the actual slice thickness measured in every field of tissue using the microcator, and BA is the block advance of the microtome which was fixed for 10 µm.

Statistical analysis

The results were analyzed by Kruskal Wallis test, using the SPSS software version 19.00 (IBM Corp., Armonk, NY, USA). $P<0.05$ was considered as significant differences.

RESULTS

Insulin administration increased mRNA levels of INS-R, Ki67, while reduced Caspase-3, IGF-1, and FOXO-1 during ovarian cycle

According to real time-PCR data, insulin treatment significantly improved the expression of mRNA levels of insulin receptor (INS-R), as well as proliferation marker (Ki67) in ovarian tissue compared to the control group (in both cases, $P<0.05$, Fig. 1). On the other hand, insulin administration significantly decreased the expression of mRNA levels Caspase-3 as a typical marker of apoptosis as well as IGF-1 and FOXO-1 in ovarian tissue compared to the control group (in the case of all three genes, $P<0.05$, Fig. 1).

Table 1. Primers design.

Genes	Primer sequences
INSR	F: GAGAGTGGTGGAGTTGAGTTGG R: TGTGGAGGATGGAGGAGGAG
Ki 67	F: AGGAAAGTAGATAGGAAGGAAG R: AGGGAGTGGTGATAGAAAGAG
FOXO1	F: AACTGAGGAGCAGTCCAAAGATG R: AACTGAGGAGCAGTCCAAAGATG
IGF1	F= GGAAGCTATGGAGTGGGAAAAG R= CCGAGAGGTGGAGTGATTTGA
Caspase3	F= AGTGGGACTGATGAGGAGATGG R= AGTGGAGTACAGGGAGAAGGA
β-actin	F= TCAGAGCAAGAGAGGCATCC R= GGTCATCTTCTCACGGTTGG

Insulin administration augmented the concentrations of reproductive hormones during ovarian cycle

Based on hormonal analysis, insulin treatment significantly improved the concentration of FSH ($P<0.05$, Fig. 2A), LH ($P<0.05$, Fig. 2A), and estradiol ($P<0.01$, Fig. 2B). However, this increase was not significant for progesterone (Fig. 2B).

Insulin administration altered histological parameters during ovarian cycle

At the end of the experiment, histological analyses showed that the total volume of ovarian tissue in mice receiving insulin was significantly reduced compared to mice in the control group ($P<0.05$, Fig. 3B).

Likewise, the results obtained from the cell count indicated a significant decrease in the total number of ovarian antral follicles ($P<0.001$, Fig. 2A), Graafian follicles ($P<0.01$, Fig. 2B), and the total number of corpora lutea ($P<0.001$, Fig. 2B) following the use of insulin compared with the control group. On the contrary, the results revealed a significant rise in the total number of both ovarian primordial and primary follicles in insulin-treated mice compared to the control group ($P<0.001$ and $P<0.05$, respectively) (Fig. 2A).

DISCUSSION

In the present study, the data showed the level of mRNA expression in genes related to insulin receptor and Ki67 significantly increased, and the level of mRNA expression in genes related to executioner caspase-3, IGF-1 and FOXO-1 significantly decreased. On the other hand, the data of this study showed that, the Serum level of FSH, LH and Estradiol as well as the number of primordial and primary follicles significantly increased. It is right to point that, the insulin receptor is a tyrosine kinase receptor that upon binding insulin, catalyzes the phosphorylation of several intracellular substrates, including the insulin receptor substrate proteins (IRSs), GAB-1, Shc, APS, p60DOK, SIRPS, and c-Cbl. Each of these substrates interacts with a series of signalling proteins which lead to initiation of different signalling pathways (Saltiel and Pessin, 2002; Shaw et al., 2011). Following phosphorylation, the binding of the regulatory subunit of insulin receptor to IRSs forms an active heterodimer which phosphorylates membrane phosphatidylinositol residues in the 3′ position of PIP3 to form PDK1/2 and thereafter activates Akt/PKB (Dupont and Scaramuzzi, 2016). On the Oder hand, mTORC2 is activated by insulin and controls cell survival, metabolism, and cytoskeletal organization (Yoon et al., 2017). These pathways can lead to reduction of apoptosis and insulin may have reduced gene expression of executioner caspases-3 in these pathways.

As previous studies have shown, FSH can enhance cell proliferation via mTOR and/or ERK and inhibit apoptosis via Akt1 and FOXO3a

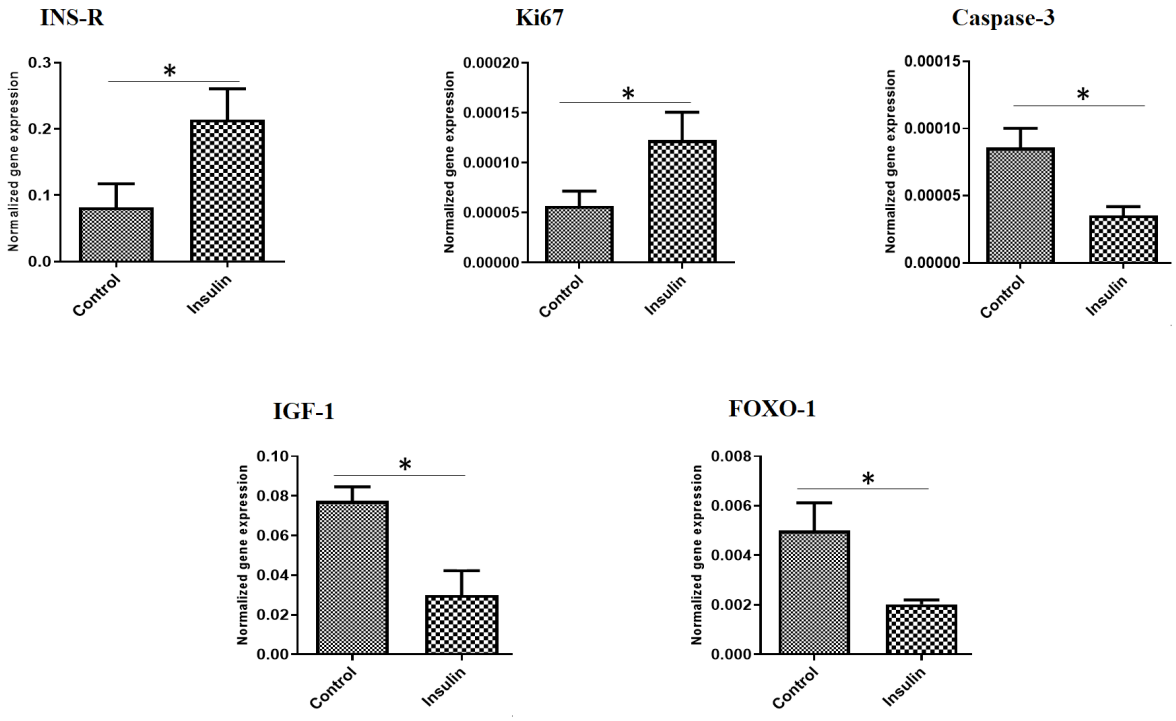

Fig. 1.- The effect of insulin administration on the expression of genes involved in the mechanism of insulin function, proliferation and apoptosis during ovarian cycle of NMRI mice Insulin injection significantly increased mRNA levels of INS-R (*P<005), Ki67 (*P<005), while significantly reduced caspase-3 (*P<005), IGF-1 (*P<005), and FOXO-1 (*P<005) in treated mice compared with the control mice.

(Dupont and Scaramuzzi, 2016). In this regard, in present study, the data showed that the serum level of FSH has increased in response to insulin so that it can be said, by increasing FSH, insulin has been able to increase proliferation and expression of Ki67 and also reduce apoptosis. Based on previous studies, it is reported that, the expression and activity of FOXO1 are modulated by LH and FSH via PI3K/Akt pathway (Liu et al., 2009). Therefore, it can be said that, increased level of LH and FSH have led to modulation of FOXO1 gene expression, after insulin injection.

On the other hand, insulin signalling via AKt1 and FOXO1 can increase the level of LH-stimulated steroidogenesis. Therefore, elevated level of LH can lead to increase steroidogenesis. There are

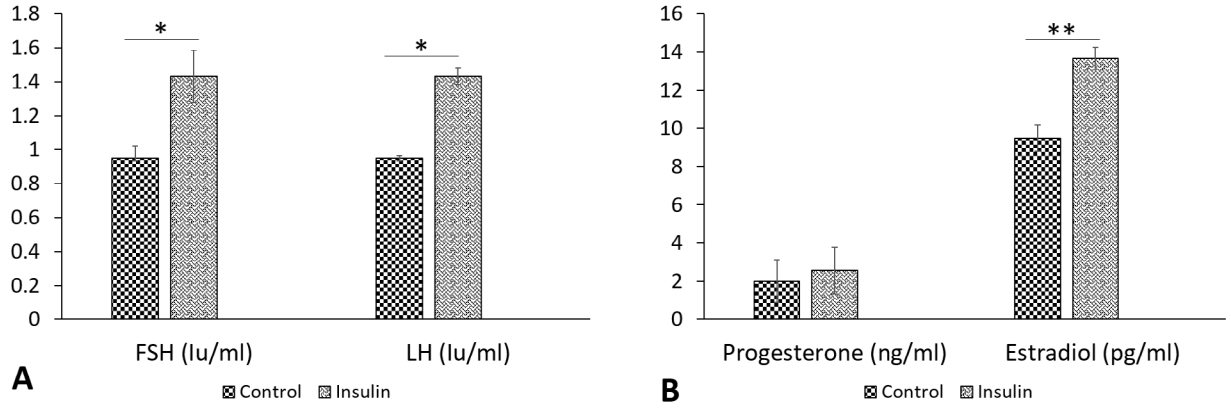

Fig. 2.- The effect of insulin administration on hormonal alterations during ovarian cycle of NMRI mice Insulin injection significantly improved the concentration of FSH (*P<005), LH (*P<005), and estradiol (**P<001). However, this increase was not significant for progesterone.

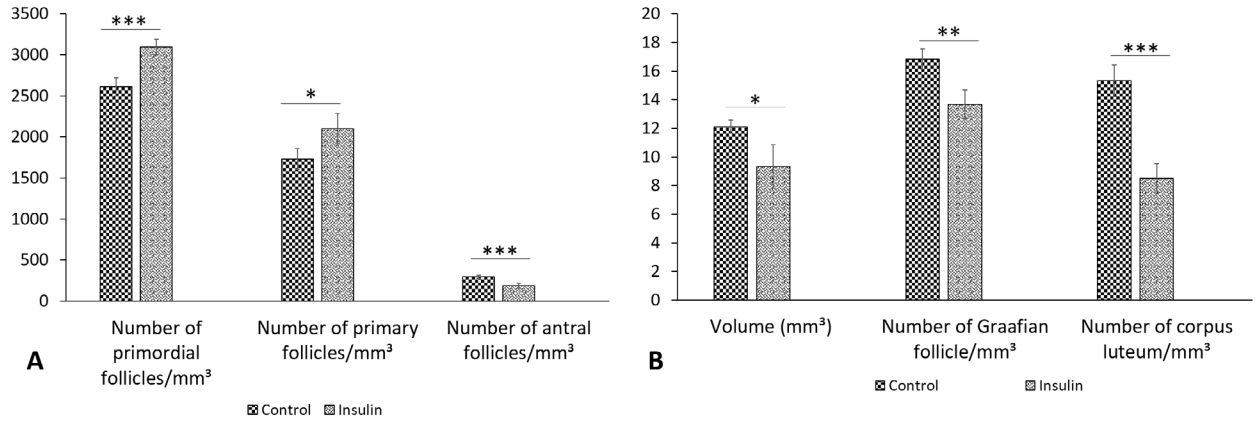

Fig. 3.- The effect of insulin administration on histological changes during ovarian cycle of NMRI mice Histological analyses showed that the total volume of ovarian tissue in group receiving insulin was significantly reduced compared to the control group (*P<005) Similarly, a significant decrease in the total number of ovarian antral follicles (***P<0001), Graafian follicles (**P<001), and the total number of corpus luteum (**P<0001) were observed following insulin usage compared with the control group In contrast, a significant rise in the total number of ovarian primordial and primary follicles in insulin-treated mice compared to the control mice (***P<0001 and *P<005, respectively).

many studies in which beneficial effects of Insulin on ovarian function were reported and they confirm the data of present study. For example it was reported that, the increase in the level of growth hormone may be involved in follicular development to enter the ovulatory phase, and the insulin system may support the maturation of preovulatory follicles (Shimizu et al., 2008). And it was also demonstrated that insulin, insulin-like growth factor I, and gonadotropins have significant role in granulosa cell proliferation, progesterone production, estradiol production, and insulin-like growth factor I production in vitro (Spicer et al., 1993), and following the increase in insulin-like growth factor I, this hormone is able to control tissue homeostasis, cell proliferation and apoptosis (Kooijman et al., 2006).

It was reported that insulin signalling can lead to increasing proliferation and hyperplasia of the ovarian surface epithelium, which has approximately 4–6 cell layers with a high rate of proliferation, as well as decrease in follicular integrity via upregulation of the PI3-kinase pathway (King et al., 2013). Furthermore, the data of the present study showed that the number of primordial and primary follicles in the insulin group are increased in comparison

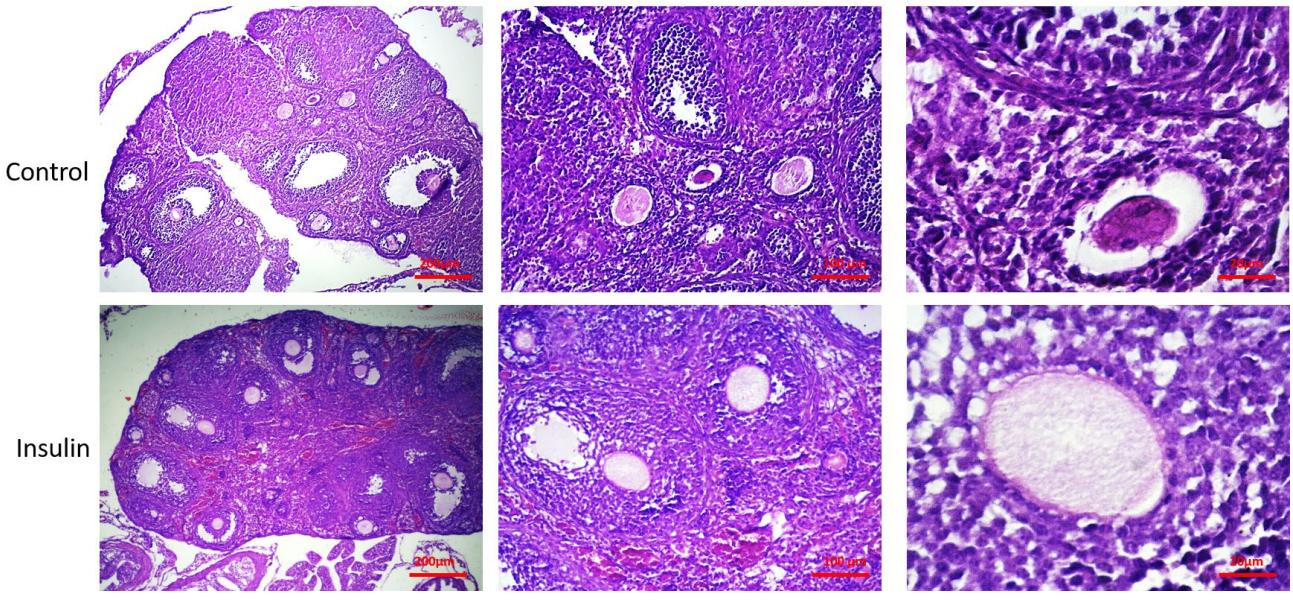

Fig. 4.- Photomicrograph of the ovaries stained with HandE (4x, 10x and 40x) in study groups.

with the control group, and there is no evidence of an increase in the number of Graffian follicle or in antral follicle while, based on the data of gene expression, it is predicted that in the gonadotropin-dependent stages of follicular development, insulin may play a significant role. Thus, it is suggested that, in future studies, the period of insulin injection should be longer for more accurate outcomes. In conclusion, based on the data of this study, it can be said that insulin improves the function of ovarian tissue during the ovarian cycle. Overall, it can be concluded that insulin administration is able to rise the expression of genes related to insulin receptor and cell proliferation, as well as the amount of female reproductive hormones, but at the same time has a dual effect on histological parameters of the ovary, including the volume of ovary as well as growing follicles.

ACKNOWLEDGEMENTS

This work has been performed at Department of Biology and Anatomical Sciences, School of Medicine, Shahid Beheshti University of Medical Sciences, Tehran, Iran (registration No: 24874). The study was funded by Cellular and Molecular Biology Research Center, Shahid Beheshti University of Medical Sciences, Tehran, Iran (Grant number:1399-24874).

STATEMENT OF ETHICS

The authors declare that all experiments protocols were approved by the Ethics Committee, Deputy of Research, Shahid Beheshti University of Medical Sciences, Tehran, Iran (IR.SBMU.RETECH.REC.1399.1120). All methods were carried out in accordance with relevant guidelines and regulations.

REFERENCES

BENDSEN E, BYSKOV A, ANDERSEN CY, WESTERGAARD LG (2006) Number of germ cells and somatic cells in human fetal ovaries during the first weeks after sex differentiation. *Human Reprod,* 21: 30-35.

CHANG AS, DALE AN, MOLEY KH (2005) Maternal diabetes adversely affects preovulatory oocyte maturation, development, and granulosa cell apoptosis. *Endocrinology,* 146: 2445-2453.

COX NM (1997) Control of follicular development and ovulation rate in pigs. *J Reprod Fertil, Supplement,* 52: 31-46.

DAS D, ARUR S (2017) Conserved insulin signaling in the regulation of oocyte growth, development, and maturation. *Mol Reprod Develop,* 84: 444-459.

DAS D, NATH P, PAL S, HAJRA S, GHOSH P, MAITRA S (2016) Expression of two insulin receptor subtypes, insra and insrb, in zebrafish (*Danio rerio*) ovary and involvement of insulin action in ovarian function. *Gen Comp Endocrinol,* 239: 21-31.

DUPONT J, SCARAMUZZI RJ (2016) Insulin signalling and glucose transport in the ovary and ovarian function during the ovarian cycle. *Biochem J,* 473: 1483-1501.

EBRAHIMI V, BOROUJENI ME, ALIAGHAEI A, ABDOLLAHIFAR MA, PIRYAEI A, HAGHIR H, SADEGHI Y (2020) Functional dopaminergic neurons derived from human chorionic mesenchymal stem cells ameliorate striatal atrophy and improve behavioral deficits in Parkinsonian rat model. *Anat Rec (Hoboken),* 303: 2274-2289.

EDSON MA, NAGARAJA AK, MATZUK MM (2009) The mammalian ovary from genesis to revelation. *Endocr Rev,* 30: 624-712.

FORABOSCO A, SFORZA C (2007) Establishment of ovarian reserve: a quantitative morphometric study of the developing human ovary. *Fertil Steril,* 88: 675-683.

GARZO VG, DORRINGTON J (1984) Aromatase activity in human granulosa cells during follicular development and the modulation by follicle-stimulating hormone and insulin. *Am J Obstet Gynecol,* 148: 657-662.

KING SM, MODI DA, EDDIE SL, BURDETTE JE (2013) Insulin and insulin-like growth factor signaling increases proliferation and hyperplasia of the ovarian surface epithelium and decreases follicular integrity through upregulation of the PI3-kinase pathway. *J Ovarian Res,* 6: 1-15.

KOOIJMAN R (2006) Regulation of apoptosis by insulin-like growth factor (IGF)-I. *Cytokine Growth Factor Rev,* 17: 305-323.

LEE J, PILCH PF (1994) The insulin receptor: structure, function, and signaling. *Am J Physiol Cell Physiol,* 266: C319-C334.

LIU Z, RUDD MD, HERNANDEZ-GONZALEZ I, GONZALEZ-ROBAYNA I, FAN H-Y, ZELEZNIK AJ, RICHARDS JS (2009) FSH and FOXO1 regulate genes in the sterol/steroid and lipid biosynthetic pathways in granulosa cells. *Mol Endocrinol,* 23: 649-661.

LOUHIO H, HOVATTA O, SJÖBERG J, TUURI T (2000) The effects of insulin, and insulin-like growth factors I and II on human ovarian follicles in long-term culture. *Mol Human Reprod,* 6: 694-698.

NAGAHAMA Y, YAMASHITA M (2008) Regulation of oocyte maturation in fish. *Development, Growth Different,* 50: S195-S219.

SALTIEL AR, KAHN CR (2001) Insulin signalling and the regulation of glucose and lipid metabolism. *Nature,* 414: 799-806.

SALTIEL AR, PESSIN JE (2002) Insulin signaling pathways in time and space. *Trends Cell Biol,* 12: 65-71.

SEKULOVSKI N, WHORTON AE, SHI M, HAYASHI K, MACLEAN JA (2020) Periovulatory insulin signaling is essential for ovulation, granulosa cell differentiation, and female fertility. *FASEB J,* 34: 2376-2391.

SHAW LM (2011) The insulin receptor substrate (IRS) proteins: at the intersection of metabolism and cancer. *Cell cycle,* 10: 1750-1756.

SHIMIZU T, MURAYAMA C, SUDO N, KAWASHIMA C, TETSUKA M, MIYAMOTO A (2008) Involvement of insulin and growth hormone (GH) during follicular development in the bovine ovary. *Animal Reprod Sci,* 106: 143-152.

SPICER L, ALPIZAR E, ECHTERNKAMP S (1993) Effects of insulin, insulin-like growth factor I, and gonadotropins on bovine granulosa cell proliferation, progesterone production, estradiol production, and (or) insulin-like growth factor I production in vitro. *J Animal Sci,* 71: 1232-1241.

VIRANT-KLUN I (2015) Postnatal oogenesis in humans: a review of recent findings. *Stem Cells Cloning,* 8: 49-60.

WANG J, WU D, GUO H, LI M (2019) Hyperandrogenemia and insulin resistance: the chief culprit of polycystic ovary syndrome. *Life Sci,* 236: 116940.

YOON M-S (2017) The role of mammalian target of rapamycin (mTOR) in insulin signaling. *Nutrients,* 9: 1176.

Prevalence of styloid process elongation on digital panoramic radiography in South India population from Chengalpet district

Krishnaeswari Veluchamy[1], D.H. Gopalan[2], Murali Punniakotti[3], M. Vani[1]

[1] Department of Anatomy, Karpaga Vinayaga Institute of Medical Sciences & Research Centre, Palayanoor, Madhurathagam, Tamilnadu - 603308. India

[2] Department of Anatomy, Tagore Medical College and Hospital, Chennai – 600 127, India

[3] Department of Anatomy, SRM Institute of Science and Technology, Chennai – 603 203, India

SUMMARY

The styloid process (SP) arises from the temporal bone in front of the stylomastoid foramen. Many nerves and vessels are adjacent to the SP. The length of the SP is usually 2-3 cm; if it is longer than 3 cm, it is considered elongated. The elongated SP may compress adjacent neurovascular structures, and cause neck and cervicofacial pain. This study aims to determine the prevalence of SP elongation detected on digital panoramic radiographs in the south Indian population from the Chengalpet region and its relation to gender, age, sides and types. Digital panoramic radiographs of 1000 patients with an age ranging from 10 to 80 years were retrospectively obtained from a private dental college. The subjects were divided into six age subgroups: 10-19, 20-29, 30-39, 40-49, 50-59, and 60 years and older. The apparent length of the SP was measured from the point where it left the temporal bone to its tip. SP measuring more than 3 cm were considered to be elongated. The data were analyzed by using Student's t-test and Chi-square test with a P value less than 0.05. The study findings reported that SP elongation was present in sixty-two (6.2%) patients. The prevalence of SP elongation in males was slightly higher than in females. In males, there was a statistically significant difference found between age groups. The prevalence of SP elongation was increased as the age increased. The most frequently observed type of elongation was the type I elongation. The digital panoramic radiographs are an economical, easily accessible and useful diagnostic tool for early detection of SP elongation. It was found that the elongated SP is an anatomical variation, which must be taken into account by practitioners while treating the patients with head and neck pain.

Key words: Eagle's syndrome – Elongated styloid process – Panoramic radiographs – South Indian population

INTRODUCTION

Styloid Process (SP) is derived from the Greek word *stylos*, meaning a pillar (AlZarea, 2017). The

Corresponding author:
Dr. Krishnaeswari Veluchamy M.Sc., Ph.D. Department of Anatomy, Karpaga Vinayaga Institute of Medical Sciences & Research Centre, Palayanoor, Madhurathagam, Tamilnadu - 603308. India.
Phone: 9841981803. E-mail: dr2kjai@gmail.com

Submitted: February 5, 2022. **Accepted:** April 9, 2022

https://doi.org/10.52083/RRGX7659

SP is a cylindrical, slender, needle-like projection from the inferior part of the temporal bone in front of the stylomastoid foramen (Chaurasia, 2019). The tip of the SP is attached to the stylohyoid ligament and is flanked on laterally and medially by external and internal carotid arteries (Iannucci and Howerton, 2017). Many important nerves such as the facial, glosssopharyngeal, vagus, hypoglossal nerve, and internal jugular vein are medially related to the SP (Eagle, 1937). The length of the SP may vary, but the mean radiographic length of the SP is usually 2-3 cm (Bozkir et al., 1999). The SP length which is longer than 3 cm is considered to be elongated (Keur, 1986). Eagle, an otorhinolaryngologist, first described in 1937 the term Eagle's syndrome, distinguished by the elongated SP and causing clinical symptoms such as neck and cervicofacial pain (Eagle, 1948). It has also received other names: stylohyoid syndrome (Steinman, 1968; Ettinger and Hanson, 1975; Messer and Abramson, 1975; Gossman and Tarsitano, 1977), stylalgia (Patni et al., 1986), SP neuralgia (Langland et al., 1982), cervicopharyngeal pain syndrome (Camarda et al., 1989a, b; Kay et al., 2001).

Several theories have been proposed to explain the etiology of SP elongation. It was suggested that a calcified stylohyoid and stylomandibular ligament are accountable for its elongation (Camarda et al., 1989a, b). The elongated SP exerts pressure on cranial nerves VII, IX, X, XI and XII, causing symptoms such as dysphagia, foreign body sensation in the throat, vertigo, cervicofacial pain, tinnitus (Warrier, 2019). Impingement of internal or external carotid artery by medially or laterally deviated elongated SP produces pain due to stimulation of sympathetic plexus associated with the artery (Chung et al., 2007). Internal carotid artery impingement leads to pain along the course of the artery, and may be accompanied by pain in the eye and parietal cephalgia, whereas external carotid impingement causes pain in the face below the eye (Dao et al., 2011). It may also cause cerebral stroke due to the compression of carotid arteries (Asutay, 2019). Eagle's syndrome is diagnosed by both radiographical and physical examination. More commonly, a panoramic radiograph is used to determine SP elongation.

The present study aims to investigate the prevalence of SP elongation by digital panoramic radiography, and to analyze this prevalence in relation to gender and age subgroups in the South Indian population living in the Chengalpet District. According to the literature, this was the first study investigating the prevalence of SP elongation in this region.

MATERIALS AND METHODS

The study was based on 1072 digital panoramic radiographs, which were retrospectively retrieved from the archival records of Tagore Dental College and Hospital, Department of Oral Diagnosis and Radiology. The study was approved by the institutional ethical committee (IEC/TDCH/054/2021). All the digital panoramic radiographs were taken between 2019 to 2021 using Rotograph EVO D (Villa SistemiMedicalai, Buccinasco) under standard exposure factors, as recommended by the manufacturer. The panoramic radiographs of all patients between 10 and 80 years old were included, provided that the radiograph was of good quality and showed the SP bilaterally. When the panoramic radiographs' quality was not good enough, the stylohyoid complex was not clearly identified, and SP superimposed on the temporal bone, then they were excluded from this study.

The subjects were divided into six age subgroups: 10-19, 20-29, 30-39, 40-49, 50-59, 60 years and above. The mineralized stylohyoid complexes and lengths of bilateral SPs were evaluated by using Digimizer image analysis software. The apparent length of the SP was measured from the point where it originates in the temporal bone to its tip. If the length of SP is more than 3 cm, it is considered elongated. The types and calcification pattern of elongation were determined for both right and left SPs, based on the classification proposed by Langlais et al. (1986). Their classification is shown in Fig. 1a and Fig. 1b. The collected data were entered into Microsoft Excel and analyzed by using SPSS 20.0 software. Student *t-test* and Chi-square test were used for statistical analysis. *P* values less than 0.05 were accepted as statistically significant.

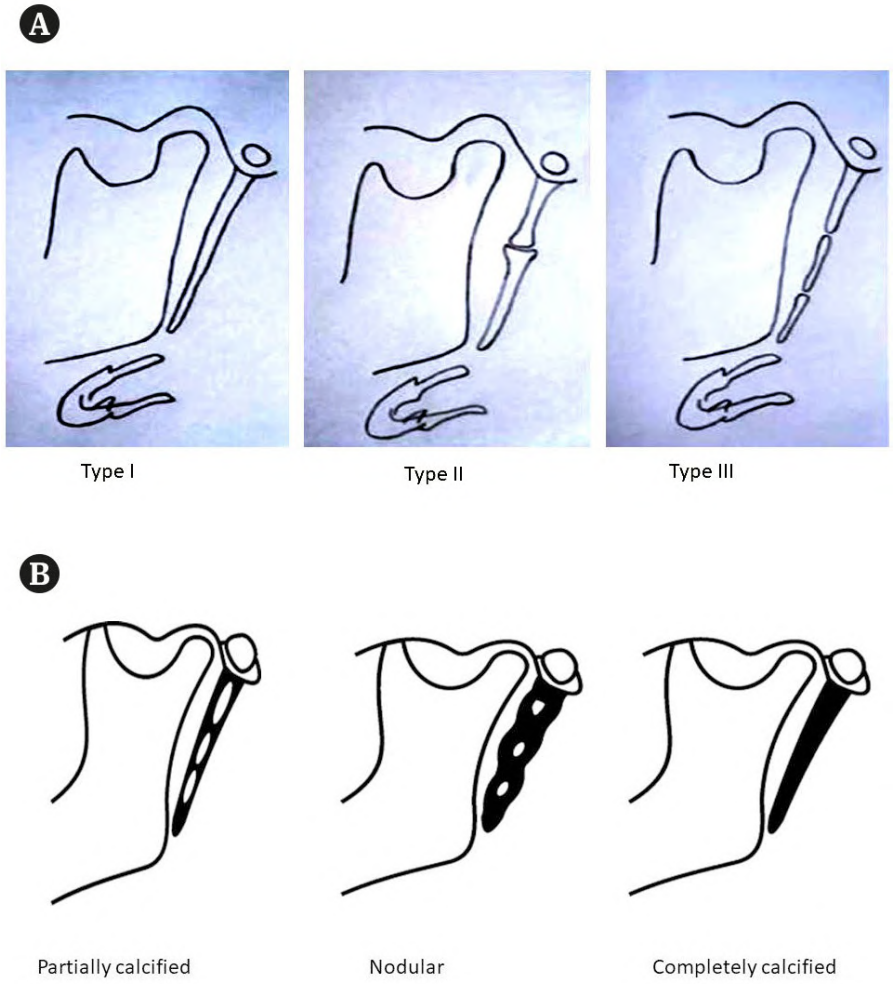

Fig.1 A- Classification of elongated styloid process (Langlais et al., 1986). Type I: uninterrupted elongation. Type II: pseudoarticulated. Type III: segmented elongation. **B-** Calcification pattern of elongated styloid process (Langlais et al., 1986).

RESULTS

Out of a total number of 1,072 digital panoramic radiographs were examined. 1,000 radiographs met our criteria and were included in this study. There were 521 male (52.1%) and 479 female (47.9%). In the study sample out of 1000 panoramic radiographs, 62 radiographs showed an elongated SP of which, 36 (6.9%) elongated SP were observed in males and 26 (5.4%) were observed in females.

Prevalence of SP elongation in relation to age in males was shown in Table 1(a). For what concerns the age groups in males, 4 out 115 (3.5%) patients between 10 and19 years old, 9 out 168 (5.4%) patients between 20 and29 years old, 2 out 81 (2.5%) patients between 30 and39 years old, 6 out 70 (8.6%) patients between 40 and 49 years old, 10 out 56 (17.9%) patients and 5 out 31 (16.1%) patients, respectively, between 50 and59 and over 60 years old showed an elongated SP. We found a statistically significant difference in the prevalence of the elongated SP in males among the age groups with a p-value lower than 0.05 (p-value<0.001). Compared to other age groups, the percentage of prevalence of SP elongation was increased in the 50-59 and above-60 age groups.

Prevalence of SP elongation in relation to age in females was shown in Table 1(b). In the case of females, 4 out 138 (2.9%) patients between 10 and 19 years old, 8 out 132 (6.0%) patients between 20 and 29 years old, 7 out 78 (8.9%) patients between 30 and 39 years old, 3 out 57 (5.3%) patients between 40 and 49 years old, 2 out 48 (4.2%) patients and 2 out 26 (5.4%) patients, respectively, between 50 and59 and over 60 years old have SP elongation. The p-value was higher than 0.05 (p-value<0.529), and showed that there

Table 1a. Styloid process elongation in relation to age in males.

	Age groups (years)	Normal	Elongated SP (%)	Total (%)	Chi-Square Value	P-value
Male	Age 10-19	111	4 (3.5%)	115(22.0%)	20.048	0.001***S
	Age 20-29	159	9 (5.4%)	168(32.2%)		
	Age 30-39	79	2 (2.5%)	81(15.5%)		
	Age 40-49	64	6 (8.6%)	70(13.4%)		
	Age 50-59	46	10(17.9%)	56(10.7%)		
	Age >60	26	5 (16.1%)	31(5.9%)		
	Total	**485**	**36 (6.9%)**	**521(52.1%)**		

Table 1b. Styloid process elongation in relation to age in females.

	Age groups (years)	Normal	Elongated SP (%)	Total (%)	Chi-Square Value	P-Value
Female	Age 10-19	134	4(2.9%)	138(28.8%)	4.145	0.529***NS
	Age 20-29	124	8(6.0%)	132(27.5%)		
	Age 30-39	71	7(8.9%)	78(16.3%)		
	Age 40-49	54	3(5.3%)	57(11.9%)		
	Age 50-59	46	2(4.2%)	48(10.0%)		
	Age >60	24	2(7.7%)	26(5.4%)		
	Total	**453**	**26(5.4%)**	**479(47.9%)**		

was no statistically significant difference in the prevalence of SP elongation in females among the age groups.

The prevalence of elongated SP in males and females according to side distribution was presented in Table 2. Out of the 26 females, 14 showed unilateral and 12 showed bilateral elongated SP, and out of 36 males 19 unilateral and 17 bilateral SP elongation were present. The percentage of the unilateral and bilateral SP elongation in males and females were almost equal. However, the percentage of unilateral is higher than that of bilateral in both male and female. But there was no statistically significant difference (*P*= 0.934) found between males and females, or betweenunilateral and bilateral distribution of elongated SP.

The Digital panoramic radiographs showing Langlais types of elongated SPs was shown in Fig. 2A to C. The distribution of types of SP elongation in both right and left side was shown in Table 3(a). The most common type of elongation observed on the right side was type I (78%). The prevalence of type II was 17%, and of type III was 5%. In the case of left side, type I was 64%, type II was 22%, and type III was 14%. The distribution of calcification pattern of SP elongation on right and left side was shown in Table 3(b). On both right and left sides, the completely calcified pattern (52% and 53%) was the most common pattern of calcification followed by partial calcification (41%and 40%) and nodular (7%) pattern, respectively.

Table 2. Distribution of elongated styloid process in males & females according to sides.

Elongated SP	Male	Female	Chi-square Value	Significance Level
Unilateral	19 (53%)	14 (54%)	0.007	0.934*** NS
Bilateral	17 (47%)	12 (46%)		
Total	36	26		

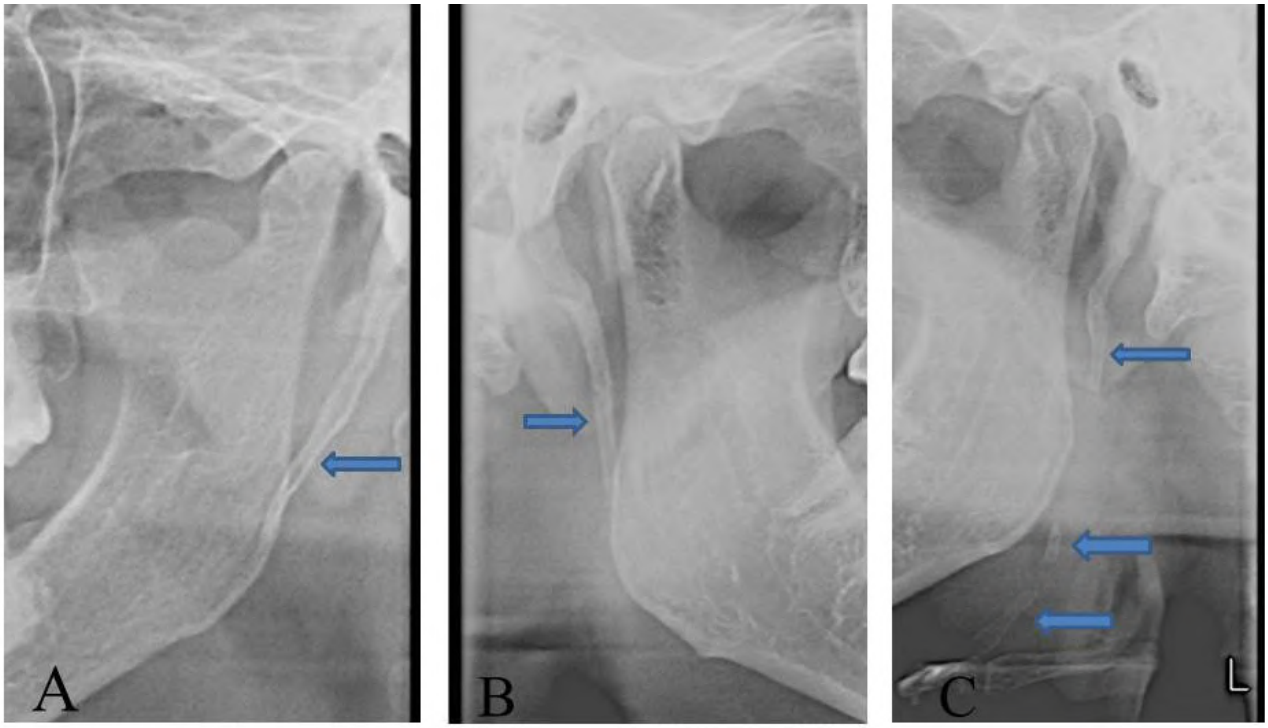

Fig. 2.- Digital panoramic radiograph showing Langlais type of elongated styloid process. **A**: Type I. **B**: Type II. **C**: Type III.

Table 3a. Distribution of types of elongated styloid process.

Elongated SP	Type I	Type II	Type III	Total
Right side	36 (78%)	8 (17%)	2 (5%)	46
Left side	29 (64%)	10 (22%)	6 (14%)	45

Table 3b. Distribution of calcification pattern of elongated styloid process.

Elongated SP	Partially calcified	Nodular	Completely calcified	Total
Right side	19 (41%)	3 (7%)	24(52%)	46
Left side	18 (40%)	3 (7%)	24 (53%)	45

DISCUSSION

The length of the SP varies from individual to individual, and from population to population. In the year 1937, Eagle, an otorhinolaryngologist, first reported that the SP that is over 3 cm was considered to be elongated, causing various clinical signs and symptoms related to the neck and cervicofacial region (Eagle 1948). Although the actual cause of SP elongation is not clear, mineralization and calcification of the tip of the SP may cause elongation. It could be due to the growth of osseous tissue at the insertion of stylohyoid ligament, or it could be due to calcification of stylohyoid ligament due to unknown processes or due to persistence of cartilaginous analog of stylohyal (Scavone et al., 2019). The resultant abnormal stylohyoid complex may irritate or exert pressure over adjacent neurovascular structures and cause clinical symptoms of Eagle Syndrome. The symptoms can be confused with some other disorders, including a wide variety of facial neuralgias, nasopharyngeal lesions, tonsillitis, otitis, oral, dental and temporomandibular diseases (Asutay et al., 2019). Hence, a detailed differential diagnosis for SP elongation should be done.

Palpation of the tip of the SP in the tonsillar fossa is indicative of SP elongation which is not normally palpable and confirmation can be done by radiographical imaging (Bagga et al., 2020). A variety of radiological approaches

are available to find out the elongated SP such as panoramic radiographs, lateral view of the skull, posterior-anterior view of the skull, and computed tomography (CT). Generally, panoramic radiography is used to detect SP elongation, because it is a simple technique and provides realistic images, allowing to replicate the SP length measurements (Chen et al., 2021).

The reported radiographic prevalence of the SP elongation varies from less than 2% to greater than 30% in the literature (Keur et al., 1986; Bozkir et al., 1999; Alpoz et al., 2014; Zaki et al., 1996). The present study exhibited that SP elongation was found in 62 out of 1000 patients, so the prevalence was 6.2%. This finding coincided with those by Austay et al. (2019), Swapna et al. (2021) and Scaf et al. (2003), who reported prevalence rates below 30%. However, this result was in contrast with the result of Chen et al. (2021) and Bagga et al. (2012), who reported that the prevalence of SP elongation was over 30%. This prevalence distribution difference in SP elongation might be due to geographical variation. The ligaments attached to the SP are more prone to ossification where the population has the habit of chewing hard foods, such as gutka and areca nut, and performing strenuous work (Bagga et al., 2012).

The prevalence percentage of elongated SP was lower in the younger age group (<19 years) compared to other age groups. This showed that the bone growth was not completed, and developmental calcification process increased as the age increased (Bruno et al., 2017). The findings by Chen et al. (2021) and Jamal et al. (2018) revealed that the length of the SP was increased with advancing age. They reported that age-related degeneration of the stylohyoid ligamentous complex and a general tendency of calcium salts deposition might be the reasons for SP elongation. Austay et al. (2019) and Gokce et al. (2008) stated that there was no correlation between the incidence of SP elongation and age. The results of the present study are also concurrent with their findings: in female, the prevalence of SP elongation was not related with age, and in the case of males, the prevalence percentage of SP elongation was higher in the groups above 50-59 years of age only.

The study results showed that the prevalence of SP elongation in males was slightly higher than in females, and this result coincides with the findings of Hettiarachchi et al. (2019) and AlZarea et al. (2017), who have reported a higher male incidence. The exact pathogenesis of SP elongation in male due to calcified and ossified bone and ligament is unclear. Explanations that have been put forward include local chronic irritation, surgical trauma, growth osseous tissue, mechanical stress or trauma during development of SP. However, this study's finding was in contrast with the findings by Ilguy et al. (2005), who observed a female-male ratio of 3:1, and Ferrario et al. (1990), who found a higher female incidence. It was suggested that endocrine disorders in women at menospause might be a reason for female predominance (Alpoz et al., 2014; Watanabe et al., 2010).

Bruno et al. (2017) and Gokce et al. (2008) reported that there was no statistically significant difference between the unilateral and bilateral distribution of SP elongation in relation to males and females. The present study's results also coincide with their findings. The most common type of elongation observed within this study was type I and the calcification pattern was the completely calcified pattern. These results were concurrent with the findings of Hettiarachchi et al. (2019) and Jamal et al. (2018). The regional factors like dietary factors might be responsible for different types and calcification patterns of elongated SP (Gokce et al., 2008).

CONCLUSION

Based on the findings of the present study, the prevalence of SP elongation in the south Indian population in the Chengalpet region was 6.2%. The prevalence rate was slightly higher in male than female. The commonest type of elongation and calcification pattern were type I and completely calcified pattern. As the age increased, the prevalence of SP elongation also increased only in males after 50 years of age. Elongated SP causes dysphagia, recurrent throat pain or foreign body sensation, facial pain and neck pain, radiating into the ear. The awareness about the prevalence rate, as well as the signs and symptoms related with elongated SP, will

be helpful for otolaryngologists, neurologists and dental surgeons. SP elongation might also include differential diagnosis in trigeminal neuralgias, migraine, myofacial dysfunctions and cervical arthritis. This knowledge will be useful for practitioners to avoid misinterpretation of the symptoms such as tonsillar pain, or pain of dental, muscular, or pharyngeal origin.

REFERENCES

ALPOZ E, AKAR GC, CELIK S, GOVSA F, LOMCALI G (2014) Prevalence and pattern of stylohyoid chain complex patterns detected by panoramic radiographs among Turkish population. *Surg Radiol Anat*, 36(1): 39-46.

ALZAREA BK (2017) Prevalence and pattern of the elongated styloid process among geriatric patients in Saudi Arabia. *Clin Intervent Aging*, 12: 611.

ASUTAY F, ERDEM NF, ATALAY Y, ACAR AH, ASUTAY H (2019) Prevalence of elongated styloid process and Eagle syndrome in East Eagean population. *Bezmialem Science*, 7(1): 28-33.

BAGGA M, BHATNAGAR D, KUMAR N (2020) Elongated styloid process evaluation on digital panoramic radiographs: A retrospective study. *J Indian Acad Oral Med Radiol*, 32(4): 330.

BAGGA MB, KUMAR CA, YELURI G (2012) Clinicoradiologic evaluation of styloid process calcification. *Imaging Sci Dentistry*, 42(3): 155-161.

BOZKIR MG, BOĞA H, DERE F (1999) The evaluation of elongated styloid process in panoramic radiographs in edentulous patients. *Turkish J Med Sci*, 29(4): 481-486.

BRUNO G, DE STEFANI A, BALASSO P, MAZZOLENI S, GRACCO A (2017) Elongated styloid process: an epidemiological study on digital panoramic radiographs. *J Clin Exp Dentistry*, 9(12): e1446.

CAMARDA AJ, DESCHAMPS C, FOREST D (1989a) I. Stylohyoid chain ossification: a discussion of etiology. *Oral Surg Oral Med Oral Pathol*, 67: 508-514.

CAMARDA AJ, DESCHAMPS C, FOREST D (1989b) II. Stylohyoid chain ossification: a discussion of etiology. *Oral Surg Oral Med Oral Pathol*, 67: 515-520.

CHAURASIA BD (2019) Styloid apparatus: Deep structures in the neck. In: Chaurasia BD (ed.). *Human Anatomy Regional and Applied Dissection and Clinical – Head, Neck and Brain*. Vol. 3. CBS Publishers, p 12.

CHEN G, YEH PC, HUANG SL (2022) An evaluation of the prevalence of elongated styloid process in Taiwanese population using digital panoramic radiographs. *J Dental Sci*, 17(2):744-749.

CHUANG WC, SHORT JH, MCKINNEY AM, ANKER L, KNOLL B, MCKINNEY ZJ (2007) Reversible left hemispheric ischemia secondary to carotid compression in Eagle syndrome: surgical and CT angiographic correlation. *Am J Neuroradiol*, 28: 143-145.

DAO A, KARNEZIS S, LANE JS 3RD, FUJITANI RM, SAREMI F (2011) Eagle syndrome presenting with external carotid artery pseudoaneurysm. *Emerg Radiol*, 18(3): 263-265.

EAGLE WW (1937) Elongated styloid processes: report of two cases. *Arch Otolaryngol*, 25(5): 584-587.

EAGLE WW (1948) Elongated styloid process: further observations and a new syndrome. *Arch Otolaryngol*, 47(5): 630-640.

ETTINGER RL, HANSON JG (1975) The styloid or Eagle syndrome: an unexpected consequence. *Oral Surg Oral Med Oral Pathol*, 40: 336-339.

FERRARIO VF, SIGURTA D, DADDONA A, DALLOCA L, MIANI A, TAFURO F, SFORZA C (1990) Calcification of the stylohyoid ligament: Incidence and morphoquantative evaluation. *Oral Surg Oral Med Oral Pathol*, 69: 524-529.

GOKCE C, SISMAN Y, ERTAS ET, AKGUNLU F, OZTURK A (2008) Prevalence of styloid process elongation on panoramic radiography in the Turkey population from Cappadocia region. *Eur J Dentistry*, 2(01): 18-22.

GOSSMAN JR Jr, TARSITANO JJ (1977) The styloid-stylohyoid syndrome. *J Oral Surg*, 35: 555-560.

HETTIARACHCHI PV, JAYASINGHE RM, FONSEKA MC, JAYASINGHE RD, NANAYAKKARA CD (2019) Evaluation of the styloid process in a Sri Lanka population using digital panoramic radiographs. *J Oral Biol Craniofacial Res*, 9(1): 73-76.

IANNUCCI MJ, HOWERTON LJ (2017) Dental Radiography: Principles and Techniques. Elsevier, St. Louis, Missouri.

İLGÜY M, İLGÜY D, GÜLER N, BAYIRLI G (2005) Incidence of the type and calcification patterns in patients with elongated styloid process. *J Int Med Res*, 33(1): 96-102.

JAMAL BT, RAVIKUMAR KK, ALYAWAR SH, MAGHRABI IN, ALSHAIKH AM, JABBAD HH, ALSOHAIBI TH (2018) Prevalence of elongated styloid process and elongation pattern on digital panoramic radiographs in Saudi Population, Jeddah. *Int J Social Rehabilit*, 3(2): 37.

KAY DJ, HAR-EL G, LUCENTE FE (2001) A complete stylohyoid bone with a stylohyoid joint. *Am J Otolaryngol*, 22: 358-361.

KEUR JJ, CAMPBELL JP, MCCARTHY JF, RALPH WJ (1986) The clinical significance of the elongated styloid process. *Oral Surg Oral Med, Oral Pathol*, 61(4): 399-404.

LANGLAIS RP, MILES DA, VAN DIS ML (1986) Elongated and mineralized stylohyoid ligament complex: a proposed classification and report of a case of Eagle's syndrome. *Oral Surg, Oral Med, Oral Pathol*, 61(5): 527-532.

LANGLAND OE, LANGLAIS RP, MORRIS CR (1982) Principle and Practice of Panoramic Radiology. W.B. Saunders, Philadelphia.

MESSER EJM, ABRAMSON AM (1975) The styloid syndrome. *J Oral Surg*, 33: 664-667.

PATNI VM, GADEWAR DR, PILLAI KG (1986) Ossification of stylohyoid ligament with pseudojoint formation. A case report. *J Indian Dent Assoc*, 58: 227-231.

SCAF G, FREITAS DQ, LOFFREDO LD (2003) Diagnostic reproducibility of the elongated styloid process. *J Appl Oral Sci*, 11: 120-124.

SCAVONE G, CALTABIANO DC, RACITI MV, CALCAGNO MC, PENNISI M, MUSUMECI AG, ETTORRE GC (2019) Eagle's syndrome: a case report and CT pictorial review. *Radiol Case Rep*, 14(2): 141-145.

STEINMAN EP (1968) Styloid syndrome in absence of an elongated process. *Acta Otolaryngol*, 66: 347-356.

SWAPNA LA, ALMEGBIL NT, ALMUTLAQ AO, KOPPOLU P (2021) Occurrence of the elongated styloid process on digital panoramic radiographs in the Riyadh population. *Radiol Res Pract*, 2021: 6097795.

WARRIER A, NANTHINI KC, SUBADRA K, HARINI DM (2019) Eagle's syndrome: a case report of a unilateral elongated styloid process. *Cureus*, 11(4): e4430.

WATANABE PC, DIAS FC, ISSA JP, MONTEIRO SA, PAULA FJ, TIOSSI R (2010) Elongated styloid process and atheroma in panoramic radiography and its relationship with systemic osteoporosis and osteopenia. *Osteoporos Int*, 21: 831-836.

ZAKI HS, GRECO CM, RUDY TE, KUBINSKI JA (1996) Elongated styloid process in a temporomandibular disorder sample: prevalence and treatment outcome. *J Prosthetic Dentistry*, 75(4): 399-405.

A study on the effects of ageing on mandibular morphology: A digital radiographic assessment

N. Harshitha, Karthikeya Patil, C. J. Sanjay, D. Nagabhushana, S. Viveka

Department of Oral Medicine and Radiology, JSS Dental College and Hospital, JSS Academy of Higher Education and Research, Mysuru-570015, India

SUMMARY

The aim of this study was to determine, compare and differentiate the morphologically related changes of the mandible in dentate males and females among different age groups on digital panoramic images, and to assess their authenticity in age estimations to provide evidence in forensics. The panoramic images were made for 420 subjects of four age groups: 12-18 years, 19-40 years, 41-60 years, and older than 60 years. The gonial angle, condylar length, ramus length, cortical bone thickness, and ramal notch width were measured and evaluated. The data obtained were then subjected to descriptive statistical analysis followed by Paired t-test and Two-way ANOVA test. On measuring angular and four-linear measurements, statistically significant differences were found among all the age groups with $p < 0.05$, and also increased on aging except for the gonial angle. Among all the parameters, the gonial angle, ramus length, and ramal notch width depicted a statistically significant difference between the right and left sides with $p < 0.05$. It is found that all parameters except the gonial angle were reliable for age determination. Hence, this study positively recommends the use of all parameters except the gonial angle for the purpose of age estimation in the field of forensics.

Key words: Digital radiographic assessment – Age estimation – Orthopantomography – Linear and Angular measurements – Mandible

INTRODUCTION

According to evolutionary biology studies, humans are descended from ancient apes (National Academy of Sciences, 1999). There are exciting developments in all fields that contribute to our understanding of human evolution (Gluckman et al., 2011). Many studies have characterised the evolution of genetically based variations in personality between age and sex groups as well as their genetic components (Ngun et al., 2011).

In legal medicine and forensic anthropology, establishing the identity of the unknown deceased person in a crime, accident, suicide, or mass tragedy, as well as for criminals who are hiding their identities, is very critical (Weisberg et al.,

Corresponding author:
Dr Karthikeya Patil, Professor and Head, Department of Oral Medicine and Radiology, JSS Dental College and Hospital, JSS Academy of Higher Education and Research, Mysore 570015, Karnataka, India. Phone: 9449822498. E-mail: dr.karthikeyapatil@jssuni.edu.in

Submitted: March 3, 2022. **Accepted:** April 9, 2022

https://doi.org/10.52083/UBHH5940

2011), and skeletal traits are among the most commonly used traits to determine a person's gender and age (Maloth et al., 2016).

The mandible exhibits many anatomical and morphological changes with the progression of age. Changes in the size and shape of the mandible are noticed along with the gradual growth and the function of jaws, which vary according to age, gender, and dental condition (Okşayan et al., 2014). The gonial area, the antegonial region, the condyle, and the ramus are some of the remodelling areas in the mandible that alter (Ghosh et al., 2010). All these areas are best viewed, measured, and evaluated by Orthopantomography (OPG), which is a commonly employed method in scientific research and criminal investigations for age and sex determination (Maat et al., 2006).

The current study aims to evaluate the morphological alterations in the mandible with ageing and dental condition by considering one angular and four linear measurements across the body and ramus of the mandible.

MATERIALS AND METHODS

In the Department of Oral Medicine and Radiology, a prospective study was conducted with the sample size of 420. After critical reviewing, the research was approved by the Institutional Ethics Committee.

The clinical examination was carried out after obtaining written consent and assent from the selected subjects, and the clinical findings were recorded in individual proforma specially designed for the study. The panoramic digital radiographs were taken using the Planmeca Promax Digital Panoramic system, under standard exposure conditions as recommended by the manufacturer.

This study included groups of young and old dentulous individuals who had complete sets of medical records and whose teeth were all intact except for third molars (present or absent), over 60 years old with at least five teeth in each quadrant, except third molars. Old denture wearers and any patients with the presence of supernumerary teeth (erupted or impacted), any systemic disease affecting the jawbone, and subjects with history or evidence of orthodontic or orthognathic treatment were excluded from the study.

In our study, all 420 subjects were categorised into 4 different age groups. Group 1 of 12-18 years, group 2 of 19-40 years and group 3 of 41-60 years were comprised of 120 (28.6%) individuals each, except for group 4 of greater than 60 years, which comprised 60 (14.3%) individuals.

The first age group in our study consists of subjects up to the age of 18 rather than 20, because development in female subjects gradually ceases by the age of 18. As a result, this may make a greater difference when comparing various age groups.

All mandibular measurements were made bilaterally using ROMEXIS DICOM viewer software (Planmeca, Helsinki, Finland). The present study was performed for about 18 months.

The parameters that were measured in our study were as follows:

- **Gonial angle:** It is formed by drawing a line between two imaginary lines that extend from the inferior border of the mandible to the ramus of the mandible.
- **Condylar length:** It is the distance between two lines drawn tangentially, one at the superiormost point of the condylar head and the other at the deepest point of the sigmoid notch's concavity.
- **Ramus length:** It is calculated by drawing two lines, one perpendicular to the ramus tangent line at the level of the most lateral image of the condyle and the other perpendicular to the ramus tangent line at the level of the most lateral image of the ramus. The distance between these two lines is the ramus length.
- **Cortical bone thickness:** The thickness of the radiopaque band is measured at the lower border of the mandible's body, where the antegonial notch begins mesially.
- **Ramal notch width:** It is the distance between the ramus tangent line and the ramus notch concavity's deepest point.

Figure 1 is a panoramic image showing the gonial angle (green line), condylar length (pink line), ramus length (blue line), ramal notch width

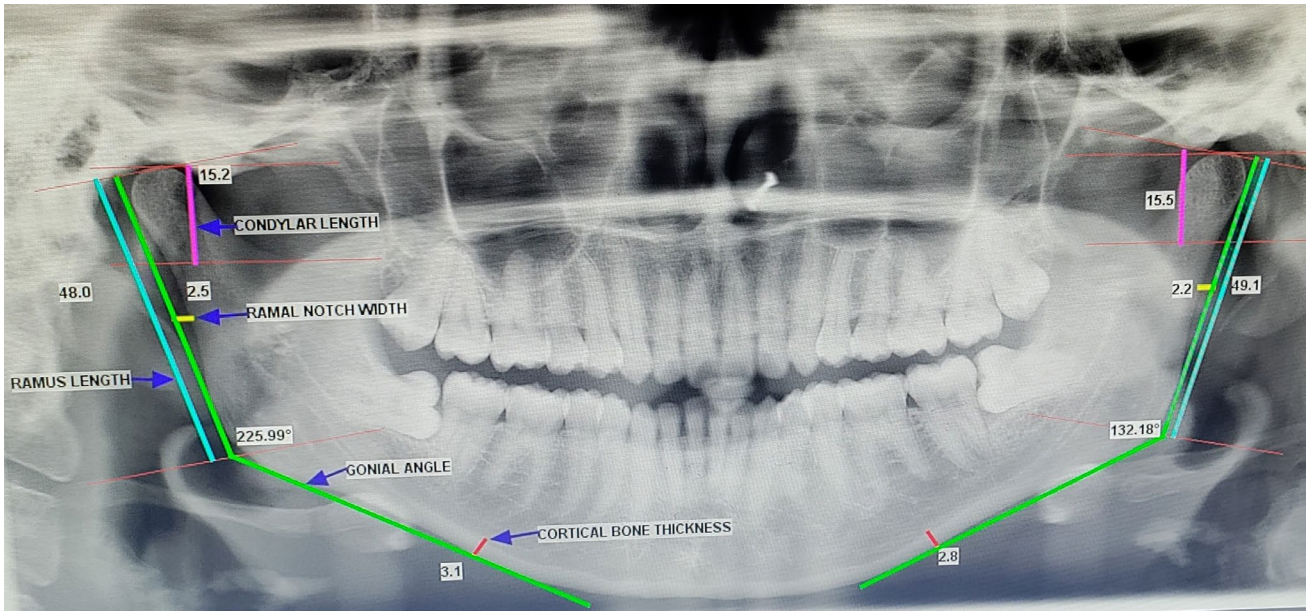

Fig. 1.- Panoramic image using Planmeca Romexis Software.

(yellow line) and cortical bone thickness (red line), which are measured using Planmeca Romexis Software.

For each variable, descriptive statistics followed by Two-way ANOVA test were determined. The difference in measures between the left and right sides of the mandible were analysed using a paired t test.

RESULTS

Gonial angle

The mean value of the Gonial Angle among groups 1 (12-18 years) was 180.8372, group 2 (19-40 years) was 180.0166, group 3 (41-60 years) was 180.6042, and group 4 (greater than 60 years) was 180.4131.

The mean value of the gonial angle was comparatively higher among the younger age group and lower among the older age group. Therefore, the gonial angle decreases as age increases.

The mean value of the gonial angle showed no significant differences between all age groups. Thus, this was found to be statistically insignificant with a p value ($p = 0.568$) (Table 1).

The right and left sides of the gonial angle showed a significant difference and were found to be statistically significant with $p < 0.05$. The gonial angle on the right side showed a significantly higher value than the left side (Table 2).

Condylar length

The mean value of the condylar length in group 1 (12-18 years) was 20.9397; in group 2 (19-40 years), it was 22.1681; in group 3 (41-60 years), it was 22.2246, and group 4 (older than 60 years) it was 22.1692.

The mean value of the condylar length was comparatively lower among the younger age group and higher among the older age group. Therefore, the condylar length increases as age increases.

The mean value of the condylar length showed a significant difference between all age groups. Thus, this was found to be statistically significant with a p value. ($p = 0.035$).

The right and left sides of condylar length showed no significant difference and were found to be statistically insignificant with $p > 0.05$.

Ramus length

The mean value of the ramus length among group 1 (12-18 years) was 65.9610, group 2 (19-40 years) was 69.8940, group 3 (41-60 years) was 70.1633 and group 4 (older than 60 years) was 70.8367.

The mean value of the ramus length was comparatively lower among the younger age group

and higher among the older age group. Therefore, the ramus length increases as age increases.

The mean value of the ramus length showed a significant difference between all age groups. Thus, this was found to be statistically significant with a p value (p = 0.000).

The right and left sides of the ramus length showed a significant difference and were found to be statistically significant with $p < 0.05$. The ramus length on the right showed a significantly higher value than on the left.

Table 1. Comparison of four Age groups (Group 1, Group 2, Group 3, Group 4) with mean values and standard deviation of gonial angle (°), 1) ramus length (mm), condylar length (mm), cortical bone thickness (mm) and ramus notch width (mm). Two-way ANOVA test for all parameters.

Descriptive Statistics				**Two-way ANOVA test**		
Variables	**Ages** (in years)	**Mean**	**Std. Deviation**	**Mean Square**	**F**	**Sig.**
Gonial angle	12-18	180.8372	6.35736	14.399	0.674	0.568
	19-40	180.0166	5.20161			
	41-60	180.6042	2.44684			
	60+	180.4131	1.92699			
Condylar length	12-18	20.9397	3.88782	58.004	3.584	0.014*
	19-40	22.1681	4.44695			
	41-60	22.2246	3.70023			
	60+	22.1692	4.06674			
Ramus length	12-18	65.9610	9.78409	522.762	7.731	0.000*
	19-40	69.8940	8.07540			
	41-60	70.1633	7.99625			
	60+	70.8367	7.07502			
Cortical bone thickness	12-18	3.3413	0.62294	5.794	11.531	0.000*
	19-40	3.6350	0.59964			
	41-60	3.8704	0.73088			
	60+	3.7517	0.91614			
Ramal notch width	12-18	2.5629	0.94160	8.275	8.419	0.000*
	19-40	2.8821	1.01761			
	41-60	2.9317	0.86233			
	60+	3.3858	1.08460			

*$P<0.05$ significance at 5% level of significance.

Table 2. Comparison of right and left sides of gonial angle (°), ramus length (mm), condylar length (mm), cortical bone thickness (mm) and ramus notch width (mm) with mean values and standard deviation. Paired T-test for all parameters.

Variables	**Sides**	**Mean**	**Std. Deviation**	**Paired differences**		**p**
				Mean	**Std. dev**	
Gonial angle	Right	236.0962	8.19937	111.24123	15.46445	0.000*
	Left	124.8550	9.76338			
Condylar length	Right	21.8139	4.19556	-0.03900	2.69601	0.767
	Left	21.8529	4.35044			
Ramus length	Right	69.2093	8.78312	0.45469	3.06425	0.003*
	Left	68.7546	8.76774			
Cortical bone thickness	Right	3.6179	0.75727	-0.03429	0.46712	0.133
	Left	3.6521	0.76497			
Ramal notch width	Right	2.7962	1.03384	-0.16167	0.69174	0.000*
	Left	2.9579	1.07159			

*$P<0.05$ significance at 5% level of significance.

Cortical bone thickness

The mean value of cortical bone thickness of group 1 (12-18 years) was 3.3413; for group 2 (19-40 years), 3.6350; for group 3 (41-60 years), 3.8704, and for group 4 (older than 60 years), 3.7517.

The mean value of the cortical bone thickness was comparatively lower among the younger age group and higher among the older age group, and again, after 60 years, the cortical bone thickness starts decreasing. Therefore, the cortical bone thickness increases as age increases, and after 60 years it starts to decrease.

The mean value of cortical bone thickness showed a significant difference between all age groups. Thus, this was found to be statistically significant with a p value ($p = 0.000$).

The right and left sides of cortical bone thickness showed no significant difference and were found to be statistically insignificant with $p > 0.05$.

Ramal notch width

The mean value of the ramal notch width for group 1 (12-18 years) was 2.5629; for group 2 (19-40 years), 2.8821; for group 3 (41-60 years), 2.9317, and for group 4 (older than 60 years), 3.3858.

The mean value of the ramal notch width was comparatively lower among the younger age group and higher among the older age group. Therefore, the ramal notch width increases as age increases.

The mean value of the ramal notch width showed a significant difference between all age groups. Thus, this was found to be statistically significant with a p value ($p = 0.000$).

The right and left sides of the ramal notch width showed a significant difference and were found to be statistically significant with $p < 0.05$. The ramal notch width on the left showed a significantly higher value than on the right side.

DISCUSSION

This study's discussion centres on a number of methodological challenges that frequently occur when attempting to estimate age at death or when providing osteological evidence that may aid in confirming identifications (Konigsberg et al., 2008). The identification of the person and the assessment of the cause of death are the two basic issues that arise when human skeletal and dental remains are discovered (Mann et al., 1990). In forensic science, determining age and gender from skeletal remains is the first step (Sairam et al., 2016).

To aid forensic identification, recent research has focused on using multiple skeleton features to assess variation linked to age and ethnicity (Franklin et al., 2008). Bones change constantly during a person's life, and those changes in the skeleton follow a chronological pattern. Knowing what changes occur in the bones can aid in determining the age of the skeleton. The skull and mandible, in addition to the pelvis, are the few additional skeletal remains that display the highest sexual dimorphism, and should be used for this purpose when accessible (Dudar et al., 1993). The mandible is considered a significant tool in age determination, because it is a strong bone that is difficult to break and disintegrate, and also because of the changes in the size and shape of the jaw bones that occur during adult life.

Radiology is critical in determining a person's age. Radiological images were utilised in the process of estimating age, which is among the most important tools in forensic science (Franklin et al., 2008). Panoramic imaging is a widely implemented technology in routine dental exams. It is a practical method for surveying dental problems, as it provides all of the necessary information on a single panoramic film. As a result, the parameters in this investigation were measured using panoramic radiography (Sairam et al., 2018).

This study assessed, correlated, and evaluated one angular (gonial angle) and four linear (condylar length, ramus length, cortical bone thickness, and ramal notch width) mandibular measurements as seen on digital panoramic radiographs in order to determine their utility in determining the age.

Gonial angle

In our present study, there was no significant difference in gonial angle between any of the

age groups, which was found to be statistically not significant with $p > 0.05$. This statement is in agreement with the studies conducted by Okşayan et al. (2014), Ceylan et al. (1998), Raustia and Salonen (1997), Fish (1979), Xie and Ainamo (2004), who also found non-significant difference in the gonial angle between the different age groups. In contrast, the study performed by Ohm and Silness (1999) found that the gonial angle increases with age and advancing edentulism. As our study did not include edentulous subjects, this could be one of the reasons for the difference observed in the increased gonial angle found by Ohm and Silness. However, on considering the dentate subjects, this study was found to be correlated with our study. Overall, this parameter (gonial angle) did not show a promising parameter for age determination.

In our study, we discovered a significant difference in the gonial angle between both sides of the jaw, which might be due to developmental variations. The above statement is in correlation with the findings by Chol et al. (2013), who also discovered a significant difference in the gonial angle between the right and left sides of the jaw, with the left side showing a greater value and $p < 0.05$. However, in our study, the gonial angle was significantly greater on the right side of the mandible and was found to be statically significant when pairing right and left gonial angles with a p value < 0.05. Another study performed by Larheim and Svanaes (1986) observed no significant difference between the right and left gonial angles. All these disagreements might be due to a disparity in sample size and the age group (14-28 years) of their study population.

Condylar length

When comparing different age groups, a study performed by Huumonen et al. (2010) revealed a significant difference in condylar length, in which the condylar length was found to be smaller in the older age group than in the younger age group. In our study, the condylar length was found to be comparatively greater in the older age group than in the younger age group. In contrast, Okşayan et al. (2014), Joo et al. (2013), Raustia and Salonen (1997), Sairam et al. (2018) and Merrot et al. (2005) revealed no significant differences in condylar length when comparing different age groups. This disagreement in the studies might be due to disparities in ethnicity, sample size, and age group. The studies that are in disagreement included edentulous subjects. Our study did not include edentulous subjects, as loss of tooth or edentulism will be associated with changes in mandibular morphology. Overall, this parameter (condylar length) appears to be a promising factor for age determination.

In addition, our study did not show a statistically significant difference in condylar length when comparing both sides of the mandible and found to be statistically insignificant with $p > 0.05$.

Ramus length

In our study, a significant difference in ramus length was observed between all age groups, which might be due to developmental variations. This statement is in agreement with the other study by Okşayan et al. (2014), who also noted significant differences in ramus length values between all age groups. However, this is not in agreement with the findings of Joo *et al.* (2013), Raustia *and* Salonen (1997) and Merrot *et al.* (2005), who reported no significant difference in the ramus length with ageing. This disagreement in the studies might be due to differences in ethnicity, sample size, and age group. The findings that were found in our study, as well as those of Sairam et al. (2018), show that ramus length increases with age. In contrast, studies by Okşayan et al. (2014) and Huumonen *et al.* (2010) observe that ramus length decreases as age increases. This disagreement might be due to the fact that our study did not include edentulous subjects, as loss of tooth or edentulism will be associated with changes in mandibular morphology. Overall, this parameter (ramus length) can be used for age determination.

In our study, a difference in ramus length was found between the right and left sides of the mandible and was found to be statistically significant, with the right side showing a higher value ($p = <0.05$).

Cortical bone thickness

In our present study, a statistically significant difference in the thickness of cortical bone was observed between all age groups of dentate subjects and was shown to be in accordance with a few other studies carried out by Joo et al. (2013) and Schwartz-Dabney and Dechow (2002). The cortical bone thickness found in our study was statistically lower in younger age groups and increased in older age groups. Our study did not include completely edentulous individuals. Hence, this factor cannot be compared with the findings involving edentulous subjects in previous studies. Overall, this parameter (cortical bone thickness) can be strongly used for age determination.

In our study, though a difference in the cortical bone thickness was found between right and left sides of the mandible, the right side showed a greater value than the left side and was found to be statistically insignificant with $p > 0.05$.

Ramal Notch width

The study by Okşayan et al. (2014), observed that ramal notch width increases with age but showed no statistically significant differences when compared with different age groups. In our study, ramal notch width was found to be statistically significant, being lower in younger age groups and increasing in older age groups. This factor is not correlated with the study conducted by Okşayan et al. (2014), who did not find any significant differences in ramus notch width when comparing different age groups. This disagreement in the study might be due to the fact that it involved only the older age group subjects (60-69 years) as well as edentulous subjects, and also due to variations in ethnicity and sample size. Our study included four different age groups, of 12 to 60 years-and-above subjects, and no edentulous subjects were included. Overall, this parameter (Ramal notch width) was found to be a promising factor for age determination.

In our study, when comparing the right and left sides, the ramal notch width was greater on left side than on right. However, this was statistically not significant with $p > 0.05$.

As this was a time-bound study, a statistically qualified minimum sample size was assessed. In the future, further studies are recommended to validate our hypothesis with the larger sample size, including various ethnicity and socioeconomic groups for age determination.

From overall results obtained in our present study, it was revealed that all parameters can be used as a tool for age estimation, as the condyle length, ramus length, cortical bone thickness and ramal notch width (all except the gonial angle) show anatomical variations between different age groups and are found to be statistically significant. Therefore, it is concluded that all linear measurements, except the angular measurement on digital panoramic images, with significant differences among different age groups, can be used in forensic anthropology as valuable tools for the estimation of age. Because linear measurements vary depending on population ethnicity, age, and dental state, there is a need to define harmonised standards for diverse populations in terms of age group and dental status. Hence, these measurements are advocated varyingly for providing evidence in forensics, especially when other bones of the skeleton are unavailable.

REFERENCES

CEYLAN G, YANÍKOGLU N, YÍLMAZ AB, CEYLAN Y (1998) Changes in the mandibular angle in the dentulous and edentulous states. *J Prosthet Dentist,* 80(6): 680-684.

CHOLE R, PATIL R, BALSARAF CHOLE S, GONDIVKAR S, GADBAIL A, YUWANATI M (2013) Association of mandible anatomy with age, gender, and dental status: a radiographic study. *ISRN Radiology,* 2013: 453763.

DUDAR JC, PFEIFFER S, SAUNDERS SR (1993) Evaluation of morphological and histological adult skeletal age-at-death estimation techniques using ribs. *J Forensic Sci*, 38: 677-685.

FRANCIS FISH S (1979) Change in the gonial angle. *J Oral Rehabil,* 6(3): 219-227.

FRANKLIN D, CARDINI A, HIGGINS PO, OXNARD CE, DADOUR I (2008) Mandibular morphology as an indicator of human subadult age: geometric morphometric approaches. *J Forensic Sci,* 4: 91-99.

GHOSH S, VENGAL M, PAI KM, ABHISHEK K (2010) Remodelling of the antegonial angle region in the human mandible: A panoramic radiographic cross-sectional study. *Med Oral Patol Oral Cir Bucal,* 15: e802–7.

GLUCKMAN PD, LOW FM, BUKLIJAS T, HANSON MA, BEEDLE AS (2011) How evolutionary principles improve the understanding of human health and disease. *Evol Appl*, 4(2): 249-263.

HUUMONEN S, SIPILÄ K, HAIKOLA B, TAPIO M, SÖDERHOLM AL, REMES-LYLY T, OIKARINEN K, RAUSTIA AM (2010) Influence of edentulousness on gonial angle, ramus and condylar height. *J Oral Rehabil,* 37(1): 34-38.

JOO JK, LIM YJ, KWON HB, AHN SJ (2013) Panoramic radiographic evaluation of the mandibular morphological changes in elderly dentate and edentulous subjects. *Acta Odontol Scand,* 71: 357-362.

KONIGSBERG LW, HERRMANN NP, WESCOTT DJ, KIMMERLE EH (2008) Estimation and evidence in forensic anthropology: age-at-death. *J Forensic Sci,* 53(3): 541-557.

LARHEIM TA, SVANAES DB (1986) Reproducibility of rotational panoramic radiography: mandibular linear dimensions and angles. *Am J Orthod Dentofacial Orthop*, 90(1): 45-51.

MAAT GJ, MAES A, AARENTS MJ, NAGELKERKE NJ (2006) Histological age prediction from the femur in a contemporary Dutch sample. The decrease of nonremodeled bone in the anterior cortex. *J Forensic Sci*, 51: 230-237.

MALOTH AK, DORANKULA SP, PASUPULA AP (2016) Lip outline: A new paradigm in forensic sciences. *J Forensic Dent Sci*, 8(3): 178.

MANN RW, UBELAKAR DH (1990) The forensic anthropologist. F.B.I Law enforcement bulletin. *Am J Phys Anthropol*, 81: 17-25.

MERROT O, VACHER C, MERROT S, GODLEWSKI G, FRIGARD B, GOUDOT P (2005) Changes in the edentate mandible in the elderly. *Surg Radiol Anat,* 27: 265-270.

NATIONAL ACADEMY OF SCIENCES (1999) Science and Creationism: A View from the National Academy of Sciences: Second Edition. Washington (DC): National Academies Press (US).

NGUN TC, GHAHRAMANI N, SÁNCHEZ FJ, BOCKLANDT S, VILAIN E (2011) The genetics of sex differences in brain and behavior. *Front Neuroendocrinol,* 32(2): 227-246.

OHM E, SILNESS J (1999) Size of the mandibular jaw angle related to age, tooth retention and gender. *J Oral Rehabil,* 26(11): 883-891.

OKŞAYAN R, ASARKAYA B, PALTA N, ŞIMŞEK İ, SÖKÜCÜ O, İŞMAN E (2014) Effects of edentulism on mandibular morphology: evaluation of panoramic radiographs. *Sci World J*, 2014: 254932.

RAUSTIA AM, SALONEN MA (1997) Gonial angles and condylar and ramus height of the mandible in complete denture wearers- a panoramic radiograph study. *J Oral Rehabil,* 24(7): 512-516.

SAIRAM V, GEETHAMALIKA MV, KUMAR PB, NARESH G, RAJU GP (2016) Determination of sexual dimorphism in humans by measurements of mandible on digital panoramic radiograph. *Contemp Clin Dent*, 7(4): 434-439.

SAIRAM V, POTTURI GR, PRAVEEN B, VIKAS G (2018) Assessment of effect of age, gender, and dentoalveolar changes on mandibular morphology: A digital panoramic study. *Contemp Clin Dent*, 9: 49-54.

SCHWARTZ-DABNEY CL, DECHOW PC (2002) Edentulation alters material properties of cortical bone in the human mandible. *J Dent Res,* 81: 613-617.

WEISBERG YJ, DEYOUNG CG, HIRSH JB (2011) Gender differences in personality across the ten aspects of the big five. *Front Psychol*, 2: 178.

XIE QF, AINAMO A (2004) Correlation of gonial angle size with cortical thickness, height of the mandibular residual body, and duration of edentulism. *J Prosthet Dent,* 91: 477-482.

Reversion of neuronal differentiation induced in human adipose-derived stem cells

Rosa Hernández[1,2,3,†], Gloria Perazzoli[1,2,†], Cristina Mesas[1,2,3], Francisco Quiñonero[1,2,3], Kevin Doello[1,4], Raul Ortiz[1,2,3], Jose Prados[1,2,3], Consolación Melguizo[1,2,3]

[1] *Institute of Biopathology and Regenerative Medicine (IBIMER), Biomedical Research Center (CIBM), Granada 18100, Spain*
[2] *Instituto Biosanitario de Granada, (ibs.Granada), SAS-Universidad de Granada, Granada 18012, Spain*
[3] *Department of Anatomy and Embryology, University of Granada, Granada 18071, Spain*
[4] *Medical Oncology Service, Virgen de las Nieves Hospital, 18014 Granada, Spain*

SUMMARY

Adipose-derived mesenchymal stem cells are a great alternative to other types of stem cells obtained from other tissues, since they are found in large numbers and are easy to obtain by liposuction and do not have ethical connotations. These cells can differentiate into neuronal lineage using induction media, although the efficacy of these media is determined by their composition. In previous studies, we have demonstrated the differentiation of human adipose-derived mesenchymal stem cells to neuronal lineage by using three induction media, Neu1, Neu2 and Neu3, each one showing a series of neuronal markers in the treated cells. In the present study, a further step is taken, since once a neuronal differentiation is obtained with these three induction media, they are removed from the medium and both morphology and neuronal markers and the ability to maintain neurosphere formation are analyzed. The results obtained show that when these induction media are withdrawn in the three cases, both the neuronal morphological characteristics and the neuronal markers are lost at different times depending on the medium used. In the case of neurospheres, the ability to maintain this shape is also lost when they are not in contact with neuronal induction factors. Therefore, although the neuronal differentiation mechanism is very promising in this type of cells, it is necessary to carry out more studies to elucidate an induction medium that allows cells differentiated into neurons to maintain neuronal characteristics over time without the need to continue applying neuronal differentiation factors.

Key words: Human adipose mesenchymal stem cells – Neurological disorders – Neuronal differentiation

ABBREVIATIONS

cAMP	Adenosine 3',5'-cyclic monophosphate
CHAT	Choline O-acetyltransferase
DMEM	Dulbecco's Modified Eagle Medium
EGF	Epidermal growth factor
ENS	Enolase
FBS	Fetal bovine serum

Corresponding author:
Dr. José Prados. Institute of Biopathology and Regenerative Medicine (IBIMER), Biomedical Research Centre (CIBM), University of Granada, Spain. Phone: +34- 958249322; Fax: +34-958246296. E-mail: jcprados@ugr.es

Submitted: March 8, 2022. **Accepted:** April 9, 2022

https://doi.org/10.52083/GUMF1586

† These authors have equal contribution

FGF	Fibroblast growth factor
FOXO-4	O4 forkhead box
GalC	Galactosylceramidase
GFAP	Glial fibrillary acidic protein
hASC	Human adipose-derived mesenchymal stem cells
HGF	Hepatocyte growth factor
IBMX	3-isobutyl-1-methylxanthine.
LIF	Leukemia inhibitory factor
MAP2	Microtubule-associated protein-2
MSCs	Mesenchymal stem cells
Neu1	Neuronal differentiation medium 1
Neu2	Neuronal differentiation medium 2
Neu3	Neuronal differentiation medium 3
NeuN	Neuronal nuclear protein
NFH	Neurofilament heavy chain
NFL	Neurofilament light chain
NFM	Neurofilament
NGF	Nerve growth factor
NPBM	Neuronal progenitor basal medium
NSE	Neuron specific enolase
PBS	Phosphate-buffered saline
SCN9A	Sodium voltage-gated channel alpha subunit-9
SNAP25	Synaptosome-associated protein-25
TAU	Tau protein
TH	Thyroxine hydroxylase
VEGF	Vascular endothelial growth factor

INTRODUCTION

The use of tissue-derived mesenchymal stem cells has great advantages for clinical use. Among them, we can find the absence of ethical implications, unlike other cell types such as embryonic stem cells (Hanley et al., 2010), their easy obtaining from different tissues such as adipose tissue (ideal tissue to obtain these cells by liposuction) (Minteer et al., 2013) and the availability of mesenchymal stem cells in fat compared with bone narrow (2% versus 0.001-0.004%, respectively) (Mahmoudifar and Doran, 2015). Human adipose-derived mesenchymal stem cells (hASCs) can give rise to different cell lines (cardiomyocytes, endothelial cells, osteoblast-like cells, etc.), which had been used in several clinical fields such as cardiovascular diseases, reconstructive plastic surgery or spine degenerative conditions, among others (Ma et al., 2017; Naderi et al., 2017; Caliogna et al., 2020). In addition, these cells exert a neuroprotective effect that may be relevant in neurological pathologies such as head trauma, ischemic stroke, and Alzheimer's disease (Sánchez-Castillo et al., 2022) and were able to improve controlled cortical impact injury in rats reducing neuroinflammation (Ruppert et al., 2020). Furthermore, hASCs can also derive in a neuronal lineage, as demonstrated by Safford et al. (2002), using valproic acid, hydrocortisone, insulin, butylated hydroxyanisole, and epidermal and fibroblast growth factor (EGF and FGF). However, this differentiation was unstable (between 3 and 4 days), and was not accompanied by a functional evaluation. Krampera et al. (2007) used a differentiation medium (which included valproic acid and butylated hydroxyanisole, among others) and Schwann cells, demonstrating a significant increase in the expression of typical markers of differentiated cells. B-mercaptoethanol has also been used to produce neuronal differentiation associated to factors such as EGF, retinoic acid or butylated hydroxyanisole (Cardozo et al., 2011).

The functionality of this differentiation was also not studied, although some different markers were established for neuronal cells. Li et al. (2013) obtained neuronal differentiation markers after differentiation with β-mercaptoethanol, butylated hydroxyanisole and platelet-rich plasma. We have recently shown that three media of neuronal induction, using EGF and FGF combined with leukemia inhibitory factor (LIF), vascular endothelial growth factor (VEGF) or nerve growth factor (NGF), among others, induced a significant differentiation of hASCs to neural-type cells (Hernández et al., 2021). However, whatever the induction method, it is vital to verify the maintenance of the neuronal markers expression to verify the functionality of these differentiated cells. In this regard, NeuN, MAP2, NSE, NFM, NFH and NFL markers stand out (Jang et al., 2010; Salehi et al., 2016). For neuronal differentiation to last over time, the expression of these neuronal

markers must also be prolonged. Therefore, it is important to know their expression changes since a loss of these markers would imply a reversal of this differentiation.

The aim of this study is to determine the degree of reversion of the neuronal characteristics acquired by mesenchymal cells induced by different culture media and to determine if there are permanent changes in their phenotype. This would allow us to determine the degree of neuronal phenotype that is maintained in cells that could be used in neurological disorders.

MATERIALS AND METHODS

Obtention of hASCs from human adipose tissue

Adipose tissue samples were obtained by liposuction from three healthy patients (aged 30 to 55 years). hASCs lines were extracted and characterized as described in our study (Hernández et al., 2021). Informed consent and approval of the Ethics Committee (Nuestra Señora de la Salud Hospital, Granada, Spain, 111430/31; date 9/11/2011) was obtained. The assay was conducted in accordance with the declaration of Helsinki.

hASCs neuronal differentiation and dedifferentiation

hASCs differentiated to neuronal lineage and subsequently dedifferentiated. As described previously (Hernández et al., 2021), we used Neu1, Neu2 and Neu3 differentiation media. For Neu1 induction (Gong et al., 2018), the hASCs were maintained in DMEM, supplemented with 25 µg/ml fibroblast growth factor (FGF, Sigma-Aldrich), 0.1 mg/ml epidermal growth factor (EGF, Sigma-Aldrich) and 10 µg/ml leukemia inhibitory factor (LIF, Sigma). The medium was changed every three days for 21 days. For Neu2 induction, hASCs were maintained in HAM-F12 medium (Sigma-Aldrich), supplemented with 20 ng/ml hepatocyte growth factor (HGF, Sigma-Aldrich), 20 ng/ml vascular endothelial growth factor (VEGF, Sigma-Aldrich) and 10 ng/ml epidermal growth factor. The medium was changed every three days for 15 days. For Neu3 induction based in the procedure of Tondreau et al. (2008), hASCs were maintained in neuronal progenitor basal medium (NPBM, Lonza), supplemented with 10 mg/ml adenosine 3',5'-cyclic monophosphate (cAMP, Sigma-Aldrich), 25 ng/ml nerve growth factor (NGF, Sigma-Aldrich), 2.5 µg/ml insulin (Sigma-Aldrich) and 5 µM 3-isobutyl-1-methylxanthine (IBMX, Sigma-Aldrich) changing the medium every three days for 10 days. All cells were preserved at 37 °C in 95% humidity and 5% CO_2 atmosphere. All media were supplemented with 1% penicillin/streptomycin solution, 1% ciprofloxacin (Fresenius Kabi). In addition, after neuronal differentiation, cells were induced to undergo dedifferentiation by removal of neuronal culture media Neu1, Neu2 and Neu3, and replacement with standard medium (10 days in the case of Neu1, 7 days in the case of Neu2, and 5 days in the case of Neu3).

hASCs neurospheres formation

hASCs neurospheres were induced following previously described procedure (Yang et al., 2015). Briefly, hASCs (90% confluent) were harvested with trypsin/EDTA and plated in 6 wells plate (2.5 x 10^5 cells/ml) in DMEM/F12 medium with 2% B27 serum-free supplement (*Gibco*) for 7 days. 96-well of matrigel or agarose were prepared. Agarose (*Sigma-Aldrich)* in distilled water (0.5%) was boiled (10 minutes). 100 µl of liquid agarose was added to each well of 96-wells plate and kept at 37ºC for 30 minutes. Matrigel (*BD-Biosciences*) in distilled water (50%) was added to the 96-wells plate (100 µl). Differentiation and dedifferentiation assays were carried out only with Neu 1 medium. Neurospheres (1 neurosphere/well) in 150 µl Neu1 medium were maintained for 4 days. DMEM/F12 medium was used as control.

Western blot analysis of neuronal marker modulation

Western blot analysis using proteins obtained from total differentiated and dedifferentiated cells was performed. Firstly, cells were collected, centrifuged, and total proteins were extracted with Laemmli buffer to finally determine protein concentrations (Bradford method). For electrophoresis, 35 µg protein of each sample were heated at 95ºC for 5 min and separated in 7.5% SDS-PAGE gel. Fractions were transferred

to a nitrocellulose membrane with a 45 µm pore size (Millipore), blocked in 5% milk in PBS supplemented with 0.1% Tween-20 (Bio-Rad) (1 hour) and incubated with respective primary antibodies overnight at 4ºC: NES, GFAP, TUB-III, SCN8A, SNAP-25, FOXO-4, CHAT, MAP2, TH, ENS, TAU, and GalC (Table 1). Antibody binding was revealed by incubation with 1:2000 dilution secondary antibody (Goat anti-mouse IgG-HRP, sc-2005). Signals were detected with an ECLTM Western blot detection reagent (GE Healthcare) and β-actin (A3854, Sigma-Aldrich) 1:10000 dilution served as an internal control. Each western was performed at least two times.

RESULTS AND DISCUSSION

Morphological changes in hASCs during neuronal differentiation and dedifferentiation

Morphological changes were observed with the three neuronal differentiation protocols – Neu1, Neu2, and Neu3 – (see Methods) (Fig. 1). Neu1 induced morphological changes from day 5 (Fig. 1b) to the final induction point, in which cells with neural-like morphology appeared (Fig. 1e), i.e., showing cytoplasmic retraction towards the nucleus and a spherical cell body with long extensions that interacted with neighboring cells (Fig. 1f). Neu2 induced fewer morphological changes than Neu1 (and later -day 10-), in the form of a tendency to form organized clusters with membrane contacts between surrounding cells (Fig. 1g-k). Finally, Neu3 caused minor morphological changes, including a spindled shape involving cytoplasmic retraction towards the nucleus. Furthermore, the induction of cytoplasmic extensions was observed sometimes forming long cell chains at the end of the differentiation period (Fig.1 lm). Marei et al. (2018) verified evident morphological changes from the sixth day of induction using retinoic acid. In this differentiation process, the cells acquired a morphological modification from the third day and a neuronal appearance from the sixth day, reaching a total neuronal appearance on the fourteenth day. Compared with our study, the Neu1 differentiation media showed significant morphological changes from day 5. These changes were less noticeable when Neu2 and Neu3 were used. Thus, Neu1 differentiation medium with EGF and FGF factors improves neuronal differentiation relative to other media, including those that used retinoic acid or heparin. This may be related to the relevant role of both EGF and FGF growth factors on hASCs differentiation to a neuronal lineage (Hu et al., 2013).

Table 1. mAb antibodies used in western blot (WB).

mAbs	WB Dilution	Reference
sodium voltage-gated channel alpha subunit-9 (SCN9A)	1:400	*Na+ CP type IXa Antibody H-17, sc-130096; Santa Cruz*
synaptosome associated protein-25 (SNAP-25)	1:400	*SNAP-25 Antibody C-18, sc7538; Santa Cruz*
tubulin-III (TUB-III)	1:1000	*Anti-tubulin Antibody beta III isoform, MAB1637; Millipore*
nestin (NES)	1:500	*Nestin Antibody, sc-23927; Santa Cruz*
choline O-acetyltransferase (CHAT)	1:400	Choactase antibody E-7, sc-55557; Santa Cruz
glial fibrillary acidic protein (GFAP)	1:500	*GFAP Antibody GA-5, sc-58766; Santa Cruz*
microtubule associated protein-2 (MAP2)	1:500	*MAP2 antibody A-4, sc74421; Santa Cruz*
O4 forkhead box (FOXO-4)	1:100	*Anti-FOXO-4, sab4501887; Sigma*
tyroxine hydroxylase (TH)	1:4000	*Anti-tyrosine hydroxylase antibody, T2928; Sigma*
enolase (ENS)	1:400	*Enolase 5G10, sc-51882; Santa Cruz*
Tau protein (TAU)	1:100	*Anti-Tau antibody TAU-5, ab3931; ABCAM*
Neurofilament (NFM)	1:800	*Anti-Neurofilament antibody, 05744; Millipore*
galactosylceramidase (GalC)	1:500	*Anti-GalC antibody, mab342; Millipore*
β-actin	1:10000	*β-actin antibody,, A3854, Sigma Aldrich*

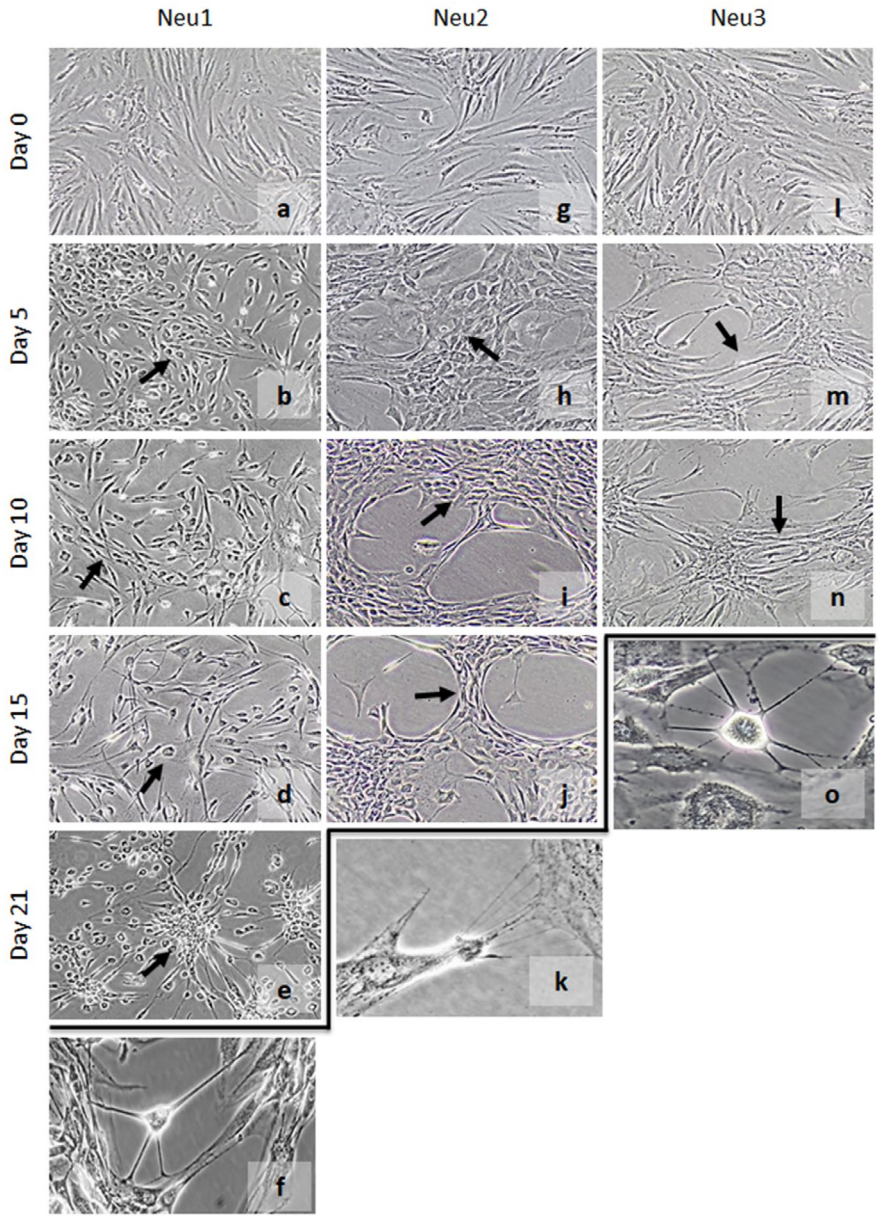

Fig. 1.- hASCs neuronal differentiation. hASCs were exposed to Neu1 (**a-e**) (21 days), Neu2 (**g-j**) (15 days) and Neu3 (**k-n**) media (10 days) (magnification 4x). Images **f, k** and **o** (magnification 20x) show intercellular cytoplasmic bridges in the last day of differentiation. Arrows point to cell morphology changes during differentiation.

Interestingly, dedifferentiation analyses showed that all cells induced with Neu1, Neu2 and Neu3 returned to their initial fibroblastic appearance, which was more pronounced in the case of Neu1. Abundant intercellular cytoplasmic bridges are also observed towards the end of dedifferentiation, more abundant in the case of Neu2 (Fig. 2). Interestingly, dedifferentiation analyses showed that all cells induced with Neu1, Neu2 and Neu3 returned to their initial fibroblastic appearance, which was more pronounced in the case of Neu1. Abundant intercellular cytoplasmic bridges are also observed towards the end of dedifferentiation, more abundant in the case of Neu2 (Fig. 2). Following Yu et al. (2011), the dedifferentiation may be related to selection that FGF and EGF in exert on these cells. In fact, Anghileri et al. (2008) demonstrated a significant loss of functionality in hASCs differentiated to neuronal lineage after seven days in culture. In our study, after remove Neu2 (HGF and VEGF included), a significant dedifferentiation was observed at the same time to Anghileri's study. However, after remove Neu1 (FGF and EGF included) the dedifferentiation was observed at 10 days. Finally, Neu3 (NGF included) was the least effective observing a cell dedifferentiation after removing media at 5 days.

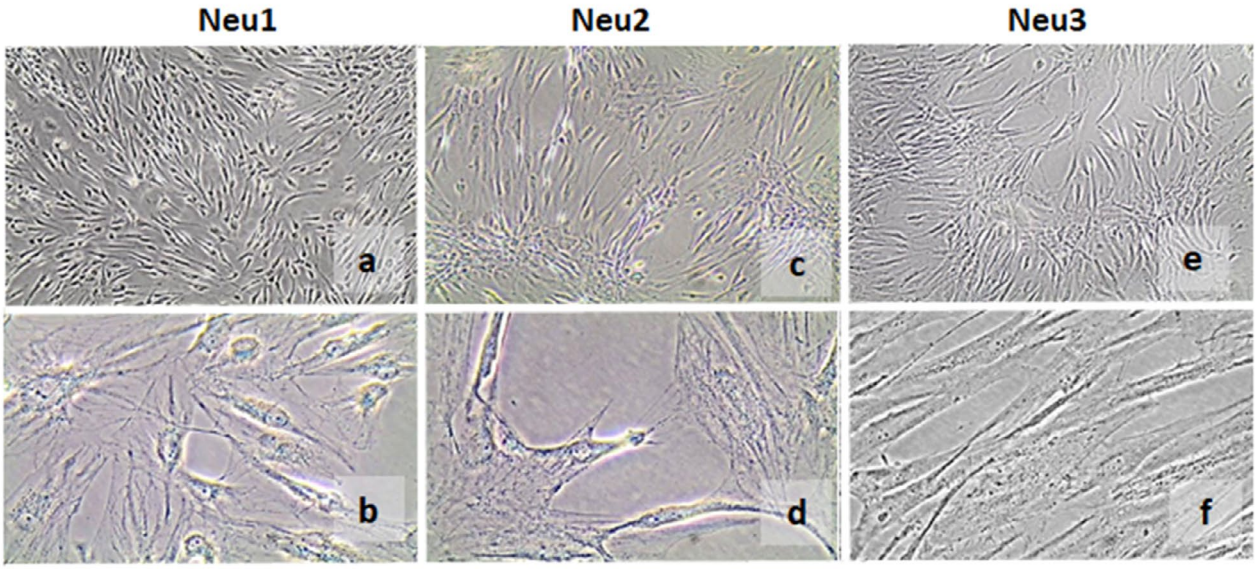

Fig. 2.- hASCs neuronal dedifferentiation. After hASCs differentiation medium was removed and cells growth until 29 days (Neu 1), 21 days (Neu2) and 15 days (Neu3). Images show dedifferentiation of hASCs cells. Magnification 4x (a,c,e) and 20x (b,d,f).

Neuronal marker modulation in differentiation and dedifferentiation of hASCs

Western blot analysis indicated a significant modulation in the expression of neuronal markers in the induced-hASCs as compared to non-induced cells. Western blot analysis showed the modulation of mature neuron markers (TAU and TH), glial markers (GFAP), and functional markers (SNAP25) cells treated with Neu1 (Fig. 3). Neu2 and Neu3 also induced an increased expression of TH and SNAP25 levels but significantly lower than those induced by Neu1; they did not induce TAU modulation and caused a significant decrease in the expression of ENS, suggesting lower neuronal differentiation compared to Neu1 (Fig. 3). For example, it has been recently observed how human-derived adipose stem cells (hASC) transdifferentiate into neuronal-like cells and increase the expression of the neuronal marker protein MAP-2 after neuronal induction. Interestingly, MAP-2 increase

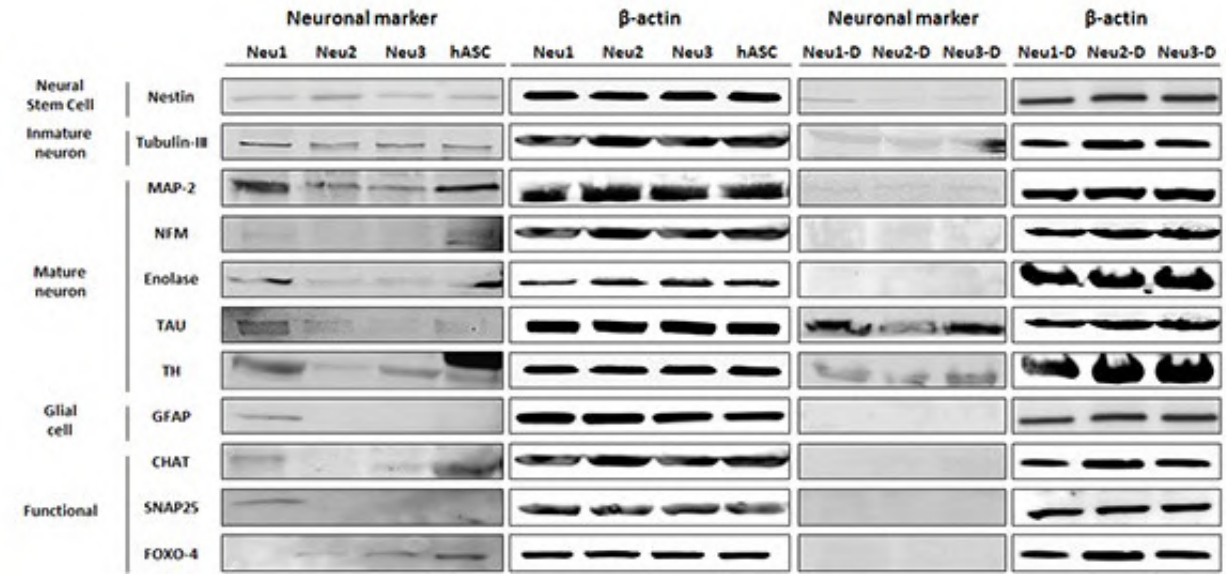

Fig. 3.- Neuronal markers determined by Western blot in hASCs control, hASCs induced with the media Neu1 (21 days), Neu2 (15 days) and Neu3 (10 days) as well as dedifferentiated cells after the differentiation process, Neu1-D (31 days), Neu2-D (21 days) and Neu3-D (15 days). β-actin served as an internal control.

has recently been pointed out as a critical fact in hASCs transdifferentiate into neuronal-type cells (González-Casacuberta et al., 2022). Thus, an expression decrease after dedifferentiation may represent a serious limitation for its applicability. To determine the reversibility of the differentiation process and corroborate the modulation of biomarkers and gene expression, an analysis of hASCs after dedifferentiation was conducted. Western blot showed a loss of expression in functional markers and in mature neuron markers (inclunding MAP2 and ENS). On the other hand, dedifferentiation after Neu2 and Neu3 exposure provoked a reduction in the expression of MAP2 and FOXO4 (Fig. 3). The expression of proteins such as TAU, GFAP and Map2 have been reported by several authors after neuronal differentiation in hASCs (Cardozo et al., 2011; Jang et al., 2010; Mostafavi et al., 2014), which indicates the acquired neuronal compromise of these cells after differentiation. NAP25 is considered a key factor to promote neuronal differentiation in rats (Bailey and Lahiri, 2006). In our study, the expression of three of these four fundamental proteins is increased by the Neu1 induction medium, suggesting that it is the best medium of the three for neuronal differentiation. In the other media studied, the modulation of these proteins is lower

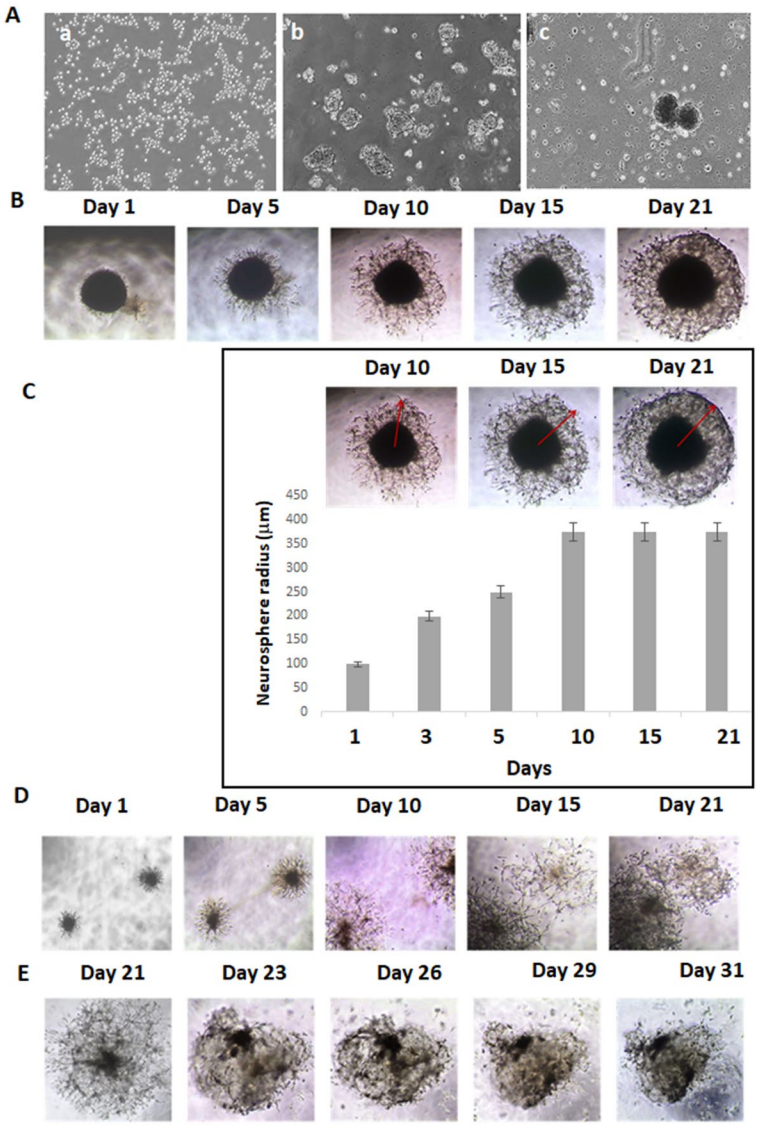

Fig. 4.- Neuronal differentiation/dedifferentiation of hASC neurospheres. **A.** Representative optical microscope image of neurosphere formation in DMEM/F12 medium supplemented with B27 during days 1 (a), 4 (b) and 7 (c). **B.** Growth of neurospheres (agarose 0.5%) after exposure to Neu 1 media (21 days). **C.** Representative images of neurospheres on days 10, 15 and 21 with determination of the extension growth (red line) (Image J). Graphic representation of growth during the 21 days. **D.** Approach and aggregation of hASC neurospheres. **E.** Morphological changes during dedifferentiation of neurospheres after removing Neu1 medium (31 days) (4x magnification).

or even show a reduction in Map2, although there are authors such as Razavi et al. (2015) that did not find significant differences in terms of Map2 expression after neuronal induction in hASCs.

Neuronal dedifferentiation in hASCs neurospheres

The differentiation/dedifferentiation assays in neurospheres were carried out only with Neu1 given the previous results. As shown in Fig. 4A, the neurospheres were formed within a few days (5 days) of the hASCs culture in DMEM / F12 medium supplemented with B27. Neurospheres maintained in the Neu1 medium grew by developing long cell extensions in the manner dendrites (Fig. 4B). These extensions grew fundamentally in the first 5 days of induction, stabilizing later (Fig. 4C). The neurospheres aggregated through long processes to finally form a single neurosphere (Fig. 4D). Analysis of the dedifferentiation process after Neu1 removal and the addition of the standard medium (10 days) showed that the neurospheres collapsed, acquiring an irregular morphology and losing the cell extensions formed during neuronal differentiation (Fig. 4E). Neurospheres derived from hASCs are associated to a greater extent with their possible clinical use in neurodegenerative diseases such as Alzheimer's. These neurospheres are characterized by high levels of Nestin (Peng et al., 2019; Yang et al., 2015). EGF and FGF together with B27 seems essential not only to the maintenance of differentiation but also the own neurospheres (Peng et al., 2019). In fact, as soon as these factors are removed from the environment, these neurospheres begin to lose neuronal differentiation.

CONCLUSION

In conclusion, previous studies demonstrated that three different media achieved effective neuronal differentiation of hASCs with remarkable results in terms of morphology changes and expression of typically neuronal markers. However, removal of the induction media induced a significant neuronal dedifferentiation. These results suggest that other strategies including a new composition of differentiation media will be necessary to avoid phenotype reversal in order to provide better therapeutic utility of the hASCs in some neurogical disorders.

ACKNOWLEDGEMENTS

This work was supported by Fundació La Marató TV3 (111430/31) and by the financial support from the CTS-107 Group from Junta de Andalucía. We thank Scientific Instrumentation Center (C.I.C) from Granada University for technical assistance.

REFERENCES

ANGHILERI E, MARCONI S, PIGNATELLI A, CIFELLI P, GALIÉ M, SBARBAT A, KRAMPERA M, BELLUZZI O, BONETTI B (2008) Neuronal differentiation potential of human adipose-derived mesenchymal stem cells. *Stem Cells Dev,* 17(5): 909-916.

BAILEY JA, LAHIRI DK (2006) Neuronal differentiation is accompanied by increased levels of SNAP-25 protein in fetal rat primary cortical neurons: Implications in neuronal plasticity and Alzheimer's disease. *Ann N Y Acad Sci*, 1086: 54-65.

CALIOGNA L, BINA V, BOTTA L, BENAZZO FM, MEDETTI M, MAESTRETTI G, MOSCONI M, COFANO F, TARTARA F, GASTALDI G (2020) Osteogenic potential of human adipose derived stem cells (hASCs) seeded on titanium trabecular spinal cages. *Sci Rep,* 10(1): 18284.

CARDOZO AJ, GÓMEZ DE, ARGIBAY PF (2011) Transcriptional characterization of Wnt and Notch signaling pathways in neuronal differentiation of human adipose tissue-derived stem cells. *J Mol Neurosci,* 44(3): 186-194.

GONZÁLEZ-CASACUBERTA I, VILAS D, PONT-SUNYER C, TOBÍAS E, CANTÓ-SANTOS J, VALLS-ROCA L, GARCÍA-GARCÍA FJ, GARRABOU G, GRAU-JUNYENT JM, MARTÍ MJ, CARDELLACH F, MORÉN C (2022) Neuronal induction and bioenergetics characterization of human forearm adipose stem cells from Parkinson's disease patients and healthy controls. *PLoS One*, 17(3): e0265256.

GONG L, CAO L, SHEN Z, SHAO L, GAO S, ZHANG C, LU J, LI W (2018) Materials for neural differentiation, trans-differentiation, and modeling of neurological disease. *Adv Mat,* 30(17): e1705684.

HANLEY J, RASTEGARLARI G, NATHWANI AC (2010) An introduction to induced pluripotent stem cells. *Br J Haematol*, 151(1): 16-24.

HERNÁNDEZ R, JIMÉNEZ-LUNA C, ORTIZ R, SETIÉN F, LÓPEZ M, PERAZZOLI G, ESTELLER M, BERDASCO M, PRADOS J, MELGUIZO C (2021) Impact of the epigenetically regulated hoxa-5 gene in neural differentiation from human adipose-derived stem cells. *Biology*, 10(8): 802.

HU F, WANG X, LIANG G, LV L, ZHU Y, SUN B, XIAO Z (2013) Effects of epidermal growth factor and basic fibroblast growth factor on the proliferation and osteogenic and neural differentiation of adipose-derived stem cells. *Cell Reprogram*, 15(3): 224-232.

JANG S, CHO HH, CHO YB, PARK JS, JEONG HS (2010) Functional neural differentiation of human adipose tissue-derived stem cells using bFGF and forskolin. *BMC Cell Biol*, 11(1): 25.

KRAMPERA M, MARCONI S, PASINI A, GALIÈ M, RIGOTTI G, MOSNA F, TINELLI M, LOVATO L, ANGHILERI E, ANDREINI A, PIZZOLO G, SBARBATI A, BONETTI B (2007) Induction of neural-like differentiation in human mesenchymal stem cells derived from bone marrow, fat, spleen and thymus. *Bone*, 40(2): 382-390.

LI H, HAN Z, LIU D, ZHAO P, LIANG S, XU K (2013) Autologous platelet-rich plasma promotes neurogenic differentiation of human adipose-derived stem cells in vitro. *Int J Neurosci*, 123(3): 184-190.

MA T, SUN J, ZHAO Z, LEI W, CHEN Y, WANG X, YANG J, SHEN Z (2017) A brief review: Adipose-derived stem cells and their therapeutic potential in cardiovascular diseases. *Stem Cell Res Ther*, 8(1): 124.

MAHMOUDIFAR N, DORAN PM (2015) Mesenchymal stem cells derived from human adipose tissue. In: Doran PM (ed.). *Cartilage tissue engineering: methods and protocols*. Springer, New York, pp 53-64.

MAREI HES, EL-GAMAL A, ALTHANI A, AFIFI N, ABD-ELMAKSOUD A, FARAG A, CENCIARELLI C, THOMAS C, ANWARUL H (2018) Cholinergic and dopaminergic neuronal differentiation of human adipose tissue derived mesenchymal stem cells. *J Cell Physiol*, *2*33(2): 936-945.

MINTEER D, MARRA KG, RUBIN JP (2013) Adipose-derived mesenchymal stem cells: biology and potential applications. In: Weyand B, Dominici M, Hass R, Jacobs R, Kasper C (eds.). *Mesenchymal Stem Cells-Basics and Clinical Application I*. Springer, Berlin, Heidelberg, pp 59-71.

MOSTAFAVI FS, RAZAVI S, MARDANI M, ESFANDIARI E, ESFAHANI HZ, KAZEMI M (2014) Comparative study of microtubule-associated protein-2 and glial fibrillary acidic proteins during neural induction of human bone marrow mesenchymal stem cells and adipose-derived stem cells. *Int J Preven Med*, 5(5): 584-595.

NADERI N, COMBELLACK EJ, GRIFFIN M, SEDAGHATI T, JAVED M, FINDLAY MW, WALLACE CG, MOSAHEBI A, BUTLER PE, SEIFALIAN AM, WHITAKER IS (2017) The regenerative role of adipose-derived stem cells (ADSC) in plastic and reconstructive surgery. *Int Wound J*, 14(1): 112-124.

PENG C, LU L, LI Y, HU J (2019) Neurospheres Induced from human adipose-derived stem cells as a new source of neural progenitor cells. *Cell Transplant*, *28*(1 Suppl): 66S-75S.

RAZAVI S, KHOSRAVIZADEH Z, BAHRAMIAN H, KAZEMI M (2015) Changes of neural markers expression during late neurogenic differentiation of human adipose-derived stem cells. *Adv Biomed Res*, 4: 209.

RUPPERT KA, PRABHAKARA KS, TOLEDANO-FURMAN NE, UDTHA S, ARCENEAUX AQ, PARK H, DAO A, COX CS, OLSON SD (2020) Human adipose-derived mesenchymal stem cells for acute and sub-acute TBI. *PLoS One*, 15(5): e0233263.

SAFFORD KM, HICOK KC, SAFFORD SD, HALVORSEN YD, WILKISON WO, GIMBLE JM, RICE HE (2002) Neurogenic differentiation of murine and human adipose-derived stromal cells. *Biochem Biophys Res Commun*, 294(2): 371-379.

SALEHI H, AMIRPOUR N, NIAPOUR A, RAZAVI S (2016) An overview of neural differentiation potential of human adipose derived stem cells. *Stem Cell Rev Rep*, 12(1): 26-41.

SÁNCHEZ-CASTILLO AI, SEPÚLVEDA MR, MARÍN-TEVA JL, CUADROS MA, MARTÍN-OLIVA D, GONZÁLEZ-REY E, DELGADO M, NEUBRAND VE (2022) Switching roles: beneficial effects of adipose tissue-derived mesenchymal stem cells on microglia and their implication in neurodegenerative diseases. *Biomolecules,* 12(2): 219.

TONDREAU T, DEJENEFFE M, MEULEMAN N, STAMATOPOULOS B, DELFORGE A, MARTIAT P, BRON D, LAGNEAUX L (2008) Gene expression pattern of functional neuronal cells derived from human bone marrow mesenchymal stromal cells. *BMC Genom*, 9: 166.

YANG E, LIU N, TANG Y, HU Y, ZHANG P, PAN C, DONG S, ZHANG Y, TANG Z (2015) Generation of neurospheres from human adipose-derived stem cells. *Biomed Res Int*, 2015: 743714.

YU JM, BUNNELL BA, KANG SK (2011) Neural differentiation of human adipose tissue-derived stem cells. In: Gimble JM, Bunnell BA (eds.). *Adipose-Derived Stem Cells: Methods and Protocols*. Humana Press, Totowa, NJ, pp 219-231.

Micro-CT to study and reconstruct fetal and infant coronary arteries: a pilot study on a novel post-mortem technique

Francesco Lupariello[1], Tullio Genova[2,3], Federico Mussano[3], Giancarlo Di Vella[1], Giovanni Botta[4]

[1] Dipartimento di Scienze della Sanità Pubblica e Pediatriche - Sezione di Medicina Legale - "Università degli Studi di Torino"; address: corso Galileo Galilei 22, 10126 Torino, Italy

[2] Department of Life Sciences and Systems Biology, UNITO, via Accademia Albertina 13, 10123, Turin, Italy

[3] CIR Dental School, Department of Surgical Sciences UNITO, via Nizza 230, 10126 Torino, Italy

[4] A.O.U. Città della Salute e della Scienza – Anatomia Patologica U, Sezione Materno-Fetale-Pediatrica; address: corso Bramante 88, 10126 Torino, Italy

SUMMARY

For a significant part of infant and fetal deaths, specific pathophysiologic processes cannot be recognized. Thus, the scientific community is called to identify novel post-mortem diagnostic tools. This manuscript proposes the results of a pilot study which reports a novel post-mortem technique to study and reconstruct fetal/infant coronary arteries. The study included human fetuses characterized by the absence of macroscopic cardiac abnormalities at post-mortem in situ examination. For the study of fetal hearts, it was used a curing radiopaque silicone rubber compound (which solidified after injection in the coronary arteries) and an X-Ray microtomography (micro-CT). After micro-CT scans, coronary arteries' branches were reconstructed throughout a specific software. At injection, it was possible to macroscopically evaluate coronary arteries' perfusion. The analysis of the three-dimensional reconstructions highlighted that the aforementioned compound reached deep branches too. This approach can be considered a novel post-mortem technique for fetal/infant hearts. Nevertheless, the manuscript also discussed the following limitations: in some spots, coronary arteries' reconstruction appeared interrupted; the compound also perfused parts of internal cardiac chambers. Until now, in the literature there are not methods that allow study with reconstruction of fetal/infant coronary arteries throughout micro-CT. The present paper pointed out the first indications for the application of this technique in human samples.

Key words: Micro-CT – Coronary arteries – Fetus – Infant – Post-mortem technique

INTRODUCTION

According to the Center for Disease Control and Prevention (CDC), each year about 3,400

Corresponding author:
Francesco Lupariello. Dipartimento di Scienze della Sanità Pubblica e Pediatriche - Sezione di Medicina Legale - "Università degli Studi di Torino", corso Galileo Galilei 22, 10126 Torino, Italy. Phone: +390116705618. E-mail: francesco.lupariello@gmail.com
Orcid: 0000-0003-2264-8521.

Submitted: March 7, 2022. **Accepted:** April 16, 2022

https://doi.org/10.52083/FCWS3396

sudden unexpected infant deaths (SUID) occur in the United States. Among them, the 37% is attributable to the sudden infant death syndrome (SIDS) and the 34.7% to unknown causes (https://www.cdc.gov/sids/data.htm). It is also important to know that the most common negative outcome of pregnancies is represented by fetal death. 2.6 million stillbirths are globally reported in 2015 (Lavezzi et al., 2019). In 2014, in the United States about 24,000 stillbirths were reported. 30% of them was attributable to unspecified causes (https://www.cdc.gov/ncbddd/stillbirth/data.html).

In the light of the above, it can be stated that, for a significative part of infant and fetal deaths, the specific pathophysiologic processes cannot be recognized, not permitting to communicate the specific cause of death to parents and to identify preventive measures (Lavezzi et al., 2019). In addition, in case of medical malpractice claims and/or inspections requested by prosecutors, the impossibility to identify a certain – or at least probable – cause of infant/fetal death is a significant limitation for forensic operators (Kettner et al., 2014; Lupariello et al., 2019; Lupariello et al., 2021; Rutty et al., 2019).

In order to reduce the number of fetal/infant deaths with unknown causes, the scientific community should be called to explore and identify novel post-mortem diagnostic tools which can allow to give new insights in pathology and forensic routine.

During standard post-mortem evaluations, a meaningful limitation is represented by the extreme difficulty to analyse and reconstruct superficial and deep coronary arteries of fetal/infant hearts. For this reason, this manuscript describes a novel post-mortem technique which can be useful to reconstruct and study these arteries. Even if until now in the scientific literature there are no clear indications about this novel tool, the abovementioned technique (capable to highlight the architecture of fetal/infant coronary arteries) could be commonly used in post-mortem examination.

MATERIALS AND METHODS

Study Samples

The study included 7 human fetuses (15 to 36 weeks of gestational age) characterized by negative prenatal ultrasonography for heart diseases. They had been referred to the Department of Pathology of the University of Turin after spontaneous demise. Parental consent for the study was obtained. All fetuses underwent post-mortem examination (24 to30 hours: interval time between miscarriage and post-mortem examination). In all cases, in situ examination of cardiovascular system confirmed the absence of macroscopic cardiac abnormalities.

Equipment

For the study of fetal hearts the authors used: a) an X-Ray microtomography (SkyScan1172, Bruker; settings: acquisition at 80KV using a 0.5mm aluminium filter at a resolution of 10 µm, 0.4° of rotation step, 180° scan, 4x frame averaging; for each sample, scanning time was fixed to 90 minutes) (Lupariello et al., 2021); b) a curing radiopaque silicone rubber compound (Microfil MV-122, Flow Tech Inc) that – initially fluid – solidifies after about 30 minutes from its injection.

Procedures

Before hearts' removal, pathologists realized a small hole in the superior surface of the aorta – just before the origin of the brachiocephalic artery. Clamping the aorta in order to block the flow towards its distal branches, pathologists injected the curing radiopaque silicone rubber compound (Microfil MV-122, Flow Tech Inc) towards coronary arteries' origins. Then, the 7 hearts were removed, fixed in 4 % aqueous buffered formaldehyde, and stored at room temperature for 20 to 30 days. Hearts were scanned by the X-Ray microtomography (SkyScan1172, Bruker) with the abovementioned settings. Finally, a three-dimensional (3D) reconstruction of hearts' coronary arteries was obtained throughout the CTvox software. Then, all 3D reconstructions were evaluated to identify possible defects and/or anomalies of perfusion. These data are reported in Table 1.

Table 1 - Summary of the results

Case number	Gestational age (weeks)	Methodology	Perfusion's pattern	Reconstruction's anomalies	Perfusion
1	17	Microfil injection towards coronary arteries' origins	Microfil perfused both right and left coronary arteries	Reconstruction's defects of deep branches	Incomplete
2	20	Microfil injection in the coronary arteries	Microfil perfused both right and left coronary arteries	Reconstruction's defects of superficial and deep branches; perfusion of parts of internal cardiac chambers	Incomplete
3	15	Microfil injection in the coronary arteries	Microfil perfused both right and left coronary arteries	Reconstruction's defects of deep branches; perfusion of parts of internal cardiac chambers	Incomplete
4	19	Microfil injection in the coronary arteries	Microfil perfused both right and left coronary arteries	Reconstruction's defects of deep branches; perfusion of parts of internal cardiac chambers	Incomplete
5	25	Microfil injection in the coronary arteries	Microfil perfused both right and left coronary arteries	Reconstruction's defects of deep branches	Incomplete
6	33	Microfil injection in the coronary arteries	Microfil perfused both right and left coronary arteries	Reconstruction's defects of superficial and deep branches; perfusion of parts of internal cardiac chambers	Incomplete
7	36	Microfil injection in the coronary arteries	Microfil perfused both right and left coronary arteries	Reconstruction's defects of deep branches	Incomplete

RESULTS

The most significant results are available in Table 1, in Figs. 1 and 2, and in **Videos 1** and **2**. At injection, thanks to the rubber compound's yellowish color, it was possible to macroscopically evaluate coronary arteries' perfusion. However, the perfusion was incomplete in all cases because the Microfil did not reach all coronary branches (Table 1). Video 1 and Fig. 1 depict the compound filling superficial coronary arteries of a fetal heart (case number one; Table 1). The three-dimensional reconstruction highlighted that Microfil perfusion also reached deep branches. Nevertheless, in some spots coronary superficial and/or deep arteries' reconstruction appeared interrupted. In addition, in some cases the Microfil also perfused parts of internal cardiac chambers (Table 1, Video 2, Fig. 2). Comparing the three-dimensional reconstructions with gross examination' findings, in all cases the X-Ray microtomography (in association with Microfil injection) demonstrated a better capability to highlight the not superficial branches of the coronary arteries.

DISCUSSION

Unlike conventional computed tomography (CT), Micro-Computed Tomography (micro-CT) is not yet implemented in clinical routine. Its resolution ability is under to 1 mm^3 (higher than CT). Nevertheless, it can be used only to analyse small samples. Indeed, in the scientific community it has been commonly used to study (in and ex vivo) animal fetuses and organs (Clark et al., 2014; Degenhardt et al., 2010; Hutchinson et al., 2017; Hutchinson et al., 2018; Lombardi et al., 2014; Liu et al., 2013; Lombardi et al., 2019; Lupariello et al., 2021).

Emerging applications of micro-CT in human samples consist of "the study of fetal/infant organs and whole fetuses, and their two/three-dimension reconstruction, representing an innovative approach because it allows: to facilitate pathologists' role in the identification of causes of fetal stillbirth and of infant death; to create digital two and/or three-dimension representations of fetal/infant organs and whole fetuses which can be easily discussed in civil and/or penal courts" (Lupariello et al., 2021). In particular, the scientific

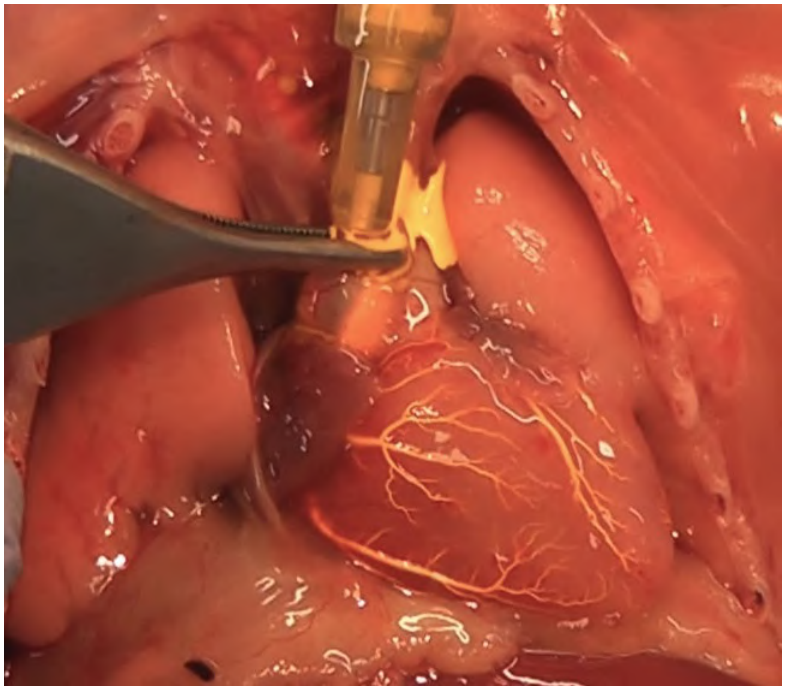

Fig. 1.- A fetal heart (17 weeks of gestational age) during Microfil injection. All superficial coronary arteries appear to be perfused by the compound. ç: aorta; +: right auricle; §: branches of the right coronary artery; *: left anterior descending artery; #: right marginal branch of the right coronary artery.

literature reports the usefulness of micro-CT – in association with Lugol solutions – in post-mortem diagnosis of human cardiac abnormalities (especially the so-called congenital heart defects – CHDs) (Hutchinson et al., 2017; Hutchinson et al., 2018; Lombardi et al., 2014; Lupariello et al., 2021; Sandaite et al., 2020).

On the contrary, until now in the scientific literature there are no indications about techniques which can allow us to reconstruct superficial and deep coronary arteries of human fetal/infant hearts. The results of this pilot study pointed out the possibility to impregnate the aforementioned arteries with the injection of a curing radiopaque

Fig. 2.- Three-dimensional reconstruction of a fetal heart (20 weeks of gestational age). Right ventricle (RV) and left ventricle (LF) show multiple defects in the reconstruction of superficial coronary arteries.

silicone rubber compound (Microfil). In addition, they highlighted the possibility to create – throughout micro-CT scans and specific software – three-dimensional reconstruction of fetal coronary arteries. Therefore, this approach can be considered a novel post-mortem technique for fetal/infant hearts. It could be commonly used in pathologists' routine especially when anomalies of not superficial/deep branches of the coronary arteries could have caused the demise.

The present study demonstrated a better capability of micro-CT to highlight the not superficial branches of the coronary arteries. On the contrary, due to their extremely small diameter, these branches are hardly distinguishable at standard gross examination of fetal/infant hearts, not allowing a complete analysis. The latter is a significant limitation in case of suspected fetal unexplained demise and sudden infant death syndrome, in which it is mandatory to exclude all cardiac anomalies for an accurate diagnosis. Thus, after proper standardization, micro-CT with coronary arteries' perfusion could be implemented as a useful ancillary tool for pathologists.

The results highlighted that the perfusion of parts of internal cardiac chambers and the impossibility to reach all the extent of some coronary arteries represent significant limitations. In particular, the study pointed out defects in the reconstruction of superficial and/or deep arteries, not allowing a complete visualization of the coronary tree. Possible explanations for these effects are, respectively: internal cardiac chambers were perfused because the Microfil was not injected directly throughout left and right coronary arteries' ostia (part of the compound went into heart cambers passing through the aortic valve); in some coronary arteries' branches there were already clots which did not allow us to complete the perfusion (the interval time between miscarriage and post-mortem examination was 24 to 30 hours). However, future studies are planned in order to solve these limitations. Indeed, preventive perfusion of coronary arteries with anticoagulant solutions and direct injection of Microfil throughout right and left coronary arteries' ostia could be suitable remedies to improve results.

REFERENCES

CLARK DP, BADEA CT (2014) Micro-CT of rodents: state-of-the-art and future perspectives. *Phys Med,* 30(6): 619-634.

DEGENHARDT K, WRIGHT AC, HORNG D, PADMANABHAN A, EPSTEIN JA (2010) Rapid 3D phenotyping of cardiovascular development in mouse embryos by micro-CT with iodine staining. *Circ Cardiovasc Imaging*, 3(3): 314-322.

https://www.cdc.gov/ncbddd/stillbirth/data.html.

https://www.cdc.gov/sids/data.htm.

HUTCHINSON JC, SHELMERDINE SC, SIMCOCK IC, SEBIRE NJ, ARTHURS OJ (2017) Early clinical applications for imaging at microscopic detail: microfocus computed tomography (micro-CT). *Br J Radiol,* 90(1075): 20170113.

HUTCHINSON JC, KANG X, SHELMERDINE SC, SEGERS V, LOMBARDI CM, CANNIE MM, SEBIRE NJ, JANI JC, ARTHURS OJ (2018) Postmortem microfocus computed tomography for early gestation fetuses: a validation study against conventional autopsy. *Am J Obstet Gynecol*, 218(4): 445.e1-445.e12.

KETTNER M, POTENTE S, SCHULZ B, KNAUFF P, SCHMIDT PH, RAMSTHALER F (2014) Analysis of laryngeal fractures in decomposed bodies using microfocus computed tomography (MFCT). *Forensic Sci Med Pathol,* 10(4): 607-612.

LAVEZZI AM, PISCIOLI F, PUSIOL T, JORIZZO G, FERRERO S (2019) Sudden intrauterine unexplained death: time to adopt uniform postmortem investigative guidelines? *BMC Pregnancy Childbirth*, 19(1): 526.

LIU X, TOBITA K, FRANCIS RJB, LO CW (2013) Imaging techniques for visualizing and phenotyping congenital heart defects in murine models. *Birth Defects Res C Embryo Today,* 99(2): 93-105.

LOMBARDI CM, ZAMBELLI V, BOTTA G, MOLTRASIO F, CATTORETTI G, LUCCHINI V, FESSLOVA V, CUTTIN MS (2014) Postmortem micro-computed tomography (micro-CT) of small fetuses and hearts. *Ultrasound Obstet Gynecol*, 44(5): 600-609.

LOMBARDI S, SCOLA E, IPPOLITO D, ZAMBELLI V, BOTTA G, CUTTIN S, TRIULZI F, LOMBARDI CM (2019) Micro-computed tomography: a new diagnostic tool in postmortem assessment of brain anatomy in small fetuses. *Neuroradiology*, 61(7): 737-746.

LUPARIELLO F, NUZZOLESE E, DI VELLA G (2019) Causes of death shortly after delivery and medical malpractice claims in congenital high airway obstruction syndrome: Review of the literature. *Leg Med (Tokyo)*, 40: 61-65.

LUPARIELLO F, GENOVA T, MUSSANO F, DI VELLA G, BOTTA G (2021) Micro-CT processing's effects on microscopic appearance of human fetal cardiac samples. *Leg Med (Tokyo),* 53: 101934.

RUTTY GN, BROUGH A, BIGGS MJP, ROBINSON C, LAWES SDA, HAINSWORTH SV (2013) The role of micro-computed tomography in forensic investigations. *Forensic Sci Int,* 225(1-3): 60-66.

SANDAITE I, LOMBARDI C, COOK AC, FABIETTI I, DEPREST J, BOITO S (2020) Micro-computed tomography of isolated fetal hearts following termination of pregnancy: A feasibility study at 8 to 12 weeks' gestation. *Prenatal Diagnosis,* 40(8): 984-990.

A retrospective study on the need of deriving ultrasonographical fetal gestational nomograms for fetal biometric parameters in the population of Udaipur Region

Hina Sharma[1], Ila Sharma[2], Dharamanjai K Sharma[3]

[1] Department of Anatomy, Geetanjali Medical College & Hospital, Udaipur, Geetanjali University India

[2] R.N.T. Medical College and Hospital, Udaipur, Rajasthan University of Health Sciences India

[3] Department of Surgery, R.N.T. Medical College & Hospital, Udaipur, Rajasthan University of Health Sciences, India

SUMMARY

Fetal gestational age is routinely calculated in sonography by the radiologists, with the dimensions of fetal biometric parameters, as the expectant mother may not remember the exact date of the last menstrual period. The expected date of delivery is then calculated accordingly and the antenatal period is managed consequently. Accurate fetal age estimation is of crucial importance for proper antenatal care in order to reduce infant mortality, and achieve the goal of delivering a healthy child. Various studies have been done to derive fetal nomograms for indigenous populations claiming that the Western data being used cannot be applied to their population. Therefore, need of deriving ultrasonographic fetal gestational nomograms for fetal biometric parameters (head circumference, abdominal circumference and femur length) for the population of Udaipur in the northwestern region of India was investigated. Fetal sonography records of pregnant women in second and third trimesters were studied. The study derived fetal gestational nomograms for fetal head circumference, fetal abdominal circumference and fetal femur length for estimating the fetal age. These nomograms were compared with the standard nomograms of Hadlock et al. used by radiologists for the same parameters. No significant difference was found between the two, and it was concluded that the routinely used nomograms may be also used for the local population of Udaipur, Rajasthan, India.

Key words: Fetal Age – Gestational Ages – Nomogram – Chronologic fetal maturity – Biometry

INTRODUCTION

Gestational age (GA) refers to the length of pregnancy after the first day of the last menstrual period (LMP). The precise estimation of gestational age is the key for successful antepartum care and for judicious explanation of antenatal tests and successful planning of appropriate intervention

Corresponding author:
Dr. Hina Sharma. 22 Hazareshwar Colony, Near Registrar Office, Udaipur, Rajasthan, India - 313001. Phone: +91 9799970949. E-mail: drsharmah@gmail.com

Submitted: December 14, 2021. **Accepted:** April 16, 2022

https://doi.org/10.52083/EGTZ2126

or treatment. The expected date of delivery is an important means for the doctor, who is responsible for the safe delivery of the child. Failure of accurate gestational age assessment can result in iatrogenic prematurity or post-maturity, both of which are associated with increased perinatal mortality and morbidity (Konje et al., 2002).

Estimation of gestational age on the basis of the LMP is most reliable and is universally followed. Yet LMP cannot be used for all patients because 10-40% of all patients seen in the antenatal clinics have no knowledge of their LMPs.

Nowadays, high-resolution ultrasound imaging makes assessment of fetal biometry at early stages of pregnancy. Ultrasound gives more objective evidence of gestational age (Otto et al., 1991). Ultrasonography is preferred over other methods, because it is noninvasive, with no radiation exposure (Nyborg et al., 2002), less expensive, usually available and safe for both mother and child. The ultrasound has been used for the examination and evaluation of high-risk pregnancies and for the diagnosis of congenital malformations (Al-Bayyari et al., 2010).

Many existing references for fetal biometric measurements have been reported by a number of investigators with results that show the uniqueness to their setting. The fetal biometric charts used in Udaipur are set from a different geographical setting, race and nutritional status. No data are available for estimation of fetal gestational age for the population of pregnant women of Udaipur. It was therefore important to conduct a study to investigate the reliability of the presently used Hadlock references for the local population of Udaipur, India. The results of this study may help in creating a baseline data on estimation of the fetal gestational age in pregnant women in the region of Udaipur.

MATERIALS AND METHODS

This retrospective, descriptive, cross-sectional study was carried out on the subjects from the Udaipur region, after obtaining ethical clearance from the institutional ethical committee of Geetanjali University (GU/UEC/EC/2014/686). Fetal biometric (Abdominal Circumference, Head Circumference, Femur Length) sonography records of pregnant women who registered for antenatal care (ANC) in Geetanjali Medical College and Hospital and Rabindranath Tagore Medical College and Hospital, Udaipur, India, were taken (as this study was a record-based retrospective study, informed consent of pregnant women could not be taken**)**. Their dates of last menstrual period (LMP) were also recorded. Records of second and third trimesters were included in the study. Care was taken to include only singleton pregnancies having regular menstrual cycles and known LMP. Records of anomalous fetuses and maternal diseases – diabetes mellitus and hypertension – were excluded from the study. Total sample size was 1212 with 659 records for the second trimester (13-28 weeks) and 553 for the third trimester (29-40 weeks). the identities of the pregnant women were not revealed.

In each of the record collected, HC, AC and FL determined by sonography were noted along with gestational age of the fetus based on the last menstrual period (LMP). Gestational age determined by fetal biometric measurements were also noted. A mean of the three parameters was then calculated and plotted for each gestational age in weeks for the second and third trimesters.

Standard nomograms by Hadlock et al. currently used for measuring fetal biometric parameters were taken from text to compare with the gestational age derived by LMP (Callen, 2007).

SPSS package was utilized for statistical analysis in this study.

The mean of all three parameters was calculated (Tables 1, 2 and 3). A comparison of the means of the parameters of the present study with standard fetal growth charts inthe second and third trimesters was done (Figs. 1, 2 and 3). Regression equations for determination of gestational age from each of the fetal parameters was calculated using SPSS. A gestational age nomogram was plotted for each parameter and in each of these the nomogram, based on the table by Hadlock et al. (Callen, 2007), was also plotted. An attempt was made to see whether these plots were in agreement with each other.

Table 1. Mean gestational age (GA) (weeks) determined from ultrasonographic measurements of fetal head circumference (HC) from 100 to 400 mm HC corresponding to 14.43 to 33.14 weeks gestational age.

HC (mm)	GA Mean weeks	HC (mm)	GA Mean weeks	HC (mm)	GA Mean weeks	HC (mm)	GA Mean weeks	HC (mm)	GA Mean weeks
100	14.43	**155**	18.28	**210**	22.85	**265**	28.55	**320**	35.72
105	14.86	**160**	18.64	**215**	23.32	**270**	29.13	**325**	36.42
110	15.14	**165**	19.37	**220**	23.76	**275**	29.71	**330**	37.11
115	15.43	**170**	19.44	**225**	24.28	**280**	30.37	**335**	37.95
120	15.82	**175**	19.84	**230**	24.91	**285**	30.91	**340**	38.59
125	16.17	**180**	20.17	**235**	25.33	**290**	31.7	**345**	39.53
130	16.45	**185**	21.21	**240**	25.91	**295**	32.13	**350**	40.28
135	16.84	**190**	21.12	**245**	26.34	**300**	32.5	**390**	31.28
140	17.14	**195**	21.39	**250**	26.86	**305**	33.63	**400**	33.14
145	17.52	**200**	21.98	**255**	27.41	**310**	34.26		
150	17.92	**205**	22.4	**260**	27.64	**315**	34.99		

Table 2. Mean gestational age (GA) (weeks) determined from ultrasonographic measurements of fetal abdominal circumference (AC) from 85 to 400 mm AC corresponding to 14.71 to 34.71 weeks GA.

AC (mm)	GA Mean weeks	AC (mm)	GA Mean weeks	AC (mm)	GA Mean weeks	AC (mm)	GA Mean weeks	AC (mm)	GA Mean weeks
85	14.71	**145**	19.57	**205**	24.86	**265**	30.35	**325**	36.06
90	15.09	**150**	20.04	**210**	25.37	**270**	30.92	**330**	36.65
95	15.5	**155**	20.48	**215**	25.81	**275**	31.48	**335**	37.13
100	15.81	**160**	20.94	**220**	26.2	**280**	31.94	**340**	37.7
105	16.26	**165**	21.33	**225**	26.69	**285**	32.31	**345**	38.14
110	16.61	**170**	21.83	**230**	27.15	**290**	32.81	**350**	38.57
115	17.11	**175**	22.19	**235**	27.19	**295**	33.29	**355**	39.09
120	17.47	**180**	22.68	**240**	28.05	**300**	33.86	**360**	39.43
125	17.92	**185**	23.15	**245**	28.47	**305**	34.28	**400**	34.71
130	18.65	**190**	23.56	**250**	29.01	**310**	34.71		
135	18.75	**195**	23.99	**255**	29.44	**315**	35.18		
140	19.16	**200**	24.39	**260**	30.08	**320**	35.63		

Table 3. Mean gestational age (GA) (weeks) determined from ultrasonographic measurements of femur length (FL) from 13 to 79 mm corresponding to 13.79 to 40 weeks GA (last reading of 89mm may be due to technical error).

FL (mm)	GA Mean weeks	FL (mm)	GA Mean weeks	FL (mm)	GA Mean weeks	FL (mm)	GA Mean weeks	FL (mm)	GA Mean weeks
13	13.79	**28**	18.41	**42**	23.47	**56**	29.11	**70**	35.7
15	14.29	**29**	18.75	**43**	23.93	**57**	29.76	**71**	36.15
16	14.5	**30**	19.14	**44**	24.33	**58**	30.14	**72**	36.62
17	15	**31**	19.47	**45**	24.67	**59**	30.62	**73**	37.11
18	15.14	**32**	19.8	**46**	25.12	**60**	30.96	**74**	37.66
19	15.61	**33**	20.16	**47**	25.49	**61**	31.41	**75**	38.12
20	15.84	**34**	20.53	**48**	25.87	**62**	31.91	**76**	38.64
21	16.15	**35**	20.89	**49**	26.2	**63**	32.4	**79**	40
22	16.4	**36**	21.27	**50**	26.77	**64**	32.83	**89**	27.57
23	16.74	**37**	21.57	**51**	27.14	**65**	33.36		
24	17.11	**38**	21.96	**52**	28.1	**66**	33.76		
25	17.41	**39**	22.36	**53**	27.92	**67**	34.2		
26	17.78	**40**	22.96	**54**	28.42	**68**	34.71		
27	18.1	**41**	23.15	**55**	28.83	**69**	35.21		

Figure 1

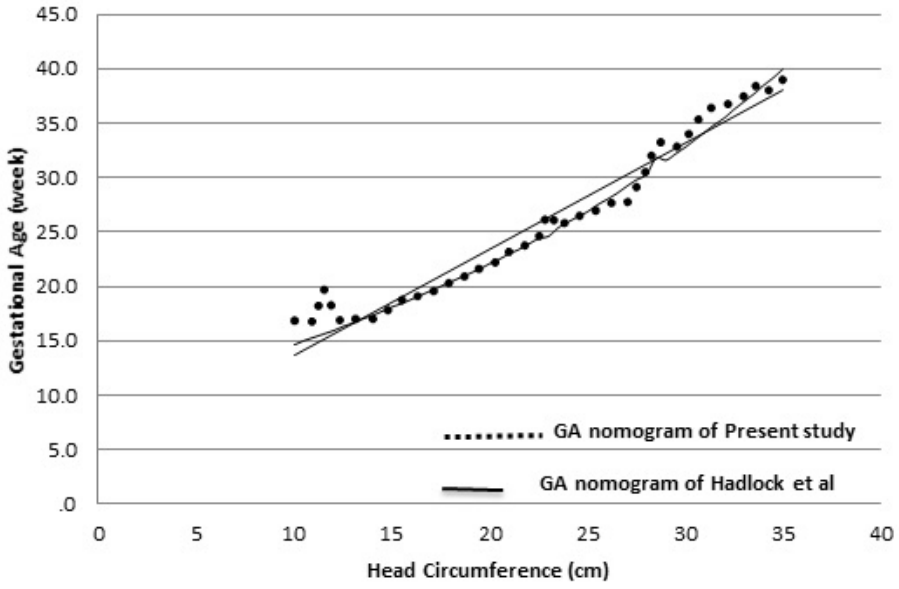

Fig. 1.- Gestational age nomograms derived from ultrasonographic Head Circumference measurements of present study vs that of Hadlock et al. (1982).

Further, Student's t test was used to evaluate statistical consonance of the present data with the table by Hadlock et al.

The correlation coefficient between gestational age by LMP method and by the three parameters (HC, AC, FL) using USG was calculated to determine a negative or positive relationship between the nomograms of the present study and that of currently used nomograms for various fetal biometric parameters.

ANOVA test was done to study the statistical difference of means for all the parameters, namely HC, AC and FL.

Figure 2

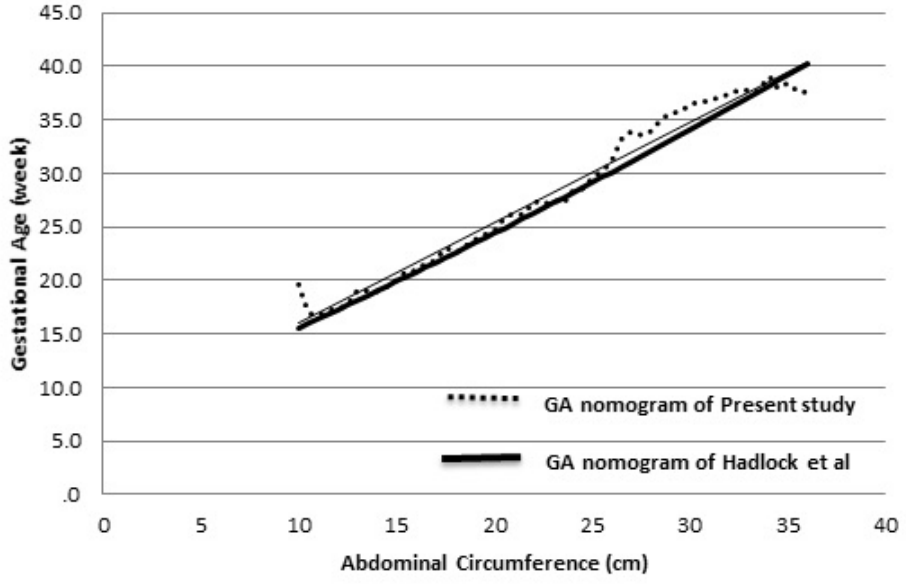

Fig. 2.- Gestational age nomograms derived from ultrasonographic Abdominal circumference measurements of present study vs that of Hadlock et al. (1982).

Figure 3

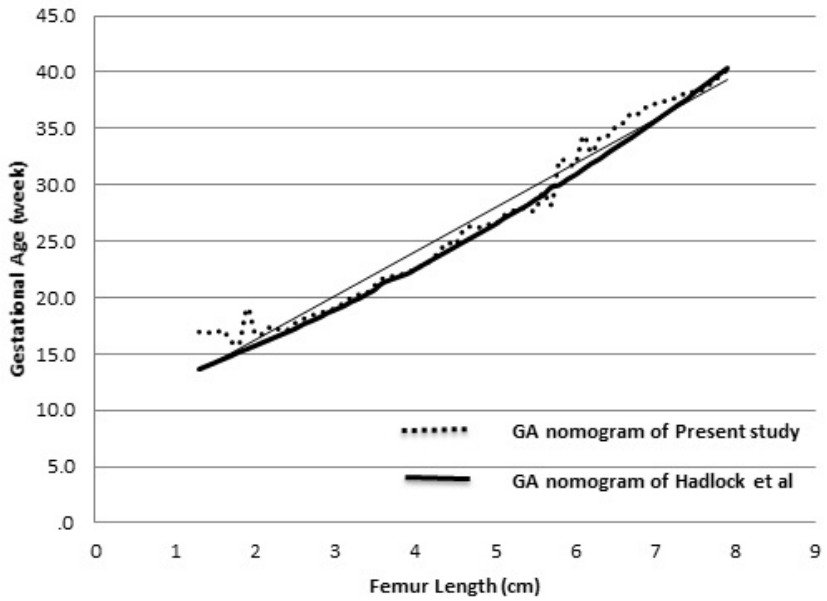

Fig. 3.- Gestational age nomograms derived from ultrasonographic Femur Length measurements of present study vs that of Hadlock et al. (1982).

In the present study, the average full-term baby's mean head circumference is 32.2 cm, with a standard deviation of 0.59 cm as compared to 33-38 cm given in text. The mean abdominal circumference in this study is 31.76 cm with a standard deviation of 0.2 cm as compared to 30.5-36.5 cm (Avery et al., 2000). The mean femur length at term (42 weeks) was found to be 70.5 cm, with a standard deviation of 0.13 cm as compared to 76-79 mm.

In this study, the mean gestational age by USG at term (42 weeks by LMP) was found to be 32.7 weeks, with a standard deviation of 5.8 weeks. The mean gestational age by USG at 28 weeks (LMP) was 27.29 weeks, with a standard deviation of just 1.31 weeks. It shows that the gestational age obtained in the second trimester was more accurate if compared to that obtained in the third trimester.

RESULTS

The mean head circumference, the abdominal circumference and the femur length were obtained for each gestational week determined by LMP. At full term, the mean head circumference was of 32.2 cm (±5.9 cm), the abdominal circumference was of 31.76 cm (±2 cm), the femur length was of 70.5 cm (±1.3 cm) (Tables 1-3).

The regression equation calculated in the present study for determination of gestational age from the head circumference is y = 0.973x + 3.958, where y = Gestational Age (weeks), x = head circumference (cm). The correlation coefficient r = 0.98, which means a strong positive relationship between the curves of the present study and that of the currently used nomogram for HC (Fig. 1).

The regression equation in the current study for the determination of gestational age from the abdominal circumference is y = 0.941x + 6.531, where y = Gestational Age (weeks), x = abdominal circumference (cm). The correlation coefficient r = 1, which means a strong positive relationship between the curves of the present study and that of the currently used nomogram for AC (Fig. 2).

The regression equation calculated in the present study for the determination of gestational age from the femur length is y = 0.973x + 3.958, where y = Gestational Age (weeks), x = femur length (cm). The correlation coefficient r = 1, which means a strong positive relationship between the curves of the present study and that of the currently used nomogram for FL (Fig. 3).

The gestational age determined by various ultrasonographic measurements of fetal biometric parameters (HC, AC, FL) was not significantly

different from that derived from LMP (P > 0.05). Student's t test showed that the difference in gestational age determined by combining all the readings of all the fetal biometric parameters by USG and gestational age determined by the LMP method in the second trimester was not significant (P = 0.39).

DISCUSSION

Available literature

It is an established fact that fetal age can be determined by the regression equations available for various fetal biometric parameters like HC, AC, FL and biparietal diameter. Different studies have found that there is a need for developing regression equations for fetal age determination of different geographical and ethnic regions (Konje et al., 2002; Al-Bayyari et al., 2010; Acharya et al., 2009; Varol et al., 2001; Snijders, 1994). The availability of such data for the population of Udaipur is scarce, and therefore this study was conducted to ascertain whether the Western data for fetal age determination by measuring fetal biometric parameters could be utilized for the local population of Udaipur.

Review of literature

According to a study on Indian women, until the end of the thrirty-fourth 34 week the growth parameters are quite same for the BPD, HC and FL, but then these parameters start lagging behind until the fortieth week (Acharya et al., 2009). However, in this study, the abdominal circumference was found to differ significantly after 30 weeks as compared to our study, where the difference was not found to be significant. In another study, significant correlations exist between BPD, AC, FL and estimated GA based upon correct last menstrual history (Varol et al., 2001). A study on the population of Africa also showed no significant ethnic differences between mothers in fetal biometry at the second trimester. They support the recommendation that ultrasound in practical healthcare can be used to assess gestational age in various populations with little risk of error due to ethnic variation (Salpou, 2008). A study of fetal biometry between weeks 14 and 40 of gestation showed that, despite methodological differences between the various studies, the meanfifth and ninety-fifth centiles were essentially the same (Snijders et al., 1994). Another previous study of fetal ultrasound biometry on Puerto Rican population, by De la Vega, showed similar fetal growth patterns as those reported from mixed US populations (De La Vega et al., 2008).

However, some studies by previous researchers have shown contrasting results. A study on a population of Jaipur, Rajasthan, India saw that sonography at 18 weeks underestimated gestational age compared with the LMP date by a median of -1.4 days (Babuta et al., 2013). Another study shows that the growth of rural Indian fetuses differs from the Western sonographic references that are generally used in clinical practice in India (Kinare, 2010). In the present study, the data consists of a mixed rural and urban population, and its sonographic references are not significantly different from the Western ones.

Inference of statistical analysis of present study

Comparison of gestational age nomogram derived from the measurements of head circumference by Hadlock et al. (1982) with our study revealed no significant difference (P value 0.36 for the second trimester and 0.28 for the third trimester). Comparison of gestational age nomogram derived from the measurements of the abdominal circumference by Hadlock et al. (1982) with our study showed no significant difference (P value 0.31 for ^{the} second trimester and 0.17 for ^{the} third trimester). Comparison of gestational age curve derived from the measurements of the femur length by Hadlock et al. (1982) with our study also showed no significant difference (P value 0.24 for the second trimester and 0.16 for the third trimester).

ANOVA test was applied and the F value was calculated to be 9.584167421, which is more than the critical value. This concludes that the difference in gestational age determined by various fetal parameters and LMP method is not significant. Thus, the present study recommends the use of conventionally used tables for determination of the gestational age of the fetus.

However, regression tables for more accurate gestational age determination for the local Indian population of pregnant women of Udaipur region have been constructed.

Impact of the present study

Regression equations for estimation of fetal age by USG measurements of fetal biometric parameters – HC, AC, FL – are now made available and can be utilized for the local population of the Udaipur region. Yet the study confirms that the previously used standard Western data is applicable to the local Indian population of Udaipur also.

CONCLUSION

Thus, to sum up, fetal age determination by sonography measurement of AC, HC and FL with utilization of already available Western nomograms was found to be applicable to a subset of the northwestern region of India, namely Udaipur.

Strengths of the study - The results of the current study are generalizable to the population of Udaipur region, reliable and versatile.

ACKNOWLEDGEMENTS

We are grateful to the Head of Department of Anatomy, Professor Dr. L.K. Jain for his guidance throughout this study; Medical Records Departments of Geetanjali Medical College and Hospital and of R.N.T. Medical College and Hospital, Udaipur, India in helping us procure the data.

REFERENCES

ACHARYA P, ACHARYA (2009) A evaluation of applicability of standard growth curves to indian women by fetal biometry. *JSAFOG*, 1(3): 55-61.

AL-BAYYARI N, ABU-HEIJA (2010) A fetal weight normograms for singleton pregnancies in a Jordanian population. *Ann Saudi Med*, 30(2): 134-140.

AVERY GB, MACDONALD MG, FLETCHER MA (2000) Neonatology. Philadelphia: Lippincott Williams & Wilkins.

BABUTA S, CHAUHAN S, GARG R, BAGARHATTA M (2013) Assessment of fetal gestational age in different trimesters from ultrasonographic measurements of various fetal biometric parameters. *J Anat Soc India*, 62(1): 40-46.

CALLEN PW (2007) *Ultrasonography in Obstetrics and Gynecology*. South Asia Edition, 5th ed. Saunders.

DE LA VEGA A, RUIZ-FEBO N, ROBERTS ZC (2008) Fetal ultrasound biometry: normative charts for a Puerto Rican population. *P R Health Sci J,* 27(1): 81-84.

HADLOCK FP, DETER RL, HARRIST RB, PARK SK (1982) Fetal head circumference: relation to menstrual age. *Am J Roentgenol*, 138(4): 649-653.

KINARE AS, CHINCHWADKAR MC, NATEKAR AS, COYAJI KJ, WILLS AK, JOGLEKAR CV, YAJNIK CS, FALL CHD (2010) Patterns of fetal growth in a rural Indian cohort and comparison with a Western European population: data from the Pune maternal nutrition study. *J Ultrasound Med*, 29(2): 215-223.

KONJE JC, ABRAMS KR, BELL SC, TAYLOR DJ (2002) Determination of gestational age after the 24th week of gestation from fetal kidney length measurements. *Ultrasound Obstet Gynecol*, 19(6): 592-597.

NYBORG W (2002) Safety of medical diagnostic ultrasound. *Seminars in Ultrasound, CT and MRI*, 23(5): 377-386.

OTTO C, PLATT LD (1991) Fetal Growth and Development. *Obstetrics Gynaecol Clinics North America*, 18(4): 907-931.

SALPOU D, KISERUD T, RASMUSS S, BIOMED CENTRAL [Online] (2008) Available from http://www.biomedcentral.com/1471-2393/8/48.

SNIJDERS RJ, NICOLAIDES KH (1994) Fetal biometry at 14-40 weeks' gestation. *Ultrasound Obstet Gynecol*, 4(1): 34-48.

VAROL F, SALTIK A, KAPLAN PB, KILI, YARDIM T (2001) Evaluation of gestational age based on ultrasound fetal growth measurements. *Yonsei Med J*, 42(3): 299-303.

Bizygomatic distance as a predictor of age and sex determination: a morphometric analysis using cone beam computed tomography

Karthikeya Patil[1], K.P. Mahesh[1], C.J. Sanjay[1], M. Aparna Vijayan[1], D. Nagabhushana[1], Aishwarya Ramesh[2]

[1] Department of Oral Medicine and Radiology, JSS Dental College and Hospital, JSS Academy of Higher Education and Research, Mysore 570015, Karnataka, India

[2] Current affiliation: Radiodent 3D, 1580, NS Road, Lakshmipuram, Mysuru, Karnataka 570004, India

SUMMARY

Despite advancements in diagnostic technologies, one of the most challenging tasks in forensic medicine is the identification of skeletal and decomposing body parts of the deceased. Estimating gender and age is also a significant issue in the identification of unknown skulls. The aim of the present study was to estimate the sexual dimorphism and variations occurring with ageing in bizygomatic distance. This was a prospective observational study performed on 180 subjects, comprising 90 males and 90 females. Linear measurements of bizygomatic distance were evaluated using cone-beam computed tomography. The study showed that there was significant difference in bizygomatic distance among different age groups and gender, with males depicting comparatively higher values than females. The results obtained were statistically significant. It was concluded that the linear measurements of bizygomatic distance on CBCT images can be used in forensic anthropology as an aid for the determination of age and sex.

Key words: Forensic science – Cone beam computed tomography – Forensic anthropology – Sex determination – Zygomatic arch

INTRODUCTION

Forensic odontology has been used to identify victims of major catastrophes (aviation, earthquakes, and tsunamis), in criminal investigations, ethnic studies, and in identifying the decomposed and disfigured bodies of drowned people, fire victims, and car accident victims. Rugoscopy, cheiloscopy, bite marks, teeth prints, radiography, photographic analysis, and molecular approaches are some of the techniques used in forensic odontology (Kavitha et al., 2009). Despite advancements in diagnostic technologies, one of the most challenging tasks in forensic medicine is the identification of skeletal and decomposing body parts of the deceased (Jehan et al., 2014). When the remains are decomposed or burnt, the DNA is destroyed; when there are no previous dental records, forensic anthropology becomes the

Corresponding author:
Dr Mahesh KP, Reader. Department of Oral Medicine and Radiology, JSS Dental College and Hospital, JSS Academy of Higher Education and Research, Mysore 570015, Karnataka, India. Phone: 9845189703. E-mail: dr.kpmahesh@jssuni.edu.in

Submitted: February 23, 2022. **Accepted:** April 18, 2022

https://doi.org/10.52083/WGES2700

preferred technique to aid in person identification (Nunes Rocha et al., 2021). Estimating gender and age is also a significant issue in the identification of unknown skulls (Jehan et al., 2014).

Unknown deceased bodies are difficult to identify, and it has serious legal and social consequences. Comparison of X-ray images of the deceased with those of missing individuals is a means of appropriate identification, especially after significant post-mortem alterations (Jehan et al., 2014; Riepert et al., 2001). However, if significant post-mortem alterations have occurred, routine forensic procedures for person identification may be futile (Teke et al., 2007).

Various parameters, including the circumference of the head, the length of the supraorbital margin, the mastoid process and the mandibular ramus, the height of the mandibular symphysis, the shape and length of the palate, the circumference of the occipital condyle, the size of the teeth, the foramen magnum, the maxillary, sphenoid, and frontal sinuses, the bizygomatic distance, and the sella turcica, have lately been used to identify age and gender in unidentified human remains (Teke et al., 2007; Uthman et al., 2012).

Because of bone fragmentation, identification can be particularly difficult in mass disasters like explosions, warfare, accidents, etc. The skull, pelvis, and femur are the most effective for determining age and sex. Radiography can help by providing precise measurements to which equations can be applied for age estimation as well as sex determination (Uthman et al., 2012). Since most of the bones that are used conventionally for sex determination are typically fractured or partial when recovered, it has become important to employ denser bones that are more frequently retrieved intact (Jehan et al., 2014; Mathew et al., 2020). Although the skull and other bones may be extensively disfigured in victims, the zygomatic bones and maxillary sinus have been reported to be intact (Jehan et al., 2014; Paknahad et al., 2017; Sujatha et al., 2017; Aishwarya et al., 2021).

Teeth and facial bones are resilient in the human body and may resist decomposition or destructional pressures even when subjected to high forces and/or temperature fluctuations (Kumar et al., 2015). Radiographs are a useful tool in forensic sciences, as they can record particular anatomical features. Radiographic identification has been used for a long time, and the process is efficient and relatively simple. Records can be obtained from both live and deceased people, and it is less expensive than DNA technology (Kumar et al., 2015). In forensic anthropology, several radiographic techniques, such as measurements on dry skulls, conventional radiography, computed tomography (CT), and cone-beam computed tomography (CBCT), have been used to assess various parameters for determining an individual's sex and age (Paknahad et al., 2017; Abu El Dahab et al., 2018). CBCT is a new way to look at craniofacial structures with great dimensional accuracy (Paknahad et al., 2017; Abu El Dahab et al., 2018). CBCT has been also used in a number of investigations, including 3D reconstruction, bitemark analysis, age estimation, person identification and anthropological assessment, with promising results (Tambawala et al., 2016). In much of the literature on maxillary sinus dimensions and bizygomatic distance, it has been proved that these can be used in age estimation and sex determination. These structures are well appreciated in CBCT images (Aishwarya et al., 2021).

The purpose of this study is to evaluate the reliability of bizygomatic distance as a predictor for age and sex determination of an individual using CBCT imaging.

MATERIALS AND METHODS

This is a prospective observational study performed on 180 subjects, comprising 90 males and 90 females. The study samples were selected by a simple purposive sampling method. The population origin of the sample is homogeneous. Ethical clearance of the study has been obtained from the Institutional Ethical Committee. The study subjects were then divided into 3 groups based on chronological age, and each group was comprised of 30 males and 30 females.

Group I: 20-40 years (30 males and 30 females).

Group II: 41-50 years (30 males and 30 females).

Group III: 51-60 years (30 males and 30 females).

Eligibility criteria

Inclusion criteria

- Subjects willing to be part of the study signed an informed consent form.
- Subjects without malocclusion and without a previous history of orthodontic treatment.
- Radiographs are devoid of any developmental anomalies or pathologies, including fractures.
- Radiographs that are free of any artefacts.

Exclusion criteria

- Subjects with missing or partially erupted maxillary teeth other than the third.
- Ideal CBCT images with poor diagnostic quality and images that do not clearly show the maxilla, including the zygomatic arch.
- Radiographs with any maxillofacial pathologies or trauma.

A clinical examination was carried out after obtaining written informed consent from the subjects eligible for the study. Clinical findings were recorded in an individual proforma specially designed for the study. Individuals satisfying the eligibility criteria were subjected to CBCT examinations at fixed operating parameters based on the build of the subject by adopting the requisite radiation protection measures. Linear measurements of bizygomatic distance were performed on axial sections using Planmeca Romexis 5.3 (3D Software).

Each of these measurements was repeated twice by the same observer at an interval of 15 days. An average of these measurements was taken into consideration to avoid intra-examiner variations.

Bizygomatic distance

Bizygomatic width is measured as the maximum distance between the most prominent points on the right and left zygomatic arches on an axial section (Fig. 1, an axial section showing maximum bizygomatic distance).

Statistical analysis

The collected data was tabulated and statistically analysed, and a comparison was made between different age and sex groups. The mean value, SD, p value, and t value were calculated separately. The collected data was then subjected to descriptive statistics, one-way ANOVA, and independent

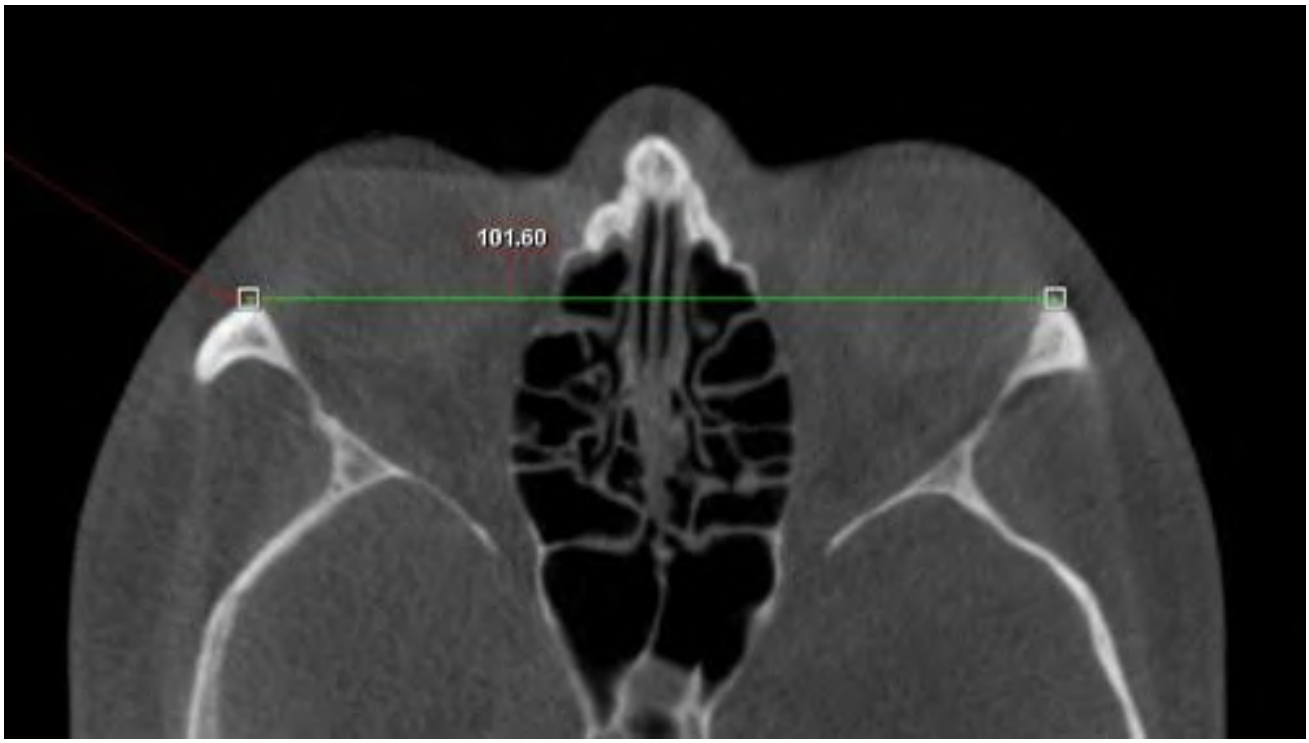

Fig. 1.- An axial session showing maximum bizygomatic distance.

sample tests. p value of less than or equal to 0.05 was considered to be statistically significant. The statistical analysis was performed using SPSS software version 22.0.

RESULTS

The study population consisted of 180 patients, of which 90 (50%) were males and 90 (50%) were females. The mean value of bizygomatic distance in Group I, Group II and Group III were calculated separately and subjected to statistical analysis.

Age

The mean values of the bizygomatic distance among Group I, Group II, and Group III were 94.9530, 94.6140, and 92.2085, respectively (Table 1 indicates comparison of mean bizygomatic distance between different age groups). The highest mean value of bizygomatic distance was observed in Group I. The data collected when subjected to one-way ANOVA to evaluate co-relation between age group and study parameter (bizygomatic distance) were statistically significant with a p value of 0.008 (Table 2 indicates correlation of bizygomatic distance with age groups). There was a significant difference in bizygomatic distance among the age groups.

Sex

The mean value of the bizygomatic distance was calculated for males (n = 90) and females (n = 90). The mean value among males was 97.0693 and among females was 90.7810, with a standard deviation of 4.75505 for males and 3.75127 for females (Table 3 indicates comparison of mean of bizygomatic distance between males and females). The correlation between the bizygomatic distance and sex of the study population was calculated using an independent sample t-test. A significant difference was noted in the bizygomatic distance between males and females, with males depicting comparatively higher values than females. The results obtained were statistically significant, with p = 0.00 and t = 9.850 (Table 4 shows the correlation of bizygomatic distance with sex).

Regression ANOVA

Independent variable: Age

The results when subjected to regression ANOVA (Table 5 – depicting regression ANOVA) with age as the independent variable, revealed an F value of 3.256 with a p value of 0.073. Regression ANOVA showed no significant difference between age and bizygomatic distance.

DISCUSSION

Forensic science has made a lot of progress in a short period of time. Identity is described in the realm of forensic science as the identification of a person's individuality, whether living or dead (Rao, 2010). Age, sex, ethnicity, and physical characteristics such as weight, height, complexion, cornea, hair colour, and facial contour can be all used to identify a person. Bizygomatic distance shows a wide range of variability in each

Table 1. Comparison of mean bizygomatic distance between different age groups (descriptive statistics).

Age groups	N	Mean	SD	Std Error
Group I 20-40	60	94.9530	5.31207	.68579
Group II 41-50	60	94.6140	4.81731	.62191
Group III 51-60	60	92.2085	5.43289	.70138

N= number of subjects, SD= Standard deviation

Table 2. Correlation of bizygomatic distance with age groups (One way ANOVA).

	Sum of Squares	df	Mean Square	F value	P value
Between Groups	268.673	2	134.336	4.979	.008

df= degrees of freedom

Table 3. Comparison of mean of bizygomatic distance between males and females (descriptive statistics).

Parameter	Sex	N	Mean	SD	Standard Error
Bizygomatic distance	M	90	97.0693	4.75505	.50123
	F	90	90.7810	3.75127	.39542

N= number of subjects, SD= Standard deviation

Table 4. Correlation of bizygomatic distance with sex (independent sample test).

Parameter	t	df	Sig. (2-tailed)	Mean Difference
Bizygomatic distance	9.850	178	.000	6.28833

t= t value, df= degrees of freedom, Sig= significance probability

Table 5. Regression ANOVA.

	Sum of Squares	df	Mean Square	F value	Sig.
Regression	90.605	1	90.605	3.256	.073
Residual	4953.577	178	27.829		
Total	5044.182	179			

The independent variable is Age. df= degrees of freedom, Sig= significance probability

individual according to different age groups and sex (Aishwarya et al., 2021). According to a few studies, the accuracy rate of estimating age from a skeleton is 92% since it can anatomically tolerate major traumas (Aishwarya et al., 2021).

The current study was designed to investigate the reliability of the bizygomatic distance as a method for age estimation and sex determination by utilizing Cone-Beam Computed Tomographic (CBCT) images of 180 subjects comprising of 90 males and 90 females.

Riepert et al. (2001), in their study on the identification of unknown dead bodies by x-ray image comparison of the skull using the x-ray simulation programme FoXSIS, aimed at enhancing the objectivity of X-ray image comparison for identifying unidentified deceased people. The results of the study concluded that the skull breadth, biorbital breadth, and bizygomatic breadth were the most consistent parameters throughout different positions (Kavitha et al., 2009).

In a study by Jehan et al. (2014) on sexual dimorphism of the bizygomatic distance and maxillary sinus using CT scan, to the aim was find out whether the bizygomatic distance, the AP diameter and breadth of the maxillary sinus, and the intermaxillary distance could be used to determine gender using a CT scan. A statistically significant difference was observed in the bizygomatic distance between males and females. In the current study, CBCT was used to measure the bizygomatic distance, and the results obtained were consistent with this study and were statistically significant with a p value of 0.00.

Abu El Dahab and colleagues (2018), in their study to investigate the possibilities of sex identification using radiographic maxillary sinus measurements in an Egyptian population sample, found that all measurements of males showed higher mean values than females. In their study, the mean value of bizygomatic distance among males was 93.5, and among females it was 88.7, which has proved statistical significance. These results were consistent with the results obtained in our study, wherein the mean value among males was 97.06, and among females was 90.78. The results showed a statistically significant difference between males and females.

Mathew et al. (2020), in their study on 3D evaluation of the maxillary sinus in gender determination, a cone beam computed tomography study found that the overall values of maxillary sinus dimensions measured, including bizygomatic distance, were significantly greater in males when compared to females with $p< 0.05$ (Mathew

et al.,2020). The results obtained in the present study also showed similar results, with higher values of bizygomatic distance in males than in females.

A study on morphometric evaluation of bizygomatic distance and maxillary sinus width as a dimorphic tool using CBCT by Chaurasia et al. (2016), conducted in 202 study subjects, revealed a statistically significant difference in bizygomatic distance between males and females, but no statistical difference was observed among different age groups. These results were in accordance with our present study, where a significant difference was noted in the bizygomatic distance between males and females, with males depicting comparatively higher values than females. There was a significant difference in bizygomatic distance among the different age groups.

In a study by Meral et al. (2021) on estimation of sex from computed tomography images of skull measurements in an adult Turkish population, they evaluated the skull measurements of 300 males and 300 females. Maximum cranial length, maximum cranial breadth, bimastoid diameter, bizygomatic diameter, and bigonial breadth were measured by computed tomography. They found a significant difference between males and females with an accuracy of 88%. Results of the present study were in accordance with this previous study with a significant difference in bizygomatic distance between males and females.

González-Colmenares et al. (2019), in their study on sex estimation from skull base radiographs in a contemporary Colombian population, measured five parameters, including maximum cranial base length, foramen magnum length and breadth, maximum cranial breadth, and bizygomatic breadth. Sexual dimorphism was observed in all the variables statistically, whereas in the present study only bizygomatic distance was considered, which showed sexual dimorphism.

In our previous study on bizygomatic distance and maxillary sinus dimensions as predictors for age estimation using CBCT, the results showed a difference in mean values among different age groups, although it was statistically non-significant (Aishwarya et al., 2021). But the results of the present study showed a significant difference in bizygomatic distance among the age groups, and the results were statistically significant with a p value of 0.008.

CONCLUSION

The current study sought to determine whether bizygomatic distance could be used as a good predictor of age and gender. The results obtained in the present study revealed that bizygomatic distance shows anatomical variations between different ages groups and sex groups. Males revealed statistically significant higher values than females. The bizygomatic distance also showed significant difference among different age groups. Therefore, it can be concluded that the linear measurements of bizygomatic distance on CBCT images can be used in forensic anthropology as an aid for age estimation and sex determination. Interpopulation differences do not allow establishing a range of standardized measurements.

REFERENCES

ABU EL-DAHAB O, DAKHLI I (2018) The role of cone beam computed tomography in sex identification of a sample of Egyptian population using maxillary sinus predictors. *Oral Surg, Oral Med, Oral Radiol*, 6(1): 4-9.

AISHWARYA R, PATIL K, MAHIMA VG, CJ SANJAY, NAGABHUSHANA D, DESHPANDE PS (2021a) Bizygomatic distance and maxillary sinus dimensions as predictors for age determination: A morphometric analysis using cone beam computed tomography. *Indian J Forensic Med Pathol,* 14(2): 91-96.

AISHWARYA R, PATIL K, MAHIMA VG, JAISHANKAR HP, SANJAY CJ, NAGABHUSHANA D (2021b) Bizygomatic distance and maxillary sinus dimensions as predictors for sex determination: A morphometric analysis using cone beam computed tomography. *Int J Current Res Rev*, 13(16): 10-16.

CHAURASIA A, KATHERIYA G (2016) Morphometric evaluation of bizygomatic distance and maxillary sinus width as dimorphic tool - A CBCT study. *Int J Maxillofacial Imaging*, 2(4): 123-128.

GONZALEZ-COLMENARES G, SANABRIA MEDINA C, ROJAS-SANCHEZ MP, LEON K, MALPUD A (2019) Sex estimation from skull base radiographs in a contemporary Colombian population. *J Forensic Legal Med*, 62: 77-81.

JEHAN M, BHADKARIA V, TRIVEDI A, SHARMA SK (2014) Sexual dimorphism of bizygomatic distance and maxillary sinus using CT scan. *IOSR J Dental Med Sci*, 13(3): 91-95.

KAVITHA B, EINSTEIN A, SUNDHARAM S, SARASWATHI TR (2009) Limitation in forensic Odontology. *J Forensic Dental Sci*, 1(1): 8-10.

KUMAR R, ATHOTA A, RASTOGI T, KARUMURI SK (2015) Forensic radiology: An emerging tool in identification. *J Indian Acad Oral Med Radiol*, 27(3): 416-422.

MATHEW A, JACOB LE (2020) 3D evaluation of maxillary sinus in gender determination: A cone beam computed tomography study. *J Indian Acad Oral Med Radiol*, 32(4): 384-389.

MERAL O, MEYDAN R, TOKLU BB, KAYA A, KARADAYI B, ACAR T (2021) Estimation of sex from computed tomography images of skull measurements in an adult Turkish population. *Acta Radiol,* 2021: 2841851211044978.

NUNES ROCHA MF, DIETRICHKEIT PEREIRA JG, ALVES DA SILVA RH (2021) Sex estimation by maxillary sinus using computed tomography: a systematic review. *J Forensic Odontostomatol,* 39(1): 35-44.

PAKNAHAD M, SHAHIDI S, ZAREI Z (2017) Sexual dimorphism of maxillary sinus dimensions using cone-beam computed tomography. *J Forensic Sci,* 62(2): 395-398.

RAO NG (2010) Textbook of Forensic Medicine and Toxicology. 2nd ed. Jaypee Brothers, New Delhi, pp 1-6.

RIEPERT T, ULMCKE D, SCHWEDEN F, NAFE B (2001) Identification of unknown dead bodies by X-ray image comparison of the skull using the X-ray simulation program FoXSIS. *Forensic Sci Int*, 117(1-2): 89-98.

SUJATHA S, KAUR A, SHARMA S, THOMAS N, PRIYADHARSHINI R (2017) Sexual dimorphism of maxillary sinus dimensions using the CBCT imaging among south Indian population. *Int J Current Res*, 9(11): 61346-8.

TAMBAWALA SS, FRENY RK, KAUSTUBH SANSARE, NIMISH PRAKASH (2016) Sexual dimorphism of maxillary sinus using cone beam computed tomography. *Egypt J Forensic Sci*, 6(2): 120-125.

TEKE HY, DURAN S, CANTURK N, CANTURK G (2007) Determination of gender by measuring the size of the maxillary sinuses in computerized tomography scans. *Surg Radiol Anat*, 29(1): 9-13.

UTHMAN AT, AL-RAWI NH, AL-TIMIMI JF (2012) Evaluation of foramen magnum in gender determination using helical CT scanning. *Dentomaxillofacial Radiol,* 41(3): 197-202.

Self-reported anatomy skills among Norwegian physicians - Need for improved postgraduate teaching provision

Camilla S. Mehlum[1], Hanan Mahmood[2], Kristoffer Ellingsen[3], Ole Øyen[4], Trygve B. Leergaard[4], Anne Spurkland[4]

[1] Innlandet Hospital Trust, Gjøvik Hospital, Dep. of child- and adolescent psychiatry, Bassengparkvegen 2, N-2821 Gjøvik, Norway

[2] University Hospital of North Norway, Harstad Site, Dep. of orthopedic surgery, St. Olavs gate 70, N-9406 Harstad, Norway

[3] Akershus University Hospital, Division Kongsvinger, Dep. of internal medicine, Parkveien 35, N-2212 Kongsvinger, Norway

[4] Division of Anatomy, Department of Molecular Medicine, Institute of Basic Medical Sciences, University of Oslo, P.O.B. 1105, Blindern, N-0317 Oslo, Norway

SUMMARY

Anatomy skills are considered essential in all aspects of medical practice, and more so now than before with increasing use of diagnostic imaging techniques and advanced surgery. In conjunction with the revision of the medical study curriculum at the University of Oslo in 2014, we investigated Norwegian physicians' assessment of their own anatomy knowledge and the educational provision of anatomical skills during and after specialization. A total of 902 Norwegian physicians divided into the specialties of general medicine, internal medicine, surgery, neurology and radiology responded to an anonymous survey.

As many as 73% of the physicians had at some time point experienced insufficient anatomy knowledge in their own practice, most commonly among surgeons and neurologists. The respondents expressed a need for supplementary educational provision in anatomy during and after specialization, and 36% were unfamiliar with such offers. Notably, dissection courses seemed unavailable during specialization.

Our findings demonstrate a requirement for an improved supply of anatomy education during and after specialization. Anatomy courses that combine dissection, radiological images and clinical application would seem desirable.

Key words: Anatomy – Anatomy education – Anatomy and medical education – Clinical anatomy – Anatomy teaching

INTRODUCTION

Anatomy skills are fundamental in most areas of medical clinical practice. Academic communities have expressed concerns about the reduction of the extent and quality of anatomy teaching in many medical curricula (Gogalniceanu et al., 2008; Drake et al., 2009, Craig; Tait et al., 2010; Drake et al., 2014; Sbayeh et al., 2016). Gogalniceanu et al.

Corresponding author:
Ole Øyen, Anatomy division, Institute of Basic Medical Sciences, University of Oslo, P.O.B. 1105, Blindern, N-0317 Oslo, Norway. E-mail: oleoy@medisin.uio.no

Submitted: April 3, 2022. **Accepted:** May 1, 2022

https://doi.org/10.52083/GQLP6804

(2008) claims that accumulated evidence indicates a worldwide decline in the absolute resources and time allocated to anatomy teaching, attributed to the high costs of maintaining dissection facilities, curricular overcrowding by non-science-based lectures, and a general disenchantment of university faculties with anatomy as a subject.

Furthermore, the significant increase in medical knowledge and technological advances already entails greater demands for detailed anatomy knowledge and technical skills during specialist education. Technological developments may also have a positive impact on acquiring anatomy skills, especially with regard to improved learning and guiding methods (audiovisual/3D programs/presentations, guiding apps). However, the development of new imaging methods and minimally invasive surgical techniques has changed the way in which anatomy needs to be viewed and abstracted. Future doctors will need to conceptualize anatomy from the perspective of angiography, ultrasound imaging, computed tomography, laparoscopy, and endoscopy. These are currently not directly addressed in many undergraduate curricula, giving rise to a discrepancy between the requirements of clinical practice and the delivery of medical school and postgraduate education.

Several institutions internationally have recently established clinically oriented anatomy courses, mainly based on macro-anatomy training on cadavers (D'Antoni et al., 2019; Meredith et al., 2019; Clifton et al., 2020). Currently, there are few clinically oriented anatomy courses for specialist training available in Norway.

With improved imaging/computational technologies and possibilities for diagnostic imaging allowing more advanced and complicated surgical procedures, we hypothesize that doctors in specialization perceive insufficient anatomical knowledge, and experience need for improved access to anatomical training also after their basic medical training.

To explore this in a Norwegian context, we surveyed physicians' assessment of their own anatomy knowledge and the demand for clinically oriented anatomy teaching among a representative sample of Norwegian physicians, being either clinical specialists or in clinical specialization.

Medical training in Norway is provided by four major universities in collaboration with the local state-owned hospitals. These four universities educate around 600 Norwegian physicians yearly. Traditionally, however, a relatively large proportion of Norwegian medical students receive their medical education abroad. Currently nearly half of these students are trained abroad (Grimstad, 2019). This is far more than the average for OECD countries. The preferred campuses have in recent years been located in Poland, Hungary, Slovakia, Denmark, Czech Republic, Latvia and Germany (accounting for more than 90% of students).

A representative sample of 902 Norwegian physicians were asked to assess their own anatomy knowledge and the perceived demand for clinically oriented anatomy teaching. The high proportion of foreign students made it possible to compare the individual outcome of anatomy teaching in Norway with that of international universities.

Our survey revealed that the majority of physicians have experienced insufficient anatomy knowledge in their own practice, most commonly among surgeons and neurologists. Physicians trained outside Norway rated their anatomy skills better than physicians trained in Norway. Our findings thus confirm a demand for improved anatomy skills among clinicians, and indicate that an offer of postgraduate clinical anatomy courses is warranted in Norway.

MATERIAL AND METHODS

Pilot study

Six physicians representing the specialties of orthopedics, gynecology and obstetrics, neurology, gastroenterological surgery, radiology and ear-nose-throat were interviewed on issues related to clinical anatomy. The information that emerged was used as the starting point for an online survey on a random sample of Norwegian physicians.

Survey

The survey was conducted in December 2015 and contained 25 questions about Norwegian physicians' assessment of their own anatomy skills and of the anatomy teaching they received during medical school and specialization (Ellingsen et al., 2016). A six-point scale of the ordinal level and nominal level was used to provide graded answers. A link to the questionnaire was sent out via email to a random sample of members of five professional specialist associations in the Norwegian Medical Association: Norwegian Internal Medicine Association, Norwegian Surgical Association, Norwegian Neurological Association, Norwegian Radiological Association and Norwegian Association for General Medicine. In each of these associations, 500 members were drawn at random (with the exception of the Norwegian Neurological Association, where all 492 members with registered email addresses were selected). A total of 2491 members were contacted (one E-mail address out of 2492 was rejected).

Ethical considerations

The survey was fully anonymous, with no registration of personal data, not requiring ethics committee approval in Norway (https://rekportalen.no/).

Statistics

Statistical analyses were performed using IBM SPSS Statistics (SPSS). Continuous variables were analyzed with T-test for comparison of means. Categorical variables were analyzed by Chi Square test. Tables and figures were created using Microsoft Office Excel.

RESULTS

Respondents

Responses were received from 902 (36.2%) physicians. Without an established relationship with the recipient, it is claimed that a response rate of >20% must be considered acceptable (Noel and Huang, 2019). Demographic data on the respondents are presented in Table 1; regarding gender, medical school (including Norway vs abroad), year of graduation and specialization status/time.

Table 1. Demographic data on the 902 respondents regarding gender, medical school (including Norway vs abroad), year of graduation and specialization status/time.

Respondent demographics n=902	
Gender n=902	Female: 452 (50,1%) Male: 450 (49,9%)
Medical school n=902	Abroad: 330 (36,6%) Oslo (UiO): 242 (26,7%) Bergen (UiB): 157 (17,4%) Trondheim (NTNU): 98 (10,9%) Tromsø (UiT): 75 (8,3%)
Year of graduation from medical school n=902	1970-79: 1 (0,1%) 1980-89: 45 (5,0%) 1990-99: 240 (26,6%) 2000-09: 436 (48,3%) 2010-15: 180 (20,0%)
Speciality status / Time in speciality n=901	In specialization: 413 (45,8%) Specialist < 5 years: 181 (20,1%) Specialist 5-10 years: 174 (19,3%) Specialist 11-20 years: 117 (13,0%) Specialist > 20 years: 16 (1,8%)
Distribution among specialities n=892	General medicine: 158 (17,7%) Internal medicine: 174 (19,5%) Surgery 210 (23,5%) Neurology 141 (15,8%) Radiology 209 (23,4%)

In our sample population, 37% of physicians had been educated abroad, which provides opportunities for comparing the individual outcome of anatomy teaching in Norway with that of international universities. The respondents were not asked about their nationality, but we know (Grimstad, 2019) that more than 95% of students, including those educated abroad, are Norwegian citizens.

Ten participants who could not be categorized into any of the specialties were excluded from analyses that dealt with distribution among specialties. Most of the respondents (95%) had completed their education after 1990.

Physicians' assessment of their own anatomy knowledge

The respondents were asked to give an assessment of their own anatomy knowledge at different times in their careers, on a graded scale from 1 to 6 (Fig. 1; 1: Too poor for good clinical practice; 6: More than sufficient for good clinical practice). The median value was 4 for 'Post medical school' and 'In specialization; current',

while increasing to 5 for 'Post specialization' and 'Specialists; current'. These stages have been defined in the legend. (Grade-partitioned data not shown).

The average self-assessment of anatomy knowledge after completing specialization (4.58) and current among specialists (4.64) was significantly higher than retrospectively assessed after completing medical studies (4.30; p <0.001) (Fig. 1). Among the specialists who reported inferior (1-3) anatomy knowledge after medical school, the anatomy knowledge after completion of specialization was assessed as significantly better (2.82 vs 4.12; p <0.001). The specialists who assessed that they had superior anatomy knowledge (4-6) after medical school reported no change after completing the specialization. Stratification of the groups according to place of study showed that physicians who had studied abroad scored their own anatomy knowledge after medical school significantly higher than physicians who had studied in Norway (4.47 vs 4.20; p <0.001), and twice as high a percentage indicated a value of 6; that is, more than adequate for good clinical practice (23.1% vs 11.6%; data not shown). When comparing the four universities in Norway, there were no significant differences (data not shown).

Surgeons and radiologists reported improved anatomy skills over time

There was no difference between the specialties regarding anatomy knowledge at graduation from university (Fig. 1).

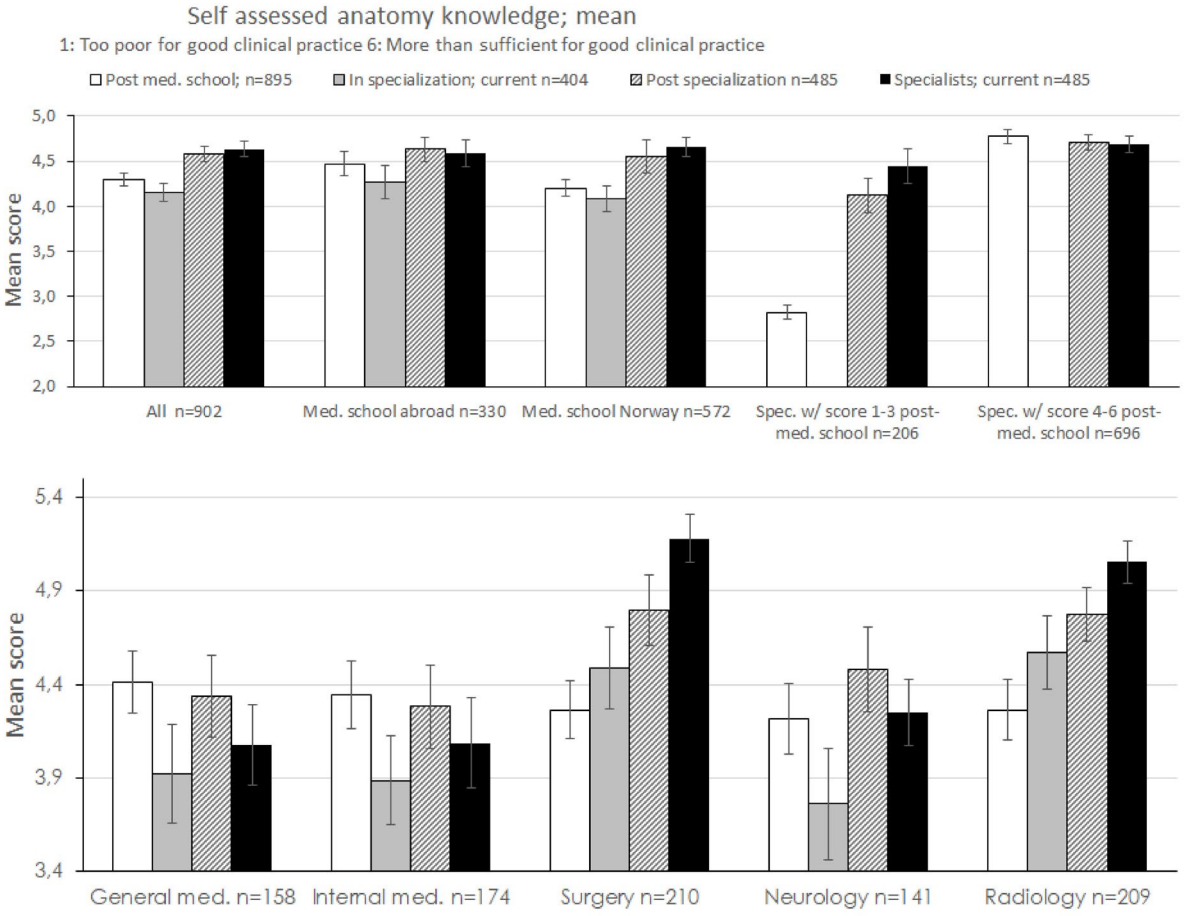

Fig. 1.- Physicians' self-assessment of anatomy knowledge at different times in their careers; average scores (grades 1-6), with 95% confidence intervals. The above panel shows the overall results and stratification according to study site (abroad vs Norway) and score at graduation (1-3 vs 4-6). In the below panel the results are broken down by specialty.

Post medical school: Retrospective assessment of anatomy knowledge at graduation from medical school. In specialization; current: Current assessment of anatomy knowledge among those currently in specialization. Post specialization: Retrospective assessment of anatomy knowledge at completion of specialization. Specialists; current: Current assessment of anatomy knowledge among current specialists.

At a later stage in their careers, surgeons and radiologists considered their anatomy skills to be significantly better than general practitioners, internal medics and neurologists (p <0.001). Surgeons and radiologists assessed their anatomy knowledge progressively better over time, while a similar trend was not present among the other specialties.

High proportion of physicians with experience of inadequate anatomy skills

As much as 73.1% of physicians reported having experienced inadequate anatomy skills in their occupational practice (Fig. 2), with the highest proportion among radiologists and neurologists and the lowest proportion among internists.

When asked about the importance of anatomy skills in the specialty, there were significantly higher scores among surgeons, neurologists and radiologists (p < 0.001). The physicians who assessed the importance of good anatomy skills in their specialty as high (value 5-6) were more likely to have experienced inadequate anatomy skills than physicians who rated anatomy skills in their specialty as less important (75.1% vs. 62.1%; p = 0.002).

The experience of inadequate anatomy skills also depended on time in the specialty. A large majority of physicians under specialization (79.0%) responded that they had experienced inadequate anatomy skills in their practice, while this proportion was lower among physicians who

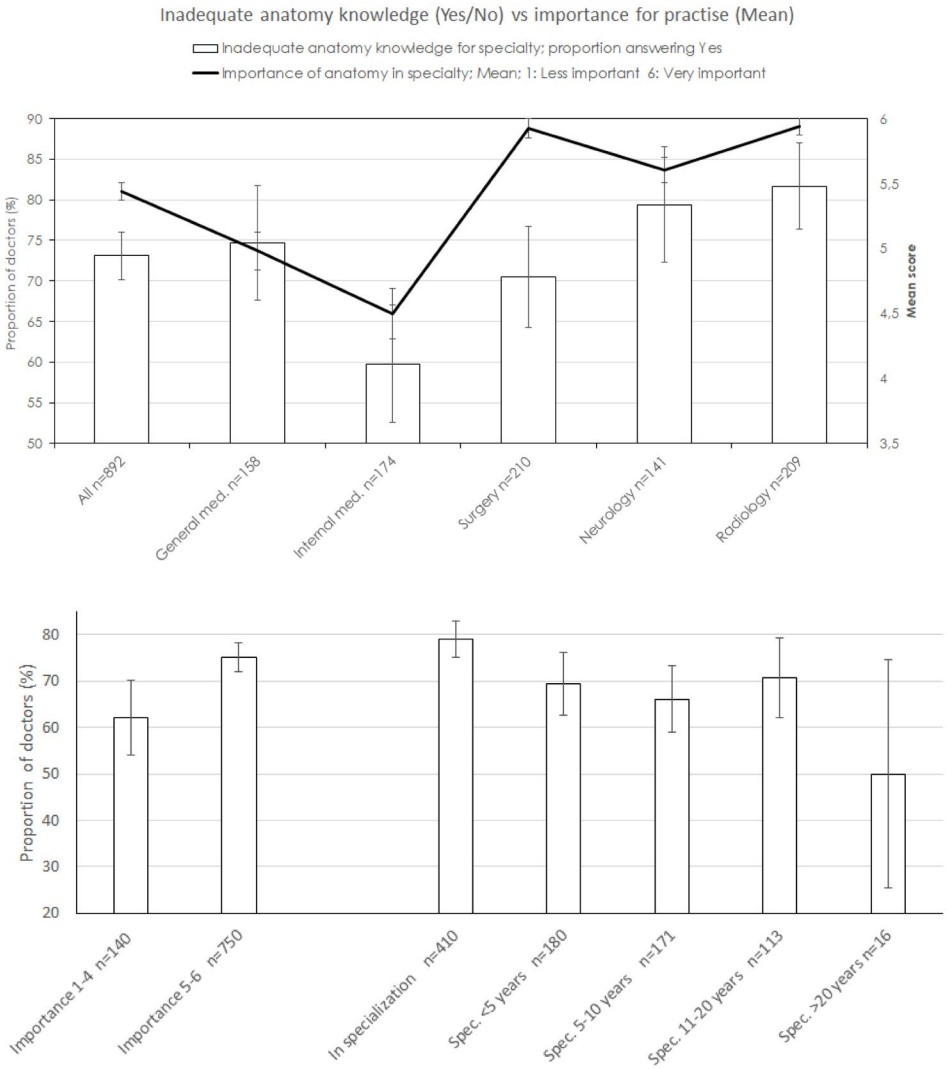

Fig. 2.- Proportion of doctors who had experienced inadequate anatomy knowledge in their practice (Yes/No), broken down by specialty (upper panel), degree of importance of anatomy in specialty and time in specialization (lower panel). The upper diagram also shows average values (solid line) for assessing the importance of anatomy in one's own specialty (1: Less important; 6: Very important). 95% confidence intervals are plotted in all graphs.

had practiced as specialists for less than 5 years (69.4%), 5-10 years (66.1%), 11-20 years (70.8%) and over 20 years (50.0%) (Fig. 2).

Among physicians who had studied abroad, a lower proportion (69%) reported inadequate anatomy skills, compared with physicians that had studied in Norway, almost reaching significance (69.2% vs 75.2%; p = 0.055; data not shown).

Anatomy teaching in medical school seemed sufficient and more relevant for clinical examinations than clinical procedures

The amount of anatomy teaching during medical school was consistently assessed as sufficient, as 77.8% entered the values 3 or 4, on a scale of 1 to 6, where 1 is too little and 6 is too much (data not shown).

Physicians educated abroad experienced the amount of anatomy teaching in medical school as significantly greater than physicians trained in Norway (4.00 vs. 3.36; p <.001) (Fig. 3; upper panel), and a higher proportion entered the values 5 or 6 (30.5% vs. 6.7%). Among physicians educated in Norway, the amount of anatomy teaching during medical school was considered significantly less at the University of Tromsø compared to the University of Oslo (UiO) (3.11 vs. 3.38; p = 0.008) and the University of Bergen (UiB) (3.11 vs 3.46; p = 0.003), but not significant compared to the Norwegian University of Science and Technology (NTNU) (3.11 vs. 3.31).

The evaluation of the relevance of anatomy teaching at university for clinical examinations and clinical procedures is shown in Fig. 3 (lower panel).

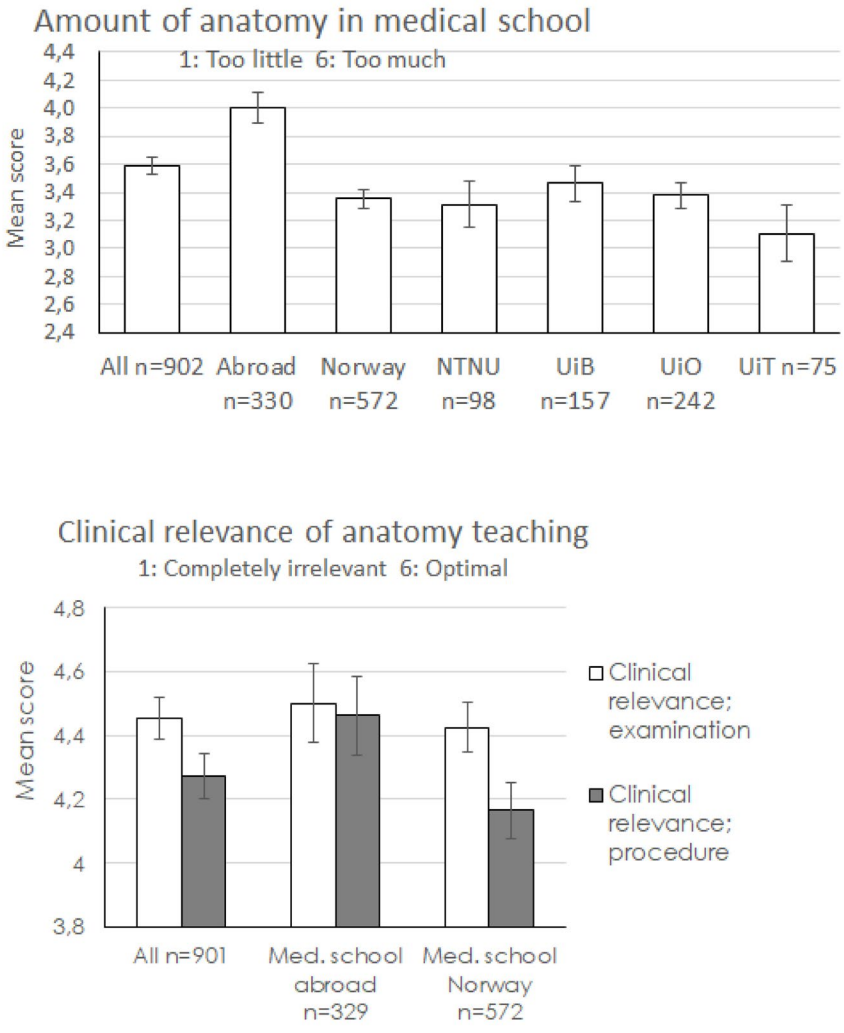

Fig. 3.- Physicians' assessment of the amount of anatomy teaching in medical school (upper panel) and the relevance of anatomy teaching for clinical examination and clinical procedures (lower panel), broken down by study site; average scores (grades 1-6), with 95% confidence intervals.

The experience of relevance to clinical procedures was indicated as significantly lower than relevance to examinations (mean value 4.27 vs. 4.45; p < 0.001). Physicians educated abroad rated the teaching's relevance for clinical procedures significantly higher than physicians educated in Norway (4.46 vs 4.16; p <0.001), and almost as high as the relevance for clinical examination (4.50).

Anatomy teaching during and after specialization was indicated as insufficient

The provision of anatomy during specialization was reported as insufficient by a predominant proportion of Norwegian physicians (Fig. 4; upper panel).

The average value for the amount of anatomy teaching during specialization was however decent (3.04), but significantly lower than that stated for the medical study (3.04 vs 3.59; p <0.001).

Radiologists (3.43; p <0.001) and internists (3.19; p = 0.033) were significantly more satisfied with the amount of anatomy teaching than the average for the other specialties.

The offer for learning and maintaining anatomy skills after medical school was considered inadequate. As much as 36.1% of physicians reported that they were not familiar with existing anatomy teaching offered to clinicians, and among the remaining 73.9% perceived the teaching provision as inadequate (value 1-3; data not shown). The neurologists were most satisfied with their anatomy training possibilities, but there was little difference between the specialties.

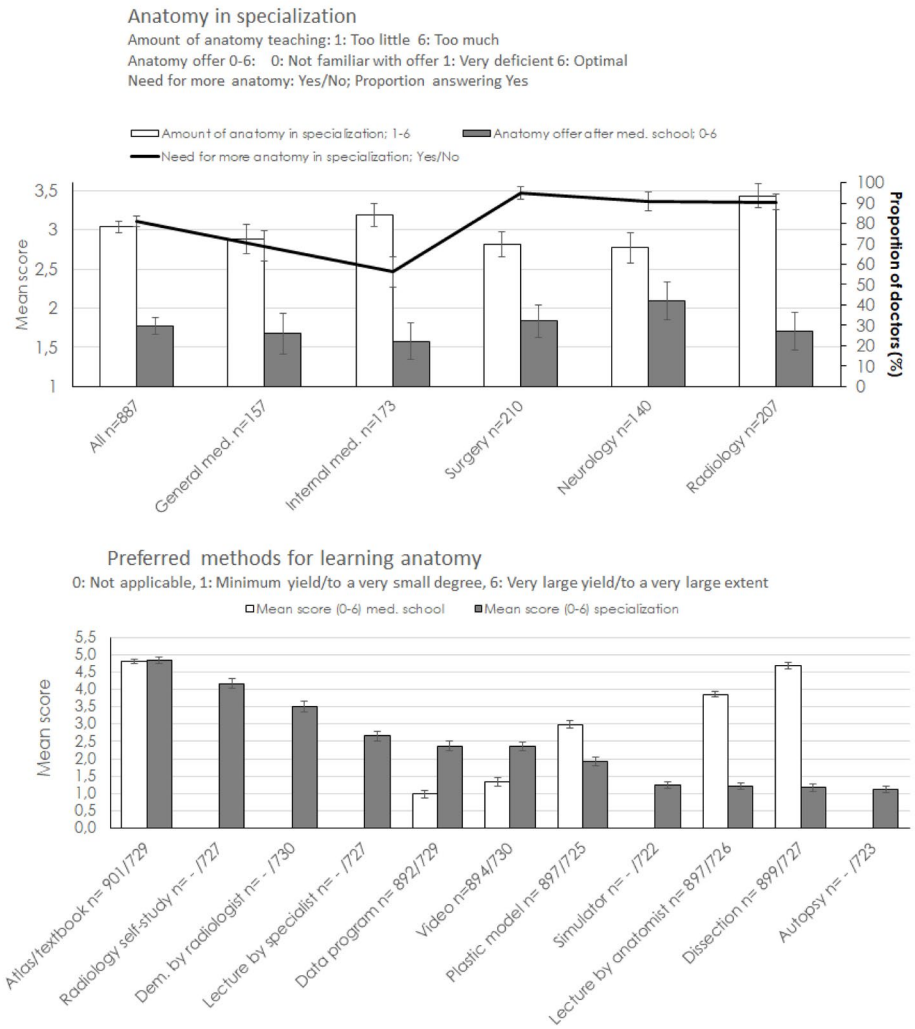

Fig. 4.- Assessment of the amount of anatomy and the availability of anatomy teaching in specialization (grades 1-6/0-6), as well as evaluation of the need for more anatomy (Yes/No) (upper panel); average scores and proportion 'Yes', with 95% confidence intervals. Average assessment of methods for learning anatomy during medical school (grades 0-6) (lower panel), with 95% confidence intervals.

Online survey/questionnaire for Norwegian physicians

A. BASIC DATA

Are you?:
Man
Woman

At which university did you study medicine?
Universitety of Oslo (UiO)
Norwegian University of Science and Technology (NTNU)
University of Bergen (UiB)
University of Tromsø (UiT)
Abroad

When did you finish medical school?
After 2010
2000-2009
1990-1999
1980-1989
1970-1979
1960-1969
Prior to 1959

What specialties do you have or are you specializing in?
[List of specialities]

Hvor lenge har du praktisert som spesialist innenfor din nåværende spesialitet?
Er under spesialisering
Under 5 år
5-10 år
11-20 år
Over 20 år

How long have you been practicing as a specialist in your current specialty?
Is under specialization
Less than 5 years
5-10 years
11-20 years
More than 20 years

B. ANATOMY IN MEDICAL SCHOOL

On a scale of 1 to 6, what do you think about the amount of anatomy teaching in medical school?
1: Too little, 2, 3, 4, 5, 6: Too much

What learning methods did you use to learn anatomy in your medical studies, and how much benefit do you think you received?
0: Not applicable, 1: Minimum yield, 2, 3, 4, 5, 6: Very large yield
- Lectures
- Selfstudy of atlas/textbook
- Dissection (The students dissect themselves)
- Self-study of ready-made preparations
- Demonstration of pre-prepared preparations by anatomy teacher or more experienced students
- Self-study of plastic models
- Videos
- Data programs, including apps

What did you think about your anatomy knowledge after graduating from medical school?
1: Too poor for god clinical practice, 2, 3, 4 , 5, 6: More than sufficient for good clinical practice

How clinically relevant do you think the anatomy teaching at the medical school was to be able to do a clinical examination?
1: Completely irrelevant, 2, 3, 4, 5, 6: Optimal

How clinically relevant do you think the anatomy teaching at the medical school was to be able to perform medical procedures?
1: Completely irrelevant, 2, 3, 4, 5, 6: Optimal

C. ANATOMY DURING SPECIALIZATION

Do you think that good anatomy knowledge is important in your specialty?
1: Less important, 2, 3, 4, 5, 6: Very important

What do you think about your anatomy knowledge right after completing your specialization?
1: Too poor for god clinical practice, 2, 3, 4 , 5, 6: More than sufficient for good clinical practice

What do you think about your anatomy knowledge now?
1: Too poor for good clinical practice, 2, 3, 4 , 5, 6: More than sufficient for good clinical practice

Have you experienced having deficient anatomy knowledge in your practice?
Yes, No

Did you need to learn more anatomy during the specialization?
Yes, No

If yes to the previous question: To what extent did you use any of these methods to learn more anatomy during the specialization?
1: To a very small degree, 2, 3, 4, 5, 6: To a very large extent
- Self-study of atlas/textbook
- Self-study of plastic models
- Dissection (of preprepared bodies)
- Lectures by experienced specialist
- Lectures by anatomist
- Exercise in the autopsy room at the hospital
- Self-study of radiological images
- Study of radiological images under the guidance of a radiologist
- Videos
- Simulators
- Data programs, including apps
- Other methods > Text field for additional information on other methods

To what extent did you use any of these methods during your specialization to learn clinical skills or procedures?
0: Not applicable, 1: To a very small degree, 2, 3, 4, 5, 6: To a very large extent
- Self-study of textbook/web sites
- Observing others executing the procedure
- Performing the procedure under supervision
- Exercise on plastic models/dolls
- Exercise on preprepared bodies/preparations
- Exercise in the autopsy room at the hospital
- Simulators
- Self-study of radiological images
- Videos explaining the procedure
- Data programs, including apps
- Other methods > Text field for additional information on other methods

If you have used radiology, simulators or carcasses to learn anatomy or clinical skills during the specialization, where have you used this?
In Norway
Abroad
Both

Do you think the teaching in your specialization is sufficient?
1: Too little, 2, 3, 4, 5, 6: Too much

D. EDUCATIONAL PROVISION

What do you think about the teaching provision in Norway to learn or maintain anatomy knowledge and clinical skills after the basic education as a doctor?
0: Not familiar with offers, 1: Very deficient, 2, 3, 4, 5, 6: Optimal

Do you have contact with medical students in your work?
Yes, No

If Yes >

What do you think about today's medical students' anatomy knowledge?
1: Very deficient, 2, 3, 4, 5, 6: Very good

Can you elaborate on your opinions about today's medical students' anatomy knowledge? Feel free to come up with examples.
Text field

Do you have any advice or comments on how you could possibly improve the offer of clinically oriented anatomy teaching at the medical school or in the continuing education of doctors?
Text field

When asked (yes/no) about the need for more anatomy in specialization, surgeons, neurologists and radiologists answered affirmatively in as much as 90-95%, significantly higher than general practitioners and internal medics.

The discepancy between the relatively high mean value for the amount of anatomy in specialization (3.04), compared with the low ratings for supply and high for need, are dealt with in the Discussion section.

Dissection was considered particularly valuable for learning anatomy in medical school

When asked about the preferred means of learning anatomy, there were a number of significant differences in the evaluation of the benefit of different methods (Fig. 4; lower panel) in medical school compared to in specialization. During medical school, studies of atlas/textbooks (average score 4.81) and cadaveric dissection courses (4.68) were valued higher than the use of computer programs (1.00) and video (1.34). For the learning of anatomy during specialization, the use of atlases and textbooks was considered significantly more valuable than studies of radiological images, which were ranked in second place (4.84 vs. 4.17; $p < 0.001$).

During specialization, dissection courses, autopsies, the use of a simulator and lectures by anatomists were considered to be relatively insignificant, and were stated as 'not applicable' by a large proportion of the respondents.

DISCUSSION

Inspired by a several year-long revision of the University of Oslo medical study plan starting in 2014, we conducted an electronic, anonymous survey regarding anatomy skills and teaching provision in anatomy, among a random sample of Norwegian physicians during specialization and ready-made specialists.

More clinically angled anatomy teaching?

Our findings regarding clinical relevance suggest a desire for more clinically angled anatomy education among physicians. As the medical knowledge base is constantly increasing and ever larger amounts of information are to be included in the medical study plan, it may be rational to make the basic anatomy teaching more clinically oriented (Drake et al., 2009; Craig et al., 2010). Furthermore, it has been reported that anatomy teaching with a clinical context improves learning and long-term memory (Bergman et al., 2008; Fincher et al., 2009) – and thus the clinical application.

Despite the findings that the amount of anatomy teaching in medical school seemed sufficient, a high proportion of physicians had experienced a lack of anatomy skills in practice. An obvious reason is that in most specialties detailed anatomy skills are required within a fairly specific area. The goal of basic education in anatomy is to provide *general* anatomy knowledge *sufficient* for good medical practice. Much of the detailed anatomy knowledge, relevant to each specialty, must therefore be acquired during specialization - in interaction with clinical application and during courses.

Assessment of ultrasound, CT and MRI images has become an important part of clinical everyday life in most specialties (Murphy et al., 2014; Geitung and Grottum, 2016). It therefore seems natural that clinically oriented anatomy teaching, both in basic and postgraduate education, should include knowledge relevant to the evaluation of radiological images (Ganske et al., 2006; Phillips et al., 2013).

Physicians educated abroad were more satisfied with their anatomy skills

Physicians who had studied abroad rated their anatomy skills as significantly better and the teaching's relevance for clinical procedures as significantly higher than physicians educated in Norway. Furthermore, a lower proportion of physicians educated abroad reported inadequate anatomy skills in their practice. This may indicate that foreign campuses have a greater volume or a more intensive type of teaching. And it may be consistent with a more progressive attitude towards clinical anatomy abroad (Meredith et al., 2019; Clifton et al., 2020). One may also wonder whether doctors educated abroad have a greater need to assert their educational status and

background (almost all of them are Norwegian citizens).

Need for strengthening of anatomy teaching during and after specialization

None of the specialist groups involved in the survey were satisfied with the teaching provision during specialization, and there seems to be a clear need for strengthening of this field. We consider that the relatively high mean value (3.04) for the amount of anatomy in specialization, compared with the low ratings for supply and high for need, may be conditioned by an unclear question, unfortunately not specifying anatomy teaching (cfr Questionnaire in Supplement).

The importance of having clinically relevant further education programs in anatomy after primary education is emphasized in a prospective UK study (Bhangu et al., 2010) in which only 14% of last-year students felt confident in their anatomy skills with regard to clinical practice. General practitioners, internists and neurologists reported declining anatomy knowledge after specialization. Several of the physicians requested targeted "refresher courses" in anatomy. But also among surgeons and radiologists, who considered their anatomy knowledge to be steadily rising from the end of medical school, more anatomy teaching was called for during specialization. Such services exist to a very limited extent in Norway today, and we are aware that Norwegian physicians have sought services in clinical anatomy abroad.

Teaching methods for courses during and after specialization

Studies of radiological images were among the most commonly used methods for learning anatomy during specialization, second only to studies of atlases/textbooks. During medical school, dissection was one of the most popular methods for learning anatomy. However, during specialization dissection was mostly considered irrelevant, presumably because dissection courses are almost unavailable. In free text fields several physicians expressed the desire for dissection and cadaver training in specialization.

It should raise concern that clinical procedures are often practised for the first time in patients. In many countries, there has been a decrease in open surgical volume among residents (Damadi et al., 2007), accompanied by diminished self-reported operative confidence and expert ratings of the operative ability (Fonseca et al., 2014). The opportunity to practice specific procedures on cadavers in advance will potentially improve patient safety (Sharma et al., 2016). Several foreign institutions offer courses where surgeons practice practical procedures on cadavers (Cabello et al., 2015; Ruiz-Tovar et al., 2019; Desai, 2021; Flynn, 2021).

Newer methods for preserving cadavers, especially the so-called "soft preservation" developed by the anatomist Walter Thiel (University of Graz, Austria), have at many universities replaced traditional formalin fixation (Thiel, 1992; Thiel, 2002; Balta et al., 2015) and opened up completely new possibilities for surgical skills training. The benefits are described as significant, with regard to natural colors and elasticity, as well as minimal formalin toxicity (Sutherland et al., 2006; Ahmed et al., 2015). This includes the possibility to perform laparoscopic procedures (Willaert et al., 2013), which is excluded on rigid, formalin-fixed carcasses.

An optimal teaching model for courses under specialization could conceivably combine dissection courses, preferably on soft-preserved carcasses, with demonstration of radiological images and the rehearsal of clinical procedures.

Limitations

The survey achieved a response rate of 36.2%. Although the sample of physicians who responded corresponded well with the Norwegian Medical Association's membership statistics in terms of campus and gender distribution, it cannot be ruled out that the respondents are particularly concerned with the topic, making the sample less representative.

We have not checked for possible confounding factors. Therefore, one should be cautious in interpreting the relationships presented as statistically significant. The questions we have

asked are partially retrospective, which obviously carries a risk of misreporting. The survey was done at the end of 2015. The teaching provision in anatomy at medical school in Oslo has changed since then. Anatomy is now taught collectively for the first two years of the study, and the exam in anatomy is conducted as a 45 minute individual oral test. We nevertheless consider our results informative and relevant for the present day situation, particularly regarding the inadequate provision of anatomy during and after specialization.

CONCLUSIONS

A remarkably high proportion (73%) of Norwegian physicians had experienced inadequate anatomical knowledge in their professional practice. The offer for learning and maintaining anatomy knowledge and skills after specialization was considered deficient. And a predominance of physicians requested an improved continuing education offer in specialization. A desirable approach would involve more clinically relevant anatomy teaching with demonstration of radiological images and rehearsal of clinical procedures, preferably using soft-preserved carcasses.

To our knowledge, there have been no previous studies on Norwegian physicians' anatomy skills. While our study is based on self-reported knowledge, future studies acquiring more objective data through knowledge tests are warranted.

REFERENCES

AHMED K, AYDIN A, DASGUPTA P, KHAN MS, MCCABE JE (2015) A novel cadaveric simulation program in urology. *J Surg Educ*, 72(4): 556-565.

BALTA JY, CRONIN M, CRYAN JF, O'MAHONY SM (2015) Human preservation techniques in anatomy: A 21st century medical education perspective. *Clin Anat*, 28(6): 725-734.

BERGMAN EM, PRINCE KJ, DRUKKER J, VAN DER VLEUTEN CP, SCHERPBIER AJ (2008) How much anatomy is enough?. *Anat Sci Educ*, 1(4): 184-188.

BHANGU A, BOUTEFNOUCHET T, YONG X, ABRAHAMS P, JOPLIN R (2010) A three-year prospective longitudinal cohort study of medical students' attitudes toward anatomy teaching and their career aspirations. *Anat Sci Educ*, 3(4): 184-190.

CABELLO R, GONZALEZ C, QUICIOS C, BUENO G, GARCIA JV, ARRIBAS AB, CLASCA F (2015) An experimental model for training in renal transplantation surgery with human cadavers preserved using W. Thiel's embalming technique. *J Surg Educ*, 72(2): 192-197.

CLIFTON W, DAMON A, NOTTMEIER E, PICHELMANN M (2020) The importance of teaching clinical anatomy in surgical skills education: Spare the patient, use a sim!. *Clin Anat*, 33(1): 124-127.

CRAIG S, TAIT N, BOERS D, MCANDREW D (2010) Review of anatomy education in Australian and New Zealand medical schools. *ANZ J Surg*, 80(4): 212-216.

D'ANTONI AV, MTUI EP, LOUKAS M, TUBBS RS, ZIPP GP, DUNLOSKY J (2019) An evidence-based approach to learning clinical anatomy: A guide for medical students, educators, and administrators. *Clin Anat*, 32(1): 156-163.

DAMADI A, DAVIS AT, SAXE A, APELGREN K (2007) ACGME duty-hour restrictions decrease resident operative volume: a 5-year comparison at an ACGME-accredited university general surgery residency. *J Surg Educ*, 64(5): 256-259.

DESAI S (2021) Cadaver Surgery and Research Lab India: MSRALC. Retrieved November 12., 2021, from https://msralc.org/surgical_skill_training.

DRAKE RL, MCBRIDE JM, LACHMAN N, PAWLINA W (2009) Medical education in the anatomical sciences: the winds of change continue to blow. *Anat Sci Educ*, 2(6): 253-259.

DRAKE RL, MCBRIDE JM, PAWLINA W (2014) An update on the status of anatomical sciences education in United States medical schools. *Anat Sci Educ*, 7(4): 321-325.

ELLINGSEN KG, MEHLUM CS, MAHMOOD DH (2016) Behov for klinisk vinklet anatomiundervisning i Norge. Prosjektoppgave Retrieved 10.11.2021, from https://www.duo.uio.no/bitstream/handle/10852/52574/Behov-for-klinisk-vinklet-anatomiundervisning-i-Norge.pdf?sequence=1&isAllowed=y.

FINCHER RM, WALLACH PM, RICHARDSON WS (2009) Basic science right, not basic science lite: medical education at a crossroad. *J Gen Intern Med*, 24(11): 1255-1258.

FLYNN, E (2021) Queens University Belfast: Postgraduate Programmes in Clinical Anatomy. Retrieved 15.11.2021, from https://www.qub.ac.uk/courses/postgraduate-taught/clinical-anatomy-msc/.

FONSECA AL, REDDY V, LONGO WE, GUSBERG RJ (2014) Graduating general surgery resident operative confidence: perspective from a national survey. *J Surg Res*, 190(2): 419-428.

GANSKE I, SU T, LOUKAS M, SHAFFER K (2006) Teaching methods in anatomy courses in North American medical schools the role of radiology. *Acad Radiol*, 13(8): 1038-1046.

GEITUNG JT, GROTTUM P (2016) Ultrasound as an integral part of the medical education. *Tidsskr Nor Laegeforen*, 136(14-15): 1192.

GOGALNICEANU P, MADANI H, PARASKEVA PA, DARZI A (2008) A minimally invasive approach to undergraduate anatomy teaching. *Anat Sci Educ*, 1(1): 46-47.

GRIMSTAD H (2019) Grimstadutvalget (appointed by the Ministry of Education): Studieplasser i medisin i Norge - Behov, modeller og muligheter. from https://khrono.no/files/2019/09/25/11745900_rapport_utredning_fra_grimstadutvalget.pdf.

MEREDITH MA, CLEMO HR, MCGINN MJ, SANTEN SA, DIGIOVANNI SR (2019) Cadaver rounds: a comprehensive exercise that integrates clinical context into medical gross anatomy. *Acad Med*, 94(6): 828-832.

MURPHY KP, CRUSH L, O'MALLEY E, DALY FE, O'TUATHAIGH CM, O'CONNOR OJ, CRYAN JF, MAHER MM (2014) Medical student knowledge regarding radiology before and after a radiological anatomy module: implications for vertical integration and self-directed learning. *Insights Imaging*, 5(5): 629-634.

NOEL H, HUANG AR (2019) The effect of varying incentive amounts on physician survey response. *Eval Health Prof*, 42(1): 71-81.

PHILLIPS AW, SMITH SG, STRAUS CM (2013) The role of radiology in preclinical anatomy: a critical review of the past, present, and future. *Acad Radiol*, 20(3): 297-304 e291.

RUIZ-TOVAR J, PRIETO-NIETO I, GARCIA-OLMO D, CLASCA F, ENRIQUEZ P, VILLALONGA R, ZUBIAGA L (2019) Training courses in laparoscopic bariatric surgery on cadaver Thiel: results of a satisfaction survey on students and professors. *Obes Surg*, 29(11): 3465-3470.

SBAYEH A, QAEDI CHOO MA, QUANE KA, FINUCANE P, MCGRATH D, O'FLYNN S, O'MAHONY SM, O'TUATHAIGH CM (2016) Relevance of anatomy to medical education and clinical practice: perspectives of medical students, clinicians, and educators. *Perspect Med Educ*, 5(6): 338-346.

SHARMA G, AYCART MA, NAJJAR PA, VAN HOUTEN T, SMINK DS, ASKARI R, GATES JD (2016) A cadaveric procedural anatomy course enhances operative competence. *J Surg Res*, 201(1): 22-28.

SUTHERLAND LM, MIDDLETON PF, ANTHONY A, HAMDORF J, CREGAN P, SCOTT D, MADDERN GJ (2006) Surgical simulation: a systematic review. *Ann Surg*, 243(3): 291-300.

THIEL W (1992) The preservation of the whole corpse with natural color. *Ann Anat*, 174(3): 185-195.

THIEL W (2002) Supplement to the conservation of an entire cadaver according to W. Thiel. *Ann Anat*, 184(3): 267-269.

WILLAERT W, VAN DE PUTTE D, VAN RENTERGHEM K, VAN NIEUWENHOVE Y, CEELEN W, PATTYN P (2013) Training models in laparoscopy: a systematic review comparing their effectiveness in learning surgical skills. *Acta Chir Belg*, 113(2): 77-95.

A review of the importance of research in Anatomy, an evidence-based science

Mariana Tapia-Nañez*, Alejandro Quiroga-Garza*, Francisco D. Guerrero-Mendivil, Yolanda Salinas-Alvarez, Guillermo Jacobo-Baca, David de la Fuente-Villarreal, Santos Guzman-Lopez, Rodrigo E. Elizondo-Omaña

Department of Human Anatomy, School of Medicine, Universidad Autonoma de Nuevo Leon, Monterrey, Nuevo León, México

SUMMARY

Considered an absolute unchanging truth, and not research-led, human anatomy has been subject to a steady decline in course hours and funding. However, this is a misconstruction, as anatomy plays an important role in the clinical and surgical field, with the need of evidence-based data, more so now than ever. Research in anatomy not only establishes an evolutionary and functional database with variability between populations, sex, and age, but develops the tools needed for patient safety, development of prostheses, technology and surgical materials, improves interpretation of imaging studies, and provides evidence of clinical and anatomical implications. Evidence-based education is an exponentially growing field in anatomical sciences, providing the best evidence for technological and pedagogical strategies integrated in the classroom and laboratory. The gold-standard cadaveric dissections are currently only one of the wide range of educational resources available, with imaging studies and clinical scenarios playing an important role. Anatomy research needs to be continued, evolving with the generations the availability of new resources and the demands of the field. This review breaks down the available data, recommendations, and guidelines, as well as the importance behind the continuing research in anatomical sciences.

Key words: Human anatomy – Anatomical variants – Anatomical sciences – Anatomy education – Evidence-based anatomy – Imaging

INTRODUCTION

Human anatomy as a discipline has historically been the study of the structure and form of the body, as well as the relationships between the different regions. It has been in constant transformation since ancient Mesopotamia and the Greek era, with documents such as the *Corpus Hippocraticum* associated with medical education, Hippocrates "Father of Medicine," and the first evidence of anatomical research and documentation (Edelstein, 1939; López Férez, 1986; Persaud et al., 2014). New dissection techniques were developed, on which Aristotle based human anatomy by comparison with animal anatomy to establish the fundamentals of clinical medicine (Blits, 1999; Crivellato and

Corresponding author:
Prof. Santos Guzmán-López or Prof. Rodrigo E. Elizondo-Omaña. Departamento de Anatomía Humana, Facultad de Medicina, Universidad Autonoma de Nuevo León, Ave. Madero y Aguirre Pequeño, Col. Mitras Centro, s/n, Col. Mitras Centro, Monterrey, Nuevo León, México, CP 64460. E-mail: dr.santos.anato@gmail.com // rod_omana@yahoo.com

Submitted: January 27, 2022. **Accepted:** March 21, 2022

https://doi.org/10.52083/EVZA1394

*The authors Mariana Tapia-Nañez y Alejandro Quiroga-Garza participated equally in the communication and are both in position as first author

Ribatti, 2007). Galen's anatomy also used animal dissection to base the theory of humoralism, as human dissection was strictly prohibited in this era, limiting the evolution of this science.

It was during the Renaissance era when research influenced the views of modern anatomy in medicine (O'Rahilly, 1997; Cosans, 2015). Leonardo da Vinci contributed with his detailed anatomical drawings based on observation. Corpses were incorporated into anatomical studies, leading to a more systematized study of the human anatomy, and an understanding of the development, structure, and functioning of the body (García Barrios et al., 1999; Álvarez Guisbert and Ro, 2007). the attempt to compensate for lacunae in knowledge was what led Andreas Vesalius to the publication of his work *De humanis corporis fabrica*. His conclusions would set the guidelines for a clear comprehension of anatomy (Malomo et al., 2006; Romero Reveron, 2007), and the beginning of a surgical revolution (Mottershead, 1980; Toledo-Pereyra, 2008; Markatos et al., 2020). However, anatomical knowledge was limited by the scarcity of dissections that reveals absolute truths to the science.

An era of cadaveric anatomy provided a more precise tool for teaching. However, learning was limited by a small sample of bodies, without consideration of the individuals' characteristics, race, diseases, or causes of death. There was a lack of variability and a belief in absolute truths that were later proved erroneous. Preservation techniques also limited the time and availability of specimens, in which structures may change in different aspects. This constrained anatomical research to only descriptive, sometimes comparative studies.

With time and the progression of technology and preservation techniques, the use of cadavers was simplified. Embalming techniques changed from alcohol immersion to the intra-arterial use of chemicals with antimicrobial properties which allowed the conservation of histological appearance, providing anatomists with a wider usability and time frame of usage (Brenner, 2014). The Thiel technique even allows for the preservation of natural colors, without the release of harmful volatile substances. Plastination, based on curable polymers, allows the dry, odorless, durable, non-toxic preservation of specimens stored at room temperature, although the technique requires expensive and specialized infrastructure (Mahajan et al., 2016). Regardless of the technique, anatomists seek to preserve the tissue for longer periods, conserving natural characteristics such as color, tissue softness, and joint mobility. This provided the modernization of gross anatomy research (Brenner, 2014; Balta et al., 2015).

With the scientific evolution of anatomical studies, the teaching of gross anatomy continued as a traditional and methodical science, as was the case for several centuries. With the use of bodies, several anatomists continued to contribute to anatomical knowledge. During the last two decades of the 20th century, the discipline began an important transformation with the incorporation of clinical anatomy and advances in teaching (Higgs, 1992; Elizondo-Omaña and López, 2008; Elizondo-Omaña et al., 2010; Estai and Bunt, 2016). Slowly, problem-based learning and computer-based learning were implemented, with research showing a clear benefit towards the understanding and application of this discipline. Students' interest peaked with the study of clinical cases and the use of digital tools to learn anatomy, complemented with dissections (Walsh and Bohn, 1990; Levine et al., 1999; Older, 2004; Yiou and Goodenough, 2006; Papa and Vaccarezza, 2013). This allowed for the modernization of research, education, and the teaching of anatomy (Drake et al., 2009; Mitchell and Batty, 2009; Sugand et al., 2010; Khalil et al., 2018).

CURRENT PERSPECTIVE

Modern medicine has been transitioning into an evidence-based practice. Gross anatomy, seen as a discipline not research-led, has been subject to a steady decline in the curricula as a stand-alone subject (Yammine, 2014b; McBride and Drake, 2018). Gross human anatomy cannot be left behind. Vertical integration of anatomy has been implemented in many universities, providing assessment strategies to assure that anatomical knowledge and education be kept to the needed standard (Bregman et al., 2011). Senior students

and more mature medical residents who have developed broader clinical reasoning can integrate anatomical knowledge (Rajan et al., 2016; Morgan et al., 2017; Quiroga-Garza et al., 2020). Anatomy research must be maintained and furthered purposefully.

Research in anatomy has been developed with the objective not only of establishing the prevalence of variability between different populations, sex, and age, but also of understanding the clinical implications it may have. A detailed study of anatomy helps healthcare providers increase patient safety during surgical procedures, aids in the development of prostheses, technology and surgical materials, improves the interpretation of imaging studies, and provides evidence for these. This is not only through the use of human bodies, but also imaging studies and the use of trans-operative surgical videos. This is what must be called an evidence-based anatomy (EBA) (Yammine, 2014a).

EVIDENCE-BASED ANATOMY

The study of anatomy is relevant to modern medicine, creating a high value in patient safety during surgical procedures (Clifton et al., 2020; Dee et al., 2021). Previous studies have demonstrated that an important percentage of *mala praxis* lawsuits are due to surgical errors attributed to "ignorance about anatomical variations" (10%) (Cahill and Leonard, 1999) and "abnormal or difficult anatomy" (13%) (Rogers et al., 2006).

The Evidence-Based Medicine (EBM) concept was first described in 1992 (Guyatt et al., 1992). It proposed a shift from a pathophysiological comprehension, non-systematized, intuition-based clinical practice to an EBM that requires efficient literature searching and the application of guidelines and recommendations based on the evaluation of the best available evidence (Guyatt et al., 1992; Sackett et al., 1996; Phillips, 2014). Evidence is hierarchically classified from the highest impact (Level 1, i.e., systematic reviews of randomized controlled trials) to the lowest (Level 5, i.e., expert opinions) (Uman, 2011; Phillips, 2014; Henry et al., 2017).

Most anatomical studies in the literature are cross-sectional or prevalence-based with epidemiological ends (Yammine, 2014a). These include anatomical structure measurements with a range of "normality" and its statistical description, inconstant structure frequencies, and inferential basic statistics looking for associations between variables or groups (sex, age, ethnicity).

As it is difficult to perform randomized controlled trials for anatomical studies, meta-analytical results of anatomical studies are considered the base of the EBA. Systematized guidelines for the realization of anatomical systematic reviews have been published (Yammine, 2014a; Henry et al., 2016). This has aided in understanding anatomical variations, which may be due to the differences in population, ethnicity, age, sex, medical history, as well as methodological discrepancies (Rodríguez-Niedenführ et al., 2001; Bergman's Comprehensive Encyclopedia of Human Anatomic Variation, 2016; Abou-Foul and Borumandi, 2016; Ling and Smoll, 2016; Martínez-González et al., 2017; Popieluszko et al., 2018; Santos et al., 2018; Hernandez-Trejo et al., 2020; Muñoz-Leija et al., 2020) For these reasons, AQUA (Anatomical Quality Assessment) guidelines were published as recommendations for researchers to ensure a higher quality of anatomical studies as well as publications (Henry et al., 2016; Henry et al., 2017; Henry, Skinningsrud, et al., 2018; Henry, Vikse, et al., 2018).

RESEARCH IN ANATOMY

Research in anatomy has shifted during the last couple of decades. This is most evident in anatomy journals and publications. Although basic gross anatomy regarding structure, function, development, and evolution is still widely published, a much larger field has opened with a refocus of traditional journals, and the emergence of new journals to publish anatomical research oriented towards the clinical and surgical application, and the advances in the educational field, which has exponentially grown.

Medical education has been constantly changing with a direct impact on modern anatomy teaching. Contemporarily, more

anatomy courses are being part of an integrated curriculum in medical schools. Course hours have had a downward trend in the last two decades, due to curricular approaches, class size, and other parameters. However, this trend seems to be stabilizing (Drake, 2014; McBride and Drake, 2018; Salinas-Alvarez et al., 2020). It has evolved from the days of long and continuous lectures to the promotion of active learning, where people might benefit more from different learning styles (visual, auditory, kinesthetic, others) (Carmichael and Pawlina, 2000; Gregory et al., 2009; Andrew Jay et al., 2013; Morton and Colbert-Getz, 2017). Additionally, integration with clinical medicine throughout the course gives students a reason to learn (Lachman and Pawlina, 2006; Drake, 2014; Drake et al., 2014). Through these activities, anatomical education aims to generate in the student acquisition of anatomical knowledge and the development of clinical reasoning skills (Elizondo-Omaña and López, 2008; Elizondo-Omaña et al., 2010; Quiroga-Garza et al., 2020; Gonzalez-Navarro et al., 2021).

Evidence-based education is also guiding the integration of curricula and the approach to teaching anatomy. Educational journals are on the rise, with an increased number of submissions, publications, and citing. Educational studies need to follow recommendations of competency-based objectives to improve the quality of reports, avoiding the over-use of technology (Ganguly, 2010; Cohen et al., 2015; Estai and Bunt, 2016; Clunie et al., 2018; Krebs et al., 2021). Systematic reviews and meta-analyses are providing the best evidence for the implementation of technological and pedagogical strategies integrated into anatomy education (Bergman et al., 2008; Campos et al.,, Sugand and Mirza, 2013; Akçayır and Akçayır, 2017; Li et al., 2017; Clunie et al., 2018; Langlois et al., 2020). However, these must be evaluated and adapted to each environment and individual circumstance in each school and university.

The integration of classroom knowledge and laboratory activities is an important competence. Traditionally, dissection has been the pillar of anatomy, developing professional, bioethical, and psycho-emotional skills in students (Elizondo-Omaña et al., 2005; Ghosh, 2017; Quiroga-Garza et al., 2017). However, obtaining human tissue may be a challenge for several reasons including financial, ethical, legal, and cultural (AbouHashem et al., 2015; Quiroga-Garza et al., 2017; Ciliberti et al., 2018; Habicht et al., 2018; Hasselblatt et al., 2018; McBride and Drake, 2018; Champney et al., 2019; Kostorrizos et al., 2019; Zhang et al., 2020). Cadaver use is decreasing, with alternatives for learning gross anatomy on the rise (McBride and Drake, 2018; McMenamin et al., 2018). A variety of technological educational resources have emerged in recent years to solve these obstacles, with a wide range of peer-reviewed articles discussing their effectiveness (Vázquez et al., 2007; Estai and Bunt, 2016; Zargaran et al., 2020; Krebs et al., 2021).

Imaging has become an increasingly important component in the teaching of anatomy, enhancing the quality and efficiency of learning (Pawlina and Drake, 2015; Grignon et al., 2016; Royer, 2016; Patel et al., 2017). Clinical cases ensured engagement between anatomical knowledge and clinical scenarios, promoting clinical reasoning to encourage learning outside the classroom settings and ultimately improving the decision-making skills (Elizondo-Omaña et al., 2010, 2020; Perumal et al., 2016; Dinesh Kumar et al., 2020; M. Muñoz-Leija et al., 2020; Salinas-Alvarez et al., 2020). Three-dimensional (3D) printing includes an accurate duplication of anatomical structures with both visual and haptic value, and financial alleviation (AbouHashem et al., 2015; Vaccarezza and Papa, 2015). Students can actively interact with the models, creating an integration of kinesthetic and visual learning, highly valuable with complicated anatomical structures (Erolin, 2019). More recently, augmented- and virtual-reality technologies allow students to manipulate a virtual 3D model of an anatomical structure and navigate around them. Interactive hologram teaching technology is currently being developed and experimented (Kuehn, 2018; Darras et al., 2019; Pennefather and Krebs, 2019).

All these tools have aided in the purpose of anatomical studying and its implications in clinical scenarios. However, for a student to integrate this knowledge, the transfer must be vertical. Many

anatomy courses are now spread throughout the curricula, providing senior students with an anatomical review in each clinical rotation. (Bregman et al., 2011; Rajan et al., 2016; Morgan et al., 2017). Constant exposure helps students recall the anatomical knowledge needed, to improve their clinical thinking and reasoning, significantly improving their assessment and understanding (Murphy et al., 2014; Osborn et al., 2014).

THE IMPACT OF IMAGING IN ANATOMICAL RESEARCH AND EDUCATION

The change in understanding gross human anatomy due to imaging techniques cannot be overestimated, as their nature allows users to visualize it in the living (Ganguly, 2010). X-rays, ultrasound, computerized tomography, magnetic resonance imaging, and digital subtraction angiography, have advanced the quality and precision of anatomical research. It broadens the options of protocol design and methods, facilitates a larger sample size, and enhances the confidence interval. The imaging software provides millimetric precision to measurements in an objective, reliable, and reproducible manner. It facilitates access to deep structures without the necessity of laborious and lengthy dissections that could alter its structural integrity. Most hospitals count with imaging databases, which upon approval of the Research and Ethics Committees, are of easy access, making them an attractive and effective method for anatomy researchers (Tregaskiss et al., 2007; Elizondo-Omaña and López, 2008; Elizondo-Omaña et al., 2010; Grignon, Oldrini and Walter, 2016; Kobatake and Masutani, 2017).

Imaging also revolutionized anatomy education. It allows an easier and three-dimensional understanding of anatomy for students. Typical anatomy can be compared to pathological findings. Ultrasounds can be used to view real-time anatomy. It has aided in the development of anatomical virtual and augmented reality. All these, without the need for expensive dissection laboratories (Machado et al., 2013; Phillips et al., 2013; Pawlina and Drake, 2015; Estai and Bunt, 2016; Moro et al., 2017).

ANATOMICAL VARIANTS AND THEIR IMPORTANCE IN CLINICAL SCENARIOS

Normalis means "by the rule or pattern". "Normal anatomy" refers to the ideal, typical, mean, natural, or most frequent (Moore, 1989). However, in the study of anatomy, normality involves a range of normal variations. Abnormal variables can be major or minor, derived from aberrant development processes during the formation of a structure by genetic, chromosomal, or environmental influences (Sañudo et al.,, 2003; Bergman's Comprehensive Encyclopedia of Human Anatomic Variation, 2016).

Galen and Vesalius noted variations in their respective investigations. Expressions like "always", "usually", "frequently", "more frequently", "sometimes", "not always", "rarely" and, "very rarely", can be found in their works (Straus et al., 1943). Centuries and several dissections were the basis to establish the concepts of normality, abnormality, and variations of the human body, thanks to the reported knowledge in works of many biologists, clinicians, and anatomists since the 19th century until today (Sañudo et al., 2003; Bergman's Comprehensive Encyclopedia of Human Anatomic Variation, 2016).

Despite numerous studies carried out over the years, the anatomy of structures continues to be researched. Significant variability of the shaping of systems and regions has been drawing attention for years and inspires targeted research projects. The future of anatomical research depends greatly on the imaging methods for anatomical variabilities. These can be gathered into three categories: morphometrical, consistency, and spatial (Yammine, 2014a).

Anatomical variability is valuable not only from the anatomical point of view but also in the clinical aspect, due to their implications (Cahill and Leonard, 1999; Rogers et al., 2006). For example, the atypical variations of the anterior cerebral artery and the communicant anterior artery increase the risk of stroke (Jiménez-Sosa et al., 2017). To understand the pathophysiology of compartment syndrome of the foot and develop viable treatment options, a clear knowledge

of the foot compartments is needed (Vazquez-Zorrilla et al., 2020). At a diagnostic level for perineural metastasis, it is useful to keep in mind the variations in the asymmetry of the skull base canals (Barrera-Flores et al., 2017). At a surgical level, to avoid complications in a paranasal sinuses surgery, ethmoidal roof variations and differences between gender must be considered (Muñoz-Leija et al., 2018). At a treatment level, the location (origin, pattern, branches) of the bronchial arteries is vital for their embolization to control massive hemoptysis (Esparza-Hernández et al., 2017), or of the external carotid artery when performing a neck procedure (Herrera-Núñez et al., 2020). Justification of procedures, such as the measurement of the pelvic and birth canal to determine cephalopelvic disproportion were an indication for a cesarean section (Vázquez-Barragán et al., 2016). The physiological changes of the recto-vaginal septum due to gynecological history influence the risk of fistulae formation (Rodríguez-Abarca et al., 2020). The influence of a higher hippocampal volume to achieve remission in depression (Zarate-Garza et al., 2021). Facilitating a procedure such as right internal jugular vein catheterization by increasing its size with a degree of head-down tilt position (Garcia-Leal et al., 2021). Determining the associated musculoskeletal symptoms or evolutionary effects new tendencies may cause, such as the morphological changes of the hand due to chronic use of smart devices (Fuentes-Ramírez et al., 2020).

Anatomical studies have proven to be beneficial in the development of prostheses of the inferior (Adam et al., 2002) and superior limbs (Wood et al., 1989; Boileau and Walch, 1997; Pearl, 2005; Mansat et al., 2013), vertebral column screws and material (Morales-Avalos et al., 2012; Ramos-Davila et al., 2021), the development of hearing devices (Van De Water, 2012; Guzman-Perez et al., 2021), among others (Fantini et al., 2013; Negi, Dhiman and Sharma, 2014; Saunders et al., 2014). Defining the anatomy of clinical implications behind these will continue to be a valuable tool in medical development and patient safety.

ANATOMICAL EDUCATION IN A MILLENNIAL GENERATION

Currently, the millennial generation (born between 1980-1996), is the most prevalent in medical students (Ruzycki et al., 2019). New generations appear as cultural and technological changes emerge over time. It is important to understand the differences and needs of current generations in medical education, as this shared context confers a set of shared values and beliefs among generation members (Borges et al., 2006; Krebs et al., 2021). In consequence, each generation differs in career expectations, personal life, and education.

Medical education has been in a continuous adaptation to meet generational needs and maintain with technological advances, attempting to improve the education and training of future physicians. Millennials are the first ones to grow up with computer access in parallel with internet growth; they are confident with technology and prefer self-study using electronic resources. This generates a challenge, primarily for the older academic staff, due to the generation and technology (Smith, 2005; Ganguly, 2010; Eckleberry-Hunt and Tucciarone, 2011; Birden et al., 2014; Ruzycki et al., 2019). Educators must focus on assuring any technological or pedagogic tool emphasizes the core values behind medical education and professionalism (Krebs et al., 2021).

FUTURE PERSPECTIVES

Anatomical sciences are pillars of medical education. Even with the decline of anatomy hours, it is a science integrated into the curriculum, being taught at all levels as the medical student advances in their training. (Drake, 2014; Drake, McBride, et al., 2014; McBride and Drake, 2018; Salinas-Alvarez et al., 2020).

Anatomical knowledge and its application are continuous through the student evolution from a medical student to a resident, to an attendant. Its importance goes beyond the surgical specialties, although there is a clear advantage in patient safety and advancement. Evidenced-based studies must be performed.

REFERENCES

ABOU-FOUL AK, BORUMANDI F (2016) Anatomical variants of lower limb vasculature and implications for free fibula flap: Systematic review and critical analysis. *Microsurg*, 36(2): 165-172.

ABOUHASHEM Y, DAYAL M, SAVANAH S, ŠTRKALJ G (2015) The application of 3D printing in anatomy education. *Med Edu Online*, 20(1): 29847.

ADAM F, HAMMER DS, PAPE D, KOHN D (2002) Femoral anatomy, computed tomography and computer-aided design of prosthetic implants. *Arch Orthop Traum Su*, 122(5): 262-268.

AKÇAYIR M, AKÇAYIR G (2017) Advantages and challenges associated with augmented reality for education: A systematic review of the literature. *Educ Res Rev*, 20: 1-11.

ÁLVAREZ GUISBERT O, CAMPOHERMOSO RODRÍGUEZ O (2007) Evolución histórica conceptual de la Terminología Anatómica. Cuadernos Hospital de Clínicas, 52(1): 113-117.

ANDREW JAY E, STARKMAN SJ, PAWLINA W, LACHMAN N (2013) Developing medical students as teachers: An anatomy-based student-as-teacher program with emphasis on core teaching competencies. *Anat Sci Edu*, 6(6): 385-392.

BALTA JY, CRONIN M, CRYAN JF, O'MAHONY SM (2015) Human preservation techniques in anatomy: A 21st century medical education perspective. *Clin Anat*, 28(6): 725-734.

BARRERA-FLORES FJ, VILLARREAL-DEL BOSQUE N, DÍAZ GONZÁLEZ-COLMENERO A, GARZA-GONZÁLEZ C, MORALES-ÁVALOS R, PINALES-RAZO R, ELIZONDO-RIOJAS G, GUZMÁN-LÓPEZ S, ELIZONDO-OMAÑA RE (2017) Perineural spread-susceptible structures: a non-pathological evaluation of the skull base. *E Eu Arch Oto-Rhino-L*, 274(7): 2899-2905.

BERGMAN'S Comprehensive Encyclopedia of Human Anatomic Variation (2016) Shane Tubbs R, Shoja MM, Loukas M (eds.). John Wiley & Sons, Inc. https://doi.org/10.1002/9781118430309

BERGMAN EM, PRINCE KJAH, DRUKKER J, VAN DER VLEUTEN CPM, SCHERPBIER AJJA (2008) How much anatomy is enough? *Anat Sci Edu*, 1(4): 184-188.

BERGMAN EM, VAN DER VLEUTEN CP, SCHERPBIER AJ (2011) Why don't they know enough about anatomy? A narrative review. *Med Teach*, 33(5): 403-409.

BIRDEN H, GLASS N, WILSON I, HARRISON M, USHERWOOD T, NASS D (2014) Defining professionalism in medical education: A systematic review. *Med Teach*, 36(1): 47-61.

BLITS KC (1999) Aristotle: Form, function, and comparative anatomy. *Anat Rec*, 257(2): 58-63.

BOILEAU P, WALCH G (1997) The three-dimensional geometry of the proximal humerus: implications for surgical technique and prosthetic design. *J Bone Joint Surg*, 79(5): 857-865.

BORGES NJ, MANUEL RS, ELAM CL, JONES BJ (2006) Comparing millennial and generation X medical students at one medical school. *Acad Med*, 81(6): 571-576.

BRENNER E (2014) Human body preservation - old and new techniques. *J Anat*, 224(3): 316-344.

CAHILL DR, LEONARD RJ (1999) Missteps and masquerade in American Medical Academy: Clinical anatomists call for action. *Clin Anat*, 12(3): 220-222.

CAMPOS P, SUGAND K, MIRZA K (2013) Holography in clinical anatomy education: A systematic review. *Int J Surg*, 11(8): 706.

CARMICHAEL SW, PAWLINA W (2000) Animated PowerPoint as a tool to teach anatomy. *Anat Rec*, 261(2): 83-88.

CHAMPNEY TH, HILDEBRANDT S, GARETH JONES D, WINKELMANN A (2019) BODIES R US: Ethical views on the commercialization of the dead in medical education and research. *Anat Sci Edu*, 12(3): 317-325.

CILIBERTI R, GULINO M, GAZZANIGA V, GALLO F, VELLONE V, DE STEFANO F, SANTI P, BALDELLI I (2018) A survey on the knowledge and attitudes of Italian medical students toward body donation: ethical and scientific considerations. *J Clin Med*, 7(7): 168.

CLIFTON W, DAMON A, NOTTMEIER E, PICHELMANN M (2020) The importance of teaching clinical anatomy in surgical skills education: Spare the patient, use a sim! *Clin Anat*, 33(1): 124-127.

CLUNIE L, MORRIS NP, JOYNES VCT, PICKERING JD (2018) How comprehensive are research studies investigating the efficacy of technology-enhanced learning resources in anatomy education? A systematic review. *Anat Sci Edu*, 11(3): 303-319.

COHEN ER, MCGAGHIE WC, WAYNE DB, LINEBERRY M, YUDKOWSKY R, BARSUK JH (2015) Recommendations for reporting mastery education research in medicine (ReMERM). *Acad Med*, 90(11): 1509-1514.

COSANS CE (2015) History of Classical Anatomy. In eLS 1-7. https://doi.org/10.1002/9780470015902.a0003091.pub2

CRIVELLATO E, RIBATTI D (2007) A portrait of Aristotle as an anatomist: Historical article. *Clin Anat*, 20(5): 447-485.

DARRAS KE, SPOUGE R, HATALA R, NICOLAOU S, HU J, WORTHINGTON A, KREBS C, FORSTER BB (2019) Integrated virtual and cadaveric dissection laboratories enhance first year medical students' anatomy experience: A pilot study. *BMC Med Edu*, 19(1): 1-6.

DEE EC, ALTY IG, AGOLIA JP, TORRES-QUINONES C, VAN HOUTEN T, STEARNS DA, LILLEHEI CW, SHAMBERGER RC (2021) A surgical view of anatomy: perspectives from students and instructors. *Anat Sci Edu*, 14(1): 110-116.

DINESH KUMAR V, RAJPRASATH R, PRIYADHARSHINI NA, MURUGAN M, DEVI R (2020) Infusing the axioms of clinical reasoning while designing clinical anatomy case vignettes teaching for novice medical students: A randomised cross over study. *Anat Cell Biol*, 53(2): 151.

DRAKE RL (2014) A retrospective and prospective look at medical education in the United States: Trends shaping anatomical sciences education. *J Anat*, 224(3): 256-260.

DRAKE RL, MCBRIDE JM, LACHMAN N, PAWLINA W (2009) Medical education in the anatomical sciences: The winds of change continue to blow. *Anat Sci Edu*, 2(6): 253-259.

DRAKE RL, MCBRIDE JM, PAWLINA W (2014) An update on the status of anatomical sciences education in United States medical schools. *Anat Sci Edu*, 7(4): 321-325.

ECKLEBERRY-HUNT J, TUCCIARONE J (2011) The challenges and opportunities of teaching "Generation Y". *J Grad Med Edu*, 3(4): 458.

EDELSTEIN L (1939) The genuine works of Hippocrates. *Bull History Med*, 7(2): 236-248.

ELIZONDO-OMAÑA RE, GUZMÁN-LÓPEZ S, DE LOS ANGELES GARCÍA-RODRÍGUEZ M (2005) Dissection as a teaching tool: Past, present, and future. *Anat Rec Part B*, 285(1): 11-15.

ELIZONDO-OMAÑA RE, LÓPEZ SG (2008) The development of clinical reasoning skills: A major objective of the anatomy course. *Anat Sci Edu*, 1(6): 267-268.

ELIZONDO-OMAÑA RE, MORALES-GÓMEZ JA, MORQUECHO-ESPINOZA O, HINOJOSA-AMAYA JM, VILLARREAL-SILVA EE, GARCÍA-RODRÍGUEZ MA, GUZMÁN-LÓPEZ S (2010) Teaching skills to promote clinical reasoning in early basic science courses. *Anat Sci Edu*, 3(5): 267-271.

ELIZONDO-OMAÑA RE, QUIROGA-GARZA A, SALINAS-ALVAREZ YE, GUZMAN-LOPEZ S (2020) Breaking down large anatomy groups. *FASEB J*, 34(S1): S1.

EROLIN C (2019) Interactive 3D digital models for anatomy and medical education. *Adv Exp Med Biol*, 1138: 1-16.

ESPARZA-HERNÁNDEZ CN, RAMÍREZ-GONZÁLEZ JM, CUÉLLAR-LOZANO RA, MORALES-AVALOS R, GONZÁLEZ-AROCHA CS,

MARTÍNEZ-GONZÁLEZ B, QUIROGA-GARZA A, PINALES-RAZO R, ELIZONDO-RIOJAS G, ELIZONDO-OMAÑA RE, GUZMÁN-LÓPEZ S (2017) Morphological analysis of bronchial arteries and variants with computed tomography angiography. *BioMed Res Int*, 2017: 9785896.

ESTAI M, BUNT S (2016) Best teaching practices in anatomy education: A critical review. *Ann Anat*, 208: 151-157.

EVIDENCE-BASED MEDICINE WORKING GROUP (1992) Evidence-based medicine: a new approach to teaching the practice of medicine. *JAMA*, 268(17): 2420-2425.

FANTINI M, DE CRESCENZIO F, CIOCCA L (2013) Design and rapid manufacturing of anatomical prosthesis for facial rehabilitation. *Int J Interact Des Manuf*, 7(1): 51-62.

FUENTES-RAMÍREZ LD, ALFARO-GOMEZ U, ESPINOSA-URIBE AG, TERAN-GARZA R, QUIROGA-GARZA A, GUTIÉRREZ-DE LA O J, VILCHEZ CAVAZOS F, GUZMAN-LOPEZ S, ELIZONDO-OMAÑA RE (2020) Morphologic changes of the fifth phalange secondary to smartphone use. *Work*, 65(2): 1-5.

GANGULY P (2010) Teaching and learning of anatomy in the 21st Century: direction and the strategies. *Open Med Edu J*, 3(1).

GARCIA-LEAL M, GUZMAN-LOPEZ S, VERDINES-PEREZ AM, DE LEON-GUTIERREZ H, FERNANDEZ-RODARTE BA, ALVAREZ-VILLALOBOS NA, MARTINEZ-GARZA JH, QUIROGA-GARZA A, ELIZONDO-OMAÑA RE (2021) Trendelenburg position for internal jugular vein catheterization: a systematic review and meta-analysis. *J Vasc Access*, 11297298211031339.

GARCÍA BARRIOS C, MEJÍAS RODRÍGUEZ I, CASTILLO DEL RÍO M (1999) Origen e historia de la disección anatómica. *Rev Arch Med Camagüey*, 3(2): 1-8.

GHOSH SK (2017) Giovanni Battista Morgagni (1682-1771): father of pathologic anatomy and pioneer of modern medicine. *Anat Sci Int,* 92(3): 305-312.

GONZALEZ-NAVARRO AR, QUIROGA-GARZA A, ACOSTA-LUNA AS, SALINAS-ALVAREZ Y, MARTINEZ-GARZA JH, DE LA GARZA-CASTRO O, GUTIERREZ-DE LA O J, DE LA FUENTE-VILLARREAL D, ELIZONDO-OMAÑA RE, GUZMAN-LOPEZ S (2021) Comparison of suturing models: the effect on perception of basic surgical skills. *BMC Med Educ*, 21(1): 1-11.

GREGORY JK, LACHMAN N, CAMP CL, CHEN LP, PAWLINA W (2009) Restructuring a basic science course for core competencies: An example from anatomy teaching. *Med Teach*, 31(9): 855-861.

GRIGNON B, OLDRINI G, WALTER F (2016) Teaching medical anatomy: what is the role of imaging today? *Surg Radiol Anat*, 38(2): 253-260.

GUZMAN-PEREZ HG, GUZMAN-LOPEZ S, VILLARREAL-DEL BOSQUE IS, VILLARREAL-DEL BOSQUE N, QUIROGA-GARZA A, TREVIÑO-GONZÁLEZ JL, PINALES-RAZO R, MUÑOZ-LEIJA MA, ELIZONDO-OMAÑA RE (2021) Cochlear morphometry in healthy ears of a mexican population: A comparison of measurement techniques. *Morphologie*, S1286-0115(21)00187-9.

HABICHT JL, KIESSLING C, WINKELMANN A (2018) Bodies for anatomy education in medical schools: An overview of the sources of cadavers worldwide. *Acad Med*, 93(9): 1293.

HASSELBLATT F, MESSERER DAC, KEIS O, BÖCKERS TM, BÖCKERS A (2018) Anonymous body or first patient? A status report and needs assessment regarding the personalization of donors in dissection courses in German, Austrian, and Swiss Medical Schools. *Anat Sci Edu*, 11(3): 282-293.

HENRY BM, TOMASZEWSKI KA, WALOCHA JA (2016) Methods of evidence-based anatomy: a guide to conducting systematic reviews and meta-analysis of anatomical studies. *Ann Anat*, 205: 16-21.

HENRY BM, TOMASZEWSKI KA, RAMAKRISHNAN PK, ROY J, VIKSE J, LOUKAS M, TUBBS RS, WALOCHA JA (2017) Development of the anatomical quality assessment (AQUA) tool for the quality assessment of anatomical studies included in meta-analyses and systematic reviews. *Clin Anat*, 30(1): 6-13.

HENRY BM, SKINNINGSRUD B, VIKSE J, PĘKALA PA, WALOCHA JA, LOUKAS M, TUBBS RS, TOMASZEWSKI KA (2018a) Systematic reviews versus narrative reviews in clinical anatomy: Methodological approaches in the era of evidence-based anatomy. *Clin Anat*, 31(3): 364-367.

HENRY BM, VIKSE J, PEKALA P, LOUKAS M, TUBBS RS, WALOCHA JA, JONES DG, TOMASZEWSKI KA (2018b) Consensus guidelines for the uniform reporting of study ethics in anatomical research within the framework of the anatomical quality assurance (AQUA) checklist. *Clin Anat*, 31(4): 521-524.

HERNANDEZ-TREJO AF, CUELLAR-CALDERON KP, TREVIÑO-GONZALEZ JL, YAMAMOTO-RAMOS M, CAMPOS-COY MA, QUIROGA-GARZA A, GUZMAN-AVILAN K, ELIZONDO-RIOJAS G, ELIZONDO-OMAÑA RE, GUZMAN-LOPEZ S (2020) Prevalence of facial canal dehiscence and other bone defects by computed tomography. *Eur Arch Oto-Rhino-Laryngol*, 277(10): 2681-2686.

HERRERA-NÚÑEZ M, MENCHACA-GUTIÉRREZ JL, PINALES-RAZO R, ELIZONDO-RIOJAS G, QUIROGA-GARZA A, FERNANDEZ-RODARTE BA, ELIZONDO-OMAÑA RE, GUZMÁN-LÓPEZ S (2020) Origin variations of the superior thyroid, lingual, and facial arteries: a computed tomography angiography study. *Surg Radiol Anat*, 42(9): 1085-1093.

HIGGS J (1992) Developing clinical reasoning competencies. *Physiotherapy*, 78(8): 575-581.

JIMÉNEZ-SOSA MS, CANTU-GONZALEZ JR, MORALES-AVALOS R, DE LA GARZA-CASTRO O, QUIROGA-GARZA A, PINALES-RAZO R, ELIZONDO-RIOJAS G, ELIZONDO-OMAÑA RE, GUZMÁN-LÓPEZ S (2017) Anatomical variants of anterior cerebral arterial circle: a study by multidetector computerized 3D tomographic angiography. *Int J Morphol*, 35(3). 1121-1128.

KHALIL MK, ABDEL MEGUID EM, ELKHIDER IA (20189 Teaching of anatomical sciences: A blended learning approach. *Clin Anat*, 31(3): 323-329.

KOBATAKE H, MASUTANI Y (2017) Computational anatomy based on whole body imaging. Springer Berlin Heidelberg.

KOSTORRIZOS A, KOUKAKIS A, SAMOLIS A, PROTOGEROU V, MARIOLIS-SAPSAKOS T, PIAGKOU M, NATSIS K, SKANDALAKIS GP, TROUPIS T (2019) Body donation for research and teaching purposes: The contribution of blood donation units in the progress of anatomical science. *Folia Morphol*, 78(3): 575-581.

KREBS C, QUIROGA-GARZA A, PENNEFATHER P, ELIZONDO-OMAÑA RE (2021) Ethics behind technology-enhanced medical education and the effects of the COVID-19 pandemic. *Eur J Anat*, 25(4): 515-522.

KUEHN BM (2018) Virtual and augmented reality put a twist on medical education. *JAMA*, 319(8): 756-758.

LACHMAN N, PAWLINA W (2006) Integrating professionalism in early medical education: The theory and application of reflective practice in the anatomy curriculum. *Clin Anat*, 19(5): 456-460.

LANGLOIS J, BELLEMARE C, TOULOUSE J, WELLS GA (2020) Spatial abilities training in anatomy education: a systematic review. *Anat Sci Edu*, 13(1): 71-79.

LEVINE MG, STEMPAK J, CONYERS G, WALTERS JA (1999) Implementing and integrating computer-based activities into a problem- based gross anatomy curriculum. *Clin Anat*, 12(3): 191-198.

LI KHC, KUI C, LEE EKM, HO CS, SUNNY HEI SH, WU W, WONG WT, VOLL J, LI G, LIU T, YAN B, CHAN J, TSE G, KEENAN ID (2017) The role of 3D printing in anatomy education and surgical training: A narrative review. *MedEdPublish*, 6(2).

LING XY, SMOLL NR (2016) A systematic review of variations of the recurrent laryngeal nerve. *Clin Anat*, 29(1): 104-110.

LÓPEZ FÉREZ JA (1986) Hipócrates y los escritos hipocráticos: origen de la medicina científica. *Epos: Revi Filolog*, 2: 157-175.

MACHADO JAD, BARBOSA JMP, FERREIRA MAD (2013) Student perspectives of imaging anatomy in undergraduate medical education. *Anat Sci Edu*, 6(3): 163-169.

MAHAJAN A, AGARWAL S, TIWARI S, VASUDEVA N (2016) Plastination: An innovative method of preservation of dead body for teaching and learning anatomy. *MAMC J Med Sci*, 2(1): 38.

MALOMO AO, IDOWU OE, OSUAGWU FC (2006) Lessons from history: Human anatomy, from the origin to the renaissance. *Int J Morphol*, 24(1): 99-104.

MANSAT P, COUTIÉ AS, BONNEVIALLE N, RONGIÈRES M, MANSAT M, BONNEVIALLE P (2013) Resurfacing humeral prosthesis: Do we really reconstruct the anatomy? *J Shoulder Elb Surg*, 22(5): 612-619.

MARKATOS K, CHYTAS D, TSAKOTOS G, KARAMANOU M, PIAGKOU M, MAZARAKIS A, JOHNSON E (2020) Andreas Vesalius of Brussels (1514-1564): his contribution to the field of functional neuroanatomy and the criticism to his predecessors. *Acta Chir Belg*, 120(6): 437-441.

MARTÍNEZ-GONZÁLEZ B, REYES-HERNÁNDEZ CG, QUIROGA-GARZA A, RODRÍGUEZ-RODRÍGUEZ VE, ESPARZA-HERNÁNDEZ CN, ELIZONDO-OMAÑA RE, GUZMÁN-LÓPEZ S (2017) Conduits used in coronary artery bypass grafting: A review of morphological studies. *Ann Thorac Cardiovas Surg*, 23(2): 55-65.

MCBRIDE JM, DRAKE RL (2018) National survey on anatomical sciences in medical education. *Anat Sci Edu*, 11(1): 7-14.

MCMENAMIN PG, MCLACHLAN J, WILSON A, MCBRIDE JM, PICKERING J, EVANS DJR, WINKELMANN A (2018) Do we really need cadavers anymore to learn anatomy in undergraduate medicine? *Med Teach*, 40(10): 1020-1029.

MITCHELL R, BATTY L (2009) Undergraduate perspectives on the teaching and learning of anatomy. *ANZ J Surg*, 79(3): 118-121.

MOORE KL (1989) Meaning of "normal." *Clin Anat*, 2(4): 235-239.

MORALES-AVALOS R, ELIZONDO-OMAÑA RE, VÍLCHEZ-CAVAZOS F, MARTÍNEZ-PONCE DE LEÓN AR, ELIZONDO-RIOJAS G, DELGADO-BRITO M, CORTÉS-GONZÁLEZ P, GUZMÁN-AVILÁN RI, PINALES-RAZO R, DE LA GARZA-CASTRO O, GUZMÁN-LÓPEZ S (2012) Vertebral fixation with a transpedicular approach. Relevance of anatomical and imaging studies. *Acta Ortoped Mex*, 26(6): 402-411.

MORGAN H, ZELLER J, HUGHES DT, DOOLEY-HASH S, KLEIN K, CATY R, SANTEN S (2017) Applied clinical anatomy: the successful integration of anatomy into specialty-specific senior electives. *Surg Radiol Anat*, 39(1): 95-101.

MORO C, ŠTROMBERGA Z, RAIKOS A, STIRLING A (2017) The effectiveness of virtual and augmented reality in health sciences and medical anatomy. *Anat Sci Edu*, 10(6): 549-559.

MORTON DA, COLBERT-GETZ JM (2017) Measuring the impact of the flipped anatomy classroom: The importance of categorizing an assessment by Bloom's taxonomy. *Anat Sci Edu*, 10(2): 1306.

MOTTERSHEAD S (1980) The teaching of anatomy and its influence on the art and practice of surgery. *Br Med J*, 280(6227): 1306-1309.

MUÑOZ-LEIJA MA, ORDÓÑEZ RIVAS FO, BARRERA-FLORES FJ, TREVIÑO-GONZÁLEZ JL, PINALES-RAZO R, GUZMÁN-LÓPEZ S, ELIZONDO-OMAÑA RE, QUIROGA-GARZA A (2020) A proposed extension to the elongated styloid process definition: A morphological study with high-resolution tomography computer. *Morphologie*, 104(345): 117-124.

MUÑOZ-LEIJA MA, ZARATE-GARZA P, JACOBO-BACA G, QUIROGA-GARZA A, SALINAS-ALVAREZ Y, MARTINEZ-GARZA J, ELIZONDO-OMAÑA R, GUZMÁN-LÓPEZ S (2020) Modifications to the delivery of a gross anatomy course during the COVID-19 pandemic at a Mexican medical school. *Eur J Anat*, 24(6): 507-512.

MUÑOZ-LEIJA MA, YAMAMOTO-RAMOS M, BARRERA-FLORES FJ, TREVIÑO-GONZÁLEZ JL, QUIROGA-GARZA A, MÉNDEZ-SÁENZ MA, CAMPOS-COY MA, ELIZONDO-ROJAS G, GUZMÁN-LÓPEZ S, ELIZONDO-OMAÑA RE (2018) Anatomical variations of the ethmoidal roof: differences between men and women. *Eur Arch Oto-Rhino-L*, 275(7): 1831-1836.

MURPHY KP, CRUSH L, O'MALLEY E, DALY FE, O'TUATHAIGH CM, O'CONNOR OJ, CRYAN JF, MAHER MM (2014) Medical student knowledge regarding radiology before and after a radiological anatomy module: implications for vertical integration and self-directed learning. *Insights Imaging*, 5(5): 629-634.

NEGI S, DHIMAN S, SHARMA RK (2014) Basics and applications of rapid prototyping medical models. *Rapid Prototyping J*, 20(3).

O'RAHILLY R (1997) Philatelic introduction to the history of anatomy. *Clin Anat*, 10(5): 337-340.

OLDER J (2004) Anatomy: A must for teaching the next generation. *Surgeon*, 2(2): 79-90.

ORSBON CP, KAISER RS, ROSS CF (2014) Physician opinions about an anatomy core curriculum: A case for medical imaging and vertical integration. *Anat Sci Edu*, 7(4): 251-261.

PAPA V, VACCAREZZA M (2013) Teaching anatomy in the XXI century: New aspects and pitfalls. *Sci World J*, 2013: 310348.

PATEL SG, BENNINGER B, MIRJALILI SA (2017) Integrating ultrasound into modern medical curricula. *Clin Anat*, 30(4): 452-460.

PAWLINA W, DRAKE RL (2015) New (or not-so-new) tricks for old dogs: Ultrasound imaging in anatomy laboratories. *Anat Sci Edu*, 8(3): 195-196.

PEARL ML (2005) Proximal humeral anatomy in shoulder arthroplasty: Implications for prosthetic design and surgical technique. *J Shoulder Elb Surg*, 14(1 Suppl): S99-S104.

PENNEFATHER P, KREBS C (2019) Exploring the role of xR in visualisations for use in medical education. *Adv Exp Med Biol*, 1171: 15-23.

PERSAUD TV, LOUKAS M, TUBBS RS (2014) A history of human anatomy. Charles C. Thomas Publisher. https://doi.org/10.3138/cbmh.35.2perdicoyianni-paleologou

PERUMAL V, DANIEL B, BUTSON R (2016) Learning analytics of clinical anatomy e-cases. In: Kei Daniel, B. (eds) *Big Data and Learning Analytics in Higher Education*. Springer. pp. 253-263.

PHILLIPS AW, SMITH SG, STRAUS CM (2013) The role of radiology in preclinical anatomy. a critical review of the past, present, and future. *Acad Radiol*, 20(3): 297-304.

PHILLIPS B, BALL C, SACKET D, AL, E (2014) Oxford Centre for Evidence-based Medicine – Levels of Evidence. Centre for Evidence Based Medicine.

POPIELUSZKO P, HENRY BM, SANNA B, HSIEH WC, SAGANIAK K, PĘKALA PA, WALOCHA JA, TOMASZEWSKI KA (2018) A systematic review and meta-analysis of variations in branching patterns of the adult aortic arch. *J Vasc Surg*, 68(1): 298-306.

QUIROGA-GARZA A, REYES-HERNÁNDEZ CG, ZARATE-GARZA PP, ESPARZA-HERNÁNDEZ CN, GUTIERREZ-DE LA O J, DE LA FUENTE-VILLARREAL D, ELIZONDO-OMAÑA RE, GUZMAN-LOPEZ S (2017) Willingness toward organ and body donation among anatomy professors and students in Mexico. *Anat Sci Edu*, 10(6): 589-597.

QUIROGA-GARZA A, TERAN-GARZA R, ELIZONDO-OMAÑA RE, GUZMÁN-LÓPEZ S (2020) The use of clinical reasoning skills in the setting of uncertainty: a case of trial femoral head migration. *Anat Sci Edu*, 13(1): 102-106.

RAJAN SJ, JACOB TM, SATHYENDRA S (2016) Vertical integration of basic science in final year of medical education. *Int J Appl Basic Med Res*, 6(3): 182.

RAMOS-DÁVILA EM, MELÉNDEZ-FLORES JD, ÁLVAREZ-PÉREZ R, BARRERA-FLORES FJ, MARTÍNEZ-COBOS MC, PINALES-RAZO R, QUIROGA-GARZA A, ZARATE-GARZA P, SANCHEZ-GOMEZ A, GUZMAN-LOPEZ L, ELIZONDO-OMAÑA RE (2021) Occipital condyle screw fixation viability according to age and gender anatomy: A computed tomography-based analysis. *Clin Neurol Neurosurg*, 200: 106358.

RODRÍGUEZ-ABARCA MA, HERNÁNDEZ-GRIMALDO EG, DE LA FUENTE-VILLARREAL D, JACOBO-BACA G, QUIROGA-GARZA A, PINALES-RAZO R, ELIZONDO-OMAÑA RE, GUZMAN-LOPEZ S (2020)

Gynecological influencing factors on the rectovaginal septum's morphology. *Int Urogynecol J*, 32(6):1427-1432.

RODRÍGUEZ-NIEDENFÜHR M, VÁZQUEZ T, NEARN L, FERREIRA B, PARKIN I, SAÑUDO JR (2001) Variations of the arterial pattern in the upper limb revisited: A morphological and statistical study, with a review of the literature. *J Anat*, 199(5): 547-566.

ROGERS SO, GAWANDE AA, KWAAN M, PUOPOLO AL, YOON C, BRENNAN TA, STUDDERT DM (2006) Analysis of surgical errors in closed malpractice claims at 4 liability insurers. *Surgery*, 140(1): 25-33.

ROMERO REVERON R (2007) Andreas Vesalius (1514-1564). Fundador de la anatomía humana moderna. *Int J Morphol*, 25(4): 847-850.

ROYER DF (2016) The role of ultrasound in graduate anatomy education: Current state of integration in the United States and faculty perceptions. *Anat Sci Edu*, 9(5): 456-467.

RUZYCKI SM, DESY JR, LACHMAN N, WOLANSKYJ-SPINNER AP (2019) Medical education for millennials: How anatomists are doing it right. *Clin Anat*, 32(1): 453-467.

SACKETT DL, ROSENBERG WMC, GRAY JAM, HAYNES RB, RICHARDSON WS (1996) Evidence based medicine: what it is and what it isn't. **BMJ**, 312(7023): 71-72.

SALINAS-ALVAREZ Y, QUIROGA-GARZA A, MARTINEZ-GARZA JH, JACOBO-BACA G, ZARATE-GARZA PP, RODRÍGUEZ-ALANÍS KV, GUZMAN-LOPEZ S, ELIZONDO-OMAÑA RE (2020) Mexican educators survey on anatomical sciences education and a review of world tendencies. *Anat Sci Edu*, 11: 1-11.

SANTOS PV DOS, BARBOSA ABM, TARGINO VA, SILVA N DE A, SILVA YC DE M, BARBOSA F, OLIVEIRA A DE SB, ASSIS T DE O (2018) Anatomical variations of the celiac trunk: a systematic review. *Arqui Brasil Cir Dig*, 31(4). e1403.

SAÑUDO JR, VÁZQUEZ R, PUERTA J (2003) Meaning and clinical interest of the anatomical variations in the 21st Century. *Eur J Anat*, 7 (Suppl 1): S1-S3.

SAUNDERS AL, WILLIAMS CE, HERIOT W, BRIGGS R, YEOH J, NAYAGAM DA, MCCOMBE M, VILLALOBOS J, BURNS O, LUU CD, AYTON LN, MCPHEDRAN M, OPIE NL, MCGOWAN C, SHEPHERD RK, GUYMER R, ALLEN PJ (2014) Development of a surgical procedure for implantation of a prototype suprachoroidal retinal prosthesis. *Clin Exp Ophthalmol*, 42(7): 665-674.

SMITH LG (2005) Medical professionalism and the generation gap. *Am J Med*, 118(4): 439-442.

STRAUS JR, WILLIAM L, TEMKIN O (1943) Vesalius and the problem of variability. *B Hist Med*, 14(5): 609-633.

SUGAND K, ABRAHAMS P, KHURANA A (2010) The anatomy of anatomy: A review for its modernization. *Anat Sci Edu*, 3(2): 83-93.

TOLEDO-PEREYRA LH (2008) De humani corporis fabrica surgical revolution. *J Invest Surg*, 21(5): 232-236.

TREGASKISS AP, GOODWIN AN, BRIGHT LD, ZIEGLER CH, ACLAND RD (2007) Three-dimensional CT angiography: A new technique for imaging microvascular anatomy. *Clin Anat*, 20(2): 116-123.

UMAN LS (2011) Systematic reviews and meta-analyses. *J Can Acad Child Adolesc Psych*, 20(1): 57-59.

VACCAREZZA M, PAPA V (2015) 3D printing: a valuable resource in human anatomy education. *Anat Sci Int*, 90(1): 64-65.

VAN DE WATER TR (2012) Historical aspects of inner ear anatomy and biology that underlie the design of hearing and balance prosthetic devices. *Anat Rec*, 295(11): 1741-1759.

VÁZQUEZ-BARRAGÁN MÁ, GARZA-BÁEZ A, MORALES-AVALOS R, MARTÍNEZ-GONZÁLEZ B, JACOBO-BACA G, PINALES-RAZO R, QUIROGA-GARZA A, DE LA FUENTE-VILLARREAL D, ELIZONDO-RIOJAS G, ELIZONDO-OMAÑA RE, GUZMÁN-LÓPEZ S (2016) Pelvimetry by reformatted computed tomography in 290 female pelvis: morphometric variations regarding age. *Int J Morphol*, 34(1): 298-304.

VAZQUEZ-ZORRILLA D, MILLAN-ALANIS JM, ALVAREZ-VILLALOBOS NA, ELIZONDO-OMAÑA RE, GUZMAN-LOPEZ S, VILCHEZ-CAVAZOS JF, FERNANDEZ-RODARTE BA, QUIROGA-GARZA A (2020) Anatomy of foot compartments: a systematic review. *Ann Anat*, 229: 151465.

VÁZQUEZ R, RIESCO JM, JUANES JA, BLANCO E, RUBIO M, CARRETERO J (2007) Educational strategies applied to the teaching of anatomy. The evolution of resources. *Eur J Anat*, 11 (Suppl 1): S31-S43.

WALSH RJ, BOHN RC (1990) Computer-assisted instructions: a role in teaching human gross anatomy. *Med Edu*, 24(6): 499-506.

WOOD JE, MEEK SG, JACOBSEN SC (1989) Quantitation of human shoulder anatomy for prosthetic arm control-I. Surface modelling. *J Biomech*, 22(3): 273-292.

YAMMINE K (2014a) Evidence□based anatomy. *Clin Anat*, 27(6): 847-852.

YAMMINE K (2014b) The current status of anatomy knowledge: where are we now? Where do we need to go and how do we get there? *Teach Learn Med*, 26(2): 184-188.

YIOU R, GOODENOUGH D (2006) Applying problem-based learning to the teaching of anatomy: The example of Harvard Medical School. *Surg Radiol Anat*, 28(2): 189-194.

ZARATE-GARZA PP, ORTEGA-BALDERAS JA, LUGO-GUILLEN RA, MARFIL-RIVERA A, QUIROGA-GARZA A, GUZMAN-LOPEZ S, ELIZONDO-OMAÑA RE (2021) Hippocampal volume as treatment predictor in antidepressant naïve patients with major depressive disorder. *J Psychiatr Res*, 140: 323-328.

ZARGARAN A, TURKI MA, BHASKAR J, SPIERS HVM, ZARGARAN D (2020) The role of technology in anatomy teaching: striking the right balance. *Adv Med Edu Pract*, 11: 259-266.

ZHANG X, PENG L, LI LJ, FAN W, DENG J, WEI X, LIU X, LI Z (2020) Knowledge, attitude and willingness of different ethnicities to participate in cadaver donation programs. *PLoS ONE*, 15(3): e0229529.

European Journal of Anatomy